Novel Approaches for the Control of Fungal Pathogens

Catheryn Rachel Augostine, BSc

Thesis submitted to the University of Nottingham (UK) for the degree of Doctor of Philosophy

School of Life Sciences

2022

Abstract

Fungal pathogens are a continual threat with potential impacts on human health, agriculture, food and goods security. Despite this, currently used treatments are limited to a handful of drug or fungicide classes. The limited availability of treatment options is further challenged by growing fungal resistance, tightening legislation over drug/fungicide use and evolving public opinion. In this thesis, certain novel approaches were explored for their potential in the control of fungal pathogens of humans or crops.

One approach utilised the concept of combinatorial treatments, applied specifically to synergistic interactions among natural product (NP) compounds. NPs have been questioned for their translational applications due to promiscuous activity; this study proposed the potential of synergy for potentiating antifungal activity and improving target specificity. In a high-throughput screening approach, selected NPs were screened pairwise against a wider NP chemical library. Screening of 800 NP combinations revealed 34 pairs that were potentially synergistic in their inhibitory effects on yeast growth. Moreover, scaled-up validation tests for three combinations of particular interest showed that synergy was present against several important pathogens. One synergistic combination was explored mechanistically and found to promote synergistic mitochondrial membrane depolarization and ROS formation. This work indicated the potential for synergistic NP combinations in fungal pathogen control.

An additional study focussed on relationships between NP interactions and their underlying mechanisms of synergy, focusing on a particular triangle of NP interactions (involving two synergies but also no interaction). Results indicated that the NP sclareol, found to synergise with a number of other NPs, could also induce synergy between the previously non-synergistic pair of compounds. Results supported that this action of sclareol involved uncoupling of oxidative

phosphorylation, which may be an activity that enables synergies against fungal pathogens more widely.

An additional approach explored the potential of collateral sensitivity (CS) as a potential drug-repurposing strategy against azole-resistant *Candida albicans*. CS is where resistance to one drug is linked to sensitivity to another, so offering means to target drug resistant strains. Two azole-resistant clinical isolates of *C. albicans* showed hypersensitivity to several non-antifungal drugs, particularly aminoglycosides. The mutants were slow growers, but slow growth was not sufficient to explain the hypersensitivity, neither were the isolates' alleles of *erg11*, the gene encoding the lanosterol demethylase targeted by azoles. Moreover, the hypersensitivity was not reproduced in other azole-resistant isolates. Mechanistic studies pointed to a possible role for cell wall glycosylation or integrity defects in the original two isolates. Further work expanded the search for CS compounds against azole-resistant *C. albicans* through a screen of a 1,280-compound library. The results did not identify any hit compounds, but reproducibility and dosage concerns meant that hit compounds could have been missed.

A final approach set out to assess mechanistic bases for reported fungal anti-attachment properties of certain polymer materials. One strategy was an accelerated evolution experiment, designed to select *C. albicans* variants hyper-attaching to polymer. However, attachment propensity did not change, indicating resilience of the anti-attachment material properties. Another strategy examined cell wall properties that may affect anti-attachment, in *C. albicans* and the plant pathogen *Zymoseptoria tritici*. Results with selective fluorescent probes highlighted certain cell wall components that were enriched in polymer-attaching or glass-attaching cells. This offers a path for understanding cell properties important for (anti-) attachment to the polymer materials, valuable for informing design of improved polymers.

Taken together the three approaches explored in this thesis offer exciting potential for bolstering efforts to control fungal pathogens, providing bases for further mechanistic and possible translational development.

Publications Related to Work in this Thesis

Augostine, C. R. & Avery, S. V. 2022. Discovery of natural products with antifungal potential through combinatorial synergy. *Front. Microbiol*., 13, 866840.

Davies, C. R., Wohlgemuth, F., Young, T., Violet, J., Dickinson, M., Sanders, J., Vallières, C. & Avery, S. V. 2021. Evolving challenges and strategies for fungal control in the food supply chain. *Fungal Biol. Rev.,* 36, 15-26.

Vallières, C., Hook, A. L., He, Y., Crucitti, V. C., Figueredo, G., **Davies, C. R.,** Burroughs, L., Winkler, D. A., Wildman, R. D., Irvine, D. J., Alexander, M. R. & Avery, S. V. 2020. Discovery of (meth)acrylate polymers that resist colonization by fungi associated with pathogenesis and biodeterioration. *Sci. Adv.*, 6, eaba6574.

Acknowledgements

Firstly, I would like to acknowledge my faith in my Lord and saviour Jesus Christ, who is the rock on which I have built my life. During this PhD journey there have been many highs and lows, yet I have continually found peace knowing God is with me, He has guided, and He will continue to guide me.

Importantly, I would like to express my gratitude to my supervisor Professor Simon Avery for his continued support and encouragement to progress not only in my project, but also in my own personal scientific development.

During my PhD experience I have been fortunate to have had such great colleagues and I would like to thank all B44 for their support, advice and fun, particularly in the tough days. I would like to thank Dr. Cindy Vallières for her guidance during the early stages of my project and for continued support. Moreover, I want to thank the technical team who enabled our day-to-day experiments to continue with ease. In particular, I would like to thank Matt Kokolski who always goes above and beyond for the Fungal Biology group.

And finally, I would like to thank my friends and family; who's continued encouragement has been invaluable on this PhD journey. I thank my Dad, Mom, sister, brother and my family-in-love, who have always encouraged me to persevere and pursue what I enjoy. Last but by no means least, I would like to express my deepest gratitude to my wonderful husband, Marinus, for always being my encourager, supporting me through every season and bringing me so much joy, life is a truly amazing adventure by your side.

Contents

List of Figures

List of Tables

List of Abbreviations

A-488	Alexafluor-488
ACM	Aspergillus complete medium
AIBN	Azobisisobutyronitrile
AODMBA	(R)-α-Acryloyloxy-β,β-dimethyl-γ-butyrolactone
AOHPMA	Acryloyloxy-2-hydroxypropyl methacrylate
A.U	Arbitrary units
BER	Berberine
BSA	Bovine serum albumin
CCCP	Carbonylcyanide-3-chlorophenylhydrazone
CFU	Colony forming unit(s)
CUR	Curcumin
CS	Collateral sensitivity
DAPI	4’,6-Diamidino-2-phenylindole
DMI	Demethylase inhibitor
DMSO	Dimethyl sulfoxide
DMPA	2,2-Dimethoxy-2-phenylacetophenone
EUG	Eugenol
ESC	β-escin
FDA	Food and Drug Administration
FICI	Fractional inhibitory concentration index
FITC	Fluorescein isothiocyanate
HS-R	Hypersensitive and azole-resistant
iCEMA	Isocyanatoethyl methacrylate
IFD	Invasive fungal diseases
mMAOES	Mono-2-(Methacryloyloxy)ethyl succinate
MIC	Minimum inhibitory concentration
NP(s)	Natural product(s)
OD	Optical density
PAMP	Pathogen associated molecular pattern
PBS	Phosphate-buffered saline
PCR	Polymerase chain reaction
PEGDA	Polyethylene glycol diacrylate
PDA	Potato dextrose agar
PDB	Potato dextrose broth
PFA	Polyformaldehyde
PM	Paromomycin
PTE	Pterostilbene
PTI	PAMP-triggered immunity
R6G	Rhodamine 6G
ROS	Reactive oxygen species
RPMI	Roswell park memorial institute medium
SCL	Sclareol

SD	Standard deviation
SDHI	Succinate dehydrogenase inhibitor
SEM	Standard error of the mean
SNP	Single nucleotide polymorphism
TFP	Trifluoperazine dihydrochloride
UV	Ultra-violet light
XTT	Tetrazolium salt, 2,3-bis[2-methyloxy-4nitro-5-sulfophenyl]2H-tetrazolium-5-carboxanilide
WHO	World Health Organisation
YPD	Yeast extract, peptone, plus dextrose (2%)
YPE	Yeast extract, peptone, plus ethanol (2%)
YPG	Yeast extract, peptone, plus glycerol (2%)

COVID-19 Impact Statement

The COVID-19 pandemic had personal and research specific impacts affecting my PhD. From a personal level, continuing with my PhD during the pandemic did bring with it several anxieties over the feeling of 'losing time' on my PhD, fears for my own and families health, particularly as my family were working as front-line workers.

Firstly, the lab lockdown of five months impacted research progress and meant it was difficult to mitigate the impact as we had no idea when or how things were going to open up. However, whilst in lockdown I was able use the time available to co-first author a review article, as well as planning a timeline of experiments to complete. On lab return, occupancy was an issue, which meant for two months we were operating on 66% time in the lab on a one week off, two weeks on rota. In addition, when the lab reopened, there were issues with delayed consumables deliveries, particularly the use of single-use plastics such as 96-well microtiter plates (which I needed for several planned experiments). Moreover, my project involved collaboration with other facilities in which access was disrupted and instrument training was delayed/online for several months after the university re-opened.

Additionally, as a mandatory part of my BBSRC-DTP, I was informed to plan to continue with organising a three-month professional internship for PhD students (PIP). I successfully arranged and carried out my PIP in Hannover, Germany (August 2020). The impact of the COVID-19 pandemic, despite my two-month funded extension has affected the output of my PhD, with several research questions unanswered. Despite these unforeseen circumstances I was able to publish, including first-authored review and primary research papers. Moreover, I was able to attend and present at a conference (BMS, Cranfield 2022) where I was awarded the best oral talk prize and despite optimisation/time challenges, make experimental progress in all areas of my PhD.

Chapter 1 – General Introduction

1.1 Fungal pathogens: the problem

The estimated number of fungal species is continually debated, with estimates ranging from 2.2 million to 3.8 million species (Hawksworth and Lucking, 2017). Within this vast diversity, fungal species have numerous important roles including beneficial roles in medicine, food and drinks production, nutrient recycling and decomposition (Bourdichon et al., 2012, Scherlach et al., 2013). However, a small proportion of this diversity is responsible for devastating socioeconomic impacts concerning human health, agriculture, food security and biodeterioration.

1.1.1 Fungal pathogenesis in humans

Fungi pathogenic to humans are estimated to comprise around 300 species, with the majority causing extremely rare mycoses (Garcia-Solache and Casadevall, 2010, Kim, 2016, Anonymous, 2017). Despite their limited relative representation within the fungal kingdom, fungal pathogens of humans are known to seriously impact the health of over 150 million people per year, leading to > 1.6 million annual cases of mortality (Bongomin et al., 2017). This mortality rate is higher than annual deaths from drug-resistant tuberculosis and malaria, further highlighting the significance of these fungal pathogens (Calderone et al., 2014). *Candida*, *Aspergillus*, *Pneumocystis* and *Cryptococcus* spp. are the most common cause of life-threatening fungal diseases, where complex interplay exists between the opportunistic pathogen and the human host to establish and maintain infection (Nosanchuk, 2013). Infections commonly occur in patients that are immunocompromised (e.g. undergoing chemotherapy or carrying HIV) but infections in healthy people are also increasing, as the number of immunocompromised people is also increasing (Anonymous, 2017). The eukaryotic nature of fungal pathogens

presents an additional hurdle for eradication of infection, as drug targets that affect the fungus but not the host are harder to find. This, coupled with growing resistance to the current antifungal drug arsenal, highlights the need for novel, effective antifungal control methods (Ben-Ami, 2018). Recently the World Health Organization (WHO) released their first global report of a fungal priority pathogens list. In the report, WHO proposed an effort to systematically prioritise fungal pathogens with aims to guide research, development and public health actions, whilst also recognising the unmet research and development needs and perceived public health importance of fungal pathogens (WHO, 2022). This part of the introduction will discuss fungal pathogens of humans, with a particular focus on *Candida albicans*.

1.1.1.1 Candida albicans

Fungal pathogens of humans are often characterised as opportunistic pathogens, which can be defined as when a pathogen initiates infection through taking advantage of an opportunity within the host that is not usually available, such as a weakened immune system or altered microbiota (Gostinčar et al., 2018). One significant opportunistic pathogen, *Candida albicans*, exists commensally in ~50% of people as a beneficial constituent of the microbiota, highlighting the potential vulnerability to infection (Höfs et al., 2016, Kim, 2016, Ben-Ami, 2018). Number of cases of infection by opportunistic fungal pathogens are growing, exacerbated by medical procedures that render a patient compromised, including indwelling medical devices and through the use of antibiotics that disrupt the microbiota (Min et al., 2020). In response to an altered host environment, fungi are able to initiate infection using multiple strategies which includes switching cell morphology (Min et al., 2020) or cell surface epitope presentation (Hall, 2015), producing cytotoxic peptides (e.g. candidalysin produced by Ece1p) (Moyes et al., 2016) and forming impenetrable structures such as biofilms (Nobile and Johnson, 2015).

1.1.1.2 Morphology switching, molecular memory and immune-evasion in human fungal pathogenesis

It is well known that fungal pathogens can adopt different morphological forms inside the host to remain virulent, or to evade host immunity and this has been likened to "shape shifting" (Min et al., 2020). Morphological transitions are evident in the four major genera of pathogenic fungi (*Candida, Aspergillus, Pneumocystis* and *Cryptococcus* spp.). A link between switching from yeast to hyphal forms and the impact this has on pathogen virulence, immune evasion and adaptation to different host niches is particularly well reported in *Candida albicans*. One example is illustrated by an attenuation of virulence in mutants unable to form hyphae (Lo et al., 1997) or in mutants that are trapped in the filamentous form (Murad et al., 2001). Regulation of the hyphal switch and development in *C. albicans* has been well-established and is controlled through complex genetics (Lu et al., 2014), environmental signals such as hypoxia, nutrient conditions (Lu et al., 2013), the introduction of serum, alkaline pH, elevated temperature and quorum sensing (QS). One example is the production of the QS molecule farnesol, which is capable of regulating the hyphal switch through repression of Ras-1 (cAMP/protein kinase A) signalling pathway to prevent hyphal formation (Davis-Hanna et al., 2008). Farnesol blocks hyphal development by suppression of the cAMP pathway, specifically through inhibition of adenyl cyclase (Cyr1) activity (Hall et al., 2011). This dimorphic switch in *C. albicans* has been discussed as a potential therapeutic target, whereby preventing the yeast-hyphal transition might prevent pathogen adhesion whilst also modulating the immune response e.g., avoidance of excessive inflammation (Saville et al., 2006, Jacobsen and Hube, 2017). Large-compound based screening has proved successful for the identification of compounds that inhibit the hyphal transition such as the small molecule inhibitor filastatin, which also prevented *C. albicans* adhesion and impaired biofilm formation (Fazly et al., 2013).

In addition to morphogenesis, fungal pathogens can also utilise alternative (to glucose) carbon-sources as forms of molecular 'memory' to promote immune

cell evasion. The dimorphic species *C. albicans* is able to resist killing within phagocytic cells, enabling infection to continue to disseminate within the host. Williams and Lorenz (2020) demonstrated that the pathogen can utilise alternative carbon sources such as amino acids and *N*-acetylglucosamine alongside glucose. This alternative carbon source utilisation was shown to promote stress resistance and virulence within the host (Williams and Lorenz, 2020). The authors proposed that differences in response to alternative carbon sources (aside from glucose) suggests *C. albicans* uses the carbon source as 'niche-specific' priming signals to allow stress recognition and adaption to virulence (Williams and Lorenz, 2020). The ability to anticipate and utilise a fluctuating environment to facilitate virulence within the host has been discussed as fungal 'memory' (Brown et al., 2019). One example of fungal memory is found in the use of glucose by *C. albicans* as a protection strategy against acute oxidative stress and neutrophil killing. It is hypothesised that upon exposure to the host bloodstream, the fungal cells detect glucose as a carbon source and activate an anticipatory stress response allowing them to evade immune cell killing (Rodaki et al., 2009).

Alongside fungal memory, *C. albicans* is capable of evading host immune-recognition through control of cell surface epitopes. In response to different environmental conditions within the host, cell wall carbohydrates, also referred to as pathogen associated molecular patterns (PAMPs) are constantly changing, which render the interaction with the host highly dynamic (Hall, 2015). One example of this immune-evading activity of *C. albicans* can be observed in the cell wall remodelling changes of the pathogen upon encountering an acidic environment, representative of the conditions in the vaginal mucosa. Cottier et al., (2019) found that fungal PAMPs (chitin and β-glucan) in yeast cells become unmasked upon exposure to the acidic environment and this unmasking was time-dependent. The PAMPs then underwent remasking at later timepoints in response to QS molecules. Interestingly, cell wall unmasking of these PAMPs also coincided with an enhanced phagocytosis rate (Cottier et al., 2019). This example exaggerates how immune evasion through cell wall

remodelling is complex and highly dynamic in response to the host environment. Evidently, the ability of fungal pathogens to successfully establish infection within the human host is complex and involves multiple 'tactics'.

1.1.1.3 Biofilm formation and its role in human fungal pathogenesis

In addition to changing morphology and potential for developing immune linked memory, fungal pathogens are able to form complex, impenetrable structures termed biofilms. A biofilm can be defined as an assemblage of microbial cells (comprised of ≥ 1 species) attached to a surface and encased within a matrix of extracellular material (polysaccharide) produced by the organism (Donlan, 2002). Biofilms have been extensively studied in different pathogens and research efforts have described multi-gene regulatory systems, underlying biofilm establishment. Biofilms are reported to be responsible for 65% of microbial infections, presenting a dangerous clinical problem (Jamal et al., 2018). Fungal biofilm formation consists of several stages; adherence, initiation, maturation and dispersion (Jamal et al., 2018). A schematic of this process is shown in Figure 1.1.

The process of adhesion in *C. albicans* biofilm formation has been well-researched and is known to be influenced by additional factors including quorum-sensing molecules, host hormones, stressful conditions and the presence of other microorganisms (Parsek and Greenberg, 2005, Frade and Arthington-Skaggs, 2010, Desai and Mitchell, 2015). Biofilm formation by *C. albicans* begins with adherence of the yeast cells to a substrate which then proliferate across the surface before the production of filamentous projections. The biofilm master regulator protein Bcr1 and several of its downstream targets such as Als1 in yeast cells and Hwp1 in hyphal cells are important for cell adherence and maturation, (Nobile et al., 2006). Moreover, another major cell wall protein that mediates surface binding in *C. albicans* is the adhesin Eap1. Genetic studies with a *eap1Δ/Δ* deletion mutant confirmed its importance in adherence, where the mutant has reduced adherence to polystyrene and is defective in biofilm formation both *in vitro* and *in vivo* (Li et al., 2007). Alongside

the abovementioned adhesins, there are several other proteins and many transcriptional regulators which have been shown important for adherence (Finkel et al., 2012). The success of the adherence step is essential for biofilm formation, therefore it not surprising that adherence is tightly genetically controlled and dynamic in response to a broad range of conditions (Nobile and Johnson, 2015).

Following adherence of the yeast cells, initiation of the biofilm begins, culminating in a morphologically heterogeneous cell population. The importance of the hyphal form is viewed as maintaining the architectural stability of the biofilm, displaying 'scaffold-like' properties that enable adherence of the hyphae to each other and to yeast cells (Nobile and Johnson, 2015).

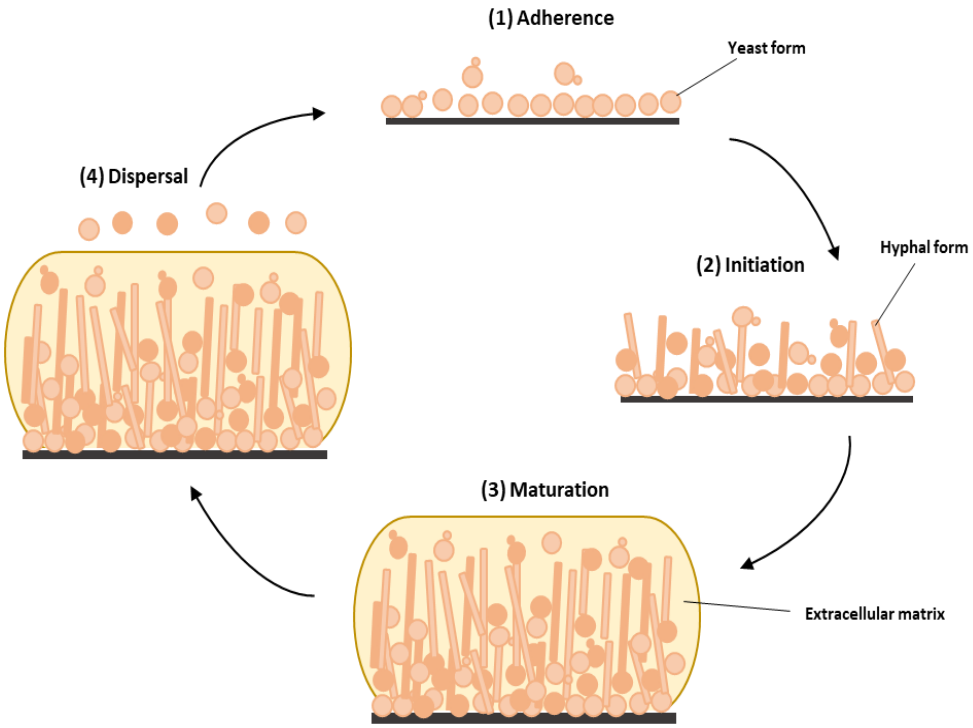

Figure 1.1. Schematic biofilm formation in *c. albicans*. Biofilm formation is divided into the four key stages, adherence, initiation, maturation and dispersion, a self-perpetuating process leading to further infection and biofilm formation. This figure is adapted from Lohse et al (Lohse et al., 2018).

Subsequent biofilm formation involves the maturation step, where the extracellular matrix (ECM) is formed. ECM regulation is likely to be linked to the core biofilm transcriptional regulators, however the involvement of these regulators has not yet been elucidated (Rodriguez et al., 2020). The ECM provides a protective physical barrier that surrounds the cells in the biofilm and is composed of proteins (55%), carbohydrates (25%) and lipids (15%) amongst other constituents (Zarnowski et al., 2014). Alongside the structural role of the ECM, it can also sequester or absorb antifungal drugs, reducing their bioavailability to act on fungal cells and contribute to antifungal resistance, the biofilm renders the organism more resistant to pharmacological intervention through slow or incomplete drug penetration (Stewart, 1996, Ceri et al., 1999, Nett et al., 2010). Besides the ECM, intrinsic drug tolerance in *C. albicans* biofilms is also attributed to the upregulation of drug efflux pumps which is sustained throughout biofilm development (Ramage et al., 2002a) and existence of persister cells. Persister cells of *C. albicans* have a heightened drug tolerance through their ability to exist in a state comparable to dormancy (Li et al., 2015). Efficient targeting of persister cells is important for effective management of biofilms (Wuyts et al., 2018).

The dispersal of *C. albicans* cells happens throughout biofilm development, but particularly after biofilm maturation. Dispersion is primarily of the yeast form, with these cells also possessing enhanced adherence and virulence in murine models (Uppuluri et al., 2010). Dispersal is also enhanced through the quorum sensing (QS) molecule farnesol, which prevents the hyphal transition and enhances the dispersal of yeast cells to disseminate in the host (Ramage et al., 2002b). Much is known about the pathogenesis of *C. albicans*, including virulence factors described above such as dimorphism and ability to form biofilms. Other examples, less relevant to the research described in this thesis, include phenotypic switching, thigomotropism (Watts et al., 1998), the production of toxins by the hyphal form such as candidalysin (Moyes et al., 2016) and robust stress responses (Mayer et al., 2013).

1.1.2 Fungal pathogenesis in plants

Fungi (and oomycetes) also destroy up to a third of all food crops per year, which would be sufficient to feed an additional 600 million people (Anonymous, 2017). Controlling fungal crop pathogens is of principal importance, with pre-harvest losses still exceeding 20% of total yield (Fisher et al., 2018). The most economically damaging fungal species include: *Magnoporthe oryzae* which infects crops such as wheat and rice (Ou, 1980), *Botrytis cinerea,* with a broad host range (van Baarlen et al., 2007), various *Fusarium spp.* pathogens such as *F. oxysporum,* a soil borne pathogen induces vascular wilt on a wide range of plants and *F. graminearum* which is particularly damaging to cereal crops (Dean et al., 2012) and wheat pathogens *Puccinia* spp. (Zadoks, 1985) and *Zymoseptoria tritici* (Palmer and Skinner, 2002).

Further emphasis on the urgency to control fungal crop pathogens is exemplified by the ability of several species to infect a broad host range. A simultaneous and non-controllable infection of rice, maize, potatoes and soybean combined would result in 61% of the world's population being without food (Almeida et al., 2019). Therefore, it is not surprising that the global market for chemical agents used to control fungal phytopathogens, i.e., fungicides, is valued at $13.4 billion per annum (Garside, 2019). A growing global population coupled with impacts of climate change that allow fungal crop diseases to migrate geographically, amplifies the need for successful fungal control to protect food security (Garcia-Solache and Casadevall, 2010, Fones et al., 2020).

1.1.2.1 Host-pathogen interactions and infection structures in fungal plant pathogenesis

The management of fungal crop pathogens is complicated by the ability of several fungi to establish infections without displaying visible symptoms. This is seen in biotrophic fungal pathogens such as *Z. tritici* and also in necrotrophic pathogens with the capability to remain quiescent until conditions conducive for infection progression arise (e.g. growth of foliar tissue) (Hua et

al., 2018, Francisco et al., 2019). These host-pathogen interactions call for improved diagnostics whilst also complicating decision-making on the timing of fungicide applications (Bosch et al., 2020).

Developing an understanding of the infection cycle of plant pathogenic fungi is important not only for biological insight but also for informing appropriate prevention strategies. Many plant pathogenic fungi have evolved elaborate infection structures to secure nutrients from the host (Mendgen and Deising, 1993). For example, the hemibiotroph *M. oryzae* produces melanised conidia that develop melanised appressorium (specialised infection cell) structures. The turgor pressure building inside the appressorium leads to rupture of plant epithelial cells and penetration of infecting hyphae (Kankanala et al., 2007, Ryder et al., 2022). During the biotrophic stage of infection the pathogen accumulates and secretes effectors to avoid and suppress plant defences (Khang et al., 2010). When the plant cells are full of fungal hyphae they die, reflecting the necrotrophic infection stage (Kankanala et al., 2007). This is one example of a complex infection process that plant pathogenic fungi may use to colonise the host plant.

1.1.2.2 Points of infection, dispersal and persistence in fungal plant pathogenesis

An additional hurdle facing crop protection from fungal disease is that pathogens initiate infection at different entry points, dependent on the pathogen and crop. *Fusarium oxysporum* in the soil infects plants by entering through the root system, causing vascular wilt on a wide range of plants (Leslie and Summerell, 2006). Alternatively, infection may start at above-ground plant surfaces, as is the case for *M. oryzae.* Some fungal crop pathogens can infect throughout plant development. One example is the necrotrophic pathogen *B. cinerea,* reported to cause disease in 400 plant species, which can infect the plant from the seedling stage with continued disruption even up to post-harvest ripening stages if conditions are appropriate (Williamson et al., 2007). The success of *B. cinerea* is likened to flexible infection modes and high

reproductive output (Cheung et al., 2020). This complicates treatment as fungicide application strategies will depend on the crop being used and knowledge of the progress and stage of pathogen infection.

Furthermore, fungal crop pathogen infectivity and persistence is enabled through the ability of spores (sexual and asexual) to hijack external factors to promote infection. Firstly, fungal spore dispersal (and subsequent plant colonisation) is promoted by wind and rain-splash (McCartney, 1994). Secondly, it is known that fungal spores can 'piggy-back' onto pollinators such as bees and insects (Goddard et al., 2010). da Silva et al. (2016) reported that flower-visiting birds enable spore dispersal over large spatial scales (> 10 km). The study suggested that this method of fungal spore dispersal can also be directed, where spores are deposited in favourable conditions for the fungus (da Silva et al., 2016b). Moreover, alongside benefits for dispersal, fungi can remain in a state of dormancy within the soil in the form of 'resting spores'. One example is the sclerotia (a hardened mass of fungal mycelium) formed by the phytopathogen *Sclerotinia sclerotium,* otherwise known as white mould (Jones and Watson, 1969). The sclerotia from this broad-spectrum phytopathogen are able to remain viable in the soil for at least eight years (Adams and Ayers, 1979) and can seed plant infection again whenever the conditions are conducive. Another example of assisted dispersal can be observed in the symbiosis between bark beetles and plant pathogenic fungi, where fungal induced wood rot feeds beetle larvae, cumulating in plant death (Six and Wingfield, 2011). One notable example is observed in Dutch elm disease. This ability of phytopathogenic fungi to disperse and remain viable in the soil complicates the treatment of fungal crop pathogens and emphasises the need for integrated disease management (IDM).

1.1.2.3 Complications for fungal plant pathogen management

Management of fungal crop pathogens typically involves an IDM approach that encompasses agricultural practices (carried out by growers e.g. tillage and crop

rotation) and planting of resistant crop cultivars (Rojas Tayo et al., 2018). Despite the important contribution of these practices, control of many plant pathogenic fungi is inherently reliant on the application of fungicides (O'Driscoll et al., 2014, Heick et al., 2017). In modern agriculture, most fungal pathogens can theoretically be controlled using an IDM approach; however major epidemics still occur with substantial yield losses, such as the ongoing problem of Panama disease (tropical race 4). The disease is caused by the soil-borne fungus, *F. odoratissimum* and threatens global production of bananas, particularly as the commonly grown Cavendish banana variety is extremely susceptible to disease (Maymon et al., 2020). This example also alludes to anthropogenic and climate change influences upon fungal pathogen spread and emergence in new regions (Fones et al., 2020). Similar to the challenges facing the control of human fungal pathogens, the current fungicide options are too limited in agriculture, faced with growing resistance and toxicity concerns, hence there is an urgent need to discover novel tools for management.

1.1.3 Fungal disruption in food spoilage and material biodeterioration

Spoilage is responsible for losses of up to 30% of stored-foods across retailers and consumers in industrialised countries (FAO, 2011). The spoilage of stored-foods is defined by negative effects upon the organoleptic product quality (e.g. aesthetics, texture, taste, toxins). Fungi are a major source of spoilage, where their biological robustness enables persistence (Selbmann, 2019). Airborne fungal spores (either sexual or asexual) can be particularly problematic in contaminating foods and food factories, resulting in economic losses both during the production process and at the consumer level (Leyva Salas et al., 2017). Spoilage of stored-foods is visible across a diverse range of foods, from dairy and bakery produce extending to fruits and vegetables and is initiated by multiple fungal species including those belonging to the *Aspergillus, Penicillium* and *Zygosaccharomyces* genera (Kaczmarek et al., 2019).

Some fungi contaminating foods possess the ability to produce mycotoxins, presenting a danger also to human health; mycotoxins often go un-detected in the food source (Krisch et al., 2011). The removal of these mycotoxigenic secondary metabolites is complicated by their tolerance of heat and acid conditions (Filtenborg et al., 1996). One prominent mycotoxin is aflatoxin B_1, produced by *Aspergillus flavus* and *A. parasiticus* and recognised as a primary carcinogen. The mycotoxin can persist during food processing and be ingested through contaminated agricultural crop and animal feed, causing both health hazards and economic losses in agriculture (Qu et al., 2019). Mycotoxin control is challenging and demands close monitoring to protect human health and food safety.

Amongst the various problems listed here, fungi are also responsible for the biodeterioration of diverse, commercially-important materials including marble, paper, glass and leather. The destructive ability of fungi is evident against cultural heritage such as paintings, monuments, textiles and paper where some fungi can exert significant damage (Sterflinger, 2010). Glass is also subject to fungal biodeterioration (Drewello and Weissmann, 1997), presenting concerns particularly in the conservation and restoration of stained-glass windows. Certain fungi are well adapted to colonise and survive upon glass; where fungal spores adhere to hydrophobic surfaces, resist desiccation, have preference for acidic-neutral pH conditions and may initiate metabolism of a wide range of carbon sources (Rodrigues et al., 2014). Molecular identification of organisms on stained glass revealed the presence of multiple fungi including *Cladosporium* and *Penicillium* species, and laboratory-based experiments showed that fungal biodeterioration can be visualised from as little as 2.5 months after production (Rodrigues et al., 2014). Conventional procedures to remove fungi from stained-glass, such as repeated cleaning (water: ethanol solution 1:1) are currently inadequate in fungal removal from glass.

In the case of leather, biodeterioration by fungi can arise from the stages of processing through to use by consumers and is exacerbated by high relative humidity. Tanned leathers present a relatively rich nutrient source for fungi,

containing carbohydrates, fats and proteins (Strzelczyk et al., 1987). Common fungal contaminants of leather include members of the *Penicillium, Aspergillus* and *Trichoderma* genera. Fungicides used in the control of leather contamination have properties including high activity, broad antimicrobial spectrum, non-discolouring, low toxicity (to humans), cost effectiveness and environmental acceptability (Orlita, 2004). As elsewhere, the use of such chemical actives in the leather industry is not an ideal scenario.

1.2 Chemical methods for fungal control

Despite the diversity and spectrum of fungal pathogens or spoilage/biodeterioration agents, current control is dominated by the application of antifungals or fungicides. As fungi possess a common eukaryotic nature with humans and plants, many basic cellular functions are conserved, issues of non-host toxicity complicate novel drug/fungicide discovery (Roemer and Krysan, 2014). Anti-mycotic agents generally target cellular structures or processes that are absent or less important in the host. For example, one such distinct process is the fungal ergosterol biosynthesis pathway and ergosterol function is the target of several drugs (Ksiezopolska and Gabaldon, 2018). Across human and agricultural pathogens, multiple classes of chemicals are used including (and not limited too); demethylase inhibitors, echinocandins, polyenes, strobilurins, succinate dehydrogenase inhibitors and DNA analogues. The cellular targets of these antifungal compounds are illustrated in Figure 1.2.

1.2.1 Demethylase inhibitors

The demethylase inhibitors (DMIs) have been used since the 1970s and represent part of the core group of fungicides used in agriculture. They can be applied to winter wheat up to three times per season (Wieczorek et al., 2015). Azole DMIs are also the most commonly prescribed treatment for *C. albicans* infection (Ksiezopolska and Gabaldon, 2018). DMIs are heterocyclic compounds

that contain at least one nitrogen atom as part of the ring, and they work through preventing ergosterol biosynthesis within the fungal cell membrane. Specifically they inhibit the action of the cytochrome P450-enzyme (sterol 14α-demethylase / CYP51 / Erg11), preventing the oxidative removal of the 14α-methyl group of lanosterol and conversion to ergosterol (Marichal et al., 1985, Leroux et al., 2008). The DMI fungicides epoxiconazole and prothioconazole have been the most used fungicides for management of winter wheat diseases across Europe for several years (Jørgensen et al., 2008). The most commonly used azole in a clinical setting against *C. albicans* is fluconazole as it is inexpensive, readily bioavailable, orally administered and still remains a successful treatment option against *C. albicans* infection (Pappas et al., 2016).

1.2.2 Echinocandins

Another important antifungal drug class, often used in conjunction with azoles, is the echinocandins. Echinocandins are cyclic lipopeptides that target the transmembrane glucan synthase complex, Fks1. The Fks1 enzyme is responsible for the production of β-(1,3)-glucan and disruption of this affects cell integrity, resulting in cell rupture and death (Denning, 2002). Currently there are only three licensed echinocandins: caspofungin, micafungin and anidulafungin. All three are used to treat *Candida* sp. infection. Unlike azoles, these drugs are supplied intravenously due to their high molecular weight (Kim et al., 2007).

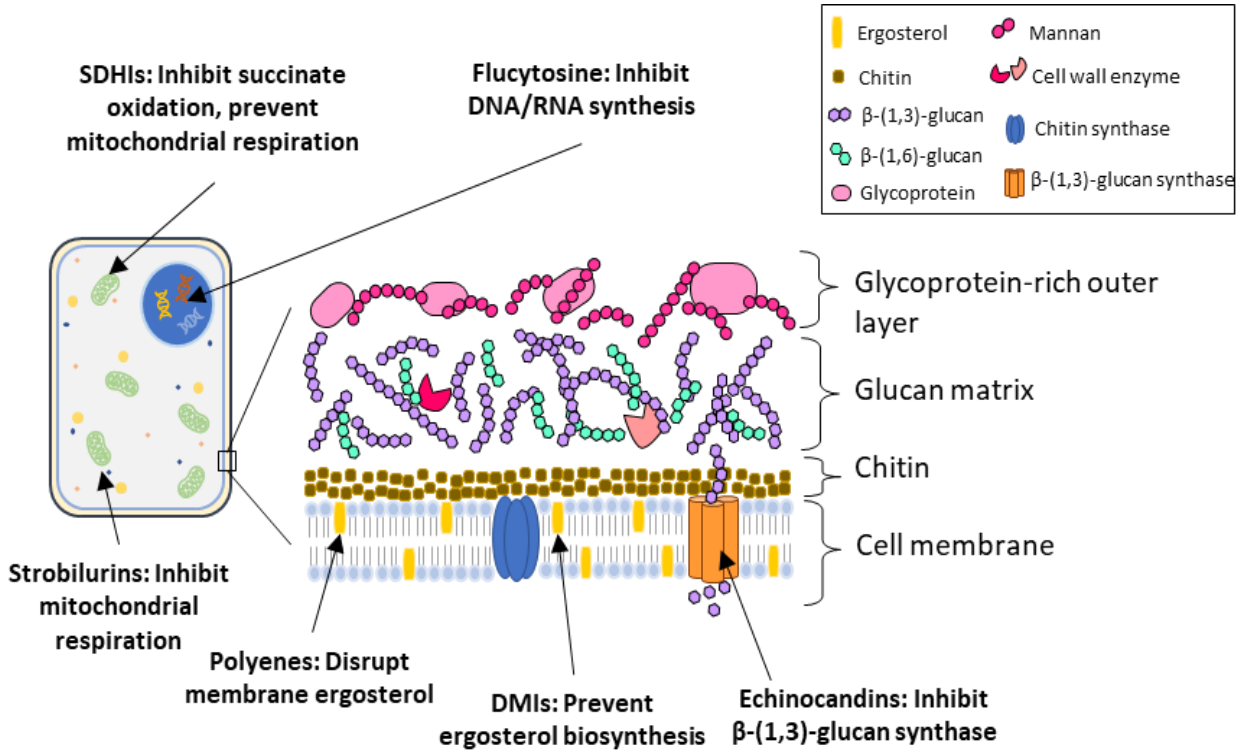

Figure 1.2. Schematic highlighting cell wall- and cell membrane- targets of some key antifungals and fungicides. Drugs/fungicides and cellular targets are labelled with an arrow followed by a brief description. The key in the top right inset indicates the relevant cell wall or membrane components. This figure was adapted from a similar figure in Geoghegan et al (2017). SDHI = succinate dehydrogenase inhibitor; DMI = demethylase inhibitor.

Echinocandins are now the preferred treatment for invasive candidiasis for a variety of reasons; they have a broad fungicidal activity against many of the *Candida* species (including those with elevated intrinsic azole-resistance), they remain safe beyond standard dosage concentrations and display limited drug-drug interactions, retaining efficacy in combination (Sucher et al., 2009, Pappas et al., 2016, Ksiezopolska and Gabaldon, 2018). Clinical evaluation of the echinocandin anidulafungin, compared with fluconazole, indicated an increased overall success of candidiasis treatment (*C. albicans*) with anidulafungin (76% vs 60%) (Reboli et al., 2007, Antinori et al., 2016). Standard therapy of candidiasis utilises initial therapy with fluconazole followed by caspofungin treatment. Moreover, echinocandins are relatively penetrative in biofilms, an important advantage considering that biofilm formation is a key hurdle in *Candida* treatment (see Fungal pathogenesis in humans (Antinori et al., 2016).

1.2.3 Polyenes

Treatments for human fungal pathogens also include polyene agents. Polyenes are poly-unsaturated organic compounds consisting of at least three alternating double and single carbon-carbon bonds (Andreoli and Monahan, 1968). Polyenes that are used clinically include amphotericin B (AmB) and nystatin. Polyenes have the broadest spectrum of antifungal activity of any clinically available agent, however their mechanism has sparked concerns regarding non-specific toxicity (Andriole, 2000). The primarily accepted mechanism of AmB involves binding to ergosterol in the fungal cell membrane followed by the formation of pores/channels, resulting in loss of membrane permeability, cell leakage and cell death (Gallis et al., 1990). Two mechanisms by which polyenes span the lipid bilayer have been shown, either by a conformational thinning of the membrane or by tandem insertion into both monolayers (Kristanc et al., 2019). More recently, another mechanism of AmB was proposed, where AmB is adsorbed in perpendicular orientation to the membrane surface in the form of large aggregates and acts as a ‘sponge’ that

draws ergosterol out of the cell membrane, leading to cell death (Gray et al., 2012). However, this hypothesis is still under experimental scrutiny (Haro-Reyes et al., 2022). AmB binds ergosterol with up to 10 times more avidity than to cholesterol and therefore can exhibit selective antifungal activity (Kotler-Brajtburg et al., 1974). Moreover, lipid formulations of AmB have reduced non-specific activity and reduced host nephrotoxicity (Hiemenz and Walsh, 1996).

1.2.4 Strobilurins

The strobilurin class of agricultural fungicides (also known as quinone-outside inhibitors [QoIs]) were first sold in 1996 and by 1999 transactions totalled $620 million which represented 10% of the global fungicidal market (McDougall, 2001, Bartlett et al., 2002). Strobilurins are a single-site class of fungicide that inhibit mitochondrial respiration through binding at the Q_o site of cytochrome b, which is part of the cytochrome bc1 complex (located within the inner mitochondrial membrane of the fungus, complex III). Upon strobilurin binding, electron transfer between cytochrome b and c1 is blocked which culminates in the prevention of nicotinamide adenine dinucleotide (NADH) oxidation and adenosine triphosphate (ATP) production essential for fungal growth (Becker et al., 1981). The strobilurin fungicides were widely used due to their curative (inhibition of the fungus even in early initial infection) and systemic (absorbed into the plant, continue activity during growth) properties (Bartlett et al., 2002). However the single-site mechanism of action of this fungicide has been undermined by the development of resistance (Feng et al., 2020).Succinate dehydrogenase inhibitors

The succinate dehydrogenase inhibitors (SDHIs) have played important roles in crop protection from various pathogens since their discovery in the 1960s(Schmeling and Kulka, 1966) followed by the first introduction of carboxin in 1969, and are still deemed the fastest growing class of fungicide regarding the production of new compounds (Umetsu and Shirai, 2020). The introduction of new SDHIs in Europe from 2010 (e.g. bixafen and isopyrazam) has been

successful for treatment of phytopathogens including the wheat pathogen *Z. tritici* (Yamashita and Fraaije, 2018). Chemically, SDHIs show diversity within the core moiety (part of the molecule) which promotes binding and *in vivo* activity, however an amide bond is a common classifying feature (Walter et al., 2011). SDHIs specifically target the fungal succinate ubiquinone oxidoreductase (SDH) mitochondrial enzyme, an essential component of the respiratory chain (complex II). Upon binding to the SDH ubiquinone binding site (Q-site) the SDHI physically blocks access of the substrate and prevents succinate oxidation and therefore respiration (Georgopoulos et al., 1972). The SDHIs harbour a broad spectrum fungicidal activity (Avenot and Michailides, 2010).

1.2.5 Analogues

In addition to the abovementioned classes of drugs, a group of chemicals defined as analogues are also used to treat fungal infections of humans. The pyrimidine analogue 5-fluorocytosine (5-FC) is used against *Candida* spp. and *Cryptococcus neoformans*. 5-FC enters the cell through a permease enzyme and becomes incorporated into the yeast RNA leading to inhibition of protein synthesis (Ghannoum and Rice, 1999). Fungal selectivity is achieved through the prodrug pharmacology of 5-FC, which requires conversion to an active drug once taken up into the fungal cell. Resistance to 5-FC in *C. albicans* is observed in both laboratory and clinical settings and is the result of loss of pyrimidine salvage enzymes and resistance to 5-FC uptake. 5-FC is particularly used as an adjunct (applied to assist the primary treatment) in the treatment of *Candida endocarditis* and central nervous system candidiasis (Ben-Ami, 2018). Despite being a generally successful treatment, potential problems of non-specific toxicity (e.g. bone marrow depression and hepatotoxicity) must be considered before administration (Vermes et al., 2000).

1.3 Current concerns over use of antifungals and fungicides

Regardless of the abovementioned successes and continued need for chemical control of problematic fungi, future reliance upon chemical control is challenged by concerns such as evolving public opinions, tightening regulatory restrictions and the emergence of fungicidal resistance (Sparks et al., 2019).

1.3.1 Changing public opinion

To satisfy the demand of an ever-growing population, predicted to reach 9.7 billion by 2050, improvements in crop protection and stored-food preservation are essential (Nations, 2019). Therefore, extensive effort has been invested in preventing food loss due to disease and spoilage. Nevertheless, public opinion shapes and informs fungal pathogen control, particularly involving crops and produce to be ingested by consumers. The use of genetically modified plants that are better able to resist infection is complicated by public safety concerns. A study in 2019 showed that public opinion was still favoured buying non GM-foods preferentially (Lefebvre et al., 2019). Moreover, in the protection of fresh produce and stored-foods, public opinion is moving toward 'green' consumerism, placing pressure on producers to move away from plastic packaging and to replace chemical preservatives with less toxic alternatives in 'clean label' products (Campêlo et al., 2019). The future of fungal control for foods would appear to rest on the development of successful alternatives to many current fungicides/preservatives alongside educational marketing, to ensure acceptance and acknowledge consumer concerns.

1.3.2 Tightening regulations

As mentioned above, chemical and drug regulations are strict as a consequence of concerns such as non-host toxicity and environmental impacts. An example of this is seen in the restriction of amphotericin B prescriptions, despite previous use as a front-line treatment against *C. albicans*, non-specific effects

upon human cholesterol has limited more widespread use. Amphotericin B can also incur significant nephrotoxicity and in some cases treatment results in extended hospital stays and increased mortality (Bates et al., 2001). There is careful deliberation over the use of pyridine/pyrimidine analogues as antifungals, where they inhibit protein synthesis via competitive incorporation into the fungal nucleic acid (Ghannoum and Rice, 1999). Their invasive and non-specific activity heightens the need for careful administration and, therefore, they are not advised for routine use in the treatment of fungal infections in humans (Ben-Ami, 2018).

Moreover, chemicals used in crop protection and food preservatives are facing growing regulatory pressure. One example is seen in the ban of a multi-site inhibitor, chlorothalonil from usage within the European Union in 2019. Chlorothalonil provides broad-spectrum, contact protection, where large concentrations of the fungicide accumulate within fungal cells to react with thiols and initiate the formation of glutathione-fungicide derivatives, inhibiting thiol-dependent enzymes (Tillman et al., 1973). This activity prevents spore germination and therefore infection. However this high reactivity sparked concerns over toxicity in the surrounding environment, with fears that the compound can interfere with multiple biochemical processes outside of the fungal pathogen, therefore leading to the ban (European Commission, 2019). Similarly, the non-specific toxicity of SDHI fungicides are gaining much research attention and are being experimentally tested using zebrafish as a model organism for (eco)toxicity studies (Strähle et al., 2012). Studies assessing SDHI toxicity have focussed on the acute toxicity, developmental toxicity, long-term toxicity and neurotoxicity of the fungicide (Yanicostas and Soussi-Yanicostas, 2021). A crucial finding from SDHI toxicity studies in zebrafish indicates that adverse effects are initiated at environmentally relevant concentrations, e.g. at 29 nM in the case of the SDHI, boscalid (Qian et al., 2021). These findings add pressure to reduce the use of SDHI fungicides in agricultural settings, which would further limit available control measures.

1.3.3 Fungicide and antifungal resistance

Excessive and/or prolonged over-use of certain drug classes, particularly those that have a single-site mechanism of action (MOA), have exacerbated the development of fungal resistance (Fisher et al., 2018). In addition, wider factors related to the intrinsic nature of the fungus, such as airborne spore dispersal, facilitate the rapid spread of resistance. The spread of airborne spores enables field-to-field transmission of resistance (Torriani et al., 2015). The spread of antifungal resistance through environmental exposure is also observed in the human fungal pathogen *Aspergillus fumigatus*. The human pathogen has acquired azole-resistance through exposure to azole drugs in the environment (Snelders et al., 2009). Fungicide resistance is present against all major drug classes and in multiple fungal pathogens. Despite the mass of research effort that has been dedicated to understanding antifungal/fungicide resistance, our mechanistic understanding is incomplete, such as how certain fungal species are intrinsically resistant or can acquire resistance to multiple drugs with ease (Sanglard, 2016). This section will briefly discuss known resistance mechanisms to some currently used fungicides and antifungals. In Table 1.1 the mechanism of action, cellular impact and suitability of the antifungals and fungicides discussed above are summarised.

Drug Class	Mechanism of Action	Cellular Impact	Suitability
Demethylase inhibitors (DMIs)	Prevent lanosterol to ergosterol conversion (prevent oxidative removal of 14α-methyl group of lanosterol).	Toxic accumulation of lanosterol. Cell membrane composition altered.	Medicine and agriculture. Inexpensive, readily bioavailable and orally administered.
Echinocandins	Inhibit transmembrane glucan synthase complex (Fks1 in *Candida albicans*).	Prevent β-(1,3)-glucan synthesis, disrupt cell integrity, result in cell rupture.	Medicine. Require intravenous administration due to high molecular weight. Three licensed echinocandins.
Polyenes	(1) Binding ergosterol in cell membrane (2) Act as a ergosterol 'sponge' (3) Induce mitochondrial oxidative burst.	(1) Form pores in the membrane, lead to cell leakage (2) Draws ergosterol out of membrane (3) Loss of metabolic activity.	Medicine. Problems of non-specific host toxicity and high production costs.
Analogues	Transported into the fungal cell and incorporates into fungal RNA.	Inhibit protein synthesis in place of uridylic acid or by thymidylate synthetase inhibition.	Medicine. Pro-drug pharmacology reduces host-toxicity but heightens risk of resistance development. Used in combination with other antifungals.
Strobilurins	Inhibit mitochondrial respiration through binding to complex III of the electron transport chain (ETC) (Qo site of cytochrome bc1)	Blocking NADH oxidation leads to prevent ATP synthesis, preventing metabolic activity and promoting cell death.	Agriculture. Widely used due to curative/systemic properties. Single site activity promotes resistance development. Concerns of ecological/human toxicity.
Succinate dehydrogenase inhibitors (SDHIs)	Target the succinate ubiquinone oxidoreductase (SDH) enzyme in complex II of the ETC.	Upon binding this blocks substrate site preventing succinate oxidation and metabolic activity, leading to cell death.	Agriculture. Fastest growing class of fungicide with broad spectrum activity. Concerns of ecological/human toxicity.

Table 1.1. Summary table of key antifungals and fungicide mechanisms of action described in the above text, cellular impact and suitability in medicine and/or agriculture.

1.3.3.1 Demethylase inhibitors

Resistance mechanisms to DMIs have been studied extensively, particularly those conferring azole resistance in key pathogens such as *C. albicans, A. fumigatus* and *Z. tritici*. All pathogens can develop resistance against azole treatment though alterations in the DMI target gene *CYP51* in *A. fumigatus* and *Z. tritici* and *ERG11* in *C. albicans*. Many non-synonymous SNPs have been validated for their involvement in azole-resistance. Alterations within the DMI target gene alter Erg11 protein structure, preventing successful drug binding. Mutations commonly found together in *A. fumigatus CYP51* include tandem repeats (TR) of 46 base pair fragment that is duplicated in the promoter region combined with mutation from a tyrosine to phenylalanine codon at codon position 121 and threonine to alanine at position 289 ($CYP51^{TR46/Y121F/T289A}$) and 34 TR in the promoter region with amino acid substitution of leucine to histidine at position 98 ($CYP51^{TR34/L98H}$) (Chowdhary et al., 2014, Verweij et al., 2016). Many SNPs conferring azole resistance in *C. albicans* have been reported, including hotspots of resistance (at codon positions 105 to 165, 266 to 287, and 405 to 488) that are especially permissive to amino acid substitution (Marichal et al., 1999). Many SNPs leading to single amino acid substitutions have been validated for their contribution to azole resistance (Flowers et al., 2015). Additionally many amino acid alterations in *CYP51* have been identified in *Z. tritici*, such as the valine to alanine substitution at codon position 136 (V136A) which was first identified in 2003 and has now been recorded across most of Europe (Jørgensen et al., 2020).

Alongside mutations in the target site of azoles, resistance mechanisms such as overexpression of the target genes (*ERG11, CYP51*) have been reported in azole-resistant isolates of the described fungal species (Heilmann et al., 2010, Cools et al., 2012, Buied et al., 2013). Overexpression in *A. fumigatus* can be the result of tandem repeated elements either 46 or 34 base pairs within the *CYP51A* promoter region. These TR elements reduce the affinity for promoter binding at the CGAAT binding complex (CBC), which in turn leads to

upregulation of *CYP51A* (Gsaller et al., 2016). Another major source of azole resistance is seen in the upregulation of drug efflux pumps including ATP-binding cassette (ABC) transporters and transporters of the major facilitator superfamily (MFS). Overexpression of these efflux pumps can result in increased drug-efflux activity often accompanied by a multidrug resistance phenotype (Sanglard et al., 1995, Tobin et al., 1997, Slaven et al., 2002, Coste et al., 2004, Omrane et al., 2015). Fortunately, despite growing resistance, DMIs still offer substantial effectiveness in the control of fungal pathogens (Jørgensen et al., 2008, Gao et al., 2018).

1.3.3.2 Echinocandins

Acquired resistance to echinocandins has been observed in all major *Candida* species. Resistance mutations in clinical isolates are mostly observed in single amino acid substitutions within a conserved gene 'hotspot' within *FKS1* and *FKS2,* which encode β-(1,3)-glucan synthase subunits (Ben-Ami, 2018). The echinocandins remain effective for the majority of infections, with *C. glabrata* exhibiting the greatest level of resistance, with resistance in *C. auris* also growing (Healey and Perlin, 2018, Rybak et al., 2022). Mutations in the *FKS* genes are a useful diagnostic to preclude echinocandin treatment failure. Such mutants in *C. albicans* exhibit classical costs of resistance such as a reduced growth rate and reduced fitness (in the absence of echinocandin) alongside echinocandin resistance (Ben-Ami et al., 2011). Moreover, echinocandin-treated *C. albicans* display elevated chitin levels, suggesting a drug-tolerance strategy enabling organism survival and potential time to develop *FKS* mutations (Yang et al., 2017). Less is known about echinocandin resistance mechanisms in *A. fumigatus* due to more limited usage of echinocandins in this case. Some echinocandin-resistant *A. fumigatus* isolates have been identified with mutations in the *FKS1* gene (Jimenez-Ortigosa et al., 2017). A novel mechanism of echinocandin resistance has also been identified in *A. fumigatus*, resulting from stress-induced changes in the lipid microenvironment surrounding the β-(1,3)-glucan synthase. The study

found that exposure to caspofungin induces ROS and cellular stress which triggers alteration to plasma membrane lipids, specifically prominent increases in the abundance of dihydrosphingosine and phytosphingosine surrounding the glucan synthase, rendering it insensitive to echinocandins (Satish et al., 2019). It is predicted that as echinocandin treatment of *Aspergillus* infection is expanding, resistance due to changes in the lipid microenvironment will be more readily observed amongst *A. fumigatus* infections (Satish and Perlin, 2019).

1.3.3.3 Polyenes

Neither primary nor acquired resistance to polyenes, specifically amphotericin B, is readily observed outside of the *Pneumocystis spp*. A study found that resistance development is restricted due to detrimental fitness costs incurred, such as hypersensitivity to oxidative stress and neutrophil killing, therefore resistant mutants cannot survive in the host (Vincent et al., 2013). Acquired resistance is rare and involves a reduction in ergosterol biosynthesis through inactivation of proteins essential for the biosynthesis leading to ergosterol depletion (Sanglard and Odds, 2002). An additional study found that amphotericin B resistant strains harboured *ERG* gene mutations (in *ERG2*, *3*, *5* and *11*) that also conferred resistance to fluconazole (Jensen et al., 2015).

1.3.3.4 Strobilurins

As mentioned earlier, the single-site MOA of the strobilurin class of fungicide has encouraged the rapid development of resistance. Fungal resistance was reported during field trials and then at low frequencies in a wider field setting just two years after the first approval and use of strobilurins (Heaney et al., 2000). Fraaije et al. (2003) correlated a change of glycine to alanine at codon position 143 (G143A) in the mitochondrial cytochrome b gene with QoI resistance in *Z. tritici*. In a follow up study two years later, all QoI-resistant isolates had the A143 allele. This rapid spread of resistance was shown to be

driven by the polycyclic dispersal of asexual conidia (Fraaije et al., 2005). The G143A mutation provides complete resistance against the strobilurins and is now present in over 25 different species of phytopathogenic fungi (Fisher et al., 2020). In addition, the role of airborne ascospores in spreading resistance was assessed, showing resistant alleles can spread up to 85 m within the crop (Fraaije et al., 2005). Both asexual and sexual spores play key roles in the spread of resistance to strobilurins, weakening their practical application in agriculture.

1.3.3.5 Succinate dehydrogenase inhibitors

To prevent or delay SDHI resistance in *Z. tritici*, the Fungicide Resistance Action Committee (FRAC) proposed a preventative strategy of SDHI application with a mixing partner (preferably an azole). The mixing partner must have a different MOA and be sufficient on its own to control the pathogen (Fraaije et al., 2012). Co-formulations of SDHI and DMIs have been practically shown to improve *Z. tritici* control *vs* DMIs applied alone, with the co-formulation also increasing yield (Wieczorek et al., 2015). Despite such measures, the risk of resistance development is still regarded as moderate to high (He et al., 2020). In addition to laboratory studies, SDHI-resistant field isolates have been identified harbouring both target site-specific (SDH subunit mutations) and non-target site specific mutations (overexpression of drug efflux pumps) (Avenot and Michailides, 2010, Kirikyali et al., 2017). SDHI resistance can also be selected from pre-existing genetic variation in SDHI susceptibility that exists within the population, emphasising the importance of agronomic practices and carefully-managed fungicide application to prevent widespread resistance (Yamashita and Fraaije, 2018).

1.4 Fungal control methods outside of antifungals or fungicides

The control of fungal pathogens of humans is improving with better diagnostics, which can assist in deciding treatment strategies. Additionally, in the control of

fungi impacting agriculture, informed agronomical practices, resistance breeding, and biocontrol pose promising options for fungicidal alternatives. In the prevention of fungal spoilage of fresh produce and stored foods, the application of biopreservation and/or electrolysed or ozonated water treatments and coatings/films (potentially incorporating actives that prevent fungal colonisation) represent novel alternatives. These are described in more detail below.

1.4.1 Alternative control methods for human pathogens

Improvements in treatment of invasive fungal diseases (IFDs) rely on early, accurate diagnosis of the pathogen. Therefore improving diagnosis has been one key focus of clinical mycology research (Kozel and Wickes, 2014). Previously IFD diagnosis predominately relied upon traditional methods such as microscopy, histopathology and culturing, which demands personnel with a high-level of mycology-specific training that is further complicated by growth in the range of known pathogenic fungal species (Steinbach et al., 2003).

The improvement in IFD treatment has been supported through the rapid identification of at-risk patients, followed by an earlier, convincing diagnosis. Identification of at-risk patients can be challenging in a clinical environment due to the presence of multiple disease states with diverse displays of symptoms including asymptomatic infections (Formanek and Dilling, 2019). Improvements in IFD diagnosis have rapidly developed with the enhanced accessibility of molecular techniques that enable rapid, sensitive evaluation whilst retaining minimal invasiveness. In the identification of *Aspergillus* and *Candida* species, polymerase chain reaction (PCR) can be utilised, harbouring a multitude of platforms/targets and high accuracy (Clancy and Nguyen, 2013, Lamoth and Calandra, 2017). Furthermore, in the identification of *Aspergillus* species another recent advancement is seen in a recently commercialised point lateral flow device (LFDs) with immunochromatographic assays introduced by LDBio Diagnostics (Lyon, France) for detection of *Aspergillus* species antibodies

(*Aspergillus* IgG-IgM ICT) with > 90 % specificity (Piarroux et al., 2019). Evidently LFDs have proven their worth elsewhere, during the coronavirus pandemic.

Alternative approaches for improving control of IFD include the use of phage therapy. There is emerging evidence of a bacteriophage from *Pseudomonas aeruginosa* with inhibitory activity against both *A. fumigatus* and *C. albicans* and the mechanism of the bacteriophage is likely to involve inhibition of fungal metabolism through iron sequestration (Penner et al., 2016). Clinical evaluation is needed to elucidate the full potential of antifungal phage therapy (Górski et al., 2018, Formanek and Dilling, 2019). Another area of development for the control for IFD is the use of nanoparticles or nanomaterials. Nanoparticles (or nanomaterials) as a potential treatment offer advantages over currently used drug regimens, such as reducing toxicity due to improved target specificity (Kou et al., 2018) and to slow the development of antimicrobial resistance (Morones-Ramirez et al., 2013). Metallic nanoparticles have attracted particular research attention for antifungal control (Leon-Buitimea et al., 2021). One example is silver nanoparticles, which have shown to exhibit inherent inhibitory activity against cases of aspergillosis (Ogar et al., 2015), candidiasis, specifically *C. auris* (Lara et al., 2020), and mucormycosis (George et al., 2011).

A final developing area for IFD control is observed in the discovery of polymers that prevent fungal attachment. As abovementioned, many human fungal pathogens can form biofilms within the host, this can be problematic also upon indwelling medical devices e.g. catheters. Passively preventing attachment and therefore preventing biofilm formation poses a promising strategy to control IFD and slow resistance development (Vallières et al., 2020). Targeting attachment and anti-attachment polymers are discussed further in Chapter 5.

1.4.2 Alternative control methods for plant pathogens

As mentioned above, agronomical practices can help in the control of fungal crop infections. These include crop rotation and avoidance of large

monocultures, particularly in crops that grow in close proximity with the objective of subduing pathogen growth by removing the plant host and implementing soil-tillage. Despite being widely used, current evidence suggests that agronomical practices are less important for the development of fungal infection than monitoring meteorological conditions (which can inform when fungal infection is most likely) (Bankina et al., 2018).

Through recent years there has been extensive research into resistance breeding and genetically modified (GM) crop cultivars that exhibit enhanced ability to fend off fungal pathogens. The need for resistance breeding is exaggerated by a reliance on crop monocultures and poor agronomical practices, which have facilitated the invasion of fungal pathogens (Moscou and van Esse, 2017). Aspects altered in resistance-bred plants can include modification of processes such as pathogen recognition and effectors, defense signalling and regulation, or modification of recessive/susceptible genes (gene expression to remove/alter host factors needed for pathogen infection) and dominant resistance genes (gene overexpression to engineer host resistance) (van Esse et al., 2020). However, the successful introduction of resistant cultivars demands durability in the field (Brown et al., 2015). The partially resistant wheat cultivar 'Altigo' reduces the expression of *Z. tritici* of plant cell wall degrading enzymes and therefore promotes enhanced survival, but the cultivar alone is not completely resistant (Ors et al., 2018). The success of resistant cultivars normally remains dependent on the application of fungicides. There have been several successes in the development of resistance cultivars, but this is clouded by several key challenges (Li et al., 2020). One drawback of GM resistance cultivars is that elevated resistance to disease often negatively influences plant growth, with impacts for crop yields and the demand for more sustainable food production (Ning et al., 2017)

Another strategy for chemical-free crop protection is the use of biocontrol agents. The practical application of biocontrol organisms has been encouraged by the European Union since 2009 in line with advocating the use of non-chemical control (van Lenteren et al., 2017). Biological control can be simply

defined as the use of a living organism to reduce the population of the undesirable organism. There are three general types of biocontrol; natural (ecosystem services), conservation (protection of naturally-occurring pests) and classical (natural enemy release) (Parnell et al., 2016, van Lenteren et al., 2017).

Biological control agents include diverse antagonistic microorganisms such as fungi, bacteria or viruses. Biocontrol of fungal pathogens has been reviewed at length elsewhere, for example Rashad and Moussa (2020). One biocontrol example is the bacterial strain *Bacillus velezensis* LM2303, which exhibits potent antifungal activity. One study showed that this bacterium can be effective in control of several pathogenic fungi, including against the *Fusarium graminearum* agent of fusarium head blight, displaying a control efficiency of 72.3% in a field trial experiment (Chen et al., 2018). Moreover, fungal species themselves are valuable as biocontrol agents, helped by the ease of their mass cultivation and *in vitro* maintenance. For example, application of the fungi *Trichoderma harzianum* and *T. viride* against wheat infection by the fungus *Puccinia graminis* led to considerable reduction in disease, improved wheat growth and yield as well as an enhanced plant defense enzyme production (El-Sharkawy et al., 2018, Rashad and Moussa, 2020). The study attributed the disease reduction to the production of various secondary metabolites with anti-spore germination properties, such as L-lactic acid (El-Sharkawy et al., 2018).

The mechanisms of biocontrol against fungal crop pathogens commonly involve competition for space and nutrients coupled with the synthesis of antifungal substances and secondary metabolites (e.g. lipopeptides, enzymes) (Pal and Gardener, 2006). In addition biocontrol also exerts indirect control benefits such as inducing plant resistance and growth regulators (Shafi et al., 2017, Majewska et al., 2017). Current biocontrol agents do not provide complete control and they are commonly applied in combination with fungicides or additional biocontrol agents (Del Pilar Martinez-Diz et al., 2021). This is because biocontrol agents used in isolation are often poorly effective in the field

environment, which can be for reasons linked to poor formulation or poor timing of the application(s) (Marian and Shimizu, 2019).

A final example of an alternative control strategy to treat plant fungal pathogens is ribonucleic acid (RNA)-based therapeutics. RNA-therapeutics offer several advantages over small molecule inhibitors, including the variety of RNA-species and ability to alter the expression of a targeted gene (Cai et al., 2018). Many phytopathogenic fungi utilise cross-kingdom RNA interference to silence gene expression and weaken the host immune system. However, host plants are also capable of releasing short RNA molecules to silence the pathogens' virulence genes. This phenomenon has been exploited to limit pathogen infection using spray-application of host-induced silencing RNAs onto the host plant. One example of spray-induced silencing using RNAi was described in a study from Koch et al. (2016). The authors sprayed long non-coding double-stranded RNAs (targeting ergosterol biosynthesis) on to barley leaves and this provided protection against *F. graminearum* infection, both in leaves sprayed directly as well as non-sprayed (Koch et al., 2016). Further research is needed to improve the efficiency RNA uptake and action in the pathogen as well as improve stability and cost of production, but this example demonstrates the potential of RNAi-based applications in agriculture.

1.4.3 Alternative control against fungal food spoilage and biodeterioration

For control of fungal food spoilage, bio-preservatives such as lactic acid bacteria (LAB) and antagonistic yeasts have attracted attention because they exhibit inherent inhibitory antifungal activity (described below), importantly, without the synthesis of toxic metabolites. LABs have been used in an array of different foods to control fungal spoilage, including fresh foods, bakery and dairy products.

Antifungal LABs have gained FDA and EU approval for use in food, further supporting their application through satisfying the major concern of product

safety and gaining consumer approval. Permeation with LAB protective mixed cultures successfully extended the 'shelf' life of refrigerated cheese by at least 3 weeks (Schwenninger and Meile, 2004). Moreover, antagonistic yeasts can be incorporated to fruits to control spoilage due to fungi such as *Botrytis cinerea* (Wei et al., 2014). Both LAB and antagonistic yeasts offer a natural method of fungal spoilage control. They may inhibit spoilage fungi by different mechanisms. These include competition for nutrients and space and the production of bacteriocins (LABs) which disrupt the fungal cell membrane or through the synthesis of antifungal hydrolases (antagonistic yeasts) (El Ghaouth et al., 2003, Oliveira et al., 2014, Ribes et al., 2018).

In the protection of fresh and stored foods, chemical sanitisers can offer some alternative to fungicides, e.g. dissolved hypochlorite salts to reduce the fungal load (Kaczmarek et al., 2019). A critical element here is the avoidance of disinfection by-products generated after the application of chemical sanitisers (Tudela et al., 2019, Gil et al., 2019). Two technologies that help with this are the use of electrolysed and ozonated water, with the latter having the least issue with disinfection by-products but a lower efficacy against microbial pathogens (Koseki and Isobe, 2007, Degala et al., 2019, Wohlgemuth et al., 2020).

In the area of microbial biodeterioration one main aim is to preserve quality of the commercial product, particularly during long-term storage. In the control of fungal spoilage of leather, antifungal chemicals and sanitisers are commonly deployed in various steps of leather processing. Despite providing fungal protection this control is costly, labour-intensive and raises concerns regarding environmental safety (Kanagaraj et al., 2020). One potential alternative here is the use of short wave radiation, such as UV irradiation. A study by Jhahan et al. (2022) utilised UV-C light irradiation against vegetable- or chrome-tanned leather and demonstrated that a 60 minute irradiation treatment provided improved protection against *A. flavus* and *A. niger* compared with previously used 15 minute leather irradiation and no irradiation. Importantly, any UV-C treatment should not be directly damaging to the leather itself. Besides more

sector-specific approaches like this for fungal control, some novel approaches are potentially cross-sector (e.g. relevant to human health, agriculture, spoilage, biodeterioration) and so are covered earlier in this chapter.

1.5 Summary and Thesis aims

In summary, fungal pathogens and spoilage fungi continue to pose a detrimental threat to human health, agriculture and food and goods security. In the control of fungal pathogens, there is currently an over-reliance on a small number of antifungal drugs and a dwindling number of fungicides. While there are advances in non-chemical control, there is a growing need to accelerate these and/or develop novel, sustainable control approaches. Furthermore, the development of fungal resistance is evident across all approved agents and the discovery of control methods that may specifically target resistant organisms is of particular interest. Approaches such as improved diagnostics, biocontrol and nanotechnology can help to alleviate the pressure from chemical control. Despite this there are several additional possible areas of development which have not been adequately exploited and which may offer further potential in the area of fungal control.

1.5.1 Aims and Objectives

This thesis addresses the growing problems and concerns facing fungal control. To do this, three different methods of fungal control are explored. These particular approaches are introduced in more detail in the Introductions to the relevant thesis chapters. Specifically, the aims of this thesis are:

1. Employ high-throughput screening to identify novel-acting natural product synergistic combinations with broad-spectrum antifungal activity.

2. Investigate a complex triangle of natural product interactions, to help elucidate and inform bases for understanding antifungal synergies.

3. Use a drug-repurposing approach in investigating non-antifungal drugs that may have selective activity against antifungal (azole)-resistant *Candida albicans*.

4. Explore fungal traits that may be important for anti-attachment properties of materials [(meth)acrylate polymers] that passively resist fungal colonization.

Chapter 2 – Discovery of Natural Products with Antifungal Potential through Combinatorial Synergy

This study was published in April 2022 in: **Augostine and Avery (2022);** ***Frontiers in Microbiology*** (DOI: 10.3389/fmicb.2022.866840) and this Chapter has been embedded as the published manuscript with incorporation of PhD examiner comments .

2.1 Abstract

The growing prevalence of antifungal drug resistance coupled with slow development of new, acceptable drugs and fungicides has raised interest in natural products (NPs) for their therapeutic potential and level of acceptability. However, a number of well-studied NPs are considered promiscuous molecules. In this study, the advantages of drug-drug synergy were exploited for discovery of pairwise NP combinations with potentiated antifungal activity and, potentially, increased target specificity. A rational approach informed by previously known mechanisms of action of selected NPs did not yield novel antifungal synergies. In contrast, a high-throughput screening approach with yeast revealed 34 potential synergies from 800 combinations of a diverse NP library with four selected NPs of interest (eugenol, EUG; β-escin, ESC; curcumin, CUR; berberine hydrochloride, BER).

Dedicated assays validated the most promising synergies, including between EUG + BER, CUR + sclareol and BER + pterostilbene (PTE) [fractional inhibitory concentrations (FIC) indices ≤ 0.5 in all cases], where minimum inhibitory concentrations were reduced to 35 mg L^{-1} (BER) and 7.9 mg L^{-1} (PTE). These three combinations synergistically inhibited a range of fungi, including human or crop pathogens *Candida albicans, Aspergillus fumigatus, Zymoseptoria tritici* and *Botrytis cinerea*. Further investigation indicated roles for mitochondrial membrane depolarization and ROS formation in the synergistic mechanism of EUG + BER action. This study establishes proof-of-principle for utilising high-throughput screening of pairwise NP interactions as a tool to find novel antifungal synergies. Such NP synergies, with potential also for improved specificity, may help in the management of fungal pathogens.

2.2 Introduction

Fungi can have devastating socio-economic impacts through human disease, crop disease and food spoilage (Brown et al., 2012, Almeida et al., 2019, Avery et al., 2019, Fones et al., 2020). As fungi share many conserved cellular functions with potential host eukaryotes (humans, plants), discovery of effective antifungal drugs or fungicides is challenging while resistance is growing to existing agents, accentuating the need for discovery of novel measures for fungal control (Roemer and Krysan, 2014, Fisher et al., 2018). On top of this, tightening of regulations and shifting of public attitudes away from the use of traditional chemical actives calls for different approaches to fungal control. Natural products are one group of compounds which are more acceptable in this landscape (Campêlo et al., 2019, Atanasov et al., 2021).

Natural products (NPs) are increasingly reported in inhibitor discovery programmes. Natural products in cancer and infectious disease therapeutics already form the backbone of > 50% of drugs being used today, either directly or indirectly (Newman and Cragg, 2016, Rodrigues et al., 2016). Antibiotics are a key example of NP use, including where the antibiotic chemical scaffold has been 'copied' from NPs (Wright, 2019). Moreover, the use of NPs in their native form is not to be underestimated considering that they have been molded throughout evolution to provide benefit to producing organisms, possessing underlying properties required for biological activity (Wright, 2019). Furthermore, regulatory hurdles are commonly lower for NPs. For example, in the application of essential-oil (EO) NPs for food preservation, the European Regulation No. 1334/2008 defines EOs and their active components as flavouring preparations and flavouring substances respectively. This allows EOs with these properties or which are natural constituents of the product not to be labelled as a preservative, also satisfying 'clean label' demand of consumers. Nonetheless, each NP should be judged by its own merits (Debonne et al., 2018, Davies et al., 2021). Despite the numerous advantages of NPs, in recent years several NPs have also been designated promiscuous molecules, having

undesirable molecular properties (such as aggregation and membrane perturbation) (Bisson et al., 2016). Related to this, several NPs are very commonly identified as 'hits' in high-throughput screens. These selected NPs have been referred to as pan-assay interference compounds (PAINs) and, in certain cases, invalid metabolic panaceas (IMPs), which are unlikely to progress to lead compounds (Baell and Walters, 2014, Bisson et al., 2016, Baell, 2016). Therefore, enhanced specificity of action is one consideration in discovery of lead NPs of interest.

Another popular strategy for addressing current challenges of disease (e.g. fungal-) control is the use of drug combinations (Tyers and Wright, 2019). One advantage is that resistance to one drug within the combination may be compensated by the second agent, while rapid pathogen removal can theoretically slow resistance development, where additional mutations would be necessary to overcome the combinatorial inhibition (Spitzer et al., 2017, Tyers and Wright, 2019). Pairs of drug activities may produce additive, antagonistic or synergistic interactions. Understanding such interactions is important and the potential risk of antagonism between antifungal drugs, for example, has been highlighted (Thomson et al., 2017). Conversely, with drug-drug synergy, the advantages include the use of lower drug doses for effect, so lowering costs and non-specific toxicity concerns (Spitzer et al., 2017). These types of interaction can be distinguished by determination of fractional inhibitory concentration indices (FICIs) (Hsieh et al., 1993). Combinations of certain non-antifungal agents, such as paromomycin and β-escin, were reported to produce marked antifungal synergy against the human pathogen *Candida albicans*, with up to a 64-fold reduction in minimum inhibitory concentrations (MICs) compared with either agent alone (Vallières et al., 2020). A few synergistic combinations of NPs such as EOs have been described including, for example, a eugenol and thymol combination inhibiting food-borne bacterial pathogens (Liu et al., 2015). Despite the novel activities of interest that have already been uncovered by study of NPs, there remains a diversity of NPs yet to be investigated. In particular, there has yet been very

little work dedicated to discovery of NP-NP synergies. Moreover, the problem of promiscuous activities of some NPs (PAINS, IMPs), discussed above, could potentially be countered with the application of combinational synergy as this should encourage increased potency and specificity (through a common targeted function).

The application of mechanism of action (MOA) knowledge can aid the prediction and discovery of synergistic interactions, as done recently in helping to find novel anti-cancer treatments, for example (Yang et al., 2020). This targeted approach relies on prior knowledge sufficient to enable rational predictions; such as when two agents are known to target similar but not identical processes, which is one basis for synergy (Vallières et al., 2018). On the other hand, the availability of NPs in selective chemical libraries (e.g. libraries which maximise chemical diversity and/or interesting NP activities) facilitates non-targeted screening approaches, including for discovery of lead targets and novel antifungal compounds (Niu and Li, 2019). The use of high-throughput combinatorial screening of chemical-libraries, by combining these with selected compound(s)-of-interest, has recently proved an effective strategy for discovery of novel antifungal synergies (Vallières et al., 2020). The latter study used standard, non-NP chemical libraries and the approach has not previously been exploited to find NP synergies.

Considering the potential importance of NP discovery for healthcare, food and agricultural applications, this study tested the hypothesis that either rational or screening-based approaches could be used to find novel, antifungal synergies between NPs. The rational approach capitalised on prior MOA knowledge for three NPs with cell membrane-targeting actions, while wider interrogation utilised an NP-specific chemical library in combination with selected NPs of interest; eugenol, β-escin, curcumin and berberine. These NPs have previously reported to possess antifungal activity. The study shows the effectiveness of this new screening strategy for finding potent, combinatorial activities among NPs, offering additional tools in the effort to control fungal pathogens.

2.3 Materials and methods

2.3.1 Strains, culture and maintenance

The principal yeast strain backgrounds were *Saccharomyces cerevisiae* W303 (*MAT*a/*MAT*α *leu2-3,112 trp1-1 can1-100 ura3-1 ade2-1 his3-11,15 [phi+]*) and BY4743 (*MAT*a/*MAT*α *his3-1/his3-1 leu2-0/leu2-0 met15-0/MET15 LYS2/lys2-0 ura3-0/ura3-0*). A rho^0 mutant was derived from *S. cerevisiae* BY4743 by sub-culturing three times on YPD agar supplemented with 40 µg ml^{-1} ethidium bromide. It was confirmed that the resultant mutant was defective for respiratory growth by lack of growth on YPG agar (recipe as for YPD agar, below, but with glycerol replacing glucose). The *sod2Δ, ogg1Δ and ccp1Δ* homozygous diploid deletants (obtained from Euroscarf, Germany), were in the BY4743 background. Other yeast species used in this study included *Zygosaccharomyces bailli* strain NCYC1766, *Candida glabrata* BG2, *Candida albicans* SC5314 and an azole-resistant isolate, *C. albicans* J942148, kindly provided by Carol Munro and Donna MacCallum (University of Aberdeen, UK). Yeasts were maintained and grown at 30^{o}C (*S. cerevisiae*) or 37^{o}C (*C. albicans* and *C. glabrata*) in YPD broth [2% peptone (Oxoid, Basingstoke, United Kingdom), 1% yeast extract (Oxoid), 2% D-glucose]. For experimental purposes, the yeasts were streaked onto YPD agar [recipe as for YPD broth but with inclusion of 1.5% agar] from –80^{o}C glycerol stocks and cultured for at least 48 h before single colonies were picked for sub-culture to broth as described below.

Filamentous fungi used in the study were *Aspergillus fumigatus* CBS 144.89 and an azole-resistant isolate *A. fumigatus* 3216 (kindly provided by Matthias Brock, University of Nottingham, UK), *Zymoseptoria tritici* K4418 (kindly provided by Syngenta, UK) and *Botrytis cinerea* SAR109940. The filamentous fungi were routinely maintained and grown either on Aspergillus Complete Medium (ACM) at 37^{o}C for *A. fumigatus,* or Potato Dextrose Agar (PDA, Oxoid) or Potato Dextrose Broth (PDB, Sigma) at room temperature for *Z. tritici* and *B. cinerea* (Vallières et al., 2018). Strains of *A. fumigatus* from –80^{o}C glycerol stocks were grown on PDA slopes for 72 h at 37^{o}C before spores were then harvested for

use in experiments. *Z. tritici* and *B. cinerea* were cultured for 7 days from –80°C glycerol stocks prior to harvesting of pycnidia for experimental use. Where necessary, media were solidified with 1.5% agar (Sigma, UK).

2.3.2 Natural product and antioxidant chemicals

Eugenol, β-escin, curcumin, berberine hydrochloride, sclareol, capsaicin, parthenolide, ellagic acid, glutathione, L-ascorbic acid were from Sigma-Aldrich (UK); osthole and pterostilbene were from Stratech (UK) and mitoquinol from Cayman Chemical Company (UK); all other NPs were components of the Puretitre natural compound library from Caithness Biotechnologies (UK). All except eugenol and parthenolide (70% ethanol), reduced-form glutathione and L-ascorbic acid (dH_2O) were dissolved in dimethyl sulfoxide (DMSO, Sigma UK) and added to growth media from the following stock solutions prepared in those solvents: eugenol, 500 mM; glutathione, 375 mM, L-ascorbic acid, 500 mM; osthole, 200 mM; pterostilbene, 200 mM; β-escin, 50 mM; curcumin, 50 mM; berberine hydrochloride, 200 mM; sclareol, 130 mM; capsaicin, 200 mM; parthenolide, 130 mM; ellagic acid, 33.3 mM, mitoquinol, 2.94 mM. In all experiments, the final solvent was not higher than 3% and a solvent control was always included.

2.3.3 Checkerboard assays and other growth inhibition assays

All culturing and preparation for checkerboard assays adhered to EUCAST guidelines, except for the use of YPD broth, ACM or PDB instead of RPMI as medium (Arendrup et al., 2012). Briefly, for yeasts, overnight cultures in YPD broth, 120 rev. min^{-1}, 30°C or 37°C (see above), derived from single colonies, were diluted in the morning to OD_{600} 0.5 then grown in YPD for an additional four hours, to ensure the yeast cells were in exponential phase of growth, followed by dilution to OD_{600} 0.1 (*S. cerevisiae*) or 0.01 (*Candida* spp.) as used in published literature (Vallières et al., 2020, Vallières et al., 2018), before use as experimental cell suspensions in assays. For filamentous fungi, spores were

inoculated from PDA plates into ACM broth at 10^5 spores ml^{-1} (*A. fumigatus*) or into PDB at 10^4 spores ml^{-1} (*Z. tritici* and *B. cinerea*). Aliquots (50 µl) of these cell or spore suspensions were transferred to flat-bottom 96-well microtiter plates (Greiner Bio-One; Stonehouse UK) with compounds added to specified final concentrations by two-fold serial dilution. The inoculated plates were incubated for 24 h at 30°C for *S. cerevisiae and Z. bailli,* 37°C for *Candida* spp., 48 h at 37°C for *A. fumigatus* and 7-days at room temperature for *Z. tritici* and *B. cinerea.* Subsequently, OD_{600} was determined with a BioTek EL800 microplate spectrophotometer. Fractional inhibitory concentration (FIC) indices were used to assess potential synergy from the checkerboard results, calculated as:

[(Compound 1 MIC in combination) / (Compound 1 MIC alone)] + (Compound 2 MIC in combination) / (Compound 2 MIC alone)] (Hsieh et al., 1993).

FIC index values were considered synergistic at ≤ 0.5, additive between ≥ 0.5 and 1.0, and antagonistic at ≥ 4.0. For continuous growth measurements in the presence of NPs, broth cultures of *S. cerevisiae* were cultivated in 96-well microplates within a BioTek Powerwave XS microplate spectrophotometer, (Vallières et al., 2018) in YP (2% peptone, 1% yeast extract) broth supplemented with either 2% D-glucose, glycerol or ethanol. The growth was monitored from a starting OD_{600} ~0.1 with continuous shaking at 30°C for 24 h, with OD_{600} readings taken every 30 min.

2.3.4 Biofilm inhibition assay

Biofilm metabolic activity was measured using the XTT (tetrazolium salt, 2,3-bis[2-methyloxy-4nitro-5-sulfophenyl]-2H-tetrazolium-5-carboxanilide)
(Sigma, UK) reduction assay and performed as described previously (Vallières et al., 2020). Briefly, overnight *C. albicans* cultures were diluted to OD_{600} ~ 0.01 in RPMI 1640 medium and 100 µl aliquots transferred to 96-well microtiter plates (Greiner Bio-One) and placed at 37 °C. After 2 h non-adherent cells were

removed through washing with PBS, plates were incubated at 37 °C for 24 h in fresh medium. Biofilms were then washed again with PBS and eugenol and berberine added at specified concentrations, with controls without NPs. Cultures were incubated for a further 24 h, then the biofilm was washed and the XTT reaction performed using 210 μg ml^{-1} XTT and 4.2 μM menadione. Biofilm metabolic activity was measured after 2 h incubation at 490 nm using a BioTek El800 microplate spectrophotometer. The assay was performed in biological triplicate.

2.3.5 Establishment of sub-inhibitory concentrations

For initial determination of sub-inhibitory concentrations (SIC) of selected test compounds (for subsequent use in the high throughput screen), experimental cell suspensions of *S. cerevisiae* W303 in YPD were prepared from overnight cultures as described above. Aliquots (50 μl at OD_{600} 0.2) were mixed with 50 μl of YPD containing the relevant NP, from 2X solutions of the test compounds. In all conditions including solvent-matched controls, solvent concentrations were < 1% of the final assay volume. Subsequent growth was measured by OD_{600} determination with a BioTek EL800 microplate spectrophotometer, after 24 h static incubation at 30°C.

2.3.6 High-throughput screening

For high-throughput screens, the four test compounds at their SIC (750 μM eugenol, 12.5 μM β-escin, 350 μM berberine, 50 μM curcumin) were assayed in pairwise combinations against the Puretitre natural compound library (Caithness Biotechnologies, UK), comprising 200 chemicals at 10 mM, dissolved in DMSO. For the screens, aliquots (1 μl) of each library compound were combined with 49 μl YPD and added to 96-well microtiter plates (Greiner Bio-One). Aliquots (50 μl) of yeast cell suspension (prepared as described above) containing one of the four test compounds (added at double the final desired

SIC concentration, see above) were added to the 50 µl library-compound preparations in the microtiter plates. This gave final concentrations of 100 µM of each library compound in 100 µl total per well. Solvent-matched controls at 0.35% DMSO or 0.3% ethanol (70%) were used for control assays without added compounds. Subsequent growth was measured according to OD_{600} determinations with a BioTek EL800 microplate spectrophotometer after 12 h and 24 h static incubation at 30^{o}C. OD_{600} from growth with added compounds was expressed as a percentage of control growth without the compounds. Effect strength [(% growth with library compound) − (% growth with library compound + test compound)] was calculated for each combination; screen 'hits' were considered as those combinations showing an effect strength > 50, as described previously (Vallières et al., 2020). Screens were performed in duplicate.

2.3.7 Mitochondrial-membrane depolarization assay

Depolarization of the mitochondrial membrane in yeast cells was determined according to rhodamine 123 dye retention using a method adapted from previous reports (da Silva et al., 2016a, Alves et al., 2017). After 24 h of exposure to berberine and/or eugenol in checkerboard format, yeast cell suspensions were removed from 96-well plates, spun down in 1.5 ml microcentrifuge tubes at 1,900 x *g* for 3.5 min, then washed with and resuspended in 250 µl phosphate-buffered saline (PBS) before supplementation with a final concentration of 20 µg ml^{-1} rhodamine 123 (Sigma, UK) and incubation for 30 min at 30 °C in the dark. After incubation, cells were washed once with PBS and resuspended in 500 µl PBS then transferred to 5 ml falcon tubes [Becton Dickinson (BD), UK]. A BD FACS Canto A flow cytometer (blue filter; excitation at 488 nm, emission at 530 nm) was used to determine fluorescence intensity of cells. A total of 20,000 cells were evaluated per sample and each condition was assessed in technical triplicate for each independent experiment (n =4). Cellular debris was gated out from the analysis using Kaluza software, where gating was performed to separate the

bulk yeast cell population (gate A), then from (A) doublets were gated out (gate B) followed by median fluorescent intensity quantification using (B). The gating procedure was unchanged for all tested conditions. Median fluorescence intensity (MFI) values for cells treated with NP compounds were transformed to percentages relative to the MFI for minus-compound control cells. “Expected values” for combinations were calculated by multiplication of the two % MFI determinations for the corresponding individual-compound effects; these were compared with experimental values obtained for the combinations, with statistical analysis by paired t-test.

2.3.8 Fluorescent microscopy

Visualisation of *S. cerevisiae* cells was performed after 24 h treatment with the NP EUG+BER combination, rhodamine-123 staining and washing as described above. Cells were resuspended in 50 µl PBS and mounted onto coverslips. A GXML3201LED microscope equipped with a GXCAM controlled by GXCapture software (GX microscopes, Stansfield, UK) was used to collect images using the FITC filter (excitation, 495 nm; emission 519 nm) at X 40 magnification. Images were taken in biological triplicate.

2.3.9 Statistical analysis

The statistics in this thesis were performed using Prism software, using the version 9.5.1.

2.4 Results

2.4.1 Selected natural products with similar mechanisms-of-action did not reveal combinatorial synergies

It was hypothesised that the natural products eugenol (EUG), β-escin and curcumin (CUR) may act synergistically in combination. This was based on their related, reported mechanisms of action: in causing lipid peroxidation and disruption of cell membrane integrity (EUG), pore formation within the cell membrane (β-escin), and interactions with ABC drug transporters and *ERG3* gene downregulation, leading to decreased membrane ergosterol and membrane permeability (CUR) (Morton and Main, 2013, Moghadamtousi et al., 2014, Marchese et al., 2017). Checkerboard assays measuring growth of the model yeast *S. cerevisiae* were used to assess synergy. These showed that pairwise combinations of EUG, β-escin or CUR did not present any synergistic interaction: all three of the fractional inhibitory concentration (FIC) index values for these pairs of NPs were > 0.5 (Figure 2.1). In fact, both the EUG + β-escin and CUR + β-escin combinations exhibited antagonism (with FIC indices ≥2.5). The interaction between EUG and CUR was deemed additive (FIC index, 1.5). These observations were reproduced in two common laboratory strains of *S. cerevisiae,* W303 (Figure 2.1) and BY4743 (Appendix A**,** A.2.). The results did not support the starting hypothesis.

2.4.2 The metabolic microenvironment had no impact on the drug-drug interaction

An organism's microenvironment can be an important determinant of drug-drug interaction, with previous work reporting a shift from antagonism to synergism for certain antibiotic combinations when bacteria were incubated with glycerol or ethanol instead of glucose, reflecting a shift between fermentative and respirative growth (Cokol et al., 2018).

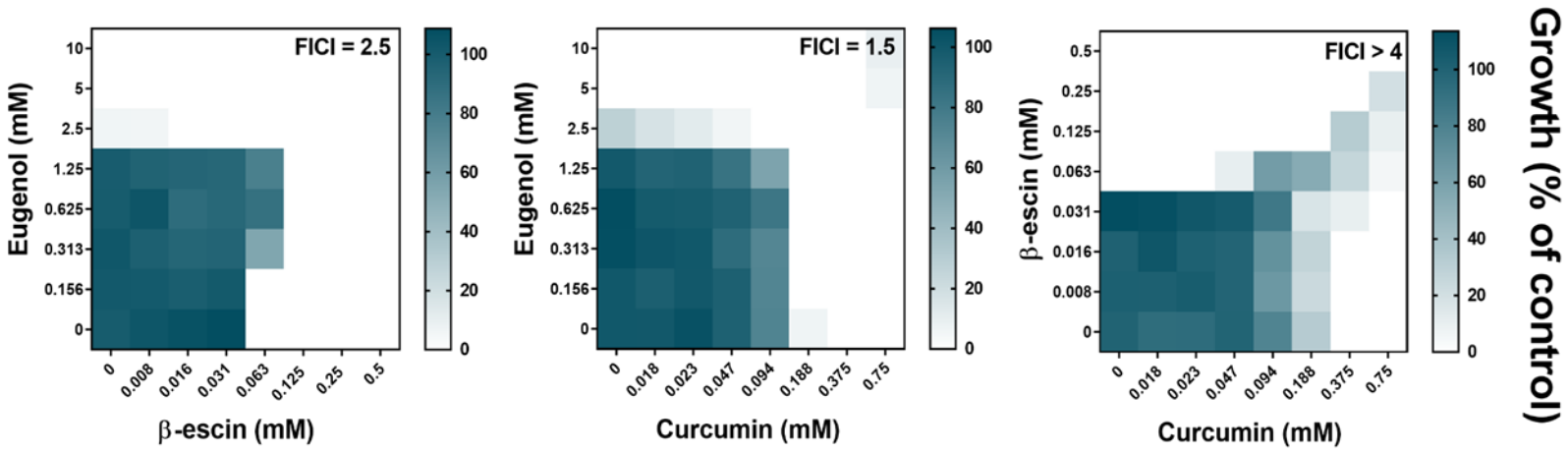

Figure 2.1. Checkerboard assays of combinatorial growth-effects of eugenol, β-escin and curcumin in *S. cerevisiae*. Assays were performed according to EUCAST procedure in YPD broth with *S. cerevisiae* W303 at the indicated concentrations of eugenol, ß-escin and curcumin. Growth values (scale to the right) represent means from three independent experiments, calculated as percentages of growth (OD_{600}) with the NPs relative to the minus-NP control. FICI, fractional inhibitory concentration index, calculated from data after 24 h growth at 30°C; growth values < 5% were assigned as no-growth (Hsieh et al., 1993). Corresponding data for *S. cerevisiae* BY4743 are shown in Appendix A, A.2.

To test for similar effects on the stability of the combinatorial interactions between EUG, β-escin and CUR, these were compared during yeast growth in different carbon sources. These experiments focused on strain W303, as strain BY4743 has defects in regulation of respiratory genes (Hon et al., 2005), affecting growth on respired substrates like glycerol and ethanol. Growth of *S. cerevisiae* W303 was only slightly slower on the respiratory substrates than on glucose, which is fermentable (**Error! Reference source not found.**A). Moreover, the antagonistic and additive combinatorial effects observed in glucose (Figure 2.1), were reproduced in the other carbon sources (**Error! Reference source not found.**B, Appendix A, A.3). The results indicate, for these combinations, that the carbon source and fermentative or respiratory metabolism were not important determinants of these NP-NP interactions.

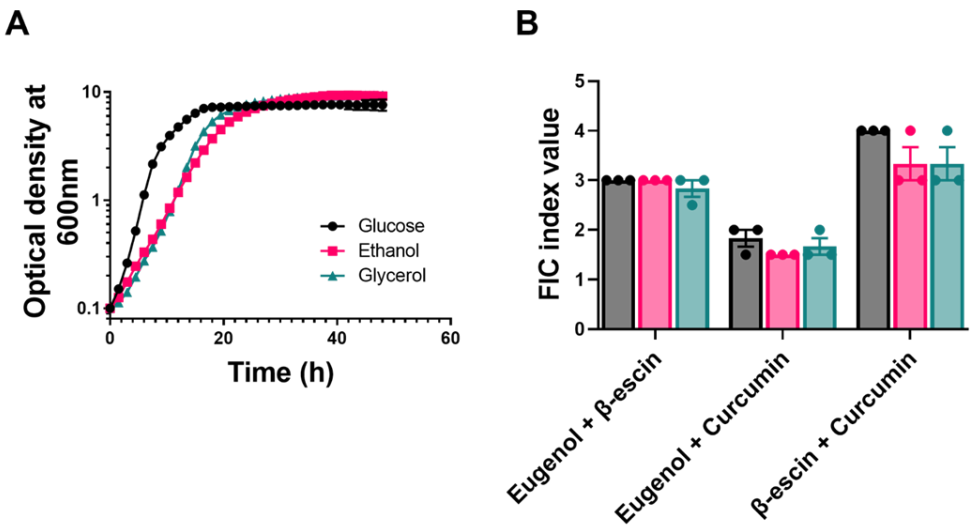

Figure 2.2. Effect of metabolic environment on the stability of combinatorial interactions. (A) Growth curves for *S. cerevisiae* W303 in YEP medium supplemented with either glucose, glycerol or ethanol (all at 2% w/v). Each point represents the mean of three independent experiments ±SEM (error bars did not exceed dimensions of the symbols). (B) *S. cerevisiae* W303 was treated in checkerboard format with combinations of eugenol, ß-escin and curcumin in YEP supplemented with 2% either of glucose (black), glycerol (pink) or ethanol (green). Percentage growth was used to calculate FIC indices. Each bar represents the mean of three independent experiments ±SEM. The corresponding checkerboard data are presented in Appendix A, A.3.

2.4.3 Screen of natural product library in combinations with selected NPs reveals multiple combinatorial antifungal candidates

To widen the net for enabling discovery of novel NP antifungal synergies, the Puretitre NP compound library (http://www.caithnessbiotechnologies.com/puretitre.html) was screened in combinations with the NPs of interest EUG, CUR and β-escin. The Puretitre library was selected as the 200 NP compounds it comprises mostly have described use in traditional medicine, possessing both high bioactivity and relatively low toxicity so enhancing translational potential. An additional screen of the library in combination with the NP berberine (BER) is described, as BER had been identified as a hit compound in an initial screen of the library with EUG (described below), and there are previous reports of antimicrobial BER

actions (Xu et al., 2009, Dhamgaye et al., 2014, Liu et al., 2015). For the combinatorial screening tests, the four selected NPs were supplied at concentrations that were very near sub-inhibitory (~10% reduction of growth yield compared to no-drug control, see Appendix A, A.4), to maximize sensitivity-of-detection of novel synergistic interactions.

The library drugs were supplied at a largely sub-inhibitory concentration (100 µM) suggested by the manufacturer and consistent with similar previous work (Vallières et al., 2020). The screens were performed in *S. cerevisiae* to encourage identification of broad-spectrum antifungal hit combinations. One reason is that pathogens such as *C. albicans* possess an intrinsic decrease in sensitivity to many NPs, which might have caused potential hit combinations to be missed but may still be effective at higher concentrations. In total, screening of 800 different NP combinations in *S. cerevisiae* revealed 34 candidate interactions of interest (Figure 2.3; raw data in Appendix A, A.1): these potential synergies (highlighted in colour, Figure 2.3) were identified according to calculated effect strength > 50 (Vallières et al., 2018, Vallières et al., 2020), from comparison of growth in the presence of each library compound either with or without the second NP (see Methods). The screens with EUG revealed six potentially synergistic interactions and with CUR, 11 hits, while no interactions of interest were found with β-escin (Figure 2.3). As mentioned above, one of the strongest interactions with EUG was with library-compound BER (detailed below) and a subsequent screen of the library in combination with BER suggested 17 potential synergies.

2.4.4 Corroboration of candidate synergies and activity against fungal pathogens

To corroborate synergistic interactions from the most promising screen combinations, checkerboard analysis was performed initially in *S. cerevisiae*. The three combinations with the greatest effect strengths from each of the three screens that indicated synergies were selected (Figure 2.4A). Synergy was

corroborated for all nine of these combinations by checkerboard analysis (Appendix A, A.5.). The most promising checkerboard result for each of eugenol, curcumin and berberine is displayed in Figure 2.4B, with the corresponding library-compound structures found in Appendix A, A.6. The other tested combinations gave FIC index values between 0.25 and ≤ 0.5 (Appendix A, A.5) but were not pursued further in this study.

For eugenol, the EUG + BER combination reduced the MICs for both compounds by up to 8-fold (Figure 2.4B). Checkerboard analysis for CUR with sclareol also indicated strong synergy, with MICs reduced by up to 4- and 8-fold, respectively, while the combination of BER with pterostilbene reduced these agents' MICs by up to 16- and 8-fold respectively.

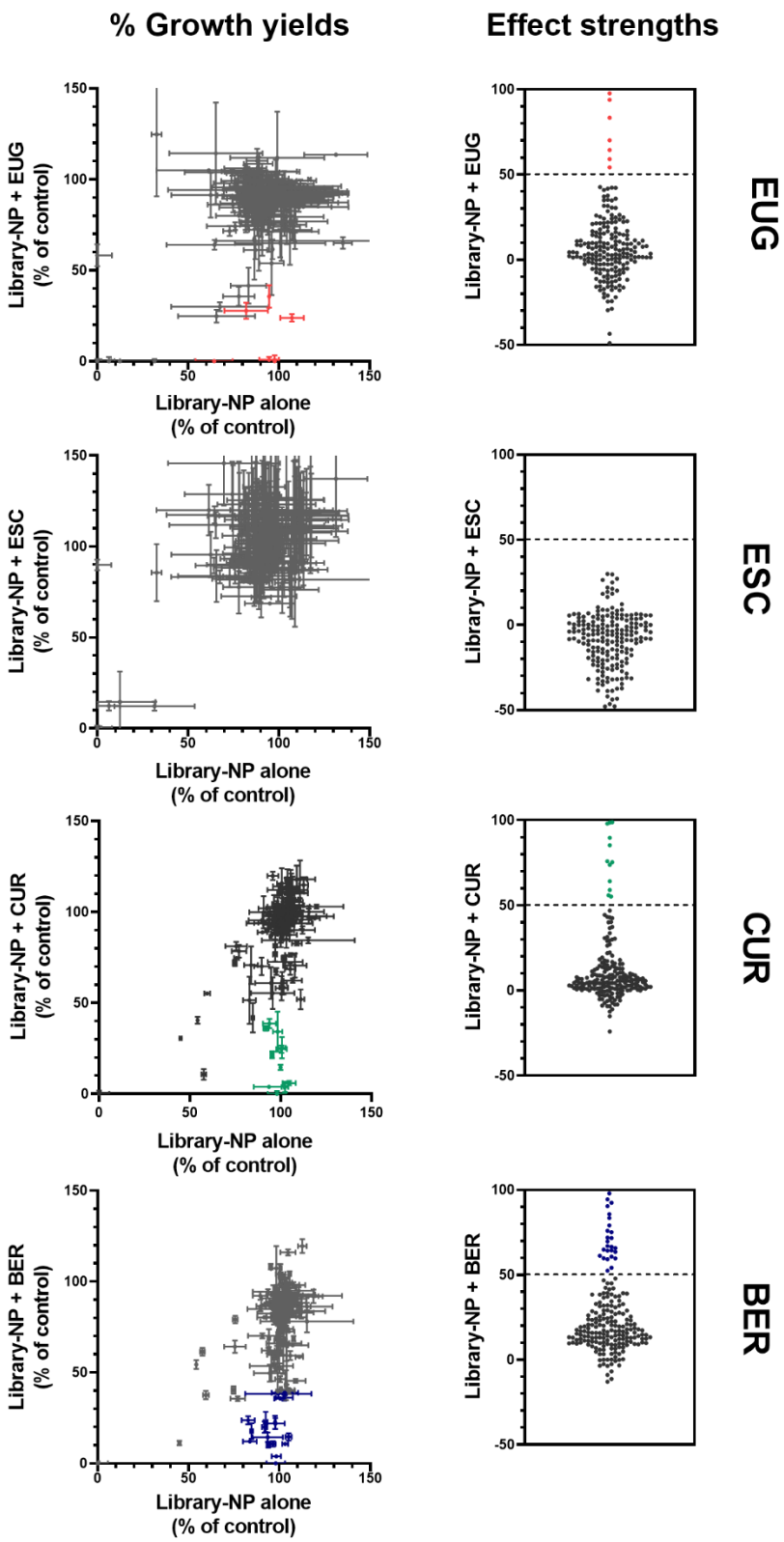
% Growth yields
Effect strengths
Library-NP + EUG (% of control)
Library-NP alone (% of control)
Library-NP + EUG
EUG
Library-NP + ESC (% of control)
Library-NP alone (% of control)
Library-NP + ESC
ESC
Library-NP + CUR (% of control)
Library-NP alone (% of control)
Library-NP + CUR
CUR
Library-NP + BER (% of control)
Library-NP alone (% of control)
Library-NP + BER
BER

Figure 2.3. Screen of library NPs in combinations with selected NPs of interest, against growth of *S. cerevisiae*. Left: normalized growth of S. cerevisiae W303 was calculated from OD_{600} values after 24 h with and without NPs, for each of the library NPs both in the absence (x axis) or presence (y axis) of 750 µM eugenol (EUG), 12.5 µM ß-escin (ESC), 50 µM curcumin (CUR) or 350 µM berberine (BER). Each point represents the mean ± SEM calculated from two independent experiments. Right: effect strengths were determined from [(% growth with library agent) − (% growth with library agent + second agent)] for the different combinations; colour is used to highlight those with an effect strength > 50. The underlying data for each combination from the screen are listed in Appendix A, A.1.

To assess the wider efficacies of the three selected combinations, they were tested against fungi that are either important human pathogens, including drug-resistant isolates (*Candida albicans, C. glabrata, Aspergillus fumigatus*); phytopathogens (*Botrytis cinerea, Zymoseptoria tritici*); or a food spoilage organism (*Zygosaccharomyces bailli*). The combinatorial effects determined from checkerboard analysis with this wider range of fungi revealed synergy in all cases, with FIC index values ranging between 0.19 – 0.5, the lowest values suggesting the strongest synergy was with EUG + BER (Table 2.1). Synergies were also retained in azole-resistant isolates of *C. albicans* and *A. fumigatus.* In addition to this, the activity of the EUG + BER combination against *C. albicans* 24 h -old biofilms was evaluated (Figure 2.5), a significant reduction in the biofilm metabolic activity was observed for the NP combination. This evidence supported our initial use of NP combinatorial screening (with *S. cerevisiae*) to find novel NP synergies that had broad antifungal spectra.

Organism	Eugenol + Berberine	Curcumin + Sclareol	Berberine + Pterostilbene
Candida albicans	0.50[a]	≤ 0.50	≤ 0.38[b]
C. albicans (azole^{R})	0.50	> 0.50	≤ 0.50
C. glabrata	0.19	≤ 0.38	≤ 0.50
Zymoseptoria tritici	0.19	≤ 0.25	≤ 0.38
Botrytis cinerea	0.25	≤ 0.25	0.26
Aspergillus fumigatus	0.25	≤ 0.25	0.50
A. fumigatus (azole^{R})	0.19	≤ 0.50	0.38
Zygosaccharomyces bailli	0.31	≤ 0.50	0.38

Table 2.1. Values for FIC index for selected NP combinations against diverse human-, plant-pathogenic and spoilage fungi.

[a] FIC index values were determined by checkerboard analysis with the indicated fungi .

[b] ≤ symbol indicates that the calculated FICI represents the highest possible FIC value for the combination; as inhibitory concentrations were not achieved at the highest doses used in checkerboards, precluding absolute MIC definition for certain agents when supplied individually.

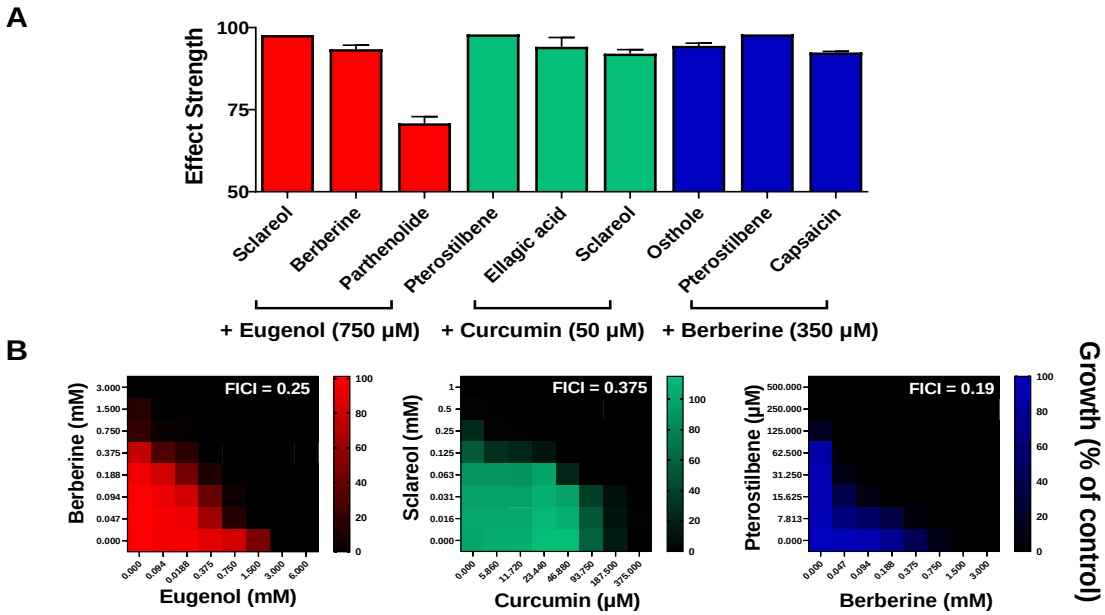

Figure 2.4. Corroboration of synergies in *S. cerevisiae.* (A) Mean effect strengths ± SEM from each screen (Figure 2.3) for selected combinations of interest (n=2). (B) Checkerboard assays of combinatorial growth-effects performed according to EUCAST procedure in YPD broth with *S. cerevisiae* W303 at the indicated concentrations of eugenol, curcumin, berberine, sclareol and pterostilbene. The growth values represent the mean of three independent experiments calculated as percentages of growth (OD_{600}) with the natural products relative to the minus-NP control, after 24 h growth at 30°C. FICI, fractional inhibitory concentration index, calculated from the data and where growth < 5% of the control was assigned as no-growth (Hsieh et al., 1993). Checkerboard data for additional combinations from (A) are presented in Appendix A, A.5.

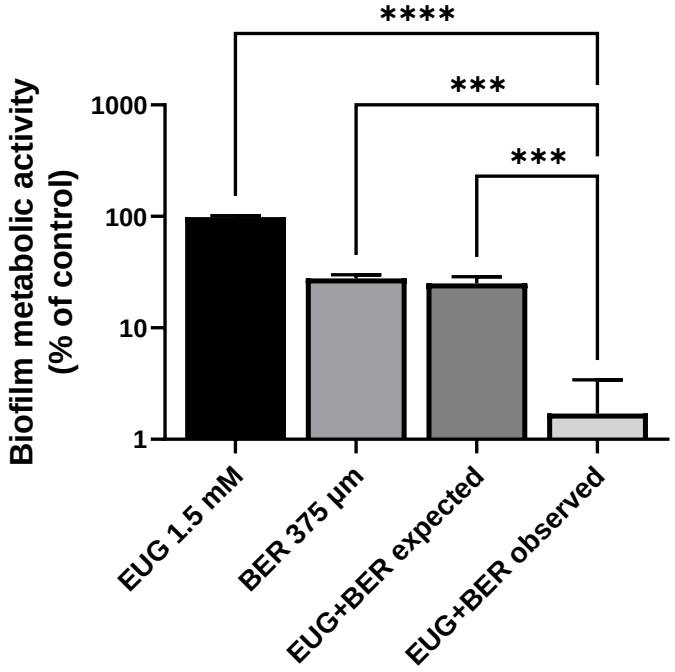

Figure 2.5. *C. albicans* biofilm metabolic activity significantly reduced eugenol and berberine synergy. Activity of EUG + BER was assessed against 24 h old *C. albicans* biofilms, when EUG + BER were added at the specified concentrations and incubated for a further 24 h before assay of metabolic activity by XTT reduction (see Methods). Data are plotted as a percentage of the solvent only (NP-free) control. Values represent means +SEM from three independent experiments: ***, $p < 0.001$; ****, $p < 0.0001$ according to a One-way ANOVA with Dunnett's Multiple Comparison post-hoc test. EUG = eugenol, BER = berberine.

2.4.5 The berberine + eugenol combination causes synergistic depolarization of the mitochondrial membrane

As the BER + EUG combination gave the strongest overall synergy it was chosen for further investigation of mechanism of synergistic action. We hypothesised that the synergy between these agents was centred on mitochondria as a target, as previous studies have indicated that each agent causes mitochondrial perturbation (and associated ROS production) as a mechanism of cell inhibition (Dhamgaye et al., 2014, Alves et al., 2017). Initially, a rho^0 mutant was tested

to assess whether the loss of mitochondrial DNA (mtDNA) could rescue the synergy between BER and EUG. The loss of mitochondrial DNA in the rho^0 mutant has also been used as a tool to study mitochondrial perturbation, to assess the involvement of mitochondrial-nuclear signalling and the impact of using only a fermentable carbon source. Synergy was retained in the rho^0 mutant but was weakened with a FIC index of 0.47 compared with 0.25 in the parental wild type ($p = 0.028$) (Appendix A, A.7.). As the result supported some role for mitochondria in the synergy, we focused next on specific mitochondrial function. Mitochondrial membrane depolarization by both EUG and BER, individually, has been reported previously (da Silva et al., 2016a, Alves et al., 2017). Furthermore, polarity is partly retained in the absence of mtDNA (Appleby et al., 1999, Vowinckel et al., 2021), consistent with the partial-retention of synergy in the rho^0 mutant shown above. Therefore, we probed mitochondrial membrane depolarization (MMD), using flow cytometric analysis of decreased retention of rhodamine 123 fluorescence by cells, at doses of EUG + BER combinations giving approximately 10%, 25% and 50% growth inhibition (Figure 2.6A). Microscopic imaging of the rhodamine-123 stained cells comparing the drug-free and NP combination treatment pointed to a decrease in fluorescence (Figure 2.6B). The flow cytometric data (presented for the intermediate dosage condition in Figure 2.6C) further corroborated that NP alone produced decreases in rhodamine 123 staining. Moreover, the effect was markedly stronger when the NPs were combined.

To indicate whether combinatorial effects on retention of the reporter were additive or synergistic, the data were normalized to median fluorescence as percentages of the no-drug controls (see Methods, 2.3.7). This enabled comparison of the outcome to be 'expected' if the combinatorial effect was additive – calculated by multiplying the two fluorescence-medians (as a % versus control without NP treatment) obtained for each NP individually – with the observed outcome for the combination (Figure 2.7A-B). In all combination concentrations tested (Figure 2.6A), the observed effects were significantly greater than those which would be expected from additive interactions,

suggesting that EUG + BER caused synergistic MMD (Figure 2.7A-B). In additional support of this, the experiment was performed in *C. albicans*, a pathogen of interest (see Appendix A, A.8). The existence of a significant difference between the observed effects which are greater than the expected values (if the interaction was additive) was also reported. As this effect was evident at combination doses including those near sub-inhibitory to growth, it implied that synergistic MMD was not a non-specific consequence of synergistic growth inhibition but consistent with a mechanistic role for MMD in the antifungal synergy between EUG and BER.

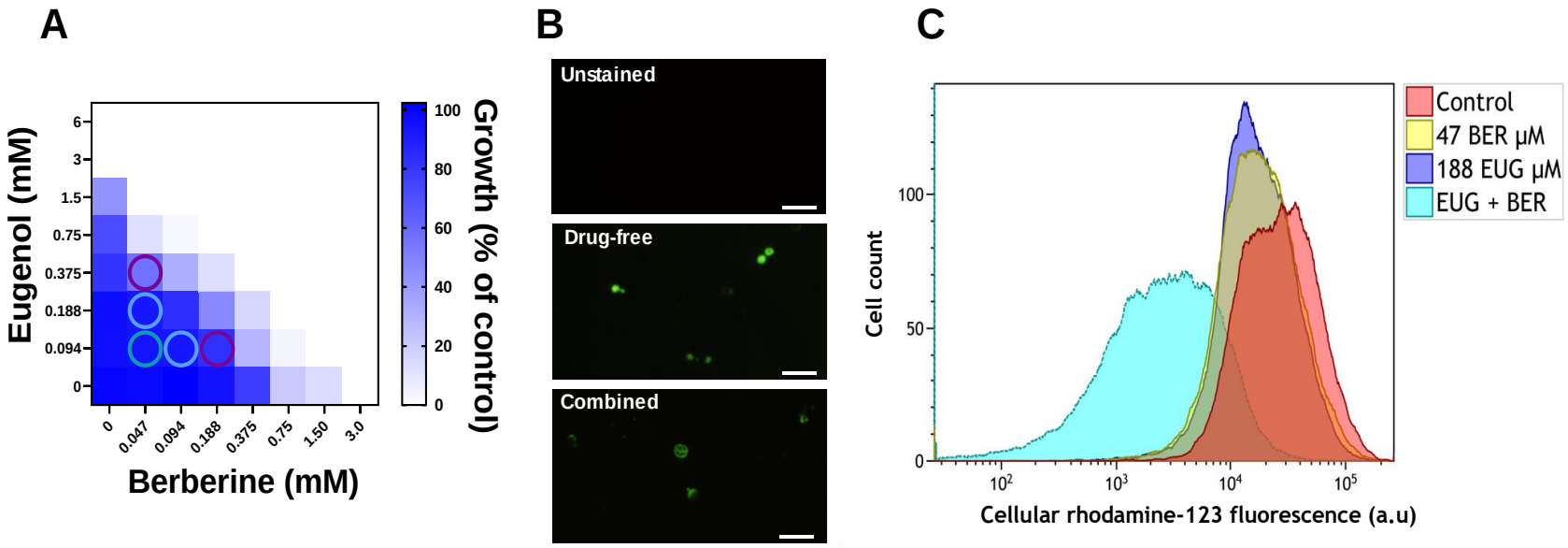

Figure 2.6. Mitochondrial membrane depolarization assessment in eugenol- and berberine-treated yeast cells. (A). Checkerboard assays of combinatorial growth-effects were performed as described in Figures 2.1 and 2.4. Combination concentrations that were subsequently tested for mitochondrial membrane depolarization are circled. (B) Microscopic imaging of *S. cerevisiae* cells treated with or without EUG and BER for 24 h, stained with rhodamine-123. Images were taken using the FITC-filter at x40 magnification, scale bar = 20 µM and the inlet describes the cell treatment. (C) Flow cytometric histograms for cells incubated for 24 h without (control) or with the indicated concentrations of EUG and BER. Cells were then stained with rhodamine 123 before analysis of fluorescence; a.u., arbitrary units.

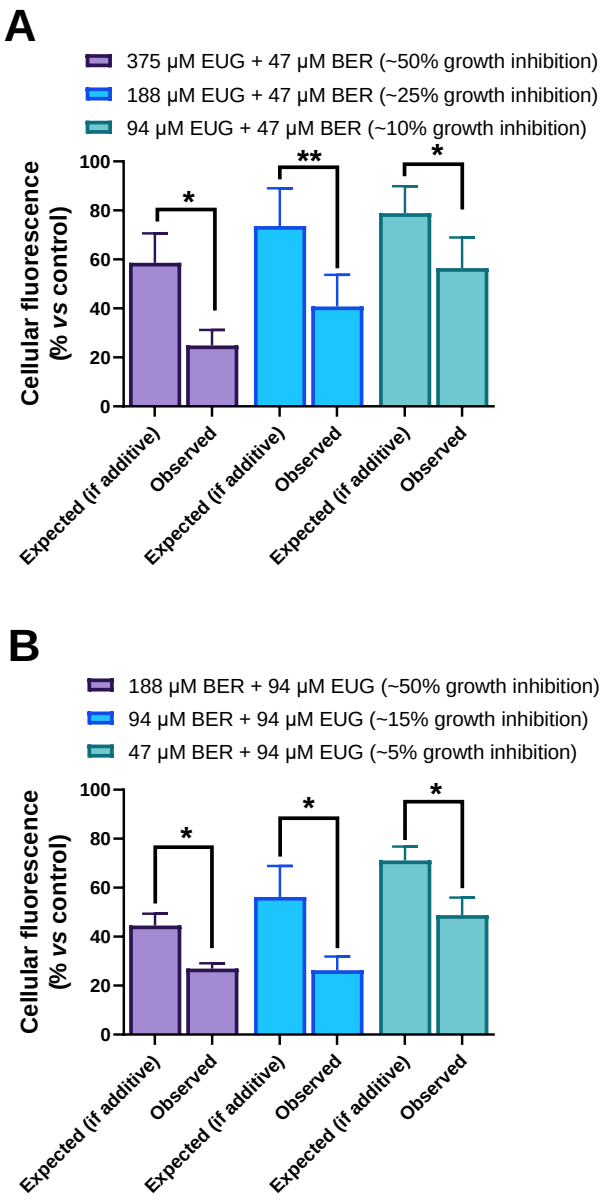

Figure 2.7. Mitochondrial membrane depolarization is significantly increased in eugenol- and berberine-treated yeast cells. (A+B) Observed effects of combinations were obtained experimentally from median fluorescence of rhodamine 123-stained cells exposed to the EUG + BER combination (derived from corresponding flow cytometric data as in Figure 2.6C), normalized to the no drug control (100%). Expected effects were calculated by multiplication of the two % median-fluorescence determinations obtained for the corresponding individual-compound effects. Values represent means +SEM from four independent experiments: *, $p < 0.05$ and **, $p < 0.01$ according to paired t-tests. EUG, Eugenol; BER, Berberine. (A) Changing EUG concentrations. (B) Changing BER concentrations.

2.4.6 Action of mitochondrial ROS in the synergy between eugenol and berberine

To further elucidate the mechanism of EUG + BER synergy, we focused on the reported effects of ROS in the individual actions of both these agents in *S. cerevisiae* (Khan et al., 2011, Dhamgaye et al., 2014). To look into the role of ROS in the NP synergy, we chose to implement a targeted approach using antioxidants with well-known properties and specific gene deletants as opposed to fluorescent-based ROS probes, which are well known to possess non-specific activity (Winterbourn, 2014). First, the effects of added antioxidants on the synergy were evaluated. Both glutathione and L-ascorbic acid significantly increased the FIC index value, beyond the threshold (≤ 0.5) that normally encompasses synergy (Figure 2.8; checkerboard data are shown in Appendix A, A.9). A similar effect was also evident for the mitochondria-targeted antioxidant, mitoquinol, where suppression of synergy appeared to be slightly stronger than for glutathione and L-ascorbic acid. The results supported the hypothesis that ROS are important for establishing the synergy between EUG + BER. These conclusions are made with the assumption the antioxidants were able to reduce intracellular ROS response.

In keeping with the earlier depolarization results for mitochondrial membrane function, and the indication that (mitochondrial) ROS production is important for the synergy, next we focused specifically on the involvement of mitochondrial ROS in the EUG + BER interaction. Deletion mutants defective for three mitochondrial antioxidant functions were tested: *Δsod2* cells lacking the mitochondrial superoxide dismutase that scavenges mitochondrial superoxide; *Δogg1* cells lacking a DNA glycosylase that protects the mitochondrial genome from oxidative damage; and *Δccp1* cells lacking the mitochondrial cytochrome C peroxidase. Checkerboard data is shown in Figure 2.9.

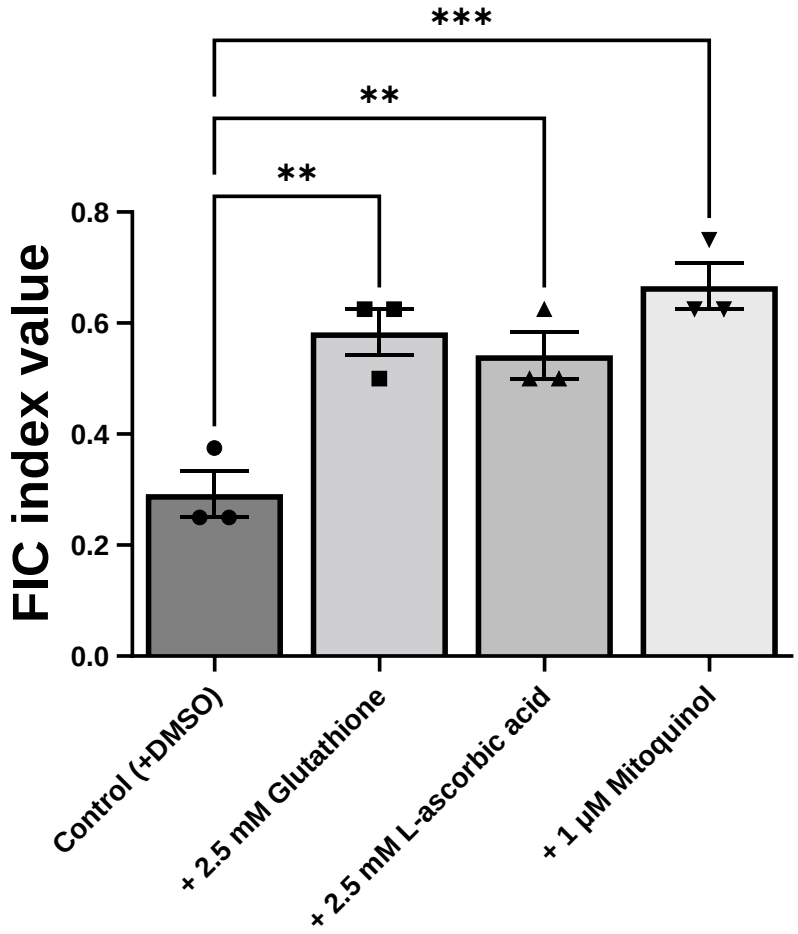

Figure 2.8. Effect of antioxidants on the eugenol plus berberine synergy. Values plotted represent mean FICI values from three independent checkerboard experiments performed with S. cerevisiae W303, as described in Figures 1 and 4, with the inclusion of the antioxidants at the specified concentrations. Bar heights show means ± SEM. **, p <0.01, ***, p < 0.001 and ****, p < 0.0001 according to a One-way ANOVA with Dunnett's Multiple Comparison post-hoc test. The relevant checkerboard data are presented in Appendix A, A.9.

Checkerboard data is shown in Figure 2.9A. The *Δogg1* and *Δccp1* deletants exhibited FIC indices with EUG + BER that were not significantly different to that of the wild type (Figure 2.9B). In contrast, synergy was accentuated in cells defective for Sod2p, reflected by an FIC index in the mutant that was ~50% of that in the wild type (Figure 2.9B). This evidence for partial suppression of the synergy by Sod2p (in wild type cells) further suggests that ROS, more

specifically, mitochondrial superoxide is important for the mechanism of synergistic eugenol–berberine action.

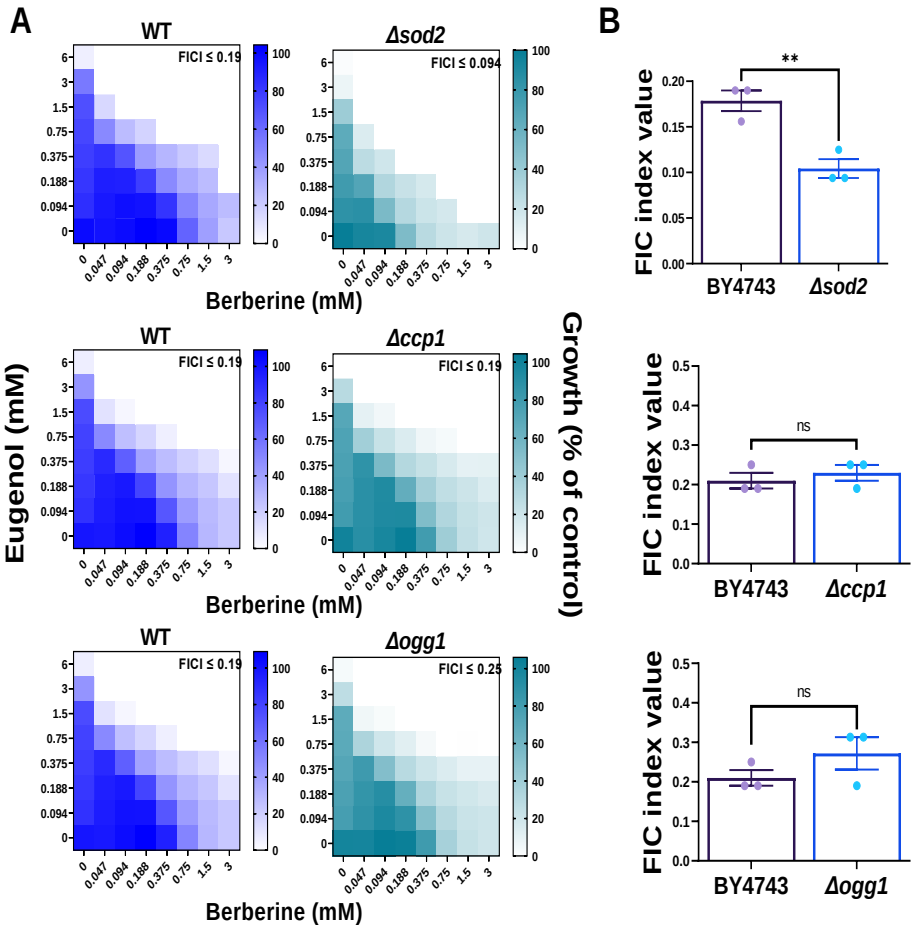

Figure 2.9. Eugenol plus berberine synergy in deletion strains defective for mitochondrial antioxidant proteins. (A) Checkerboard assays of combinatorial growth-effects performed according to EUCAST procedure in YPD broth within *S. cerevisiae* BY4743 (WT) and isogenic deletion mutants *Δsod2*, *Δccp1* and *Δogg1* at the indicated concentrations of eugenol and berberine. The growth values represent the mean of three independent experiments calculated as percentages of growth (OD_{600}) with the natural products relative to the minus-NP control, after 24 h at 30°C. FICI, fractional inhibitory concentration index, calculated from the data and where growth < 5% of the control was assigned as no-growth (Hsieh et al., 1993). (B) FIC indices are plotted from three independent checkerboards experiments, with bar-height showing mean ± SEM. **, p <0.01, unpaired t-test. ns, not significant.

2.5 Discussion

This study highlights the potential value of using NP combinations for fungal control, and how a high-throughput screening approach can enable ready discovery of novel NP synergies. The high-throughput approach proved more successful here for that purpose, compared with a rational approach based on prior mechanism-of-action knowledge. NPs have been the focus of considerable recent attention for finding novel fungal inhibitors, as concern has grown over diminishing treatment options in the face of growing resistance to existing agents (Aldholmi et al., 2019), or toxicity concerns, including environmental. This work identifies several potential lead NP synergies arising from the pairwise NP screening procedure, which display broad-spectrum inhibition of diverse pathogenic or spoilage fungi. This spectrum of fungi suggests potential for the approach to yield effective NP treatment options in crop protection, human health or food preservation; noting of course that each of these presents additional sector-specific hurdles including safety and regulatory.

High-throughput screening of individual NPs has been historically important for identifying novel compounds of interest, including in treatment of cancer, infectious disease, cardiovascular disease and inflammation (Waltenberger et al., 2016, Attiq et al., 2018, Newman and Cragg, 2020). Moreover, certain NPs have been quite well characterised, and this information can feed into the development of selective NP chemical libraries (Wright, 2019). The four compounds chosen here for pairwise screens against the NP library had all been reported previously to exhibit at least some mild antifungal activity. One advantage of combinatorial treatments is in enabling use of lower dosages of both agents – especially when there is synergy – without compromising antifungal efficacy (Vallières et al., 2018). This can be particularly important for NPs, where bioactivity of the NP alone is commonly insufficient, however the impact on host-toxicity must also be considered, particularly if the compounds also target mammalian mitochondria (Atanasov et al., 2021).

Another drawback of NPs is that often little is known about their mechanism of action, although this can of course be addressed with particular NPs of interest that attract research attention. The NPs used in this study were all selected (by us and the NP library compilers) based on available prior knowledge, including on mechanisms of action (MOAs).

This work has highlighted that commonalities in MOA between compounds, such as the reported membrane targeting actions of the three NPs initially examined here, eugenol, β-escin and curcumin, does not assure synergies when applied in combinations and can even produce antagonism between them. These combinations were also not influenced by the carbon source, being stable across respiratory and fermentative growth conditions. Nevertheless, prior knowledge is an advantage for elucidating MOAs underlying any novel synergies between NP pairs, as done here in substantiating that the production of ROS and mitochondrial-membrane depolarization appear to be important for the eugenol/berberine antifungal synergy. It is important to note that such modes of synergistic action are not necessarily the same as the primary, individual-agent MOAs, considering that synergy involves a gain of (inhibitory) activity (Vallières et al., 2020). The gain of inhibitory action during synergy may be important for countering the challenge of promiscuous activities, associated with many studied NPs (Baell, 2016). This gain of action adds specificity, as synergy typically centres on a common target of the individual agents. For potential translational applications, it is important to guard against promiscuity of action in routine NP-screening studies (Baell, 2016, Bisson et al., 2016). The exploitation of synergy offers a route to help address that.

2.5.1 Synergistic mechanism of action

Among the 34 candidate synergies identified here from 800 interactions tested, nine were chosen for validation and from these, three were taken further for additional investigation. It is encouraging that only a limited number of candidates were identified from the screen, as it supports the notion that assay

for synergy should restrict the scope for promiscuity compared with individual-NP activities. The BER + pterostilbene (PTE) combination produced up to 16-fold (BER) and 8-fold (PTE) reductions in MICs for inhibition of *S. cerevisiae* and the synergy was retained against fungal pathogens. Individually, BER and PTE have previously-reported activities against *C. albicans*, with reported MOAs linked to the Ras/cyclic AMP pathway (PTE) or membrane damage (BER) (Li et al., 2014, da Silva et al., 2016a). The CUR + SCL combination gave similar synergistic potency and spectrum as BER + PTE. Previously, CUR has been shown to downregulate the *ERG3* gene leading to decreased plasma-membrane ergosterol and accumulation of inhibitory precursors in ergosterol biosynthesis, ROS and cell death (Sharma et al., 2012). For SCL, previous literature has reported the NP to induce uncoupling of mitochondrial oxidative phosphorylation in *B. cinerea* (Mendoza et al., 2015). Accordingly, one possible explanation for the observed synergy could be centred on an interaction at the mitochondria between the uncoupling, membrane perturbation and/or ROS actions of the two drugs. Synergy commonly arises between agents that perturb a common process, potentially through a different molecular target (Vallières et al., 2018).

To test a synergistic MOA experimentally, here we concentrated on EUG + BER as this combination gave the lowest FIC index value (strongest synergy) against several of the fungal pathogens tested. Knowledge of previous indications of commonalities in fungus-inhibitory actions of EUG and BER (He et al., 2007, Das et al., 2016, Darvishi et al., 2013, Marchese et al., 2017, Dhamgaye et al., 2014, da Silva et al., 2016a) informed the consequent demonstration that the combined agents provoked a synergistic depolarization of the mitochondrial membrane, that the synergy is significantly suppressed by the addition of antioxidants and that the synergy was accentuated in cells defective for Sod2-mediated mitochondrial ROS scavenging. The focus of this study was on the mechanistic activity of the NPs themselves, future mechanistic elucidation could also investigate the synergistic role of ROS on each NP, through for example, combination of the NPs with agents known to produce ROS, such as

hydrogen peroxide. Taking this evidence together, a model for the synergistic MOA can be proposed whereby synergistic depolarization of the mitochondrial membrane potential is associated with mitochondrial dysfunction and increased mitochondrial ROS production, culminating in accentuated cellular stress and growth inhibition that is greater than a sum of the individual-NP effects.

2.5.2 Potential synergistic applications

Concerning the potential for application, one consideration is cost. Berberine and eugenol, for example, are relatively inexpensive. These are purchasable from research suppliers for less than ~10 USD per gram, whereas the equivalent pricing for the common antifungal drug amphotericin B is ~1,000 USD per gram. Regarding safety, eugenol is already used in pharmaceutical products (commonly as a local antiseptic and analgesic), as a food preservative, in agriculture (pest control) and in cosmetics and can be adminstered at 2.5 mg/kg of body weight per day in humans (FAO/WHO, 1982, Ulanowska and Olas, 2021). Similarly, numerous studies have supported the application of berberine for therapeutic purposes in humans in relation to different conditions (diabetes, anti-cancer, anti-inflammation, antioxidant and cardiovascular effects), including absorption and toxicity properties (Neag et al., 2018, Song et al., 2020). Clinical trials using berberine have used dosing at between 1–2 grams per day, a level that was deemed safe for a period of at least 6 months (Zeng et al., 2003). In the present study, the effective concentrations of these particular agents in combination were up to a maximum of 279 mg L^{-1} BER and 123 mg L^{-1} EUG (calculated from the most resistant pathogen tested, *Candida albicans*, using the average adult weight of 70 kg; 70 x 2.5 = 175 mg L^{-1} as maximum dosage). However, it is important to highlight that the effective concentrations could be quite different *in vivo* or with synergistic combinations of more-potent NPs. Accordingly, before any possible commercial or clinical use of novel drug combinations, dosaging needs to be evaluated *in-vivo* as a further criterion alongside registration and other regulatory hurdles. For the purposes

of the present study, the focus was primarily on establishing proof-of-principle, i.e. the demonstration of scope for *in-vitro* discovery of antifungal synergies among NP combinations.

Importantly, the lead combinations from this study synergistically inhibited a range of important pathogenic and spoilage ascomycete fungi, including activity against *C. albicans* biofilms (EUG + BER). This also included azole resistant isolates of *C. albicans* and *A. fumigatus*, suggesting additional potential relevance for the clinical setting where azoles are key drugs for treating invasive infection (Ben-Ami, 2018, Jenks and Hoenigl, 2018). Both NPs have also shown synergistic interactions with fluconazole against azole-resistant *C. albicans* (Quan et al., 2006, Ahmad et al., 2010a).

These previous studies exaggerate the potential of this lead combination, where future work would evaluate the synergistic activity of these NPs in combination with fluconazole as an additional potential clinical benefit. Additional future work from this study would also seek to evaluate the activity of the lead synergistic combinations against the emerging fungal pathogen, *C. auris*, for which we are awaiting arrival. Despite its potential, the strategy of using synergistic combinations must be carefully monitored and controlled, as resistance development to one agent is likely to abolish pathogen inhibition, given that the second compound may be supplied at too low a concentration to exert inhibition (Davies et al., 2021). Nevertheless, the limited range of effective drugs available for control of fungal pathogens emphasises the desirability of effective alternative options, such as that offered by combinatorial synergy. By showing that this principle can be extended successfully to NPs, this study promises a potential treasure-trove of novel synergistic interactions ripe for discovery among the diverse plant extracts and other NP sources and libraries available worldwide, beyond the potential combinations of interest revealed here.

Chapter 3 – Elucidation of Natural Product Interactions Through a Targeted Mechanism of Action Approach

3.1 Introduction

3.1.1 Developing mechanistic understanding of drug-drug interactions

A drug's mechanism of action (MOA) commonly defines the activation or inhibition of a specific biochemical event, often associated with an enzymatic process (Pritchard et al., 2013). Developing an understanding of a drug's MOA is important for its appropriate use in a clinical or agricultural setting, particularly in antifungal drug development due to the small number of available drugs (Roemer and Krysan, 2014). With combinations of different drugs, it is possible that synergism, antagonism, or no interaction can be observed (Odds, 2003). Combination therapies (or drug 'cocktails') have been a key part of successful treatment of certain complex diseases including infectious diseases and cancer (Crystal et al., 2014, Zheng et al., 2018). One strategy for the discovery of combinatorial therapies is seen in the use of systematic high-throughput testing of pairwise combinations; this strategy was used in Chapter 2 to identify promising natural product combinations (Augostine and Avery, 2022).

Despite continuing development of the understanding single-drug MOAs, there has been less attention on understanding the mechanistic detail governing drug-combination inhibitory actions (Cheng et al., 2019). Moreover, understanding the molecular mechanisms behind existing drug combinations can also assist in the discovery of new drug combinations (Yeh et al., 2006, Jia et al., 2009). Considerable research effort has focused on how drug-drug interactions can be best studied, including how they can be predicted. One example of this is seen in a study by Cheng et al (2019), where a mathematical, network-based approach was employed to describe

relationships between drug targets and disease-related proteins (from the human protein-protein interactome). One of the study's key findings was that, for each drug of a combination, the two drug-targets must not only overlap with the disease module (localised 'neighbourhoods' of disease proteins) but also be separated in the human interactome without overlapping toxicities i.e. target separate distinct 'neighbourhoods' (Cheng et al., 2019). This was unexpected as it indicates that drugs with different actions are predicted to act efficaciously in combination, whereas it might have been expected that overlapping actions, and therefore a combined effect on a given target could be more effective.

3.1.2 Studying combinations of more than two agents

The study by Cheng et al (2019) emphasized the complexity of characterising drug-combination MOAs. As discussed in Chapter 2, unexpected interactions between drugs were also noted among agents that were combined based on related actions. Moreover, in the high-throughput screening process, multiple synergistic interactions were identified and tested in several pathogens, with common compounds found in multiple synergistic combinations (Chapter 2). Combinatorial synergy can potentially arise from several types of interaction.

Anti-counteractive interactions can arise when drug-drug synergy occurs where the combinations act at different molecular targets (Jia et al., 2009). One example is seen in the synergistic effect of epigallocatechin gallate (EG, which disrupts cell wall integrity) and DL-cycloserine (CY, which inhibits cell wall synthesis) on the cell wall of *Staphylococcus aureus,* whereby EG's disruption of cell wall integrity is enhanced by CY's prevention of counter-active cell wall synthesis (Zhao et al., 2001). A second type of interaction involves complementary actions; where synergy is primarily the combined product of a positive regulation of the same pathway, or of different but related pathways that regulate the same target (Jia et al., 2009). One example is seen in the synergistic enhancement of tubulin acetylation by paclitaxel (stabilises

microtubules via acetylation) when in combination with tubacin (inhibits microtubule-associated deacetylase activity). The drugs complement each other by affecting different targets of the same pathway (Marcus et al., 2005). Finally, synergy could also be the result of facilitating actions, where the target of one drug promotes the activity (e.g., through increasing bioavailability) of the second drug (Jia et al., 2009). One example is seen in the antibacterial combination of gentamicin and vancomycin, where gentamicin penetration into the bacterial cell is enhanced through vancomycin's effect on peptidoglycan synthesis in the cell wall (Cottagnoud et al., 2003).

In the screening experiment discussed in Chapter 2, many different combination interactions were identified. From this data, three NPs were chosen for further investigation: eugenol (EUG), an essential oil isolated from clove oil (Zheng et al., 1992); curcumin (CUR), a polyphenol from the Indian spice turmeric (Ruby et al., 1995); sclareol (SCL), a plant-derived diterpene found in clary sage (Frija et al., 2011). This interaction between these NPs was chosen to form the premise for additional mechanistic investigation.

The inhibitory activity of EUG has been well-studied in bacteria and fungi. As mentioned in Chapter 2, EUG is able to depolarize the mitochondrial cell membrane, outside of this EUG activity has been linked to lipid peroxidation of the cell membrane (Braga et al., 2007), production of intracellular ROS (Das et al., 2016), disruption to ion and ATP transport (Ahmad et al., 2010b) and bacterial enzyme inhibition (Gill and Holley, 2006). These mechanisms cumulate in alterations to membrane permeability, and downstream consequences lead to cell death.

For CUR, the biological activity of the NP has been extensively researched for various clinical implementations and has been shown to have anti-tumour and antioxidant properties (Prasad et al., 2014). The antimicrobial activity of CUR has been well-studied (Moghadamtousi et al., 2014). Several studies have shown the NP to exert inhibitory activity in many areas including; iron chelation (Jiao et al., 2006), production of ROS (Sharma et al., 2010), modulation of ATP-binding cassette efflux pumps (Sharma et al., 2009) and depletion of ergosterol

through *ERG3* downregulation (Sharma et al., 2012). Despite the many studies that emphasise the potential of CUR, it has to be noted, as discussed in Chapter 2, CUR is classified as a pan-assay interference compound (PAIN) where *in vitro* results do not often translate into successful *in vivo* results, due to problems of promiscuous activity. One strategy to circumvent this problem, focused on in Chapter 2, is proposed through the use of synergistic combinations or alternatively where CUR can be used to enhance existing antifungal treatments.

Finally in the inhibitory activity of SCL, the NP has been shown to exhibit anti-cancer (Wang et al., 2015) and anti-inflammatory properties (Hsieh et al., 2017). More specifically in SCL antimicrobial activity, it has been shown to uncouple oxidative phosphorylation (Mendoza et al., 2015) and inhibit quorum-sensing through potential prevention of the upregulation of accessory gene regulator-regulated genes in *Staphylococcus aureus* (Iobbi et al., 2021). These three NPs share promise as a potential treatment against microbial pathogens.

3.1.3 Chapter Aims

This chapter aims to develop mechanistic understanding of natural product combinatorial actions using a 'triangle' interaction consisting of synergy and no interaction. Each of the three NPs within the triangle is supported by existing literature focused on their mechanisms of action in different microorganisms, so providing an ideal model for the present aim. The chapter will also concentrate upon the basis by which the compound that synergises with both other compounds in the 'triangle' (sclareol) promotes such synergy and whether this extends to a more diverse range of other antifungals. Understanding of multi-NP interactions is important as these compounds are commonly produced in mixes naturally (e.g. in plant exudates) and single-compound studies do not capture this.

3.2 Materials and methods

3.2.1 Strains, culture, and maintenance

The study utilised strains of *Saccharomyces cerevisiae* throughout. The principal strains used were W303 (*MATa/MATα leu2-3,112 trp1-1 can1-100 ura3-1 ade2-1 his3-11,15 [phi+]*) and BY4743 (*MAT*a*/MAT*α *his3-1/his3-1 leu2-0/leu2-0 met15-0/MET15 LYS2/lys2-0 ura3-0/ura3-0*). The *erg2-5Δ* homozygous diploid deletants (obtained from Euroscarf, Germany) were in the BY4743 background and phenotyping was performed by comparison with the BY4743 strain. Yeasts were maintained and grown at 30^{o}C in YPD [2% peptone (Oxoid, Basingstoke, United Kingdom), 1% yeast extract (Oxoid), 2% D-glucose]. For experimental purposes, the yeasts were streaked onto YPD agar [recipe as for YPD broth but with inclusion of 1.5% agar] from -80^{o}C glycerol stocks and cultured for at least 48 h before single colonies were picked for sub-culture to broth as described below.

3.2.2 Chemicals

All the compounds used in this study were purchased from Sigma Aldrich (UK) and are listed in Table 3.1 with the solvent and stock concentrations used.

3.2.3 Checkerboard assays

All checkerboard assays were performed as described in Chapter 2, 2.3.3. As in Chapter Two, fractional inhibitory concentration (FIC) index values were considered synergistic at ≤ 0.5, additive between ≥ 0.5 and 1.0, and antagonistic at ≥ 4.0. In experiments where the interaction of three compounds was explored, two compounds were prepared in two-fold dilution series and added to the 96-well plate (25 µl aliquots added per well), the third compound was prepared at a single concentration and added to all wells of interest (25 µl per well). In these experiments the two compounds prepared at two-fold serial dilutions and the third single compound concentration were prepared at X 4

the desired final concentration to account for the dilution within the plate. In all experiments, the control condition contained the same amount of solvent to control for any effect of solvent. The plates were inoculated with 25 µl of cells at OD_{600} 0.4 (final OD_{600} within the well 0.1, accounting for in-plate dilution). The plates with a total volume of 100 µl were then incubated statically for 24 h at 30°C. Subsequently, OD_{600} was determined with a BioTek EL800 microplate spectrophotometer. Fractional inhibitory concentration (FIC) indices were used to assess potential synergy from the checkerboard results (both with and without the third compound), according to: [(Compound 1 MIC in combination) / (Compound 1 MIC alone)] + (Compound 2 MIC in combination) / (Compound 2 MIC alone)] (Hsieh et al., 1993).

Compound	Solvent	Stock concentration
Eugenol	70% Ethanol or DMSO	500 mM
Curcumin	DMSO	50 mM
Sclareol	DMSO	130 mM
CCCP	DMSO	100 mM
α-Tocopherol	DMSO	136 mg ml^{-1}
Cadmium nitrate	DMSO	31.2 mM
Tebuconazole	DMSO	1.78 mg ml^{-1}
Amphotericin B	DMSO	2.5 mg ml^{-1}
Caspofungin	DMSO	100 µg ml^{-1}
Antimycin A	DMSO	4 mM

Table 3.1. Test compounds and chemical stock concentrations used in this study.

3.2.4 Uptake assay using Rhodamine 6G (R6G)

Checkerboard assays with *S. cerevisiae* were performed as described above and after 24 h incubation specific treatments from the checkerboard were sampled for R6G uptake analysis. This method was adapted from Maeski et al. (1998) and Revie et al. (2022). The samples (100 µl) from the 96-well plate were transferred to 1.5 ml microcentrifuge tubes and centrifuged for 3.5 min at 1900 *g*. Samples were resuspended in 250 µl phosphate-buffered saline (PBS) and R6G (Sigma-Aldrich, UK) was added at a final concentration of 10 µM. Samples were incubated for 30 min at 30^{o}C then washed twice with PBS after centrifugation for 3.5 min at 1900 *g*. Samples were resuspended in 500 µl PBS, transferred to 5 ml falcon tubes [Becton Dickinson, (BD), UK) and kept on ice before use in flow cytometry. The ID7000 Spectral Cell Analyzer (Sony Biotechnology) was used with a FITC filter (excitation at 488 nm, emission at 530 nm) to determine median fluorescence intensity. Data analysis was carried out using Kaluza software, where gating was performed to separate the bulk yeast cell population (gate A), then from (A) doublets were gated out (gate B) followed by median fluorescent intensity quantification using (B). The gating procedure was unchanged for all conditions.

3.2.5 Statistical analysis

The statistical analyses in this chapter were performed as in Chapter Two, using Prism version 9.5.1.

3.3 Results

3.3.1 Triangle of interactions with sclareol, curcumin and eugenol

As discussed in the introduction, the rationale-based and high-throughput screening explored many synergistic combinations. A closer investigation saw that in the three NPs, eugenol, curcumin and sclareol there was a triangle of interactions, where synergy was observed in two of the possible pairwise NP combinations but in not the third. The initial findings are summarised in Figure 3.1, where checkerboard assays and calculation of fractional inhibitory concentration index (FICI) values using the thresholds of FIC index values ≤ 0.5 considered synergistic, additive between ≥ 0.5 and 1.0, and antagonistic at ≥ 4.0, indicated that either eugenol or curcumin combined with sclareol produced a synergistic interaction (FICI ≤ 0.5), but not eugenol and curcumin in combination (FICI ~ 1.5) (Figure 3.1).

As discussed in the introduction there are several reported mechanisms of actions for the NPs selected. For sclareol the role of uncouple oxidative phosphorylation will be tested (Mendoza et al., 2015). In the case of curcumin, the role of *ERG3* downregulation within the ergosterol biosynthesis pathway, leading to disruption of ergosterol synthesis and consequently increased membrane permeability will be explored (Sharma et al., 2009). Finally for eugenol, again several MOAs have been researched, including induction of lipid peroxidation (Khan et al., 2011). These MOA were chosen in attempts to underpin the mechanistic reasoning for the 'triangle' of interactions between these NPs, these MOA are schematically shown in Figure 3.2.

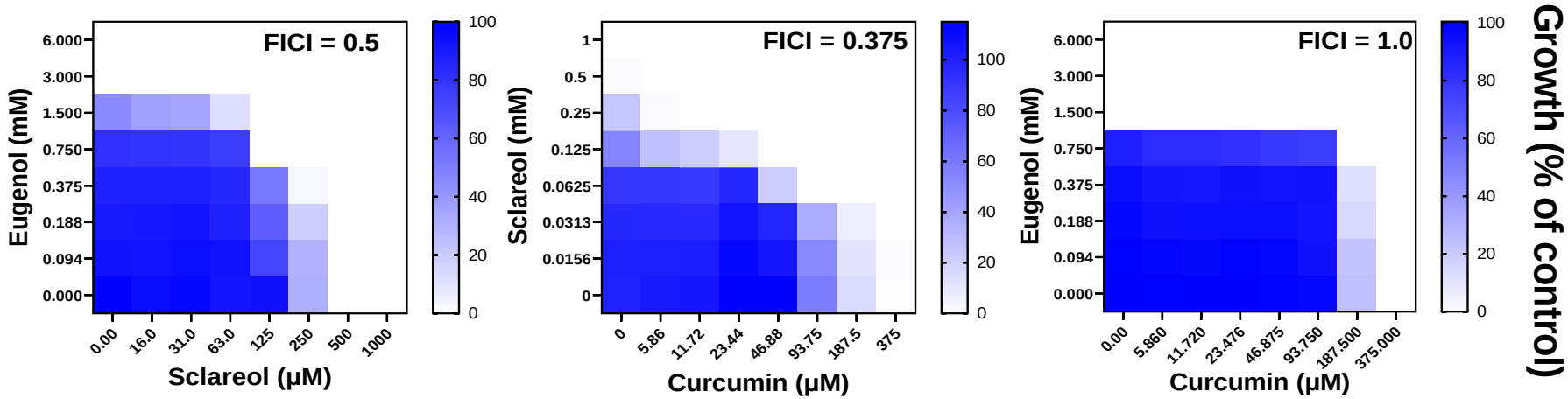

Figure 3.1 Three way interaction of natural products in *S. cerevisiae*. Checkerboard assays of combinatorial growth-effects performed according to EUCAST procedure in YPD broth in *S. cerevisiae* W303 at the indicated concentrations of eugenol, sclareol and curcumin. The growth values represent the means of three independent experiments calculated as percentages of growth (OD_{600}) with the natural products relative to the minus-NP control, after 24 h growth at 30°C. FICI, fractional inhibitory concentration index, calculated from the data and where growth < 5% of the control was assigned as no-growth (Hsieh et al., 1993).

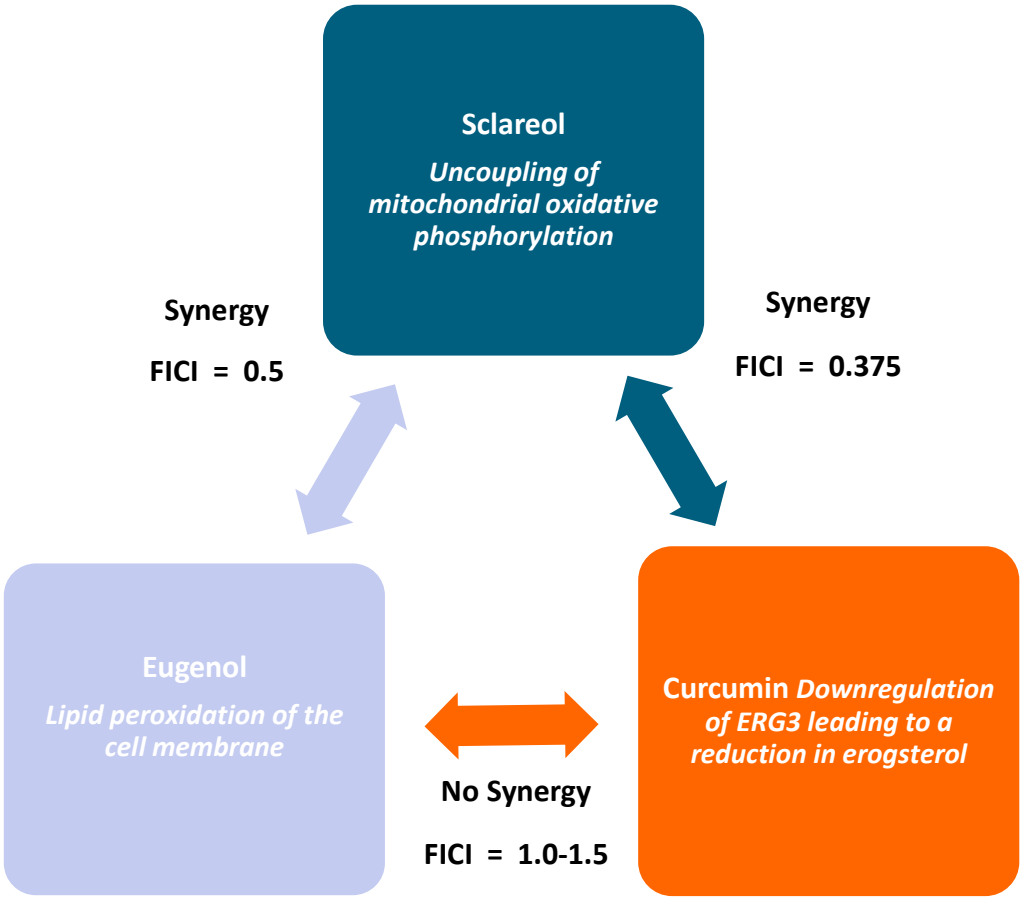

Figure 3.2. Triangle of NP interactions with mechanisms of actions chosen to explore in the three natural products. Sclareol exhibits synergy with both eugenol and curcumin, where uncoupling of mitochondrial oxidative phosphorylation was chosen to investigate (Mendoza et al., 2015). For eugenol, which shares synergy with sclareol but no interaction with curcumin, the role of lipid peroxidation of the cell membrane was explored (Alves et al., 2017). In the case of curcumin, where synergy is seen with sclareol but not with eugenol, the role of ergosterol downregulation was studied (Sharma et al., 2012). FICI = fractional inhibitory concentration index value, calculated from the checkerboard data in Figure 3.1.

3.3.2 Uncoupling of oxidative phosphorylation may be important for synergy between sclareol and eugenol or curcumin

First, the known MOA of sclareol as an uncoupler of oxidative phosphorylation was explored as a potential basis for the synergistic fungal inhibition it exhibits

when in combination with either eugenol or curcumin. The uncoupling action was mimicked using a known uncoupler of oxidative phosphorylation, carbonylcyanide-3-chlorophenylhydrazone (CCCP) (Kasianowicz et al., 1984). CCCP was combined individually with eugenol and curcumin. In both cases, the combination with CCCP gave synergistic inhibition of yeast growth (Figure 3.3). The interaction between eugenol and CCCP had a FICI value of 0.375, and between curcumin and CCCP the FICI value was 0.313. This suggested that the role of sclareol in the synergistic interactions with these two other NPs may at least in part involve the uncoupling of oxidative phosphorylation.

To assess potential of interaction also between sclareol and CCCP (e.g. competitive/antagonistic or synergistic), additional checkerboards were performed. Sclareol in combination with CCCP gave FICI values of 0.09 and 0.313, dependent on the concentrations analysed (Figure 3.4). This result indicated a synergistic interaction between these agents, potentially relating to their actions in uncoupling of oxidative phosphorylation. This indicates that using a targeted and unspecific uncoupling agent such as sclareol (mitochondrial) and CCCP (unspecific) can produce synergy.

3.3.3 Synergy between curcumin and sclareol removed in ergosterol biosynthesis mutants

As outlined in the introduction, curcumin is a well-studied NP where considerable mechanistic understanding of its actions on cells has been described (Prasad et al., 2014). In this study, first the potential involvement of curcumin-induced *ERG3* downregulation (Sharma et al., 2009) in the synergy with sclareol was considered, as this effect is at the membrane as is also the case for uncouplers. Several diploid gene-deletion mutants in the ergosterol biosynthesis pathway were tested to determine if the deletion of *ERG3* specifically would remove the synergy between curcumin and sclareol or if other genes mediating ergosterol biosynthesis, and therefore more unspecific ergosterol depletion, was important.

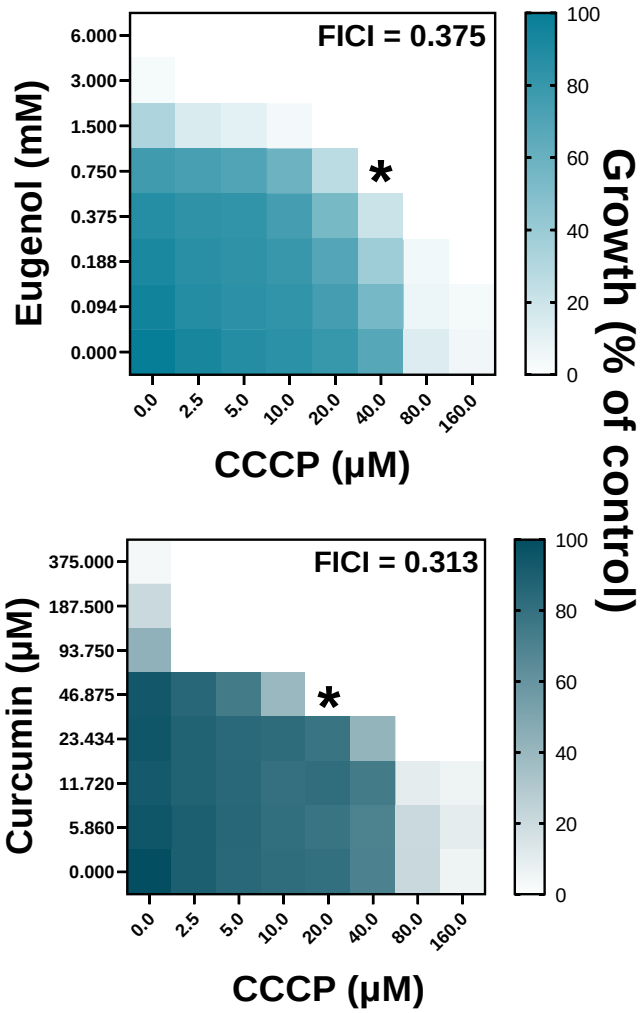

Figure 3.3. The known uncoupling agent CCCP reproduces synergy (like sclareol) with eugenol or curcumin. Checkerboard assays of combinatorial growth-effects performed according to EUCAST procedure in YPD broth with *S. cerevisiae* W303 at the indicated concentrations of eugenol, curcumin and CCCP. The growth values represented by the colour intensities are means of three independent experiments calculated as percentages of growth (OD_{600}) with the natural products relative to the minus-NP control, after 24 h growth at 30°C. FICI, fractional inhibitory concentration index values, calculated from the data and where growth < 5% of the control was assigned as no-growth. Asterisks indicate the conditions for which FICI was calculated.

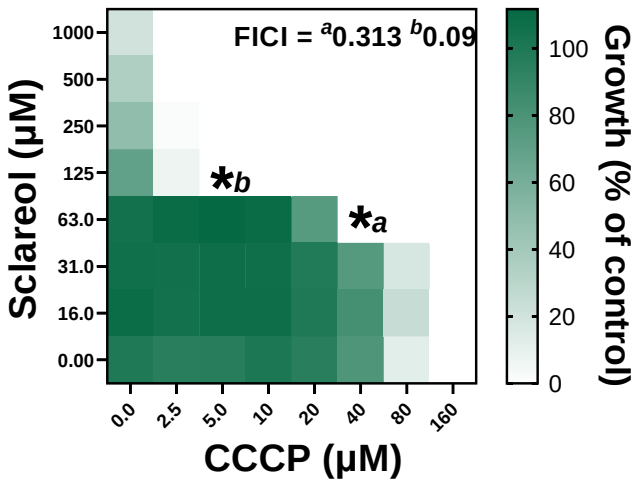

Figure 3.4. Sclareol and CCCP also exhibit a synergistic interaction. Checkerboard assays of combinatorial growth-effects performed according to EUCAST procedure in YPD broth with *S. cerevisiae* W303 at the indicated concentrations of sclareol and CCCP. The growth values represent the mean of three independent experiments calculated as percentages of growth (OD_{600}) with the natural products relative to the minus-NP control, after 24 h growth at 30°C. FICI, fractional inhibitory concentration index values, calculated from the data and where growth < 5% of the control was assigned as no-growth. *a and *b indicate the concentrations selected for calculating FICI value.

In all the *erg* deletion mutants that were tested, the FICI values were significantly raised compared to the background strain (BY4743, used to create the diploid mutants), and synergy was largely removed (FICI > 0.5) (Figure 3.5A). It is important to note that despite being non-essential genes, the *erg* mutants display slower growth and various changes in sensitivity towards other stressors, although this was not specifically tested for in this thesis. The tests of *erg* deletion strains were also extended to the interaction between curcumin and CCCP, to help relate observed phenotypes to uncoupling action more specifically. In agreement with the data for sclareol and curcumin, with the curcumin and CCCP combination all ergosterol mutants showed an increased FICI value and a loss of the synergistic interaction that was evident for the wild

type (Figure 3.5B). The raw checkerboard data for these experiments can be found in Appendix B (B.1 and B.2). The finding that cells defective for ergosterol biosynthesis are not as sensitive to the synergistic activity of curcumin and an uncoupling agent compared to the wild-type is consistent with mechanistic action of *ERG3*-downregulation by curcumin (Sharma et al., 2012) being important for the synergy, as such downregulation may be inconsequential in ergosterol-defective mutants.

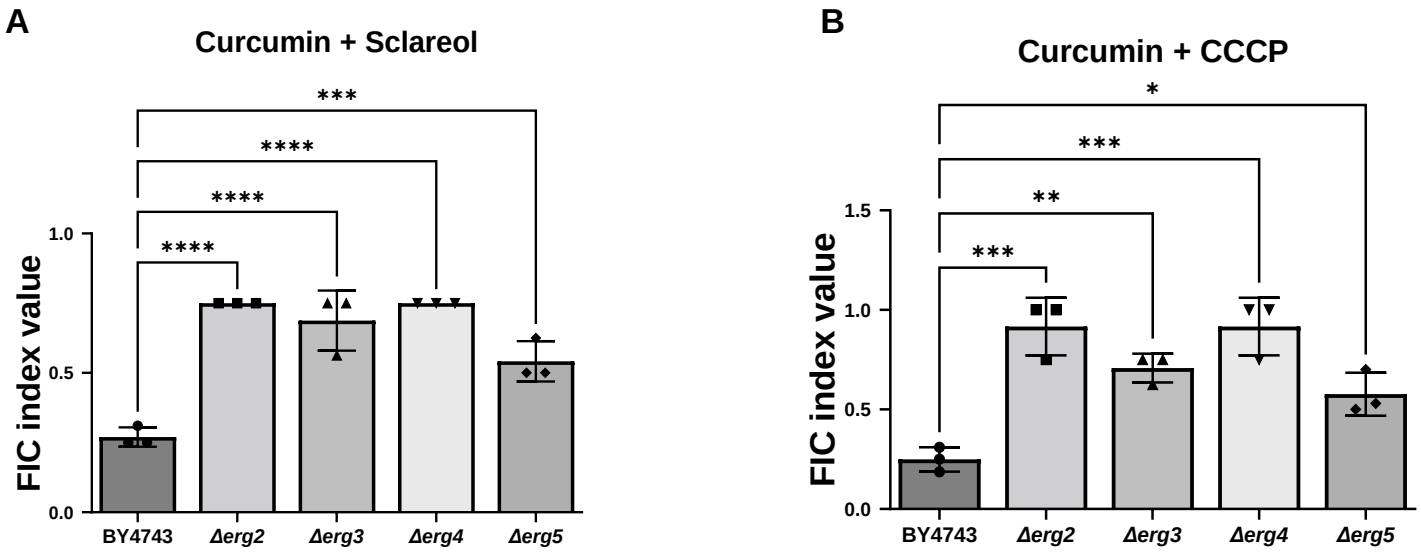

Figure 3.5. Ergosterol deletion mutants are insensitive to synergistic inhibition by curcumin combined with uncoupling agents. FICI values are calculated from checkerboard assays of combinatorial growth-effects performed according to EUCAST procedure in YPD broth in *S. cerevisiae* BY4743 and diploid deletion mutants constructed in the BY4743 background. Bar-height represents the mean of three independent experiments, ±SD. FICI, fractional inhibitory concentration index values. Raw checkerboard data can be found in Appendix B, B.1 and B.2. * $p < 0.5$ ** $p < 0.01$, *** $p < 0.001$ and **** $p < 0.0001$ according to a One-way ANOVA with Dunnett's Multiple Comparison post-hoc test.

3.3.4 The role of lipid peroxidation in the synergy between eugenol and sclareol

To investigate the role of eugenol in its synergy with sclareol, the action of eugenol as an inducer of lipid peroxidation (Khan et al., 2011) was investigated as this is a membrane targeted action (similar to discussion above for curcumin). Several agents are known to induce lipid peroxidation in their mechanism of action, including cadmium nitrate (Hussain et al., 1987, Jurczuk et al., 2004), which was selected here to mimic lipid peroxidation as a potential cause of synergy with sclareol and CCCP. In combination with cadmium nitrate, both uncouplers gave synergistic inhibition of yeast growth with FICI values in sclareol and cadmium nitrate of 0.189 and with CCCP and cadmium nitrate the FICI is higher but still synergistic at 0.5 shown in Figure 3.6.

To further test the specific role of lipid peroxidation in eugenol's synergistic action with the uncouplers, α-tocopherol (also referred to as vitamin E) was used as an agent to suppress lipid peroxidation. α-Tocopherol has been reported across different types of organism to exhibit potent antioxidant effects most specifically protecting against lipid peroxidation (Cheeseman, 1993, Shichiri et al., 2011). Checkerboards with eugenol and sclareol were set up with or without the addition of a sub-inhibitory concentration of α-tocopherol (growth effects shown in Appendix B, B.3). The checkerboard data revealed an FICI value of 0.5 for eugenol + sclareol with the DMSO solvent control (Figure 3.7A) and with the addition of α-tocopherol, the FICI value increased to ≥ 1.0, indicating absence of synergy in this condition.

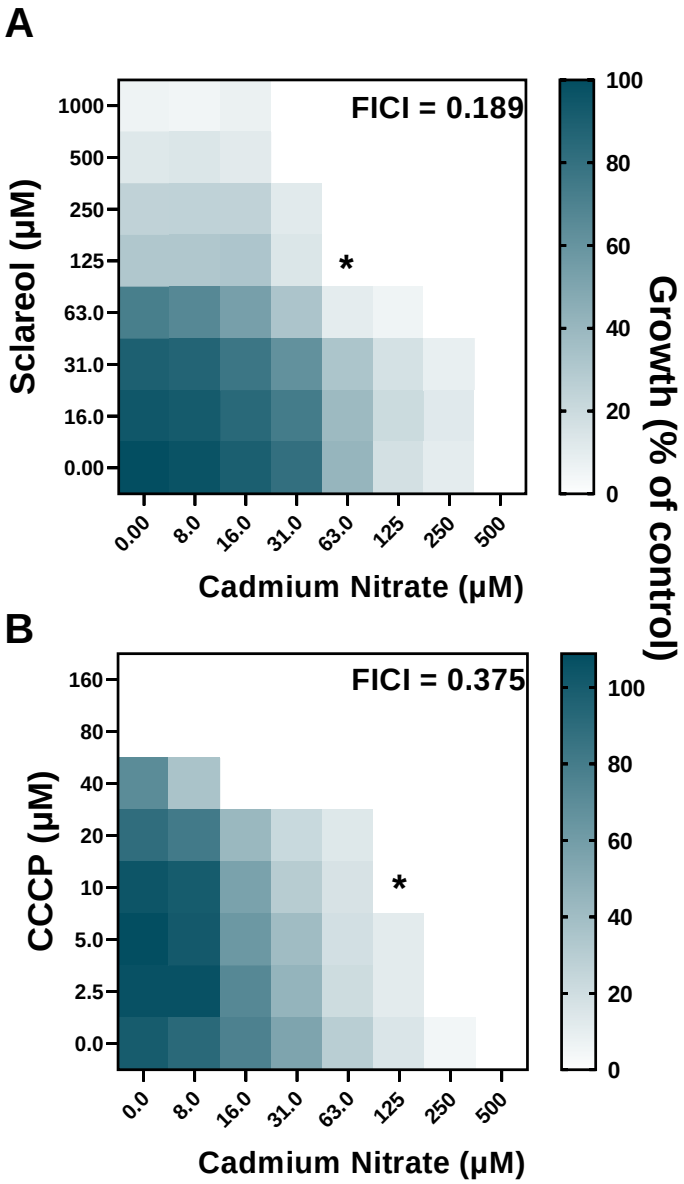

Figure 3.6. Mimicking lipid peroxidation activity using cadmium nitrate reproduces synergy with uncoupling agents. Checkerboard assays of combinatorial growth-effects performed according to EUCAST procedure in YPD broth in *S. cerevisiae* W303 at the indicated concentrations of cadmium nitrate and sclareol (A) or CCCP (B). The growth values represent the means of three independent experiments calculated as percentages of growth (OD_{600}) with the natural products relative to the minus-NP control, after 24 h growth at 30°C. FICI, fractional inhibitory concentration index values, calculated from the data and where growth < 5% of the control was assigned as no-growth (Hsieh et al., 1993). Asterisks indicate the conditions for which FICI was calculated.

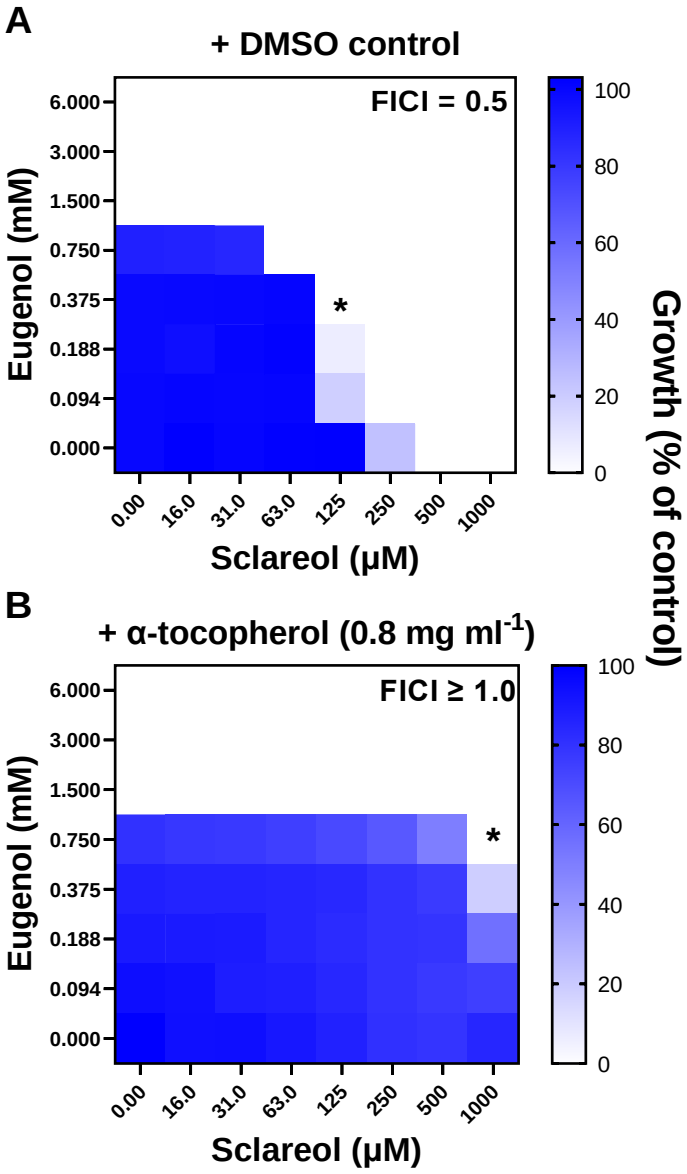

Figure 3.7. Inclusion of lipid-peroxidation suppressor α-tocopherol removes the synergy between eugenol and sclareol. Checkerboard assays of combinatorial growth-effects performed according to EUCAST procedure in YPD broth in *S. cerevisiae* W303 at the indicated concentrations of eugenol and sclareol, with the addition of DMSO as a solvent control or α-tocopherol. The growth values represent the mean of three independent experiments calculated as percentages of growth (OD_{600}) with the natural products relative to the minus-NP control, after 24 h growth at 30°C. FICI, fractional inhibitory concentration index values, calculated from the data and where growth < 5% of the control was assigned as no-growth (Hsieh et al., 1993). Asterisks indicate the conditions for which FICI was calculated.

Moreover, the interaction between the action of suppressing lipid peroxidation using α-tocopherol was further explored through combining the compound with sclareol. The checkerboard is shown in Figure 3.8, where a strong antagonistic relationship was evident with an FICI value of 5.0. This finding indicates that besides the proposed role for lipid peroxidation in the synergy between sclareol and eugenol; lipid peroxidation, or downstream consequences of lipid peroxidation, are important for the inhibitory activity of sclareol. This further points to a combined effect at cellular membranes between sclareol and eugenol.

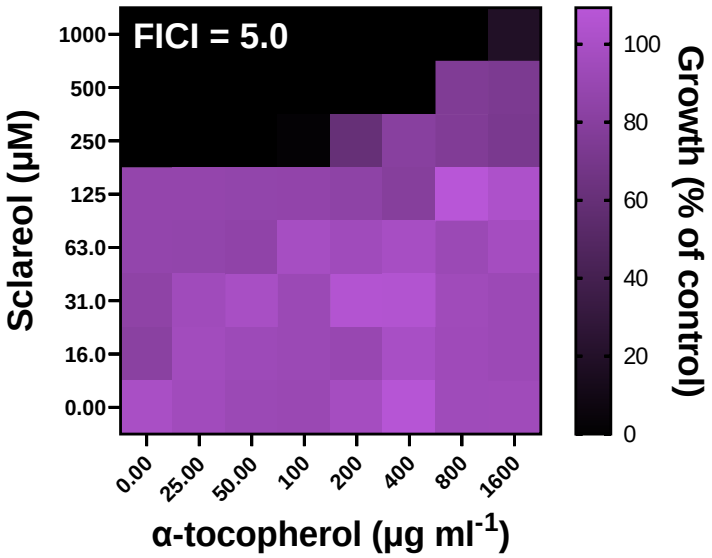

Figure 3.8. α-Tocopherol antagonises inhibition by sclareol. Checkerboard assay of combinatorial growth-effects performed according to EUCAST procedure in YPD broth with *S. cerevisiae* W303 at the indicated concentrations of sclareol and α-tocopherol. The growth values represent the mean of three independent experiments calculated as percentages of growth (OD_{600}) with the natural products relative to the minus-NP control, after 24 h growth at 30°C. FICI, fractional inhibitory concentration index values, calculated from the data and where growth < 5% of the control was assigned as no-growth.

3.3.5 Sclareol and CCCP act synergistically or additively with other cell-membrane and -wall acting antifungals

In response to the indication that uncoupling activity is important for the above synergies with both the NPs curcumin and eugenol, it was decided to test this synergy mechanism for important antifungals: the polyene, amphotericin B (Andreoli and Monahan, 1968); the demethylase inhibitor (azole), tebuconazole (Marichal et al., 1985) and the echinocandin, caspofungin (Balashov et al., 2006). All of these affect the cell membrane or cell wall. Checkerboards were conducted to assess interactions with either sclareol or CCCP. When combined with sclareol, amphotericin B and caspofungin showed synergistic inhibition of yeast growth with mean FICI values of ≤ 0.5, while sclareol with tebuconazole exhibited an additive relationship with a mean FICI value of ≤ 0.625 (Figure 3.9). In contrast, when CCCP was combined with the antifungals additive interactions were observed for both tebuconazole and amphotericin B, whereas synergy was observed in combination with caspofungin. Therefore, both uncouplers had additive relationships with the demethylase inhibitor, tebuconazole, and both were synergistic with caspofungin, but results differed for amphotericin B. In the latter case, the differing localisations of sclareol and CCCP actions (Demine et al., 2019) may underpin this difference, or that some additional activity (besides uncoupling) of sclareol accounts for its synergy with amphotericin B. Overall, the results indicate that uncouplers have the potential to enhance the inhibitory actions these major cell-wall and membrane acting antifungal actives.

3.3.6 The introduction of uncoupling activity establishes synergy between eugenol and curcumin

Following on from the individual mechanistic evaluation discussed above, it was next decided to assess whether the introduction of uncoupling activity could establish a synergistic relationship between eugenol and curcumin. It was the interaction only of these two that was non-synergistic among the combinatorial interactions of the three NPs studied in this chapter (Figure 3.1). The inclusion

of CCCP at a sub-inhibitory concentration (SIC) of 20 µM produced a synergistic relationship between eugenol and curcumin compared to the solvent control (Figure 3.10A), with the presence of CCCP decreasing the FICI value of the combination from 1.0 to 0.5. Moreover, to assess if this effect extended to sclareol, a SIC of sclareol (62.5 µM) was included with the combination; like for CCCP, the chosen concentration does not significantly decrease growth (Figure 3.10C).

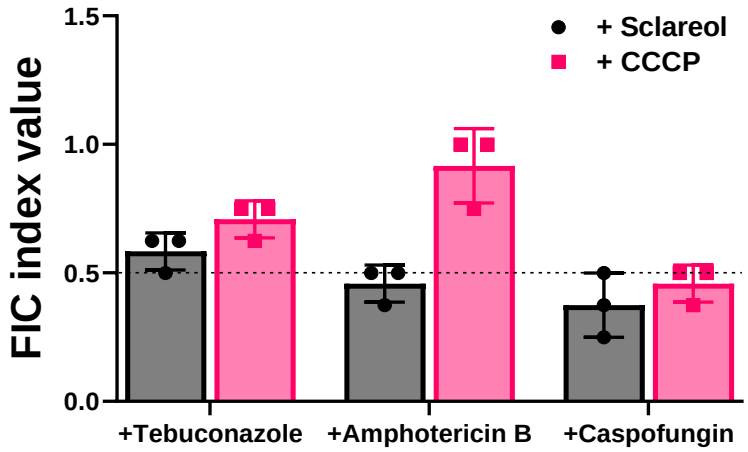

Figure 3.9. Growth inhibition by sclareol or CCCP combined with commonly used antifungals in *S. cerevisiae* W303. FICI, fractional inhibitory concentration index values were calculated from checkerboard data where growth < 5% of the control was assigned as no-growth and plotted as the mean of three independent experiments. Raw checkerboard data can be found in Appendix B, B.4. The dotted line indicates FICI value of 0.5 which reflects the standard 'cut off' point for a synergistic relationship (Hsieh et al., 1993).

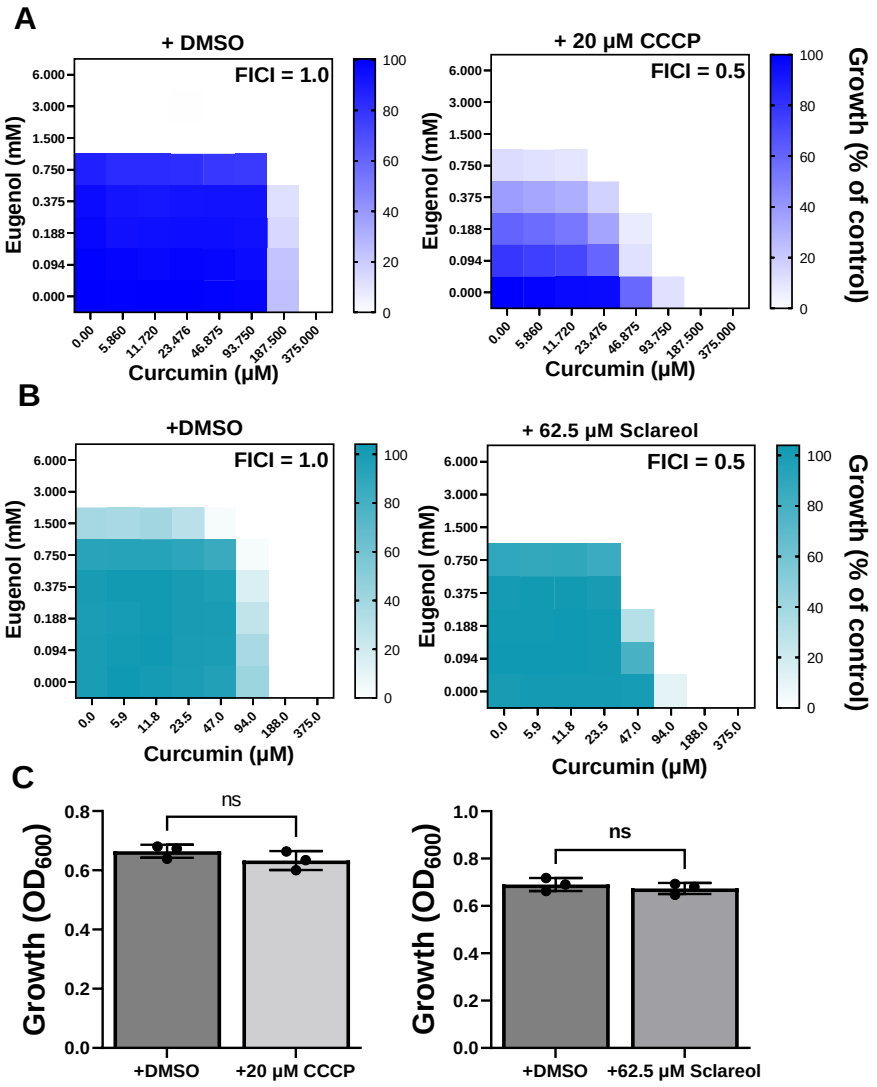

Figure 3.10. Introduction of uncoupling activity induces synergy between eugenol and curcumin in *S. cerevisiae* W303. Eugenol and curcumin combined with a sub-inhibitory concentration either of CCCP (20 µM) (A) or sclareol (62.5 µM) (B), concentrations that had no significant effect on growth yield (C) (according to OD_{600} after 24 h). Checkerboard assays were performed in adherence to EUCAST guidelines. Growth values represent the mean of three independent experiments calculated as percentages of growth (OD_{600}) with the natural products relative to the minus-NP control, after 24 h growth at 30°C. FICI, fractional inhibitory concentration index values, calculated from the data and where growth < 5% of the control was assigned as no-growth. Bar height represents mean OD_{600} after 24 h, error ±SD, ns = non-significant assessed using an unpaired t-test.

The addition of sclareol also induced synergy when added to eugenol and curcumin, where the FICI value decreased from 1.0 to 0.5 (Figure 3.10B). These findings indicate that the introduction of uncoupling activity is sufficient to induce synergy between curcumin and eugenol, but also appears consistent with the earlier results showing that the uncouplers themselves synergise with either agent alone.

3.3.7 Synergy through the inclusion of uncoupling activity potentially involves ATP depletion and membrane reorganisation

The finding that uncoupling activity can elicit synergy between eugenol and curcumin directed the next research question, where the mechanism by which the uncouplers act in this synergy-provoking manner was explored. The first hypothesis tested was that the uncoupler agents permit increased drug (NP) uptake into the cells, which would be expected to exacerbate growth inhibitory effects. Despite literature searches and consultation, no reasonably accessible methods for measuring eugenol or curcumin uptake could be identified during this study. Previously the fluoroprobe R6G has been used as a generic indicator of drug (azole) efflux activity in azole-resistant *Candida albicans* (Maesaki et al., 1999). Therefore, that approach was adapted to give a proxy of accumulation activity rather than efflux activity of cells. R6G accumulation was measured with or without the presence of CCCP. In all treatments, including the control, CCCP decreased the median R6G uptake, determined after 30 min (Figure 3.11A). The addition of sclareol also decreased R6G accumulation in all conditions, albeit less so then the effect of CCCP in the NP-treated conditions (Figure 3.11B). The data does not support the hypothesis that increased accumulation activity explains the synergy induced through the addition of uncouplers. Nevertheless, the data must be considered with caution considering that R6G uptake may not reflect that of the NPs.

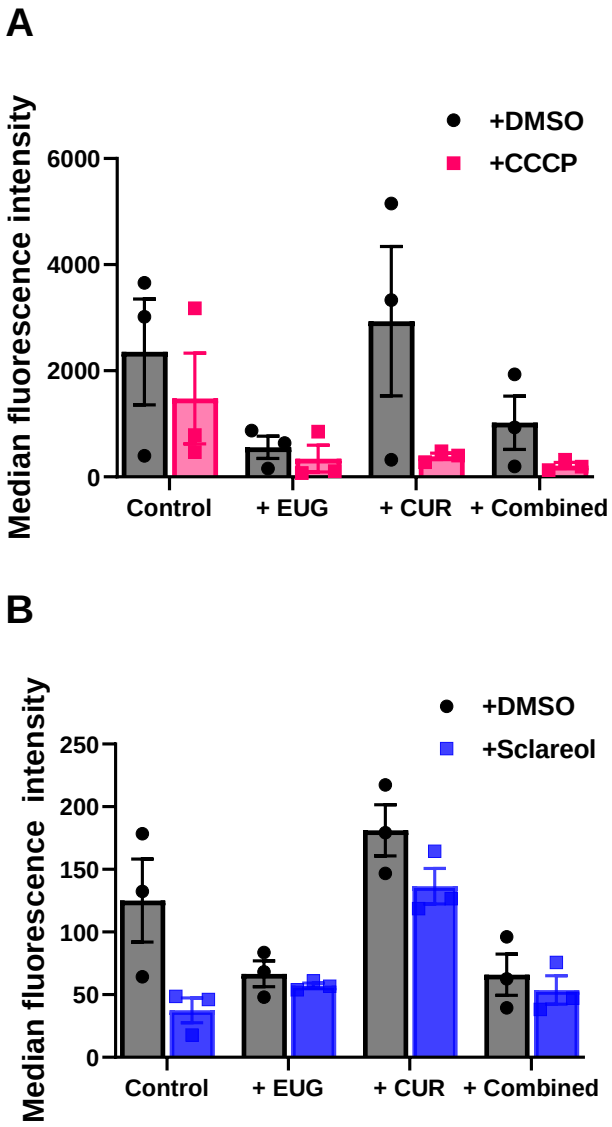

Figure 3.11. Fluorescence intensity reflecting R6G uptake by yeast cells incubated with different NPs and uncoupling agents. Cells were incubated for 24 h with the indicated agents supplied at EUG 94 µM, CUR 11.8 µM, CCCP at 20 µM and SCL at 62.5 µM. Cells were then assayed for R6G uptake. Bar height represents the median fluorescence intensity from cells incubated with R6G, measured using flow cytometry and analysed through Kaluza software. Each bar is the mean of three independent experiments, ±SD. (A) Checkerboard without CCCP indicated as '+DMSO' as the grey bar and with CCCP as the pink bar. (B) Checkerboard without sclareol indicated by the grey bar '+DMSO' and the data from with sclareol shown by the blue bars. Control = +/-CCCP or Sclareol, no eugenol or curcumin, '+EUG' = eugenol alone, '+CUR' = curcumin alone and '+Combined' indicates both NPs together. CCCP, carbonylcyanide-3-chlorophenylhydrazone, SCL, sclareol.

Additional experiments then directed to investigate one of the major downstream cellular consequences of uncoupling oxidative phosphorylation, ATP depletion. As previous research has established that uncoupling activity can result in ATP depletion (Slater, 1973, Marini et al., 2020), here antimycin A was assayed as it is a potent inhibitor of ATP production. It was tested whether antimycin A would mimic the effects of sclareol or CCCP in synergising with eugenol and curcumin. The appearance of the checkerboards results from these combinatorial assays suggested that neither eugenol nor curcumin synergised with antimycin A, at the highest usable concentration (keeping DMSO below 3% of the total volume, Figure 3.12, left panels). However, it is important to note that an inhibitory concentration of antimycin A could not be attained in these assays, so MIC could not be estimated, and the possibility of synergy (at some concentration) could not be fully ruled out. Therefore, instead of FICI, results at selected concentrations were examined. At these concentrations the combination of eugenol and antimycin A showed a significant decrease in growth compared to what would have been expected from a simple additive interaction between the compounds (Figure 3.12, right panels); unexpectedly, antimycin A alone appeared to stimulate growth, although the extent of this differed between experiments (compare upper- and lower-right panels, Figure 3.12). As this experiment was performed in 2% glucose, this saturation condition could have prevented the observation of any potential stronger effects of Antimycin A as ATP synthesis would mostly be derived from substrate level phosphorylation during fermentation rather than using the electron transport chain (Achilles et al., 2004).

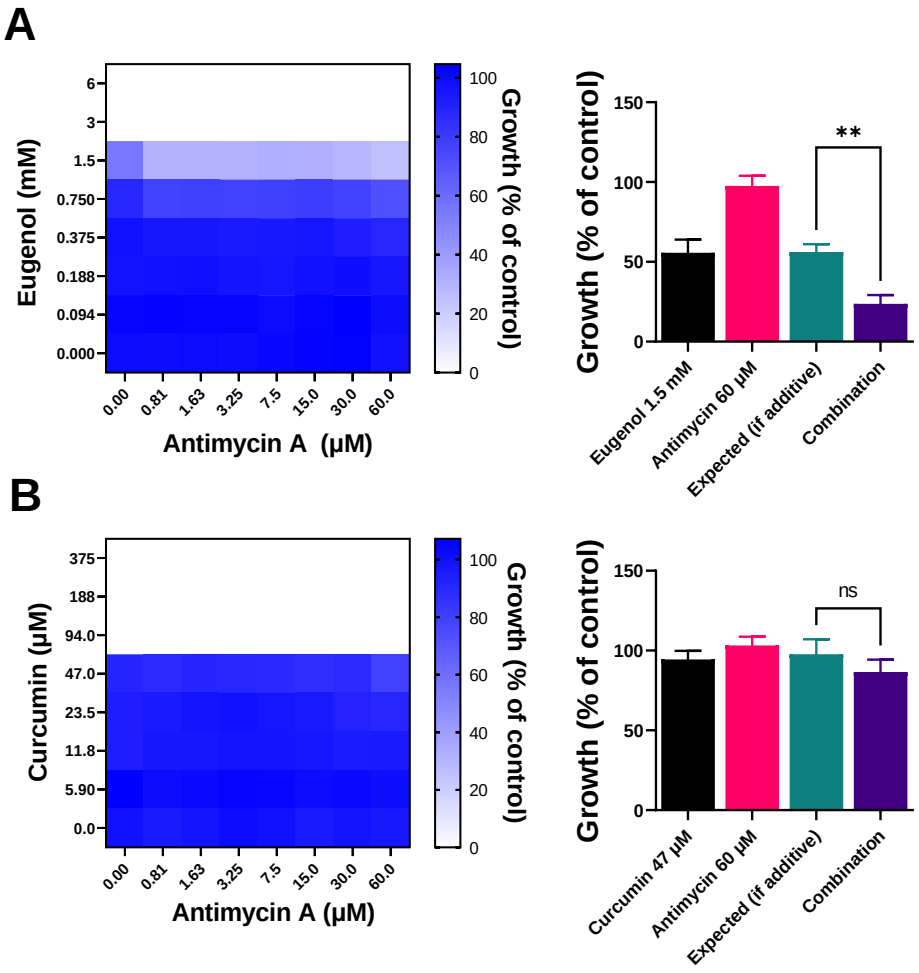

Figure 3.12. Effect of antimycin A (ATP-depleting agent) in combination with eugenol or curcumin. Checkerboards with eugenol (A) or curcumin (B) combined with antimycin A were performed according to EUCAST guidelines. Growth values represent the mean of three independent experiments calculated as percentages of growth (OD_{600}) with the addition of compounds relative to the minus-compound control, after 24 h growth at 30°C. FICI could not be calculated as the MIC for antimycin A was not attained. Selected growth comparisons are shown in the right-hand panels. Bar height represents mean OD_{600} after 24 h. Expected values were calculated by subtracting from 100% the growth inhibition observed for both compounds individually. Error ±SD. ** = $p < 0.01$, ns = non-significant assessed using an unpaired t-test.

The overall result was consistent with the hypothesis that depletion of ATP may contribute to the action of sclareol or CCCP in synergising with eugenol.

In contrast, for curcumin combined with antimycin A, the combination did not significantly reduce growth compared to what would be expected should the interaction be additive. Therefore, is seems less likely that potential ATP depletion by sclareol or CCCP is a basis for synergistic interaction with curcumin. Cellular ATP levels were not measured here, but such analyses, incorporating the investigation of intracellular pH, might help corroborate conclusions in future work. Moreover, the depletion of ATP is one of several downstream consequences of uncoupling activity, which can lead to reorganisation of the cell membrane, including potential for increased lipid peroxidation. It could be that such consequences of uncoupling activity themselves facilitate actions of agents like curcumin and eugenol at the cell membrane, e.g., the membrane reorganisation promoting easier access to the target sites of the NPs (Marini et al., 2020).

3.4 Discussion

This chapter aimed to explore mechanisms that may underlie synergistic interactions between either of two NPs (eugenol, curcumin) and a third NP (sclareol), but absence of synergy between the first two NPs. Specifically, how complementary, yet distinct mechanisms of action may promote these particular interactions between the different compounds. The results indicate that the mechanism of uncoupling oxidative phosphorylation that is characteristic of sclareol or CCCP is important for synergistic interaction with eugenol or curcumin. The uncoupler CCCP was used to help attribute this effect to uncoupling activity. The findings highlight the value of understanding the mechanism of action (MOA) of drugs and synergistic combinations and how this information can be used to develop efficacious 'drug cocktails'. Multi-compound interactions are particularly pertinent to NPs as these are thought to be produced primarily as multiple rather than single or pairs of compounds in nature.

As synergy with sclareol was common to both curcumin and eugenol, understanding the relevant action of sclareol was important here for elucidating these interactions. Sclareol has been shown to be an effective inhibitor of cancer cells and the phytopathogen *Botrytis cinerea*, with MOA in both those studies linked to mitochondrial uncoupling (Mendoza et al., 2015, Wang et al., 2015). Mitochondrial uncoupling is defined as the dissociation between generation of mitochondrial membrane potential and its function in mitochondria-dependent ATP synthesis (Demine et al., 2019). The present experimental findings imply that uncoupling activity is the relevant role of sclareol in its synergistic interactions with eugenol and curcumin. For curcumin, it was decided to investigate the relevance of reported curcumin-dependent *ERG3* downregulation (Sharma et al., 2012) in its synergistic interaction with sclareol. The findings indicated that more generally, an ergosterol biosynthesis defect is enough to remove the synergy, implying that ergosterol is a pre-requisite for the synergy, consistent with a drug-effect targeting ergosterol being responsible. Finally, for eugenol's MOA, actions of eugenol upon the

fungal cell membrane has been explored previously, where studies have indicated that disturbance of the membrane lipid bilayer and induction of lipid peroxidation are involved in eugenol's inhibitory activity (Braga et al., 2007, Khan et al., 2011, Marchese et al., 2017). Several experimental fronts suggested that lipid peroxidation was also important for the role of eugenol in the present synergy, including synergy between sclareol/CCCP with an additional lipid peroxidation agent (cadmium nitrate) and removal of synergy using a suppressor of lipid peroxidation (α-tocopherol).

Developing our understanding of a drug's MOA contributes towards our evolving ability to accurately predict how drugs may interact in their actions i*n vitro*. The approach used in this chapter, summarised above, elucidated individual MOAs and their role in a specific synergy of interest. Alternatively, other studies that focus on drug combination predictions have utilised computational approaches such as network pharmacology (understanding complex relationships from a network perspective e.g. between biological systems, drugs, targets and disease) to identify synergistic combinations; enabling predictions of effective drug combinations beyond the scope of what could reasonably be tested experimentally (Csermely et al., 2013). In this approach, drug actions are described as a network perturbation. Using a network-based approach, Lv *et al.* (2022) emphasised that knowledge of the drug target network structure alone is insufficient to predict synergistic antibiotic interactions and needs to also incorporate network proximity, which enables quantification of the relationship between targets and network interactomes of different drugs. Their study indicated that synergy amongst antibiotics has a small network proximity, where networks of drug targets overlap (but not completely). Moreover, the authors suggest that synergistic combinations act on a common biological pathway (Lv et al., 2022). With a different experimental approach, the findings from this chapter agree with Lv et al. (2022): a combined effect on a common biological process or structure (e.g. membrane function) produces synergy. It is important to recognise the practical constraints on experimentally evaluating drug combination MOAs

compared with high-throughput computational techniques whilst also acknowledging that individual drug MOA studies can improve the accuracy of predicting how drug combinations may interact. At the same time, it should be borne in mind that high-throughput experimental screens may be a more effective route to discovery of synergies than a rational approach based on knowledge of individual-drug MOAs (see Chapter 2, (Augostine and Avery, 2022)).

3.4.1 Potential importance of uncoupling activity for establishing synergies with certain natural products

The present results indicated that the uncoupling of oxidative phosphorylation was important for the identified synergies (of sclareol or CCCP) with eugenol and curcumin. Elsewhere, it is commonly found that synergy is linked to an increased accumulation of at least one of the agents into the cell (Roemhild et al., 2020). In the present study, cellular uptake activity was estimated using the R6G probe as a proxy. However, besides the fact that R6G uptake dynamics may not accurately reflect that of the NPs of interest, interpretation is complicated by the knowledge that R6G fluorescence in the cell arises through tight binding to the inner mitochondrial membrane, where R6G can act as a potent inhibitor of oxidative phosphorylation (Williams et al., 1999). This overlap in MOA between R6G and the uncoupling agents of interest emphasises how the R6G results should be considered with some caution. Ideally, methodology that enabled reliable detection of intracellular eugenol, curcumin and/or sclareol, or tagged-derivatives, would be needed to determine whether potential contributions of altered NP uptake in the synergies.

As a consequence of uncoupling of oxidative phosphorylation several downstream consequences may contribute towards arising phenotypes. The present findings (using the inhibitor of oxidative phosphorylation, antimycin A, for depleting cellular ATP) suggest that depletion of ATP could be involved in the synergy of sclareol with eugenol. It has been shown that (in cells of *Saccharomyces cerevisiae*), upon depletion of ATP, the cell membrane begins to undergo reorganisation, including lipid rearrangement (Marini et al., 2020).

It could be speculated that the downstream consequences of uncoupling involving ATP depletion and potentially membrane reorganisation could render the membrane target sites of certain NPs like eugenol (known to promote lipid peroxidation) more susceptible to detrimental effects such as lipid peroxidation, accentuating growth inhibition.

The potential for uncoupling activity to promote synergy was also considered for commonly used antifungals, where uncouplers (sclareol or CCCP) either exhibited synergistic or additive interactions when combined with amphotericin B, tebuconazole or caspofungin. This suggested that agents with uncoupling activity may act synergistically with a range of different inhibitors with varied MOA. Such potential of uncoupling activity could also be examined using a more targeted approach. For example, it is known that antagonism is prevalent amongst bactericidal and bacteriostatic antibiotics (e.g., ampicillin [-cidal] and trimethoprim [-static]) (Ocampo et al., 2014). Improving the efficacy of these antagonistic combinations would be beneficial for treatment strategies that utilise antibiotic cocktails. Antagonism is detrimental for reasons opposite to the benefits of synergy: antagonism can worsen treatment options as higher dosing is needed, raising associated toxicities and cost (Lehar et al., 2009). One example of the synergistic potential of uncoupling agents has been demonstrated in the synergistic anti-cancer effects of BAM15, a novel mitochondrial protonophore uncoupler (Kenwood et al., 2014) with inhibitors of MAPK signalling (Serasinghe et al., 2018). This study also exaggerates the potential of targeting mitochondrial function to overcome drug resistance, which is a major obstacle facing clinical treatments (Shrestha et al., 2021).

A key aim of this chapter was to understand how two agents (eugenol and curcumin) may synergise in common with a third agent (sclareol) but not synergise directly with each other. The collective data suggest that it is an action of sclareol that centres around uncoupling of mitochondrial oxidative phosphorylation (and possibly ATP depletion and/or membrane perturbation) that provokes synergy with the other two NPs. Neither eugenol nor curcumin is known to have uncoupling activity. Therefore, while both of the latter are

reported to perturb membrane function in different ways, evidently these particular membrane effects are not synergistically detrimental when combined, i.e. they affect cells independently, unlike when either is combined with the action of sclareol. One future aim could be to understand mechanistically how different types of membrane perturbation may interact to produce such different outcomes for cells.

3.4.2 Conclusions and future work

Natural product combinations and their inhibitory mechanisms are a complex, yet imperative research question. Developing our understanding on why different NPs synergise or not is important for informing future combinatorial treatments and how natural NP 'cocktails' may operate. Moreover, building on our mechanistic knowledge could help inform the search for novel, potent synergies to assist in the control and management of fungal pathogens. The study conducted here indicated that compounds with uncoupling activity can synergise with different NPs and promote synergy between pairs of compounds. As discussed elsewhere in this thesis, synergies enable the use of lower concentrations of NPs or antifungals for effective control of problematic fungi. This strategy could be of particular use where 'cocktails' of drugs are used (which have already undertaken clinical trials and regulatory examination). It would of course be important to confirm the safety and interaction status of these combinations before use (Talevi and Bellera, 2020).

The promise of using compounds which possess activity in uncoupling of oxidative phosphorylation, for synergy, could be further assessed using a high throughput screen approach, such as that of Chapter 2 but in this case using agents like sclareol and CCCP against which to screen. Moreover, to more specifically investigate the mechanism by which sclareol or CCCP as uncouplers enable synergy, as discussed above it could be insightful to assess impacts of uptake through visualisation of the NPs of interest inside the cell. Different techniques such as the use of fluorescent tagging or radiolabelling would assist in inside cell visualisation. One example of how fluorescently tagging can develop biological understanding is seen in a recent study that fluorescently

labelled caspofungin (Jaber et al., 2020) that demonstrated resistance to echinocandins in *C. albicans* could be identified through fluorescent intracellular quantification of caspofungin. The aim of fluorescently tagging NPs in our study would assist in the evaluation of whether uncoupling activity allowed an increased accumulation of the NP, leading to synergy.

The findings reported here shed some light on bases for certain NP-NP interactions in these agents' inhibitory effects on fungal cells. Identification of compounds with particular MOAs that frequently tend to interact synergistically with other potential inhibitors (e.g. uncouplers of mitochondrial phosphorylation) could also pose an attractive focus for rapid subsequent expansion of libraries of compound-compound synergies. Of course, the usual expected benefits of such synergies (reduced dosages, lower toxicity etc.) would need to be balanced against the potential risk of introducing non-specific synergies, which could affect the host.

Chapter 4 – Collateral Sensitivity: A Potential Drug-repurposing Strategy against Azole-resistant *Candida albicans*

4.1 Introduction

4.1.1 Drug-repurposing as an antimicrobial strategy

Antimicrobial resistance (AMR) is one of the greatest existing challenges to human health and is predicted to be responsible for up to 10 million human deaths annually with an associated economic burden of $100 trillion by 2050 (O'Neill, 2016). AMR is a dynamic and complex process involving gene transfer events and spontaneous mutations conferring drug resistance through various potential mechanisms (Ghannoum and Rice, 1999, Reygaert, 2018). Consequently, management of pathogenic microorganisms is constantly evolving to help protect infected hosts in both clinical and agricultural settings (Perfect, 2017). The approval of new antimicrobials is a costly and time-consuming process, with drug-development costing $2-3 billion and taking between 10-12 years until market approval (Nosengo, 2016, Boyd et al., 2021). Moreover, the probability of success is low, with only one-two drugs from a starting number of 10,000 compounds reaching Federal Drug Administration (FDA) approval (Boyd et al., 2021). However, there are routes to drug-based pathogen control that do not require new antimicrobials.

One method outside of drug-development involves the process of drug re-purposing (also termed drug repositioning/reprofiling/re-tasking/redirecting). This presents a relatively unexploited alternative approach to combat AMR but is gaining traction in both a private and public sector (Farha and Brown, 2019, Pushpakom et al., 2019). Drug-repurposing is an attractive opportunity for the discovery of new antimicrobials as it exploits compounds which have already been approved for at least one purpose, therefore which may already possess relevant toxicological data and record of safe use (e.g. from clinical trials in humans) to enable rapid re-deployment in

the clinical or elsewhere. The promise of drug-repurposing as a treatment strategy is underlined through two principles. One principle involves the 'cryptic' biological activities FDA-approved drugs possess, demonstrated by the array of side-effects they may cause (Paolini et al., 2006). This first principle of cryptic biological activity also suggests possibilities for extending their application beyond their originally intended target. The second principle is exhibited through different diseases and pathogens that may share common molecular/metabolic pathways or are influenced by similar genetic factors (Glicksberg et al., 2015). This commonality can enable the same drug to be effective across different clinical needs.

Drug-repurposing is not a new strategy and has been exploited across multiple diseases and health conditions, where often-unintentional discovery of additional therapeutic use has proved successful. One celebrated example is seen in the repurposing of sildenafil, which was originally intended to treat hypertension but was repurposed to treat erectile dysfunction and pulmonary hypertension (Farha and Brown, 2019). During the ongoing global coronavirus (COVID-19) pandemic, there have been several life-saving drugs that have been repurposed at rapid speed in order to compete with the viral spread and circumvent mortality. One key example has been the successful repurposing of remdesivir, which was considered a drug-centric repurposing approach as the drug's mechanism of action was scrutinised for potential activity against other diseases (Farha and Brown, 2019). Remdesivir is a broad-spectrum antiviral drug (an adenosine analogue) that inserts itself into the virus's nascent RNA chain, resulting in premature termination and inhibition of viral replication. Repurposing of remdesivir was informed through the effectiveness of the drug against other human coronaviruses, which was identified through another repurposing study (Agostini et al., 2018). Following a series of clinical trials, the effectiveness of remdesivir as an antiviral against COVID-19 was confirmed through the successful shortening of recovery time in adults treated with remdesivir compared with a placebo treatment (Beigel et al., 2020).

The importance of drug-repurposing during the COVID-19 pandemic has accentuated the strategy's potential as a tool to circumvent and 'keep up' with the spread of life-threatening diseases. Drug-repurposing could be exploitable across a plethora of microbial pathogens, particularly as the development of resistance to current antimicrobials continues to grow and the costly, time-consuming process of new drug discovery and development (discussed earlier).

4.1.2 Collateral sensitivity: what is it?

As a trade-off to the development of AMR by a pathogen, the organism often incurs a fitness cost, such as defective growth, altered pathogenicity or reduced nutrient uptake (Olivares et al., 2012, Melnyk et al., 2015, Basra et al., 2018). The mutational load, whilst promoting survival in the presence of one antibiotic has the capability to induce hypersensitivity to other, un-related agents – this is termed "collateral sensitivity" (CS) (Munck et al., 2014), depicted graphically in Figure 4.1. One example is observed in the > 16-fold lower MIC of tigecycline-resistant *Escherichia coli* towards nitrofurantoin, discussed below (Roemhild et al., 2020). This phenomenon has been studied both during drug discovery and based on mechanistic understanding of specific drugs and CS profiles in antimicrobial and cancer therapeutic studies. Harnessing CS proposes a new strategy to overcome AMR and to strengthen the success of antimicrobial cycling (Imamovic and Sommer, 2013). CS has been explored in strains harbouring pleiotropic mutations governing multidrug resistance: in one study, 74% of the laboratory evolved-resistant lines also exhibited certain sensitivity to other drugs (Imamovic and Sommer, 2013). Despite the existence of such studies, various questions persist in understanding the phenomena, such as the long-term impact on resistance development and the maintenance of CS in clinical settings (Pal et al., 2015).

The origins and evolution of CS are complex and relatively unexplored. Recently, Nichol et al (2019) combined mathematical modelling with *in vitro* experimental evolution in *Escherichia coli* to explore the prevalence and causes

of CS from a homogenous starting population. Whilst acknowledging the limitations of their *in vitro* evolution approach, such as not capturing the stochastic evolution of pathogenic bacteria that can occur in a clinical setting, this study highlighted that CS is not universal, but in fact rare and governed by multiple founding mechanisms (Nichol et al., 2019). The study highlighted the importance of understanding CS likelihood for gauging the probability of success in a clinical setting.

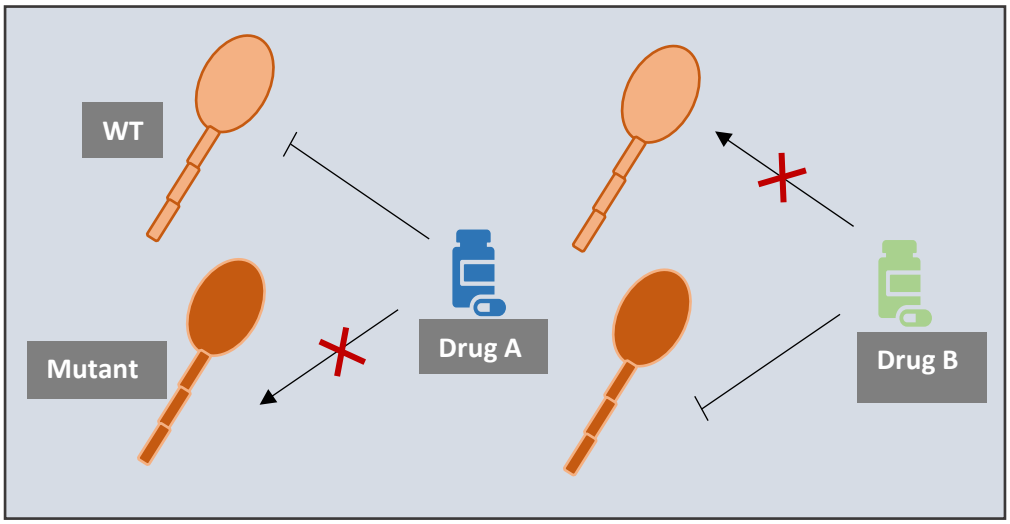

Figure 4.1. Collateral sensitivity (CS) schematic. Upon exposure to Drug A, the wild type (WT) is inhibited, whereas the mutant strain has developed resistance and is able to survive, indicated by the red cross. Subsequently, on exposure to a second, unrelated drug, (Drug B) the mutant, resistant to Drug A is now sensitive to Drug B, whereas the WT is not inhibited, indicated by the red cross. This phenomenon permits a selectivity to preferentially kill the strain resistant to Drug A. Schematic created without any known plagiarism.

An additional study conducted by Barbosa et al (2019) explored the evolutionary stability of CS in the bacterial pathogen *Pseudomonas aeruginosa*. The authors conducted a two-step evolution experiment, evolving resistance to drug A through challenging with streptomycin, producing sensitivity to drug B, piperacillin/tazobactam. These bacteria were then subject a second evolution experiment challenging the population with drug B (piperacillin/tazobactam)

alone or in combination with a low concentration of drug A (streptomycin). They found that hypersensitivity reversal/evolved resistance to drug B re-sensitised the population to drug A, and a strong killing effect was reintroduced. The work highlights that a single drug followed by combination therapy presents a promising treatment strategy (Barbosa et al., 2019). The authors also emphasised that the prevalence of CS is variable and dependent on the genetic background of the organism. Introduction of the same mutations in two closely related species (*E. coli* and *Salmonella enterica*) has been shown previously to cause opposing effects on drug resistance (Apjok et al., 2019), presenting additional complexity in the understanding of CS and the importance of clinical diagnostics. Barbosa et al (2019) conclude the success of CS treatment relies on acknowledging the critical prerequisite that CS does evolve in response to treatment and this may differ depending on the initial evolutionary path established to 'drug A' (Barbosa et al., 2017).

A study conducted by Roemhild et al (2020) revealed the existence of multiple origins and molecular mechanisms governing CS to the antibiotic nitrofurantoin (NIT, drug B). CS could occur against NIT by three different resistance profiles in the two bacterial species examined, for *E. coli* resistance to tigecycline or mecillinam produced CS towards NIT and in *S. enterica*, resistance to protamine sulphate produced CS to NIT, these drugs are 'drug A' (Roemhild et al., 2020). The CS mechanisms were based either on the (net) increase in cellular accumulation of active drug, or that the drug is able to confer increased toxicity within the cell (Roemhild et al., 2020). Mechanisms included effects on uptake dynamics (elucidated using radioactively labelled NIT) and the involvement of the SOS response, certain mechanisms being specific to only one bacterial mutant. Additionally, they showed that overexpression of nitroreductases, as an indicator of prodrug activation, conferred a moderate increase in susceptibility to NIT in all mutants, indicating a common mechanism of CS action to NIT. This study highlighted that the same hypersensitivity profile of drug resistant bacterial isolates can be the result of different mechanisms.

The authors concluded that NIT presents a candidate for the last drug in the 'drug switching regime' because of the strong CS effects it brings about.

4.1.3 Collateral sensitivity in fungal pathogens

Despite the existence of many studies of CS in bacterial pathogens, it is mostly unexplored for countering AMR in fungi. Fungal pathogens are prevalent in both clinical and agricultural settings (Denning and Bromley, 2015). The development of resistance in fungi is now observed across all classes of available drugs (discussed in the Introduction); one such example is seen in the evolved and intrinsic resistance to azole antifungals. Azole antifungals have been on the chemical market since the 1980s and their MOA involves targeting biosynthesis of ergosterol, which is a structural sterol molecule found in the fungal cell membrane but absent in humans, so presenting a fungus-specific target (Maertens, 2004). The azoles inhibit ergosterol biosynthesis through binding the lanosterol 14α-demethylase and inhibiting conversion of lanosterol to ergosterol (Arendrup and Patterson, 2017, Whaley et al., 2017, Ksiezopolska and Gabaldon, 2018). The azole class of drugs are often used clinically to treat invasive fungal infections, such as candidiasis (*C. albicans*), aspergillosis (*A. fumigatus*) and to control crop pathogens in the field (Fisher et al., 2018).

The most commonly used azole, fluconazole remains the treatment of choice for *C. albicans* infection due to it being inexpensive, readily bioavailable and orally administered (Pappas et al., 2016). However, prolonged over-use of the fungistatic drug in both clinical and environmental settings renders it prone to the rapid development of resistance (Ksiezopolska and Gabaldon, 2018). Several resistance mechanisms to azoles have been elucidated in both *C. albicans* and *A. fumigatus.* Both pathogens can develop azole resistance though alterations in the target gene *CYP51*/*ERG11* (*A. fumigatus*/*C. albicans*), with many non-synonymous SNPs shown to mediate azole-resistance (discussed in the Introduction). As well as target gene alterations, overexpression of efflux pumps can also confer resistance (Chowdhary et al.,

2014, Nishimoto et al., 2019). Resistance mechanisms toward demethylase inhibitors is discussed in more detail in Chapter One, see 1.3.3.1. Despite the development of mechanistic understanding of azole resistance, there are still questions to be answered, such as the identification of new azole-resistance mechanisms which will continue to evolve in the environment and how this will impact clinical azole resistance (Verweij et al., 2016, Gao et al., 2018). The exploration of CS in azole-resistant fungal pathogens could contribute to furthering understanding of resistance and specifically of fitness consequences that render the organisms collaterally sensitive.

The concept of CS has been discussed as a viable possibility for the control of invasive fungal pathogens but has not yet been exploited experimentally (Spitzer et al., 2017). In one study with *C. albicans,* Shi et al (2019) aimed to find agents that preferentially inhibited azole-resistant organisms. Using a co-culture system they identified five natural compounds that inhibited both azole-susceptible and azole-resistant organisms, with two compounds preferentially inhibiting azole-resistant strains (Shi et al., 2019). These two compounds were previously found to inhibit efflux pump activity and down-regulate expression of *MDR-1*. Furthermore, they showed that the *MDR-1* hyper-activation present in the azole-resistant strains used in this study, was associated with changes in cell membrane composition, such as reduced ergosterol, and led to enhanced intracellular accumulation of the natural compounds (drug B), producing hypersensitivity compared to wild-type. The selectivity of the compounds to inhibit efflux pump activity combined with the membrane alteration and increased permeability of the *MDR-1* overexpressing azole-resistant mutants contribute to the explanation behind the observed *MDR-1* activated CS. The study demonstrated potential for the treatment of resistant fungal pathogens through CS, suggesting also this could be extendable to fungi beyond *C. albicans*.

4.1.4 High-throughput screening to identify novel antifungals against emerging and drug-resistant *Candida* species

High-throughput screening has shared a role in discovering novel compounds whilst also harbouring importance in repurposing approved compounds for a different medical purpose. The promise of drug-repurposing through high-throughput screening is a growing and successful strategy to discover new antifungals. One study by de Oliveira (2019) screened an off-patent library, the Prestwick library, against three clinical isolates of *Candida auris*, the emerging fungal pathogen that has an intrinsic resistance against fluconazole, amphotericin B and echinocandins. Compounds not used as antifungals, such as suloctidil (anti-platelet) and ebselen (anti-inflammatory) were identified as hit compounds and also found to be synergistic with voriconazole and anidulafungin (de Oliveira et al., 2019). Another recent example of how high-throughput screening can be utilised against drug-resistant *C. albicans* is seen in a study by Revie et al. (2022). The authors carried out a combinatorial screening approach (alike the strategy used in Chapter 2) of a natural product library (RIKEN NPDepo) and identified many hit compounds which are synergistic with fluconazole. One compound of interest, NPD827 (an imidazopyrazoindole) was shown to synergise with fluconazole and also potentiate the efficacy of fluconazole when combined against azole-resistant isolates. NPD827 was shown to interact with fungal sterols and interfere with membrane homeostasis, resulting in inhibitory activity against *C. albicans* (Revie et al., 2022). These studies demonstrate the potential of high-throughput screening to identify compounds with activity against drug resistant *Candida* spp.

4.1.5 Chapter Aims

This study aimed to identify further the existence of, and enlighten the mechanistic understanding of, collateral sensitivity (CS) in azole-resistant *C. albicans*. Initially, the CS profile of three different azole-resistant strains was

explored against a plethora of drugs with different mode of actions. Upon identification of CS, mechanistic elucidation was performed. The occurrence of CS was further assessed using additional azole-resistance and azole-sensitive isolates. Further mechanistic analyses focussed on the involvement of altered uptake and possible glycosylation defects in the CS-displaying mutants. Additionally, a high-throughput screen was carried out with specificity for compounds which selectively inhibit azole-resistant strains, further validating CS as a treatment strategy.

4.2 Materials and methods

4.2.1 Strains, culture, and maintenance

In this study, strains of *Candida albicans* were a wild-type laboratory strain SC5314 and seven azole-resistant isolates; J942148, SCS119299X, J980280, AM2006/0180, AM2003/0041, AM2005/0334, AM2006/0101 kindly provided by Carol Munro and Donna MacCallum (University of Aberdeen, UK). In addition, four clinical *C. albicans* isolates with no known resistance (DSM 6959, ATCC 48867, ATCC 26790, ATCC10231) were kindly provided by Matthias Brock (University of Nottingham, UK). *Saccharomyces cerevisiae,* strain W303 (*MAT*a/*MAT*α *leu2-3,112 trp1-1 can1-100 ura3-1 ade2-1 his3-11,15 [phi+]*) was also used for mechanistic elucidation. Organisms were streaked onto YPD agar [recipe as for YPD broth, see below, but with inclusion of 1.5% agar] from –80^{o}C glycerol stocks and cultured for at least 48 h before single colonies were picked for sub-culture to broth. Organisms in YPD medium [2% peptone (Oxoid, Basingstoke, United Kingdom), 1% yeast extract (Oxoid), 2% D-glucose] were grown at 37^{o}C for *C. albicans* and 30^{o}C for *S. cerevisiae*. Filamentous fungi used in this chapter were *Aspergillus fumigatus* CBS 144.89 and two azole-resistant clinical isolates, 3216 and 4003, kindly provided by Matthias Brock (University of Nottingham, UK). These were routinely maintained and grown on potato dextrose agar or broth [PDA (Oxoid) or PDB (Sigma-Aldrich)] or *Aspergillus* Complete Medium (ACM; 1% Glucose, 0.1% Yeast extract, 0.2% peptone, 0.1% casamino acids, 1% aspergillus vitamin solution, 2% *Aspergillus* salt solution (ingredients listed in Appendix C, C.1-3), 0.0075% adenine), all at 37^{o}C (Vallières et al., 2018).

4.2.2 Chemicals

The chemicals used in this study were purchased from Sigma-Aldrich and Fisher chemicals. Stock solutions were prepared in water, DMSO or 70% ethanol as solvent (Table 4.1). Aliquots were added to growth media as required to give

the specified final concentrations, alongside the addition of corresponding amounts of solvent only in solvent-matched controls.

Compound	Solvent	Stock Concentration
Paromomycin	Water	500 mg ml^{-1}
Hygromycin	Water	100 µg ml^{-1}
Streptomycin	Water	50 mg ml^{-1}
Chloroquine	DMSO	50 mM
Cycloheximide	DMSO	20 mg ml^{-1}
Doxycycline	DMSO	25 mg ml^{-1}
Thialysine	DMSO	2.5 mg ml^{-1}
Tavaborole	Water	25 µg ml^{-1}
Amphotericin B	DMSO	1 mg ml^{-1}
Caspofungin	Water	500 µg ml^{-1}
Azoxystrobin	DMSO	50 mM
Cyprodinil	DMSO	100 mM
Sodium chromate	Water	100 µM
Amorolfine hydrochloride	DMSO	100 mM
Fluvastatin	DMSO	100 mM
Tunicamycin	DMSO	2 mg ml^{-1}
Eugenol	70% EtOH	500 mM
Congo red	Water	5 mg ml^{-1}
Calcofluor white	Water	1 mg ml^{-1}

Table 4.1. Chemical stock solutions used in this study.

4.2.3 Collateral sensitivity (CS) assays, hit validation and checkerboard assays

To test the sensitivity of the yeast strains to chemicals listed in Table 4.1, overnight cultures in YPD broth, 120 rev. min^{-1}, 30°C, derived from single

colonies, were diluted in the morning to OD_{600} 0.5, to ensure yeast were in exponential phase when tested, then grown in YPD for an additional four hours followed by dilution to OD_{600} 0.1 (*S. cerevisiae*) or 0.01 (*Candida* spp.). For *A. fumigatus*, spores were inoculated from PDA plates into ACM broth at 10^5 spores ml^{-1} before use as experimental cell suspensions in assays. For testing compounds for CS, culture aliquots (50 µl) were transferred to 96-well microtiter plates (Greiner Bio-One; Stonehouse UK) containing chemicals at 2X concentration (50 µl aliquots) added as specified in a 2-fold dilution series, with all dilutions and cell cultures prepared in YPD (*C. albicans*) or ACM (*A. fumigatus*) broth. The inoculated plates, with a total volume of 100 µl were incubated statically at 37°C for 24 h. OD_{600} was measured with a BioTek EL800 microplate spectrophotometer (at 0 h and 24 h). Growth was calculated as percentage of the OD_{600} attained in the control condition containing no drug (solvent and cells only). For continuous growth measurements, broth cultures of *C. albicans* or *A. fumigatus* were cultivated in 96-well microplates within a BioTek Powerwave XS microplate spectrophotometer in YPD or ACM broth. The growth was monitored from a starting OD_{600} ~0.01 (*Candida spp.*) or spore concentration of ~10^5 spores ml^{-1} (OD_{600} ~0.01) with continuous shaking at 37°C for 24 h, with OD_{600} readings taken every 30 min.

For checkerboard assays, culturing and preparation adhered to EUCAST guidelines, except for the use of YPD broth (Arendrup and Patterson, 2017). Aliquots (50 µl) of cell or spore suspensions prepared as described above were transferred to flat-bottom 96-well microtiter plates (Greiner Bio-One; Stonehouse UK) with compounds added to specified final concentrations by two-fold serial dilution (50 µl at 2X desired final concentration). The inoculated plates (100 µl per well, at 1X YPD) were incubated statically for 24 h at 30°C for *S. cerevisiae* and 37°C for *Candida albicans.* Subsequently, OD_{600} was determined with a BioTek EL800 microplate spectrophotometer. Fractional inhibitory concentration (FIC) indices were used to assess potential synergy from the checkerboard results, calculated as: [(Compound 1 MIC in

combination) / (Compound 1 MIC alone)] + (Compound 2 MIC in combination) / (Compound 2 MIC alone)] (Hsieh et al., 1993).

4.2.4 Slow growth assays

Candida albicans SC5314 was inoculated from YPD plates to YPD broth and cultured overnight at 30°C, 120 rev. min^{-1}. Overnight cultures were diluted to OD_{600} 0.5 and cultured for a further 4 h in fresh YPD before dilution of these experimental cultures to OD_{600} 0.02 (final OD_{600} in the well, 0.01) in the same medium. Two conditions were used to recreate slow growth phenotypes of drug-hypersensitive mutants. In one condition, the diluted culture aliquot was added to 96-well plates (Greiner Bio, UK) containing either YPD (2% peptone, 1% yeast extract, 2% dextrose) + paromomycin 50 mg ml^{-1} or YPD + the same volume of water (solvent control) and the growth was monitored using a BioTek Powerwave XS microplate spectrophotometer, from a starting OD_{600} ~0.01 with continuous shaking at 24°C, and OD_{600} readings taken every 30 min up to 24 h. The second condition was prepared with diluted culture aliquots containing YPD (2% peptone, 1% yeast extract, 2% dextrose) supplemented with 0.3 µl eugenol (in 70% ethanol) to a final concentration of 1.5 mM. Controls were YPD + the same volume of 70% ethanol (solvent control). The growth was monitored using a BioTek Powerwave XS microplate spectrophotometer, from a starting OD_{600} ~0.01 with continuous shaking at 30°C and OD_{600} readings taken every 30 min up to 24 h.

4.2.5 DNA extraction from *Candida albicans*

Microcentrifuge tubes (1.5 ml) of overnight *C. albicans* culture were centrifuged at 15,890 *g* for 1 min and the supernatant completely removed. Samples were resuspended in TEN buffer [100 mM Tris-Hcl (pH 8), 50 mM EDTA, 500mM NaCl] (250 µl) followed by the addition of 20% SDS (25 µl) and sterile glass beads at 50:50 (bead:volume). Tubes were incubated at 65°C for 20 min, then 90 µl of 3M potassium acetate (pH 5.3) was added tubes incubate for 15 min on ice. In a separate microcentrifuge tube, the supernatant was transferred across and

centrifuged for 10 min at 15,890 *g*. Supernatant was then transferred again, and 800 µl of 100% ethanol added, mixed and incubated for a further 10 min on ice. Samples were centrifuged for a further 10 min, the supernatant removed, and 500 µl of 70% ethanol added to wash the pellet. Centrifugation was repeated for 30 sec and the ethanol removed completely. The dry pellet was dissolved in sterile deionised water (25 – 50 µl). The DNA concentration was quantified using a DS-11 Spectrophotometer (Denovix, USA). Additionally, ratios A260/280 and A260/230 were used to estimate the purity of the DNA.

4.2.6 *ERG11* gene amplification and sequencing

Amplification of the DNA of *ERG11* gene (open reading frame) from *C. albicans* was carried out using the primers listed in Table 4.2. Amplification was performed using 50 µl volume reactions with final concentrations of: 0.5 µM of forward and reverse primer, 200 µM dNTPs (New England Biolabs, UK), 5% DMSO (NEB, UK), 5X GC Phusion Buffer (NEB, UK) and 1 Unit Phusion DNA polymerase (NEB, UK). In each 50 µl reaction, 200 ng μl^{-1} gDNA from template was included. PCR was carried out using a thermocycler with the following cycling conditions; 98°C initial denaturation (3 min), 35 cycles of [denaturation 98°C (30 sec), annealing at 50°C (30 sec), extension 72°C (90 sec or 30 sec)] with a final extension at 72°C (10 min). Sequencing was performed using the primers listed in Table 4.2 by Eurofins Genomics (France). The data were analysed using Snap Gene and Jalview software. The sequences were also compared with a further 'WT' *ERG11* sequence taken from the *Candida* Genome database, strain *C. albicans* SC5314 Assembly 22.

Amplicon	Amplicon Length (bp)	Orientation	Primer
ERG11_1	2587	Forward	**ACTGGATGCAGAACAACAACA**
		Reverse	**AAACGTCGAATCCTGGTCCT**
Amp1	413	Forward	**ATTCTTTCCATATTACTTGTCTTC**
		Reverse	**AGCAGAAACATCAGATAATTTAG**
Amp2	392	Forward	**TATGACGGTTTATTTAGGTCC**
		Reverse	**AATATAGTTGAGCAAATGAACG**
Amp3	377	Forward	**GCTTCAAGATCTTTATTTGGTG**
		Reverse	**TCACCTAAATGTAACAAGAACC**
Amp4	399	Forward	**TGGGTGGTCAACATACTTCT**
		Reverse	**TGAAACAGAATTAGCTTTGG**
Amp5	435	Forward	**CCAATTATATTGTTCCAAAAGGTC**
		Reverse	**TCGAAAGAAAGTTGCCGTTT**

Table 4.2 Primers used for *ERG11* DNA amplification and subsequent gene sequencing. Amp1-5 utilised from published primers (Spettel et al., 2019).

4.2.7 Rhodamine 6G (R6G) uptake assay

A single colony from *C. albicans* strain/isolates SC5314 (WT), J942148, J980280 and SCS119299X was grown overnight in 10 ml YPD (2% glucose) in a 50 ml Erlenmeyer flask at 30^{o}C and 150 rpm. Each culture was diluted to OD_{600} 0.5 and incubated for a further 4 h. Then 500 µl of OD_{600} 1.0 cells were supplemented with rhodamine 6G (Sigma-Aldrich, UK) to a final concentration of 10 µM and incubated in the dark with shaking (200 rpm). After 0 and 5 min incubation (with additional timepoints to establish chosen analysis points; see Appendix C, C.5.) 50 µl were removed and placed in 1.5 ml microcentrifuge tubes. Samples were centrifuged at 1900 *g* for 3.5 min and washed in phosphate-buffered saline (PBS, pH 7.2) prior to fixation. Cells were resuspended in 1% glutaraldehyde (Sigma-Aldrich, UK) on ice for 1 h, centrifuged and washed again as described. Samples were resuspended in 500 µl PBS, added to 5 ml falcon tubes [Becton Dickinson, (BD), UK) and kept on ice before analysis by flow cytometry. The Beckman Coulter FC500 flow cytometer

(FITC filter; excitation at 488 nm, emission at 530 nm) was used to determine median fluorescence intensity. Analysis was carried out using Kaluza software.

4.2.8 Flow cytometric analysis of exposed β-glucan

A single colony from *C. albicans* strain/isolates SC5314 ('WT'), J942148, J980280, SCS119299X and AM2003/0041 was grown overnight in 10 ml YPD in a 50 ml Erlenmeyer flask at 30^{o}C and 120 rpm. The cells were diluted to OD_{600} 0.2 in YPD and were further grown until mid-exponential phase, at OD_{600} 0.8 and used in analysis. Samples of cells (2 ml) were washed with PBS, resuspended in 4 % polyformaldehyde (in PBS, 2 ml) and placed on ice for 30 min, and washed twice with PBS Cells were then kept in the fridge until staining (no more than 48 h). Upon staining, 150 µl of fixed cells were place inside a U-bottom 96 well plate (Nunc, Thermo Fisher, UK) and centrifuged for 3.5 min at 1500 *g*. Samples were resuspended in PBS (+ 2% bovine serum albumin (BSA, Sigma)) and placed on ice for 30 min blocking. The supernatant was replaced with fresh PBS (2% BSA) and washed once. Cells were incubated with the primary antibody Fc-hdec1a (Invivogen, UK) at 3 µg ml^{-1} for 60 min on ice. Cells were then washed three times in PBS (no BSA). The pellet was resuspended with PBS containing 2% BSA and 1:200 diluted secondary antibody, goat anti-human tagged with Alexafluor 488 (Invitrogen, A11013, UK) and incubated in the dark for 30 min on ice. After three washes in PBS (no BSA), samples were resuspended in 100 µl PBS (no BSA) and used for flow cytometric analysis. The ID7000 Spectral Cell Analyzer (Sony Biotechnology), using the FITC filter; excitation at 488 nm, emission at 530 nm was used to determine median fluorescence intensity. Data analysis was carried out using Kaluza software, where gating was performed to separate the bulk yeast cell population (gate A), then from (A) doublets were gated out (gate B) followed by median fluorescent intensity quantification using (B). The gating procedure was unchanged for all conditions.

4.2.9 High-throughput screen of the Prestwick Chemical library

The Prestwick Chemical Library (PL) (Prestwick Chemical) was screened with drugs supplied at a final concentration of 100 µM. The final DMSO concentration in the screen, or solvent control was 1%. Screens were performed in duplicate using *C. albicans* azole-sensitive strains SC5314, ATCC 48867 and azole-resistant 21C1M1A1 strain and J980280 isolate, inoculated from YPD plates to YPD broth and cultured overnight at 30°C, 120 rev. min^{-1}. Overnight cultures were diluted to OD_{600} 0.5 and cultured for a further 4 h in fresh YPD before dilution of these experimental cultures to a final OD_{600} 0.01 in the same medium. Aliquots (50 µl in YPD) of the diluted culture were transferred to 96-well plates (Greiner Bio-One) containing Prestwick test chemical or internal DMSO control (50 µl in YPD), and cultured for 24 h at 30°C, with OD_{600} measured at 24 h in a BioTek EL800 microplate spectrophotometer. OD_{600} was expressed as percentage of growth relative to control growth (i.e., without any chemicals).

4.2.10 Statistical analysis

The statistical analyses in this chapter were performed as in Chapter Two, using Prism version 9.5.1.

4.3 Results

4.3.1 Hypersensitivity to aminoglycosides in two azole-resistant strains of *C. albicans*

The aminoglycosides have been of particular interest in the understanding and investigation of CS, with several studies in bacteria reporting that resistance to aminoglycosides is correlated with an increase in sensitivity to other drugs such as inhibitors of protein (doxycycline) and cell wall (ampicillin) synthesis (Lazar et al., 2013). Resistance to aminoglycosides can be permitted through disruption of the proton motive force (PMF) across the inner membrane; as a side effect these mutations diminish the activity of PMF-dependent major efflux pumps, preventing efflux of other antibiotics, resulting in the establishment of a hypersensitivity profile (Lazar et al., 2013). In another study, *Escherichia coli* resistant to chloramphenicol displayed CS to the aminoglycoside streptomycin (Imamovic and Sommer, 2013). Therefore, initial tests aimed to establish the status of sensitivity to aminoglycosides (initially paromomycin and hygromycin) in azole resistant and sensitive strains of *Candida albicans,* primarily to assess if the known intrinsic resistance of *C. albicans* to aminoglycosides was maintained in azole-resistant isolates. Moreover, the aminoglycosides were specifically chosen as previous data from our laboratory had indicated a hypersensitivity of two azole resistant *C. albicans* isolates to a combination of the aminoglycoside paromomycin and the drug β-escin (Vallières et al., 2020) suggesting a possible CS action underlying the result.

Initial experiments corroborated that two of the three tested azole-resistant *C. albicans* isolates were hypersensitive to the aminoglycosides paromomycin and hygromycin, minimum inhibitory concentrations (MICs) were determined as the concentration at which < 5% growth was observed, the concentrations can be found in Table 4.3. The two strains J980280 and SCS119299X shared a 16-fold higher increase in the MIC for tebuconazole than the standard laboratory strain SC5314, whereas strain J942148 had a 32-fold higher MIC. In the sensitivity to paromomycin, strains J9080280 and SCS119299X exhibited

striking hypersensitivity, with a 64-fold lower MIC than evident in strain SC5314 (Figure 4.2). In contrast, the other azole-resistant isolate did not exhibit sensitivity to paromomycin.

Strain/Isolate	MIC Tebuconazole	MIC Paromomycin	MIC Hygromycin
SC5314	≤[a] 4 μg ml^{-1}	> 50 mg ml^{-1}	100 μg ml^{-1}
J980280	64 μg ml^{-1}	≤ 0.782 mg ml^{-1}	6.25 μg ml^{-1}
SCS119299X	64 μg ml^{-1}	≤ 0.782 mg ml^{-1}	12.5 μg ml^{-1}
J942148	128 μg ml^{-1}	> 50 mg ml^{-1}	100 μg ml^{-1}

Table 4.3. Minimum inhibitory concentration (MIC) values for *C. albicans.* MIC was determined where < 5% growth was observed after 24 h incubation at 37°C. a = where the MIC could be below the stated concentration but was the lowest concentration used in the experiment.

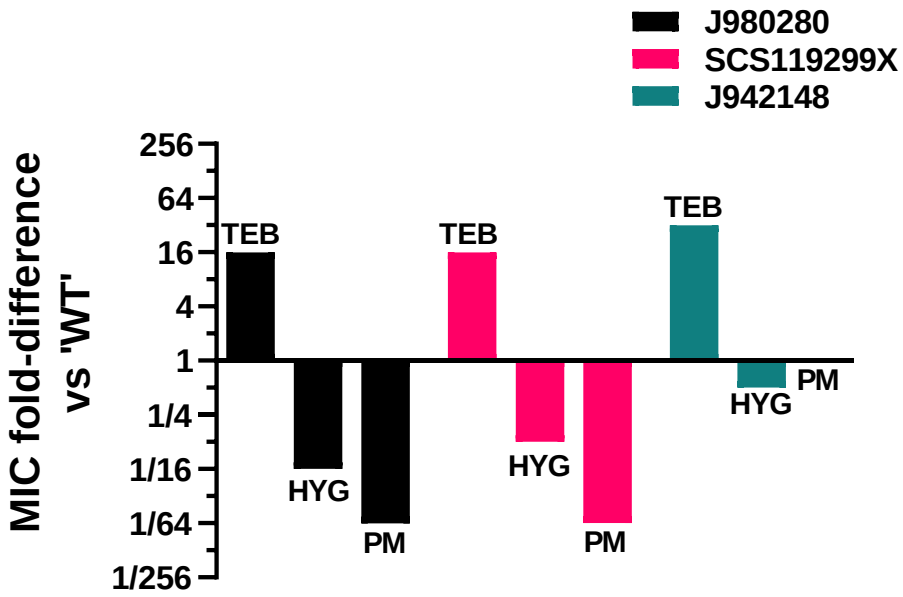

Figure 4.2. Sensitivities of three azole-resistant isolates of *C. albicans* to tebuconazole, hygromycin and paromomycin. Sensitivity was calculated as a fold difference in the minimum inhibitory concentration (MIC) compared with a standard laboratory strain (*C. albicans* SC5314, here termed 'WT'). Elevated MIC (relative to WT) to tebuconazole indicates azole resistance. TEB = tebuconazole, HYG = hygromycin, PM = paromomycin. The MIC fold difference is calculated from the mean of three independent experiments. MIC raw data can be found in Table 4.3.

In addition to testing the laboratory strain SC5314, additional isolates of *C. albicans* with a 'WT'-like profile (i.e. not displaying known drug resistance to commonly used antifungal agents (Jacobsen et al., 2014)), were tested for their paromomycin and hygromycin sensitivities and growth capabilities (Figure 4.3). Despite a relative sensitivity of DSM6959 and ATCC 48867 to both aminoglycosides compared to strain SC5314 (Figure 4.3A), these strains showed comparable growth to the laboratory 'WT' SC5314 (Figure 4.3B) and did not exhibit the same degree of aminoglycoside sensitivity as the two azole-resistant isolates (Figure 4.2). Moreover, the 'WT' isolates did not exhibit growth inhibition above 60% for paromomycin at 50 mg $ml^{-1}$and hygromycin at 100 µg ml^{-1}. This experiment suggested that the hypersensitivity observed in Figure 4.2 could be specific to certain azole-resistant isolates, termed hypersensitive and azole-resistant (HS-R).

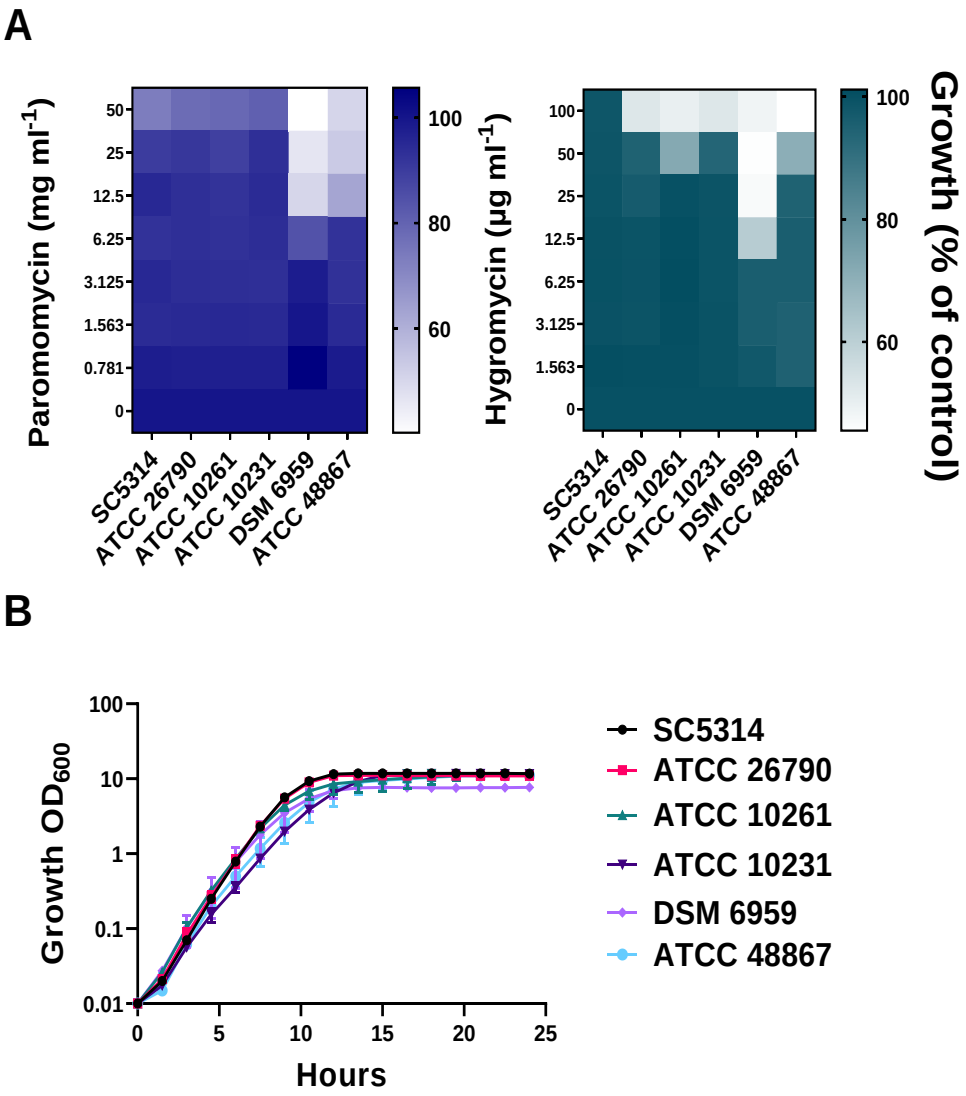

Figure 4.3. Sensitivities of five *C. albicans* azole-sensitive clinical isolates and laboratory wild-type SC5314 to paromomycin and hygromycin. (A) The sensitivity profile of the strains was measured by taking OD_{600} readings after 24 hours of incubation at 37°C with the solution mixture of aminoglycoside and YPD (+2% glucose). Heat maps represent the mean from three independent experiments. Growth was calculated as a percentage of the control (+dH_2O). (B) Growth curves based on OD_{600} across a 24-hour growth period. Cells were added at a starting OD_{600} of 0.01 and incubated in YPD at 37°C with shaking. Each point represents the mean of three independent experiments, with the error plotted ± SD.

4.3.2 Slow growth of hypersensitive mutants may partly contribute to the sensitivity profile

As discussed in the introduction, the principle behind the phenomenon of collateral sensitivity resolves around resistance to one drug which is associated with incidental consequences conferring hypersensitivity to other drugs (Imamovic and Sommer, 2013). In extreme cases the development of resistance is limited due to the toxic hypersensitivity profile exhibited; for example resistance to polyenes is not often seen (Vincent et al., 2013, Ben-Ami et al., 2011). As altered growth rate (of a resistant strain) could be one basis for other phenotypes (such as CS), the fitness of the three azole-resistant mutants was estimated by growth analysis across a 24-h period according to OD_{600}. Growth curves revealed that the two hypersensitive mutants, J980280 and SCS119299X exhibit a slower growth than WT and the non-hypersensitive mutant (J942148) (Figure 4.4A). The growth rate was calculated to enable a quantitative comparison (Figure 4.4B). Both HS-R have a significantly reduced growth rate of 0.501 and 0.542 for J980280 and SCS119299X respectively compared with 0.848 for 'WT' (growth rate units; h^{-1}). The difference between non-hypersensitive mutant J942148 growth rate of 0.785 was not significantly different to 'WT'.

To eliminate the possibility that the hypersensitivity observed is the consequence of a reduced growth rate alone, paromomycin sensitivity experiments utilising a reduction in the incubation temperature and the presence of a drug (eugenol) were performed to mimic the slower growth rate seen in the hypersensitive mutants compared to the wild type.

Slow growth observed in the HS-R (growth rates; 0.501 and 0.542) was mimicked through incubation at 24°C, with a mean growth rate of 0.515 (Figure 4.5A+C). Upon exposure to 50 mg ml^{-1} paromomycin, strain SC5314 grown at 24°C showed a small delay to growth, but some delay was also apparent at 37°C and growth was not strongly inhibited in either case. It must be mentioned that reducing temperature is not an ideal method to mimic slow growth as metabolism would be effected and could have other harmful defects aside from

drug detoxification. Moreover, the presence of eugenol (EUG) at 1.5 mM (Figure 4.5B) also reproduced a slow growth rate of 0.519 as observed in the hypersensitive mutants (Figure 4.5C) and the addition of paromomycin 50 mg ml^{-1} delayed the onset of growth. Yet, here again, the subsequent growth rate of strain SC5314 was barely affected versus the minus-paromomycin condition. Taken together, the data suggest a slight sensitization to paromomycin but not full inhibition, indicating that slow growth alone is not the sole determinant of the HS-R phenotype.

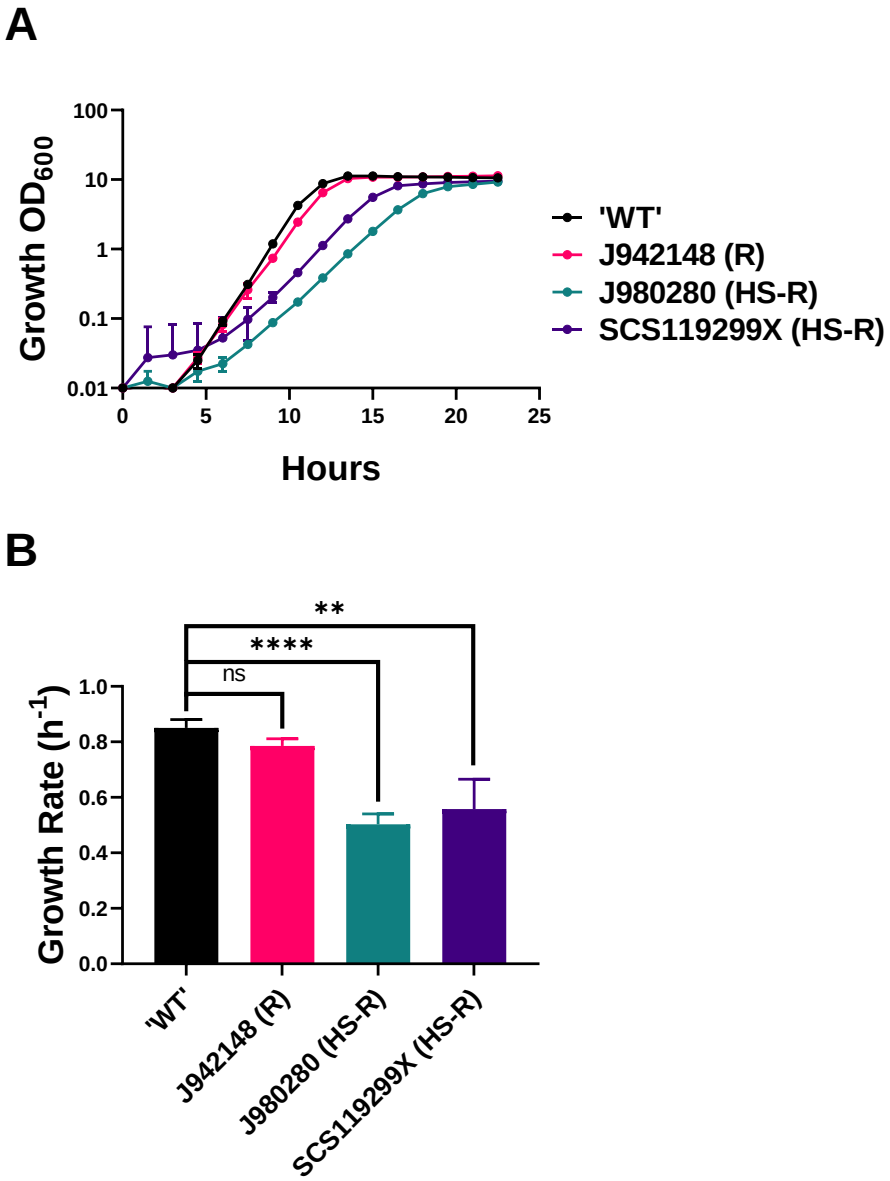

Figure 4.4. Delayed growth in aminoglycoside-hypersensitive mutants revealed through growth assays. (A) Growth curves based on OD_{600} across a 24-hour growth period. Cells were added at a starting OD_{600} of 0.01 and incubated in YPD (+ 2% glucose) at 37°C with shaking. Each point represents the mean of three independent experiment, ±SD. (B) Growth rate of each strain or isolate calculated as [(ln (2) / doubling time); where doubling time is calculated by (-0.301*3) / ($logOD_i$ -$logOD_f$) (the "3" corresponds to "3h", $_i$ = initial OD_{600}, $_f$ = final OD_{600})] and plotted. Each bar represents the mean of three independent experiments, +SD. (R)- azole-resistant, (HS-R)- hypersensitive and azole-resistant. Data statistically assessed using unpaired t-tests: ns, not significant, ** $p < 0.01$, **** $p < 0.0001$.

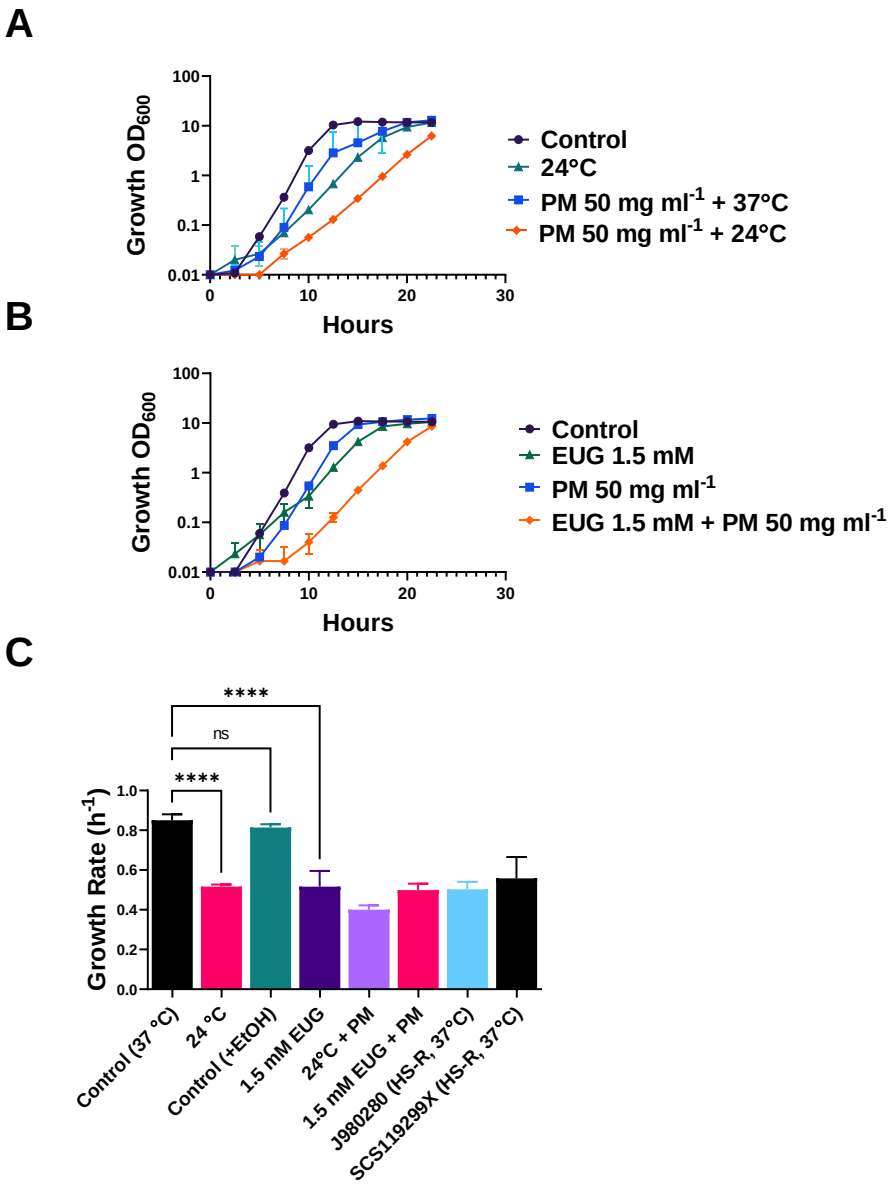

Figure 4.5. Slow growth in hypersensitive mutants is insufficient to explain paromomycin sensitivity. (A+B) Growth curves based on OD_{600} across a 24-hour growth period. Cells were added at a starting OD_{600} of 0.01 and incubated in YPD at 37°C with shaking in the conditions specified, where the final concentration of EtOH was 0.3%. PM = paromomycin, EUG = eugenol. Each point represents the mean of three independent experiments, ±SD. (C) Growth rate of strain SC5314 in each condition calculated as [(ln (2) / doubling time); where doubling time is calculated by (-0.301*3) / ($logOD_i$ -$logOD_f$) (the "3" corresponds to "3h", $_i$ = initial OD_{600}, $_f$ = final OD_{600})] and plotted. (HS-R)- hypersensitive and azole-resistant. Data statistically assessed using a One-way ANOVA with Dunnett's Multiple Comparisons post-hoc test ; ns, not significant, **** $p < 0.0001$.

4.3.3 Aminoglycoside sensitivity persists in azole-resistant *Aspergillus fumigatus*

Azole resistance is present in multiple fungi across clinical and agricultural disciplines. One example is in the filamentous fungal pathogen of humans, *A. fumigatus*, where azole-resistance is an increasing clinical burden. Due to this, mechanisms of azole resistance have been well-studied to assist with management strategies (Verweij et al., 2016). Two azole-resistant isolates with defined mutations in *CYP51* (isolate 3216; *CYP51*^{TR34,L98H} and isolate 4003 (*CYP51*^{TR46,Y121F,T289A}) [TR = tandem repeat number within the promoter, and amino acid changes in *CYP51*, for 3216; lysine to histidine at codon position 98 and for 4003; tyrosine to phenylalanine at codon position 121 and threonine to alanine at position 289]) were used to assess if the spectrum of aminoglycoside hypersensitivity is present outside of *C. albicans.*

Despite the azole-resistance mutations, both mutants grew comparably to the 'WT', just with isolate 3216 potentially showing a slight reduction in growth (Figure 4.6A). Aminoglycoside sensitivity was tested using paromomycin and hygromycin. Sensitivity to paromomycin is not shown in Figure 4.6B because at the highest usable concentration of 50 mg ml^{-1} no sensitivity was seen across all tested isolates. This does not rule out that hypersensitivity is present compared with the WT, just that it is not distinguishable at attainable concentrations. Consistent with all of the *C. albicans* isolates, sensitivity to hygromycin was evident in the two azole-resistant *A. fumigatus* mutants, with growth inhibited at a concentration approximately half that which was inhibitory to the 'WT' (Figure 4.6B). This is suggestive that azole resistance, governed by distinct changes in *CYP51* render the pathogen more sensitive to an aminoglycoside, hygromycin.

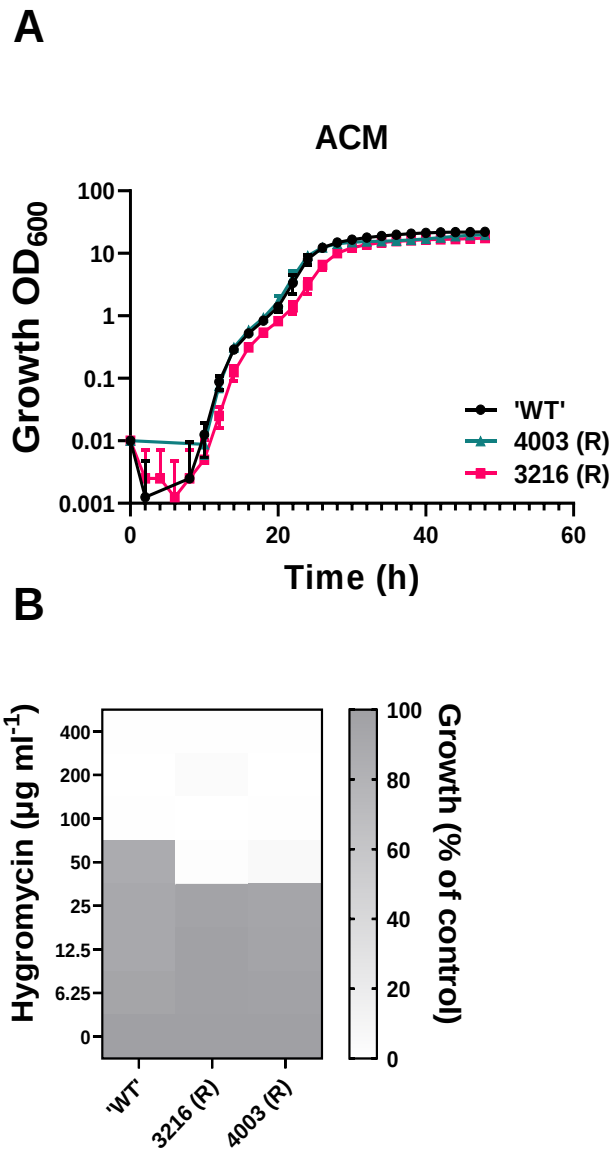

Figure 4.6. Aminoglycoside sensitivity present in azole resistant *A. fumigatus.* (A) Growth assessment of *A. fumigatus* wild-type (WT), and two azole-resistant isolates (3216 and 4003) in ACM liquid medium across a 48-hour period. Each point represents the mean of three independent experiments. Error represents ±SD. (B) Growth assessment of the *A. fumigatus* (sensitive/resistant) isolates in the presence of the aminoglycoside hygromycin over a 2-fold dilution series. Growth was determined after 48 h static incubation at 37°C using changes in OD_{600} compared to a drug-free control. Heat maps represent the mean from three independent experiments. (R)- azole-resistant.

4.3.4 Hypersensitivity phenotype is not universal, but specific to agents that act within the cell

The hypersensitivity profile of CS in bacterial pathogens is often linked to a particular process or function within the cell (Pal et al., 2015). Interference of these processes or functions can give rise to hypersensitivity to several, unrelated agents. To assess if the CS seen in the *C. albicans* azole-resistant mutants was specific to aminoglycosides, multiple agents were tested with various molecular targets and different mechanisms of action (MOA) upon the cell. The MOAs and sensitivity profiles from this experiment are listed in Table 4.4 and raw data for each compound can be found in Appendix C (C.8).

Interestingly, the HS-R phenotype was present in agents outside the aminoglycosides (paromomycin/hygromycin/streptomycin). Hypersensitivity was also consistently specific to the two azole-resistant mutants J980280 and SCS119299X (as for the aminoglycosides in Figure 4.2), with these isolates showing hypersensitivity to chloroquine, cyprodinil and azoxystrobin (Table 4.4). These compounds are from different groups of chemicals to aminoglycosides but, similarly, act intracellularly and therefore require transport across the cell membrane.

The compounds where there was no hypersensitivity include doxycycline, cycloheximide and tavaborole which are also drugs that act inside the cell, as well as caspofungin and amphotericin B which do not need uptake across the cell membrane for their actions. The results are consistent with particular intracellular target(s) or action(s) that account for the hypersensitivity. Alternatively, the hypersensitivity could arise from increased entry of specific drugs as a consequence of azole-resistance. As discussed in the introduction, mutations in *ERG11* can provide resistance to azoles through an alteration to the protein which exhibits a reduced affinity for azole binding (Whaley et al., 2017). Such protein alteration could possibly also influence mechanisms of drug transport.

Compound	Mode of Action	Sensitivity
Paromomycin Hygromycin Streptomycin	Binds to the ribosomal 40S subunit, prevent ribosomal translocation & compromise translational fidelity (Tuite and McLaughlin, 1984)	Increased (J980280 & SCS119299X)
Chloroquine	Alkalinisation of the host environment & iron depletion (Levitz et al., 1997)	Increased (J980280 & SCS119299X)
Sodium chromate	Induce translation errors by limiting sulphur-containing amino acid availability (Holland et al., 2010)	Increased
Doxycycline	Inhibition of protein synthesis when in combination with amphotericin B (El-Azizi, 2007)	None
Cycloheximide	Bind E-site of 60S ribosomal subunit inhibiting translation elongation (Schneider-Poetsch et al., 2010)	None
Tavaborole	Leucine tRNA synthetase inhibitor (Rock et al., 2007)	Increased in J980280
Cyprodinil	Potential methionine biosynthesis inhibitor (under investigation) (Mosbach et al., 2017)	Increased (J980280 & SCS119299X)
Caspofungin	Inhibit the FKS enzyme, preventing 1,3-β-D-glucan synthesis in cell wall (Balashov et al., 2006)	None
Amphotericin B	Bind ergosterol, cause pore formation, cell leakage (Andreoli and Monahan, 1968)	Reduced
Azoxystrobin	Inhibit mitochondrial respiration through binding the Qo site of cytochrome b, prevent ATP synthesis (Bartlett et al., 2002)	Increased (J980280 & SCS119299X)
Thialysine	Toxic analogue of lysine, inhibits protein synthesis (Parsons et al., 2006)	None

Table 4.4. Compounds tested to assess the sensitivity profile of the azole-resistant mutants compared to growth of 'WT' *C. albicans*. Sensitivity was classified as, increased, none or reduced. This represents significantly less growth, no significant difference or significantly more growth respectively when compared to strain SC5314 ('WT') exposed to the same concentration, $p < 0.05$. Raw data can be found in Appendix C, C.8., statistically analysed data in C9. The experiments were performed in technical triplicate for three biological experiments.

4.3.5 *ERG11* sequencing reveals the same non-synonymous SNP is present in hypersensitive mutants

Azole-resistance in *C. albicans* has multiple mutational origins. A major source of resistance is found in the synthesis of ergosterol (increased expression/mutations in *ERG11*), and another significant origin is that of increased drug efflux (Cowen et al., 2014). DNA sequencing of azole-resistant clinical isolates of *C. albicans* reveals a multitude of point mutations in the coding region of the *ERG11* gene (orthologous with *CYP51* in *A. fumigatus*) which is unsurprising as it is the target site of azole drugs in the role of inhibiting ergosterol biosynthesis (Ksiezopolska and Gabaldon, 2018). Many of these mutations have been predicted to occur within the catalytic site of the enzyme, thus rendering the azole unable to bind the Erg11 protein (Flowers et al., 2015). In the present work, it was decided to sequence the *ERG11* gene from the WT (lab strain SC5314) and the three azole-resistant mutants used in the hypersensitivity profiling above. The primers used for this are listed in Table 4.2. Analysis of the sequences obtained revealed two non-synonymous single nucleotide polymorphisms (SNP) in the coding region of the gene present in the azole-resistant strains compared with the online reference strain (*C. albicans* SC5314 Assembly 22) and our own laboratory SC5314 strain, these amino acid substitutions are highlighted in Figure 4.7 and the raw sequencing data can be found in Appendix C, C.4.

The first amino acid substitution discovered was at codon position 405, where serine was substituted with a phenylalanine (S405F) in both of the HS-R mutants SCS119299X and J980280. This change in amino acid is an important change in functional group and influences protein (O-linked) glycosylation and hydrophobicity. In both mutants the SNP of a cysteine to thymine at nucleotide position 1214 (C1214T) is responsible for the amino acid change. This mutation has been reported in the literature as a marker of azole resistance in *C. albicans* (Xu et al., 2008, Wang et al., 2009, Flowers et al., 2015, Warrilow et al., 2019). The S405F mutation has also been reported in two azole-susceptible isolates, suggestive that in these cases other acting mutations such as *ERG11*

downregulation may be present and responsible for the susceptibility phenotype (Oliveira-Carvalho and Del Negro, 2014). The two isolates harbouring the S405F variant (SCS119299X and J980280) are azole-resistant evidenced by elevated resistance to tebuconazole (Figure 4.2), consistent with S405F being involved in the resistance.

A second non-synonymous SNP is seen in the non-hypersensitive mutant, J942148 as a glycine to glutamic acid substitution at codon position 448 (G448E). The change in nucleotide is seen in a change from guanine to alanine at position 1343 in the coding region (G1343A), shown in Appendix C, C.4. This SNP has also been reported to confer azole-resistance in *C. albicans* (Xu et al., 2008, Wang et al., 2009, Xiang et al., 2013, Flowers et al., 2015, Warrilow et al., 2019). Despite being azole-resistant the isolate does not present CS. Both of the identified mutations exist in a 'hotspot' of mutation in the Erg11 protein, between residues 405-488, and are predicted to occur in the enzyme's catalytic site (Marichal et al., 1999, Flowers et al., 2015).

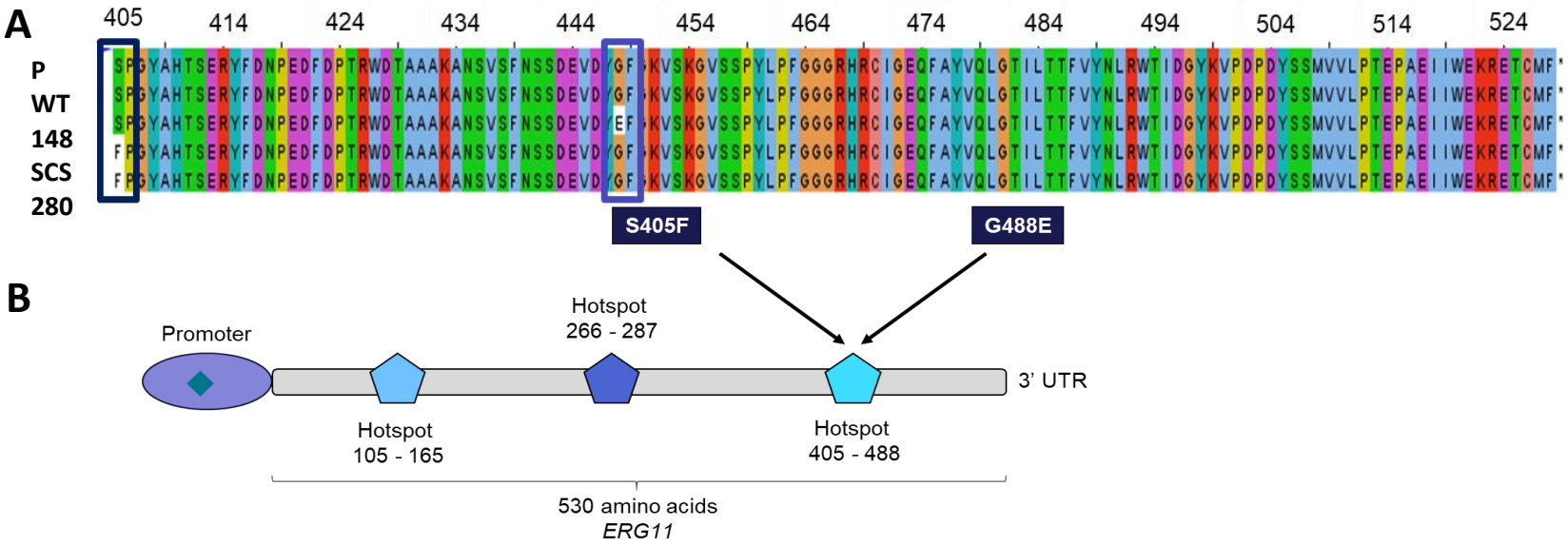

Figure 4.7. Hypersensitive mutants share the same mutation in *ERG11*. (A) Amino acid alignment from codon position 405 of the *ERG11* ORF (to the stop codon at position 529). Each row of alignment represents a different isolate: (P) published SC5314 wild-type; (WT) wild-type (laboratory strain SC5314) were used as controls, compared with azole-resistant isolates; (148) J942148, (SCS) SCS119299X and (280) J980280. The alignment was coloured with Clustal annotation in Jalview software. Two non-synonymous SNPs highlighted, S405F occurs in both the SCS119299X and J980280 isolates, indicated by the navy box. The other SNP, G448E is present only in strain J942148 shown outlined by a purple box. (B) *ERG11* gene outline with indicated hotspots of mutation, including the two mutations identified from the sequencing data, S405F and G488E which are both present in the third hotspot region of the gene. Raw DNA sequences for the *ERG11* sequencing are found in Appendix C, C.4.

4.3.6 Strains engineered with the SNP of interest do not show hypersensitivity

The DNA sequencing results revealed a common SNP in both of the HS-R isolates, an amino acid change of serine to phenylalanine arising from a through the nucleotide change of cysteine to thymine at position 1214. It was decided to assess whether this SNP could be involved in the observed aminoglycoside hypersensitivity phenotype. To address this question, strains were kindly provided by Professor Rogers (St. Jude Children's Research Hospital, Tennessee) that were constructed from a study investigating different SNPs in *C. albicans* and their involvement in azole-resistance (Flowers et al., 2015). In their work, strains were constructed in the strain SC5314 background, where both copies of *ERG11* were mutated with the SNP of interest. For the S405F amino acid change, strain SC5314 was modified with the C1214T mutation, giving strain 21C1M1A1. Moreover, to investigate the mutation of the isolate that was not hyper-sensitive, a strain carrying the glycine to glutamic acid substitution at position 448 (strain 20NA11A57A) was also provided. The strains *ERG11* gene was sequenced (using the primers listed in Table 4.2) to confirm the received strains were as requested (Appendix C, C.4 and C.5.). The received strains were also confirmed to possess azole resistance using the CLSI method outlined in the Flowers et al (2015) paper (MICs found in Appendix C, C.6).

The strains possessing mutated copies of the *ERG11* gene, 21C1M1A1 (S405F) and 20NA11A57A (G448E) were assessed for their paromomycin sensitivity (Figure 4.8). It was concluded that the S405F mutation of interest did not confer hypersensitivity when placed into the SC5314 background as the 20NA11A57A strain did not show any increased paromomycin (PM) sensitivity compared with the background SC5314. This result indicates that despite the HS-R mutants sharing a common SNP, this mutation alone is not sufficient for hypersensitivity to paromomycin (at least not in any strain background) and could benefit from whole genome sequencing to identify other potential resistance mechanisms

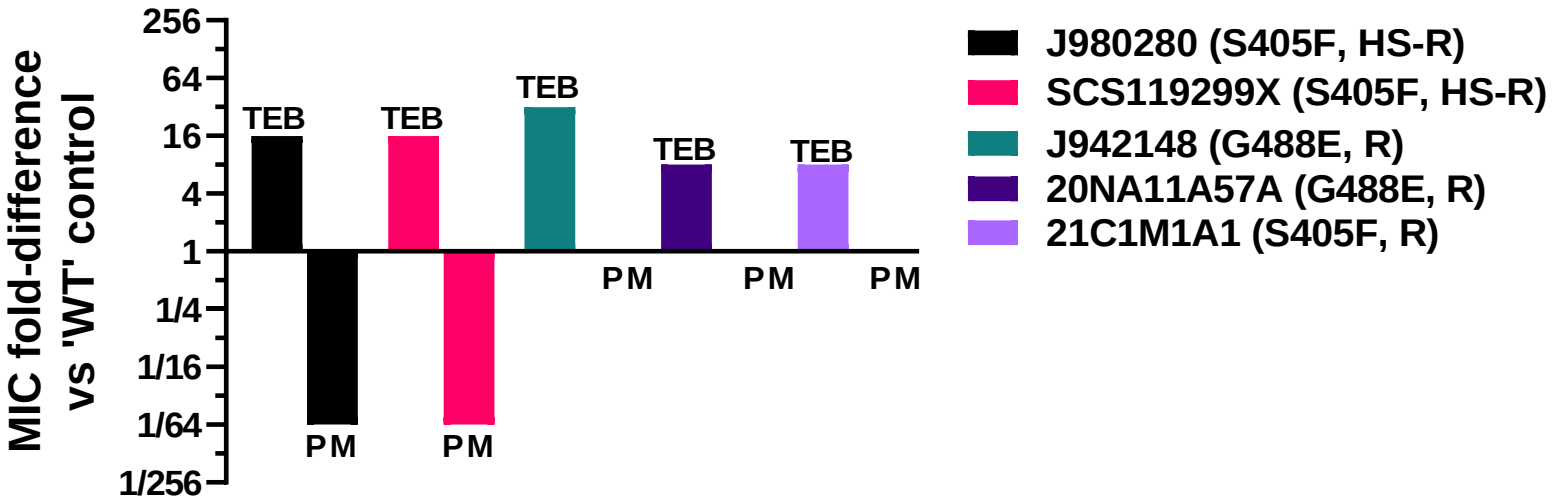

Figure 4.8. Sensitivities of three azole-resistant isolates and two engineered strains of *C. albicans* to paromomycin and tebuconazole calculated as a fold change in the minimum inhibitory concentration (MIC) compared with the laboratory wild-type (SC5314). An increase in the MIC to tebuconazole is observed across all strains as confirmation of azole resistance. Hypersensitivity to the aminoglycoside is seen in isolates J980280 and SCS119299X but absent from isolate J942148 and the two engineered strains. TEB = tebuconazole, PM = paromomycin. MIC fold change calculated from the average of three independent experiments. (S405F) = serine to phenylalanine at codon position 405 in *ERG11*, (G488E) = glutamic acid to glycine at codon position 488 in *ERG11*. (HS-R)- hypersensitive and azole-resistant, (R)- azole-resistant. Raw MIC data can be found in Appendix C, C.6.

4.3.7 Rhodamine 6G uptake as a proxy for drug uptake did not identify differences between isolates

Further potential phenotypic differences between the isolates were considered. Bacterial mechanisms of CS, as discussed in the introduction, have been grouped into two, with one of these main mechanisms being increased uptake inside the cell of the compound producing sensitivity (Roemhild et al., 2020). Therefore, the general uptake capabilities of the strains were examined using rhodamine 6G (R6G) and flow cytometry. R6G was implemented as a proxy for general uptake and was chosen due to previous use in uptake and efflux dynamics (Maesaki et al., 1999, Revie et al., 2022). A time course assay with the laboratory wild type (SC5314) was performed to establish the most appropriate incubation times for further analysis (see Appendix C, C.7). It was evident that five minutes of incubation with R6G was enough to observe uptake, as additional incubation did not appear to further increases in cellular R6G fluorescence.

The results in Figure 4.9A display the median fluorescent intensity (MFI) peaks from one representative biological replicate. The mean of four independent MFI values for each strain or isolate was plotted as a percentage of that obtained for the SC5314 strain, which was considered the wild-type (Figure 4.9B). The J942148 (R) isolate consistently exhibited a markedly lower R6G uptake compared with the SC5314 (S) strain. For the two aminoglycoside-hypersensitive isolates, SCS119299X (HS-R) and J980280 (HS-R), R6G uptake was at an intermediate level between the WT and J94218 strains. The biological replicates also revealed variability in the R6G uptake by these isolates, shown by the large SEM bars. Due to the variation in the experiments it made it difficult to evaluate potential uptake effects in these isolates. However, because uptake was not consistently elevated in the hypersensitive strains, it was concluded that uptake could not be assigned as a/the primary factor explaining the hypersensitivity phenotype using this assay. For corroboration of this, uptake of the drugs (e.g. hygromycin) themselves would

be assayed, but there was not a feasible means to do this within the timeframe of the project.

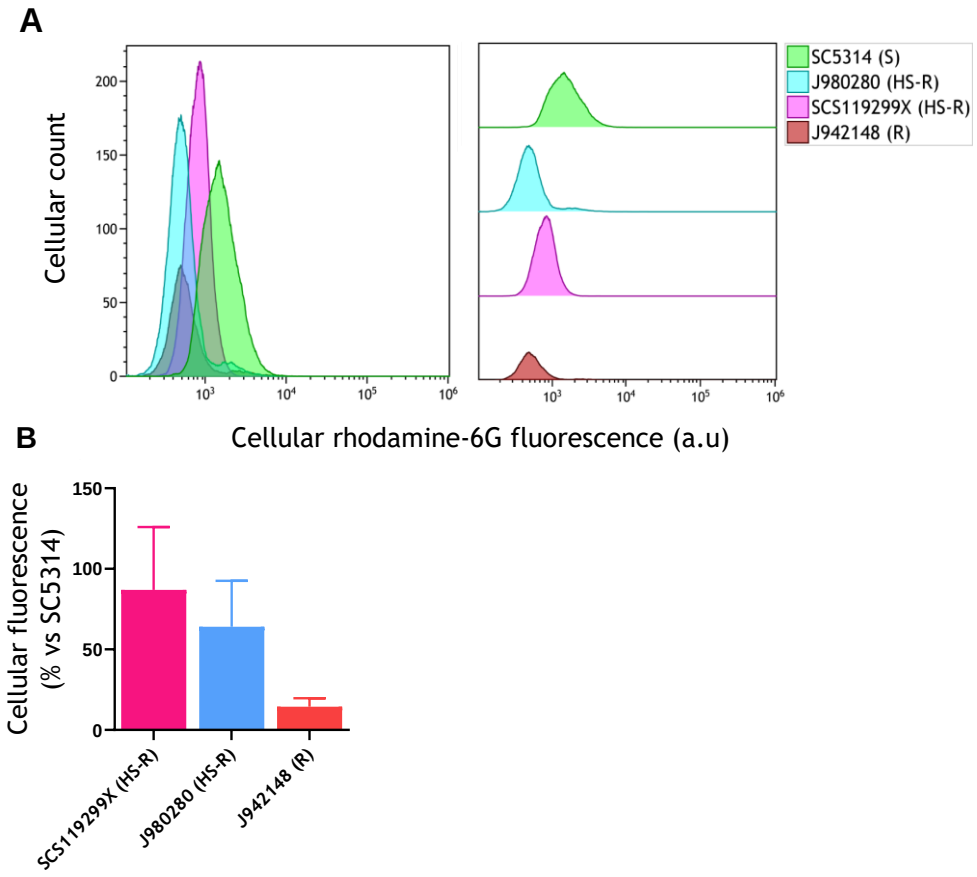

Figure 4.9. Rhodamine-6G uptake in *C. albicans* cells across a five minute incubation time analysed through flow cytometry. (A) Flow cytometric peaks from one biological repeat assessing cellular fluorescence using the rhodamine-6G probe with an incubation time of five minutes at a cell concentration of OD_{600} 2.0 in YP (+ 2% glucose) medium. The samples were then washed three times in PBS and kept on ice before analysis. Fluorescence was quantified by analysing 20,000 cells using a Beckman Coulter FC500, FITC filter. Analysis was performed in Kaluza software. (B) Data from four biological replicates expressed as a percentage of cellular fluorescence compared with SC5314 (as 100%). The data show the mean fluorescence from four independent experiments, +SEM. (R)- azole-resistant, (S)- azole sensitive and (HS-R)- hypersensitive and azole-resistant.

4.3.8 Testing of additional azole-resistant clinical isolates and 'WT' isolates for paromomycin hypersensitivity

In order to establish the incidence of paromomycin hypersensitivity amongst *C. albicans* clinical isolates, an additional ten isolates were tested. Several of the isolates had known mutations in the *ERG11* gene which were previously discussed (S405F and G448E) with an additional four isolates possessing azole-resistance (kindly provided by Dr. Donna MacCallum). In addition, it was decided to assess the paromomycin sensitivities of clinical isolates with no known drug-resistance, referred to here as additional 'wild type' controls, including DSM 6959, ATCC 48867, ATCC 26790 and ATCC 10231.

All strains outlined in Figure 4.10 were exposed to 50 mg ml^{-1} paromomycin and OD_{600} was used to assess growth across a 48-hour period. Incubation with the aminoglycoside paromomycin highlighted the striking hypersensitivity in HS-R J980280 and SCS119299X clinical isolates, which were unable to grow in this condition across the 48 h period. The results from the additional ten azole resistant isolates tested showed that paromomycin sensitivity is not a ubiquitous phenotype among azole resistant clinical isolates. In addition, minor paromomycin sensitivity is seen in the 'wild type' control DSM 6959 which has no reported drug sensitivities. It is worth noting that the DSM 6959 strain also possesses a reduced growth rate compared with the laboratory strain, as do the hypersensitive mutants, although it was shown above that this trait alone is not sufficient to account for aminoglycoside hypersensitivity.

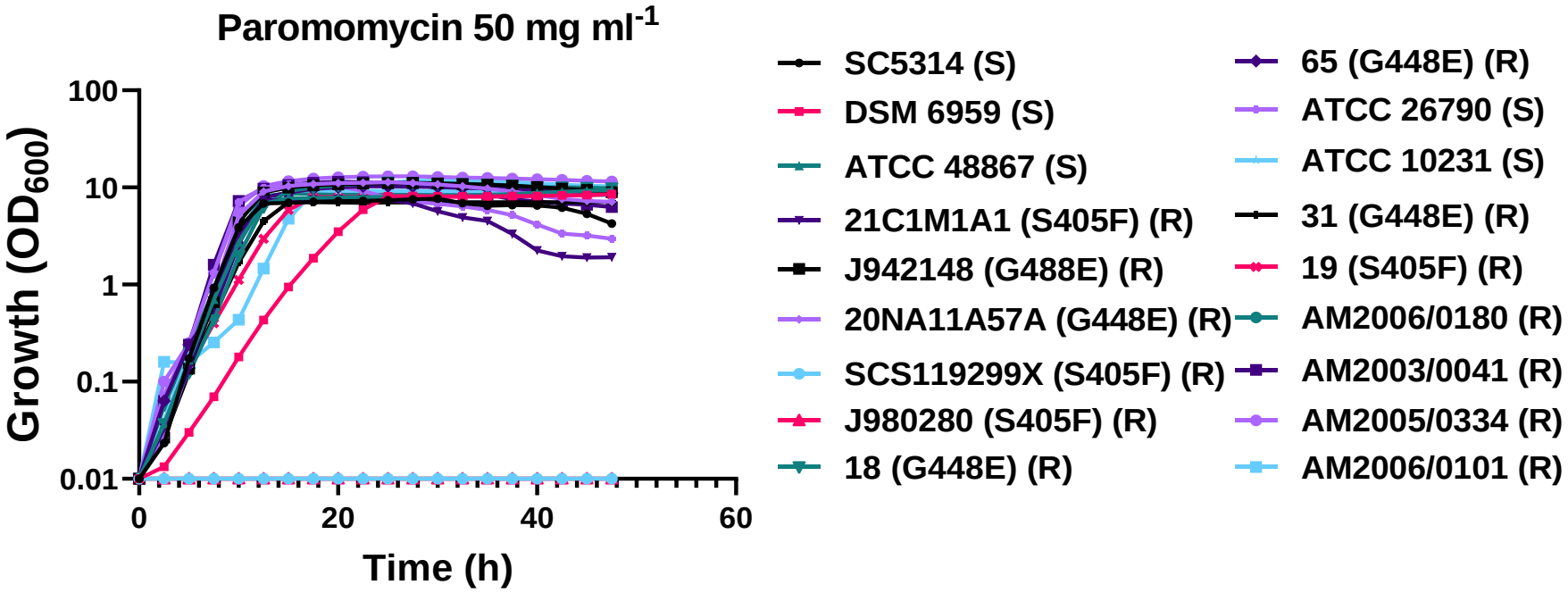

Figure 4.10. Paromomycin sensitivity assay with additional *C. albicans* strains and isolates both azole-sensitive (S), azole-resistant (R) and hypersensitive and azole-resistant (HS-R). Growth curves for the *C. albicans* strains in YPD with the inclusion of 50 mg ml^{-1} paromomycin. Each point represents the mean of three independent experiments ±SEM (error bars did not exceed dimensions of symbols).

4.3.9 Inhibition of glycosylation renders *S. cerevisiae* cells hypersensitive to aminoglycoside treatment

In the investigation into the mechanism behind hypersensitivity to aminoglycosides in the two azole resistant mutants, a previous study was noted in which *S. cerevisiae* mutants that are defective in glycosylation (an important post-translational modification) showed an aminoglycoside hypersensitivity phenotype (Dean, 1995). In their study, mechanistic elucidation of the hypersensitivity involved preincubation with tunicamycin which inhibits N-linked glycosylation (acts in the endoplasmic reticulum, blocking the formation of the protein-carbohydrate N-glycosidic linkage). This preincubation (inhibiting glycosylation) reproduced a hypersensitivity to aminoglycosides in wild-type *S. cerevisiae*. Consequently, it was hypothesized that a possible glycosylation defect in the two HS-R *C. albicans* mutants could explain their aminoglycoside hypersensitivities.

Supporting the hypothesis, when combined in *S. cerevisiae*, tunicamycin potentiated the effect of paromomycin creating a strong synergistic reaction (Figure 4.11A). This interaction was reflected by an FICI value (calculation described in Collateral sensitivity (CS) assays, hit validation and checkerboard assays) of ≤ 0.063, indicative of strong synergy. However, in *C. albicans* SC5314 this result was not reproduced, and an additive relationship was suggested by the data (FICI ≤ 0.75). An MIC value in *C. albicans* was not reached at the highest concentration attainable for either compound alone, so the FICI value reflects a maximum rather than absolute value and it cannot be ruled out that synergy is present. To assess if the effect was paromomycin-specific or was associated with other members of the aminoglycosides, hygromycin B was also used in combination with tunicamycin. Tunicamycin also produced strong synergy with hygromycin B against *S. cerevisiae,* with a FICI value of 0.094 (Figure 4.11B). Interestingly in *C. albicans*, tunicamycin did sensitise the cells to hygromycin B with a synergistic FICI value of 0.375. Taken together this data suggests that perturbation of glycosylation (through the application of tunicamycin) does sensitise cells to treatment by aminoglycosides, in particular hygromycin B.

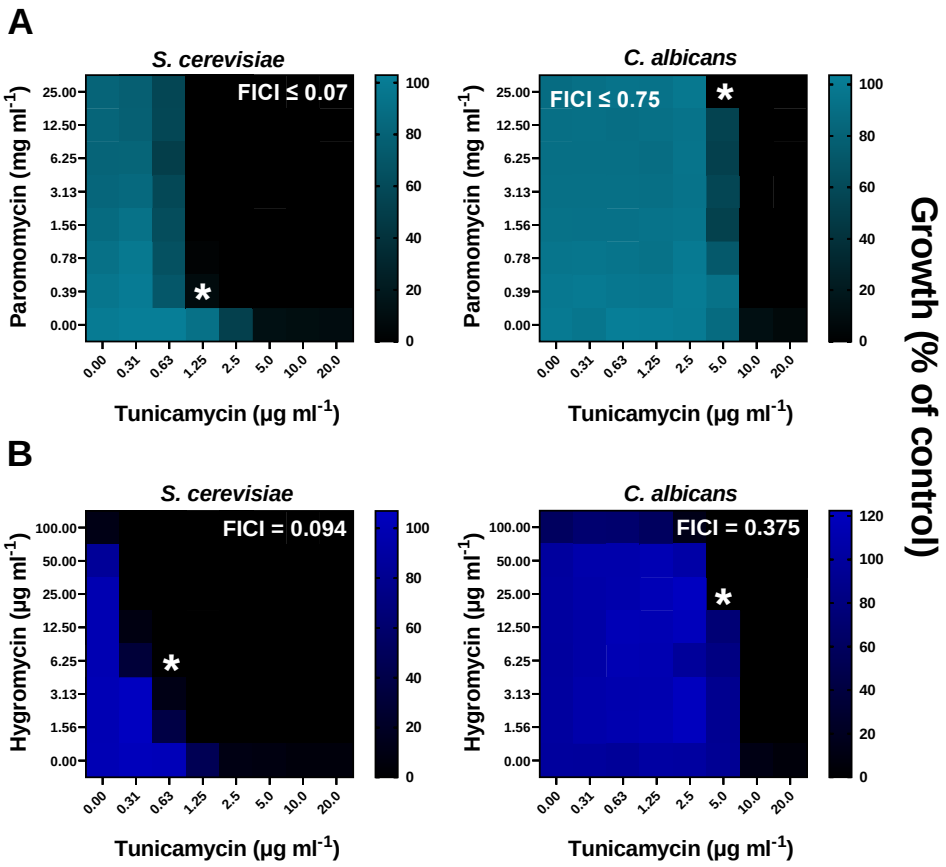

Figure 4.11. Checkerboard analysis of aminoglycosides combined with tunicamycin in laboratory strains of *S. cerevisiae* and *C. albicans*. Checkerboards were performed as per EUCAST guidelines in YPD. Growth was measured using OD_{600} after 24 h incubation at 30°C for *S. cerevisiae* and 37°C for *C. albicans*. Changes in OD_{600} were calculated as a percentage of growth compared with the solvent control. (A) Combination of paromomycin and tunicamycin, in *S. cerevisiae* strain W303 and *C. albicans*, strain SC5314. The FICI values are indicated (calculated as described in "Collateral sensitivity (CS) assays, hit validation and checkerboard assays".) (B) Hygromycin combined with tunicamycin. Each heat map represents the mean of three independent experiments and the * symbol indicates the drug concentrations at which FICI values were calculated.

To corroborate the above effect, the hygromycin and tunicamycin combination was evaluated in the three initial azole-resistant isolates used in this study, including the two aminoglycoside-hypersensitive strains. Checkerboard assays revealed synergy between the compounds in strain J942148, the azole-

resistant but not aminoglycoside hypersensitive strain, with an FICI value of 0.375 (Figure 4.12). In contrast, the two HS-R isolates (J980280 and SCS119299X) did not show synergy, with FICI values of 1.0 and 2.0. One possible explanation for this, consistent with the hypothesis, is that possible glycosylation defects of these particular strains preclude any further inhibitory effect of tunicamycin on glycosylation, so nullifying the potential for tunicamycin to synergise with the aminoglycosides.

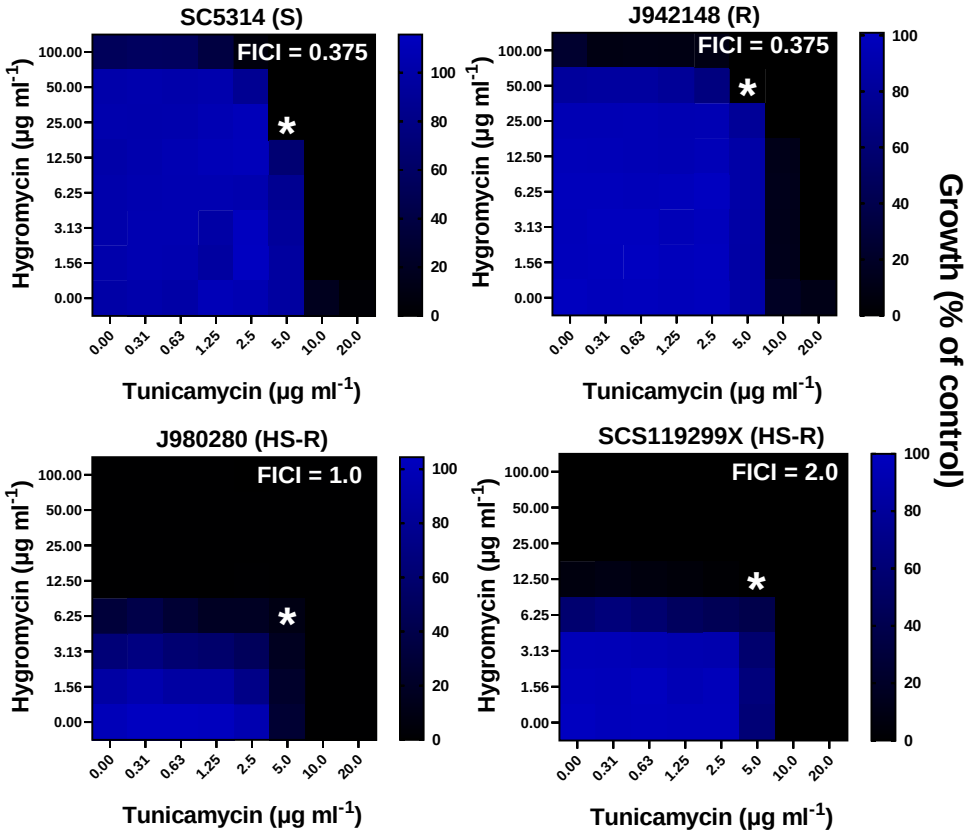

Figure 4.12. Checkerboard analysis of hygromycin combined with tunicamycin against different isolates of *C. albicans*. Checkerboards were performed as per EUCAST guidelines in YPD (+2% glucose). Growth was measured using OD_{600} after 24 h incubation at 37°C calculated as a percentage of growth compared with the solvent control. Each heat map represents the mean of three independent experiments and the * symbol indicates the drug concentrations at which FICI values were calculated for each strain tested. (S) Indicates azole-sensitive, (R)-resistant and (HS-R) hypersensitive and azole-resistant.

4.3.10 Aminoglycoside-hypersensitive isolates exhibit defects in cell wall integrity and possibly glycosylation

The above data with tunicamycin hinted towards the possibly that cell wall glycosylation could be at least partly defective in the aminoglycoside-hypersensitive strains. Cell wall targeting agents have been utilised for characterisation of cell wall glycosylation defects (Hall and Gow, 2013). One example is from Prill et al (2005) where hypersensitivity of *C. albicans* to Congo red and calcofluor white, targeting glucan and chitin synthesis respectively, were used as an indicator of cell wall glycosylation defects as a consequence of mutations in *PMT1* and *PMT2.* These genes are required for the initiation of O-linked glycosylation (Prill et al., 2005). Therefore, here, the sensitivity towards these agents was tested with *C. albicans* SC5314 (wild-type), J942148 (azole-resistant), J980280 and SCS119299X (hypersensitive and azole-resistant, HS-R). The data revealed that both of the (HS-R) isolates were significantly more sensitive than the other tested strains to both Congo red (Figure 4.13A) and calcofluor white (Figure 4.13B) with at least an 8-fold and 2-fold respective increase in sensitivity (absolute increase in sensitivity unknown because the minimum inhibitory concentration could not be attained in strain SC5314). This finding further supported the possibility that aminoglycoside-hypersensitivity in the two azole-resistant mutants may be linked to defects in cell wall glycosylation or cell wall integrity.

To further assess a role for glycosylation defects in the HS-R phenotype of the isolates, the exposure of β-(1,3)-glucan on the cell wall was considered. It is well known that the masking of β-(1,3)-glucan through protein glycosylation in *C. albicans* is linked to pathogenicity and virulence through the prevention of host-recognition (Gomez-Gaviria et al., 2021). In the present study, the levels of exposed β-(1,3)-glucan were analysed using the C-type lectin receptor, Dectin-1, which recognises β-(1,3)-glucan (Brown and Gordon, 2001). According to immune-detection of Fc-Dectin-1, the HS-R isolates had significantly less exposed β-(1,3)-glucan on the cell surface than the non-HS-R strains (Figure 4.14).

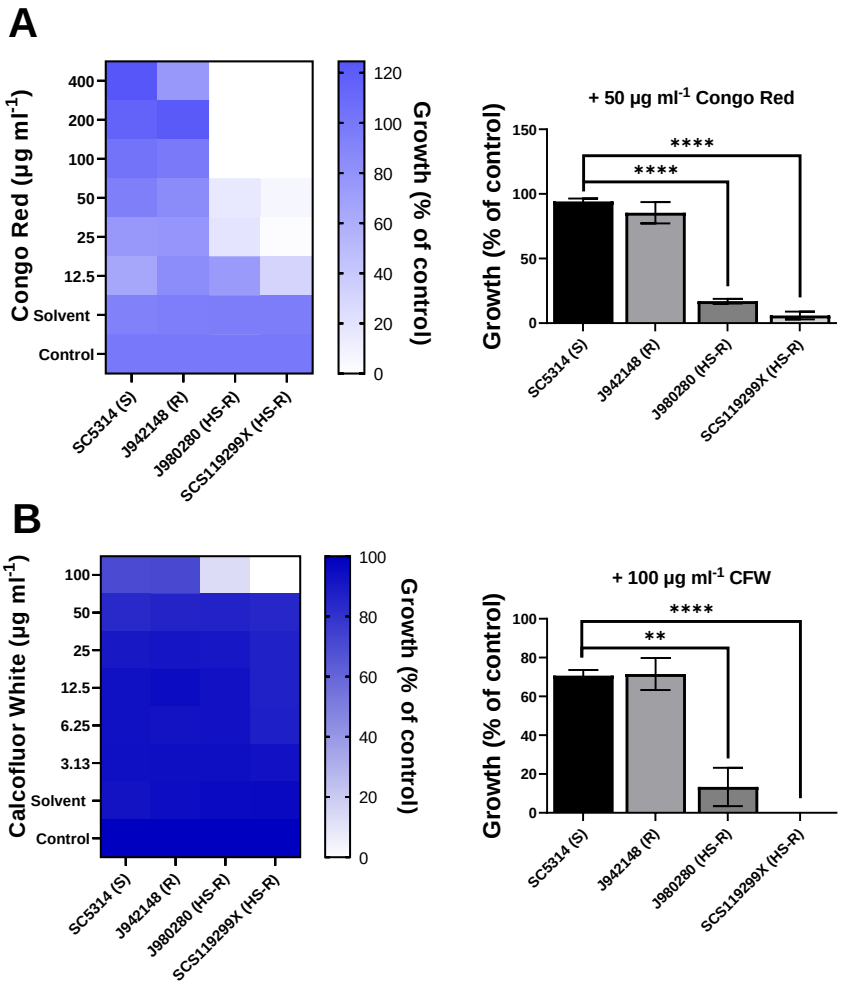

Figure 4.13. Sensitivity profiling of cell wall targeting agents against *C. albicans.* Analysis was performed in YPD (+2% glucose) and growth was measured using OD_{600} after 24 h incubation at 37°C, was calculated as a percentage of growth compared with the solvent control and plotted as a heat map. Each heat map represents the mean of three independent experiments. Bar height indicates growth expressed as a percentage of the solvent control. Unpaired t-tests were performed between SC5314 and the hypersensitive azole-resistant strains. (A) Sensitivity profiling to Congo red and (B) sensitivity profiling for calcofluor white (CFW). (S) Indicates azole-sensitive, (R)-resistant or (HS-R) implying hypersensitive and azole-resistant. Data statistically assessed using unpaired t-tests; ** $p < 0.01$, **** $p < 0.0001$.

The fluorescence histogram peaks are presented in Figure 4.14A and the median fluorescent intensity values (MFI, significantly reduced for the HS-R isolates) in Figure 4.14B. The data suggest decreased exposure of β-(1,3)-glucan in the HS-R mutants, contrary to expectation, and could indicate the isolates have less within the cell wall. To assess the composition of the cell wall in these isolates, additional experiments such as concanavalin-A or Alican blue staining would be a possible route of exploration . Microscopic images of the strain/isolates stained with Fc-Dectin-1 can be found in Appendix C (C.10).

To conclude, the mechanistic evaluation of aminoglycoside hypersensitivity in the azole-resistant mutants suggested a potential basis in cell wall integrity defects and possibly cell wall glycosylation defects. As inhibitors thought to target these functions were used to reach this conclusion, the relatedness of these inhibitors' actions was corroborated by assaying for synergy. As discussed earlier, Congo red and tunicamycin target glucan synthesis and N-linked glycan synthesis respectively (Prill et al., 2005, Hakulinen et al., 2017). The agents were combined according to EUCAST testing as described. The combination was strongly synergistic to *C. albicans* SC5314 with a highest possible FICI value of 0.188 (the actual FICI value could be lower; however the MIC of Congo red could not be reached) (Figure 4.15). This finding supports the conclusions as it helps corroborate that the two agents had related inhibitory actions in our hands, as expected.

As the collateral sensitivity (CS) angle originally pursued for the two HS-R isolates was not borne out, i.e., the hypersensitivity did not anti-correlate with azole resistance in a range of other isolates tested, it was decided at this stage of the project to stop the work on further characterisation of mechanistic bases in the two HS-R isolates and move the focus back to CS. The availability of the azole-resistant and sensitive *C. albicans* isolates was used next to cast the net wider for discovery of CS in this pathogen.

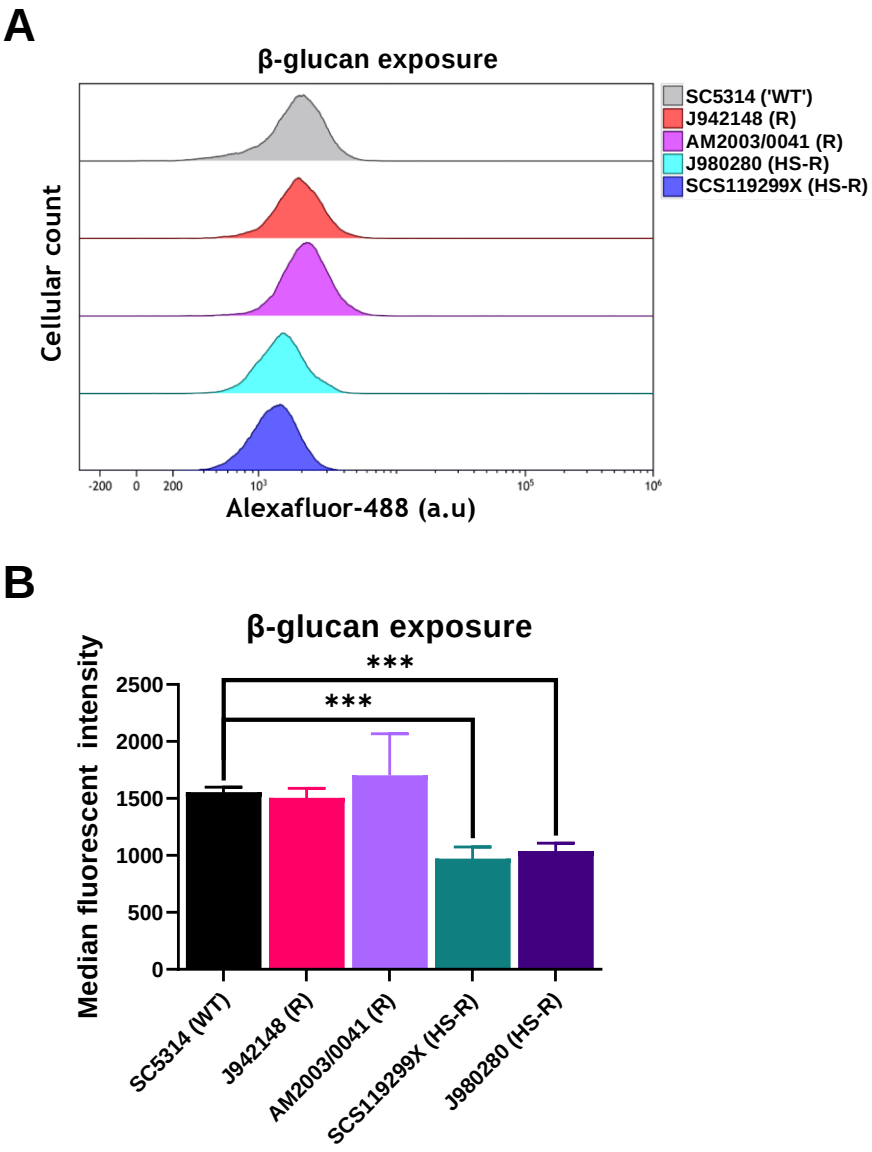

Figure 4.14. Assessment of exposed β-(1,3)-glucan through flow cytometric immune-detection of Fc-Dectin 1 staining. *Candida albicans* cells were grown to mid-exponential phase, fixed in 4% polyformaldehyde (PFA) and incubated with the primary antibody, Fc-Dectin 1 followed by an Alexafluor-488 (A-488) tagged secondary antibody. Flow cytometry was then used to quantify the levels of A-488 fluorescence for each strain. (A) Histogram peak data for each isolate. 10,000 cells were analysed per sample. Data were further analysed in Kaluza software. (B) Bar height indicates plotted median fluorescent intensity data; each bar represents the mean of three independent experiments. Error, + SD. WT = wild-type, R = azole-resistant, HS-R = hypersensitive, azole resistant. Differences statistically analysed using unpaired t-tests; *** $p < 0.001$.

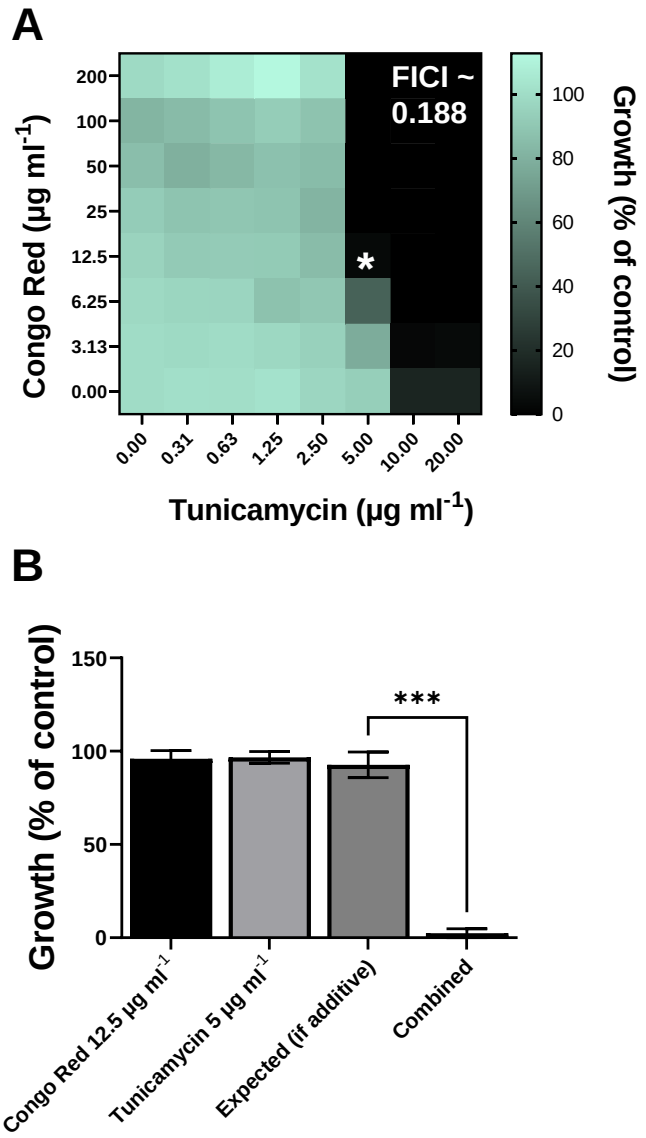

Figure 4.15. Congo red and tunicamycin act synergistically in combination against *C. albicans*. (A) Checkerboard analysis of the two agents in combination at the indicated concentrations in YEPD (+2% glucose) adhering to EUCAST guidelines. *Candida albicans* SC5314 growth was calculated as a percentage of the control well, where < 5 % growth was regarded as no growth. The heat map represents the mean of three independent experiments. (B) Percentage growth data plotted from the checkerboard format. Expected values calculated from the combined inhibition from Congo red of tunicamycin used in isolation. Bar height represents the mean of three independent experiments. Error ±SD. Unpaired t-test with *** $p < 0.001$.

4.3.11 Screening for collateral sensitivity against azole-resistant *Candida albicans*

High-throughput screening of FDA-approved chemical libraries is considered an effective way of enhancing and improving efficacy of existing antifungal treatments alongside the discovery of novel antifungal treatments (Siles et al., 2013). Related to this, screening of compound libraries has been an effective way of discovering compounds that are active against both drug-sensitive and -resistant fungal pathogens (Wall et al., 2018, Yousfi et al., 2020). Here, a high-throughput screening was adopted to see whether this approach could be applied to discover compounds that can selectively inhibit drug-resistant isolates/strains. The specific focus was on collateral sensitivity in the azole-resistant *C. albicans* isolates described earlier in this chapter, using a library of FDA approved compounds. As discussed in the introduction, azole-resistance in *C. albicans* is the result of multiple mutational origins. Therefore, to reduce the complexity of any findings from this screen it was decided to use azole-resistant mutants that possessed the same mutation, S405F, in the *ERG11* gene. Accordingly, two azole-sensitive (SC5314 and ATCC 48867) and two azole-resistant (21C1MA1 and J980280) strains/isolates were chosen to screen against the Prestwick Chemical library, containing 1280 FDA-approved compounds and used at final concentrations of 100 µM (Vallières et al., 2020).

The screen revealed that for most of the compounds, across both azole-sensitive and -resistant strains, there was no particular effect on growth of the library compounds at the concentration used in the screen (Figure 4.16). For assays with some chemicals, there was marked variability between the duplicates of the screen, and this was noted. The raw data for the screening can be found in Appendix C, C.11.

A small number of compounds which were strongly inhibitory (< 5% growth compared to solvent control) across both azole-resistant and azole-sensitive strains or isolates tested (Figure 4.17). Amongst these compounds were multiple azole-containing chemicals (miconazole, isoconazole, enilconazole, clotrimazole, sertaconazole), indicating the azole-resistant isolates/strains are

not resistant to all members of the azole family. Certain similar findings have been reported previously. For example, fluconazole-resistant strains have been reported to show susceptibility to other drugs of the azole family, e.g., miconazole (Isham and Ghannoum, 2010).

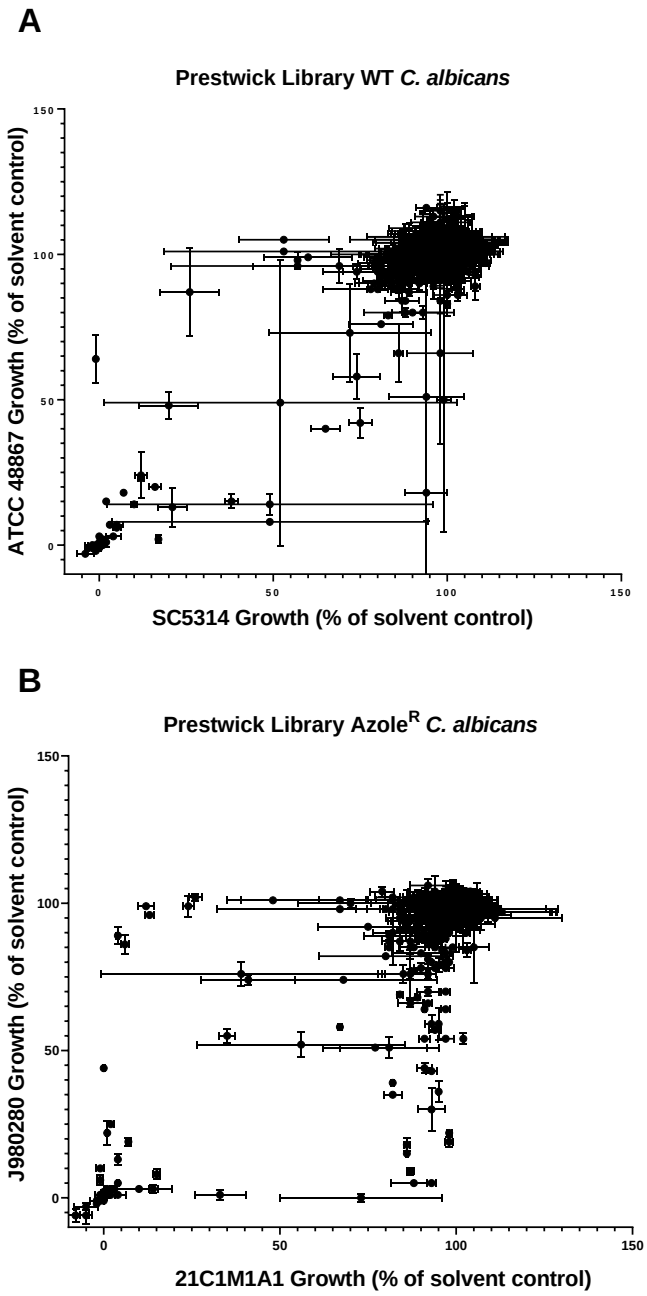

Figure 4.16. Prestwick chemical library screening against azole-sensitive (A) and azole-resistant (B) *C. albican*s. Growth is displayed as percentage growth compared to the drug-free (solvent only, DMSO) control. Each dot represents a compound from the Prestwick chemical library with growth of a sensitive (upper panel) or resistant (lower panel) strain or isolate on each axis to allow visualisation of reproducibility in strains harbouring similar susceptibilities. Screens were performed in YPD (+2% glucose) and OD_{600} was used as a growth measure across 24 h, compared to wells containing only the DMSO control. Each point is the mean of two independent experiments, ±SEM.

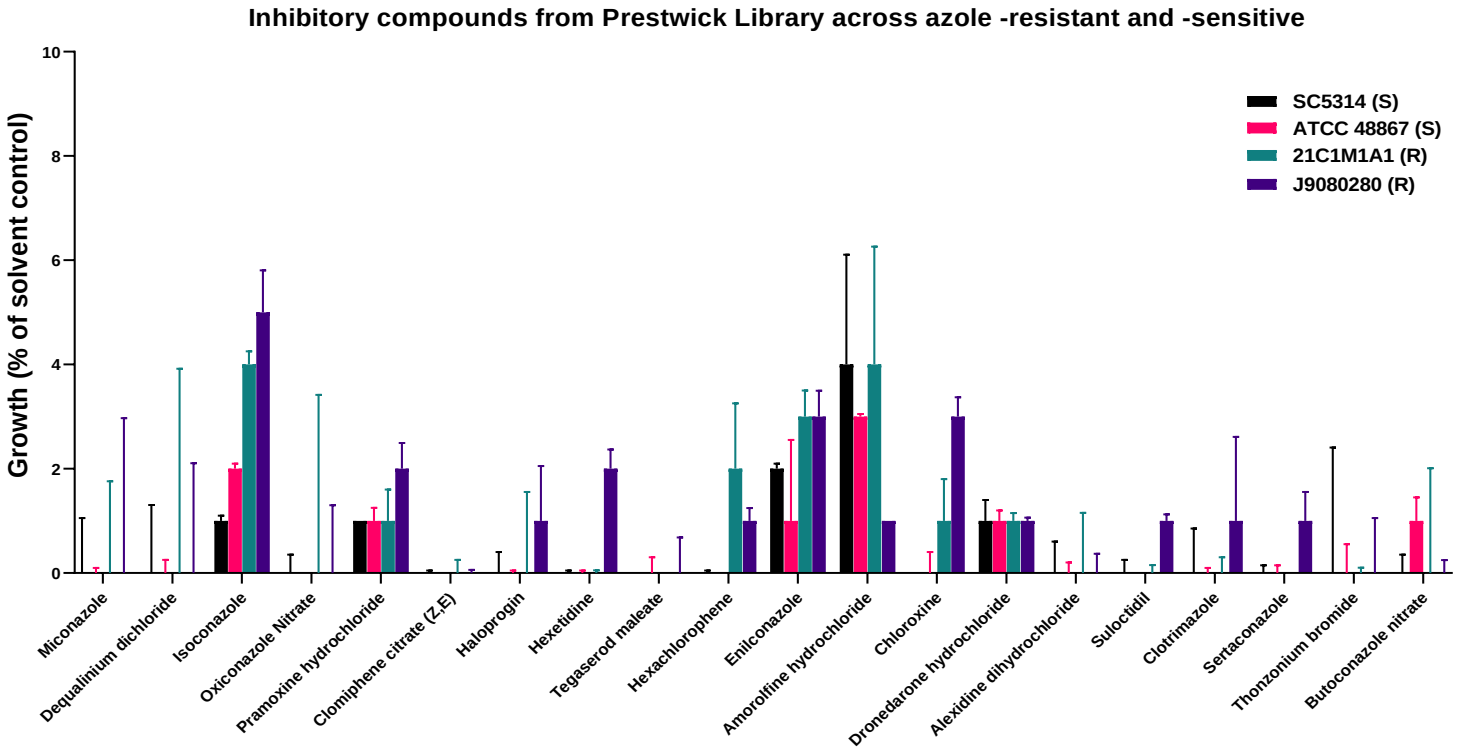

Figure 4.17. Inhibitory compounds (≤ 5% growth) across both azole-sensitive and -resistant *C. albicans.* Growth is displayed as a percentage of the solvent (DMSO) control after 24 h incubation AT 30°C with the indicated chemicals from the Prestwick Chemical library. Data derived from Fig. 4.17. (S) = azole-sensitive, (R) = azole-resistant.

4.3.12 Potential hit compound validation demonstrated that observed hypersensitivity is an artefact of the screen

Within the analysis from the 1280 chemicals, one compound appeared a potential 'hit', meaning selective inhibition of the azole-resistant strains but not the azole-sensitive strains tested. This compound was trifluoperazine dihydrochloride (TFP) (Figure 4.18). TFP was determined as a potential 'hit' as the mean growth for both azole-sensitive strains was > 70% compared with the mean of azole-resistant, which was ≤ 10%, indicating a potential seven-fold increase in sensitivity. TFP is a commonly used antipsychotic drug mostly used to treat schizophrenia. TFP has been identified as a promising antifungal against the destructive *C. auris* pathogen as part of a Prestwick Library screen (Wall et al., 2018). To corroborate the result shown in Figure 4.18, TFP was used at 100 µM against a wider range of azole-resistant and -sensitive strains or clinical isolates (Figure 4.19).

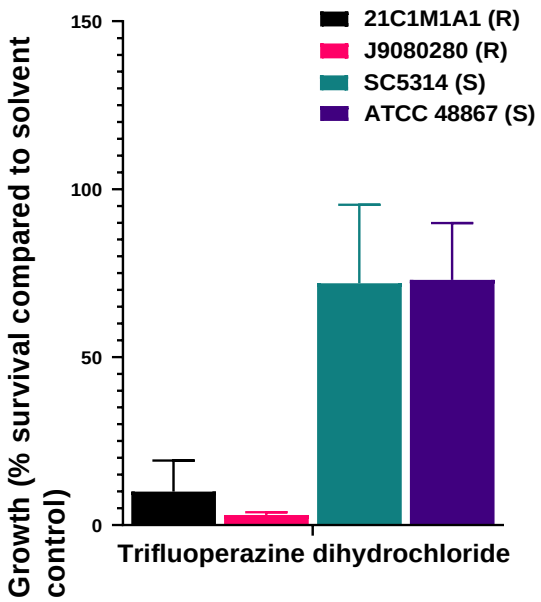

Figure 4.18. Data for *C. albicans* with trifluoperazine hydrochloride (TFP) from the Prestwick screening experiment. Growth displayed as a percentage of growth (from OD_{600} values) compared with the solvent (DMSO) control after 24 h with TFP. (R) indicates azole-resistant and (S) azole-sensitive. Screens were performed in duplicate, error +SEM.

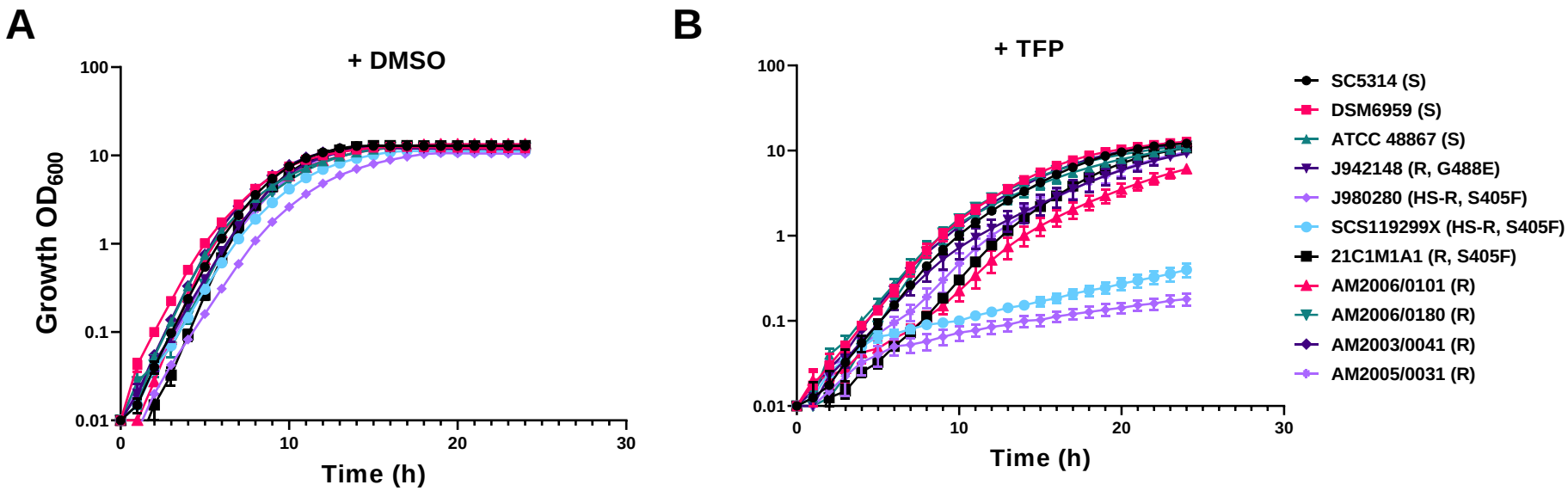

Figure 4.19. *C. albicans* trifluoperazine hydrochloride (TFP) sensitivity profiling. Growth in YPD (+2% glucose) without TFP (+DMSO) (A) and with 100 µM TFP (B) across a 24 h period was measured using OD_{600}, with readings taken every 30 minutes. Plotted values represent the mean of three independent experiments, with error plotted as ±SD (some error did not extend outside the plotted symbol). (S) = azole-sensitive, (R) = azole-resistant, (HS-R) = hypersensitive and azole-resistant, known mutations in *ERG11* are indicated after (R).

Incubation with solvent control (Figure 4.19A) or TFP 100 µM (Figure 4.19B) revealed that sensitivity in azole-resistant isolates was not specific to those containing the S405F mutation. However, this test showed that the genetically engineered strain 21C1M1A1 (S405F) was not sensitive to TFP in this repeated growth experiment, where compounds were both tested from the library and from separately made drug stocks, in contrast to its behaviour in the screen according to results from that experiment (Figure 4.18). In the dedicated growth assay, the TFP sensitivity was only observed in two isolates, SCC119299X and J980280, which were the same two isolates which also exhibited paromomycin sensitivity. The result of the TFP sensitivity assessment suggest the sensitivity observed is not linked to the S405F mutation in *ERG11*, as strain 21C1M1A1A which also has the S405F mutation does not show TFP sensitivity. The result also suggests this is not solely due to azole-resistance as other azole-resistant isolates do not exhibit TFP sensitivity. It may be that the defect in cell wall integrity/glycosylation suggested earlier for these two strains may be relevant here also, potentially rendering these two clinical isolates hypersensitive to a range of compounds.

4.3.13 Testing of additional compounds suggested a reproducibility problem with the high-throughput screening

Besides the non-reproducible result for TFP with isolate 21C1M1A1, it was noted that several chemicals gave results with high error between the screen duplicates, or large differences between either the two azole-resistant or -sensitive strains (i.e., only one azole-sensitive strain showing resistance or one azole-resistant strain showing sensitivity to a compound within the library). Considering the apparent scope for error, it was decided to further test two of these compounds with such differing results for either the azole-resistant or -sensitive strains, in case of potential false results from the screen. The two selected compounds were fluvastatin and amorolfine hydrochloride (Figure 4.20). Fluvastatin is a widely prescribed inhibitor of HMG-CoA reductase, the key enzyme in sterol biosynthesis and has been shown to be active against

C. albicans (albeit at high concentrations) and can also act synergistically with fluconazole (Chin et al., 1997). Amorolfine hydrochloride is part of the morpholine antifungal drug class that inhibits the fungal enzymes in the *ERG* biosynthesis pathway, delta-14 reductase and delta-7–delta-8 isomerase. Inhibition of these enzymes leads to depletion of ergosterol and accumulation of toxic sterols, such as ignosterol in the fungal cytoplasmic cell membrane, resulting in altered membrane permeability and, ultimately, cell death (Georgopapadakou and Walsh, 1996).

Both compounds were tested under the same conditions as the Prestwick Library screen was conducted and applied at 100 µM. It was evident that J980280 (azole-resistant) cells reproducibly retained their resistance to fluvastatin versus the other strains (Figure 4.20B). Sensitivity profiling to amorolfine hydrochloride (AH) however revealed a lack of consistency between the experiments for one of the strains. From the original screen, ATCC 48867 (S) was the only strain/isolate able to grow in the presence of AH (Figure 4.20A). When the experiment was repeated none of the four strains were able to grow (Figure 4.20C). These findings indicated that there are some issues with reproducibility variability in the screening process, particularly when the testing is scaled-up and that interpretation of the results should be taken with caution. Therefore, although the results did not reveal a novel CS effect with the azole resistant strains, it cannot be completely ruled out that such effects exist for these organisms.

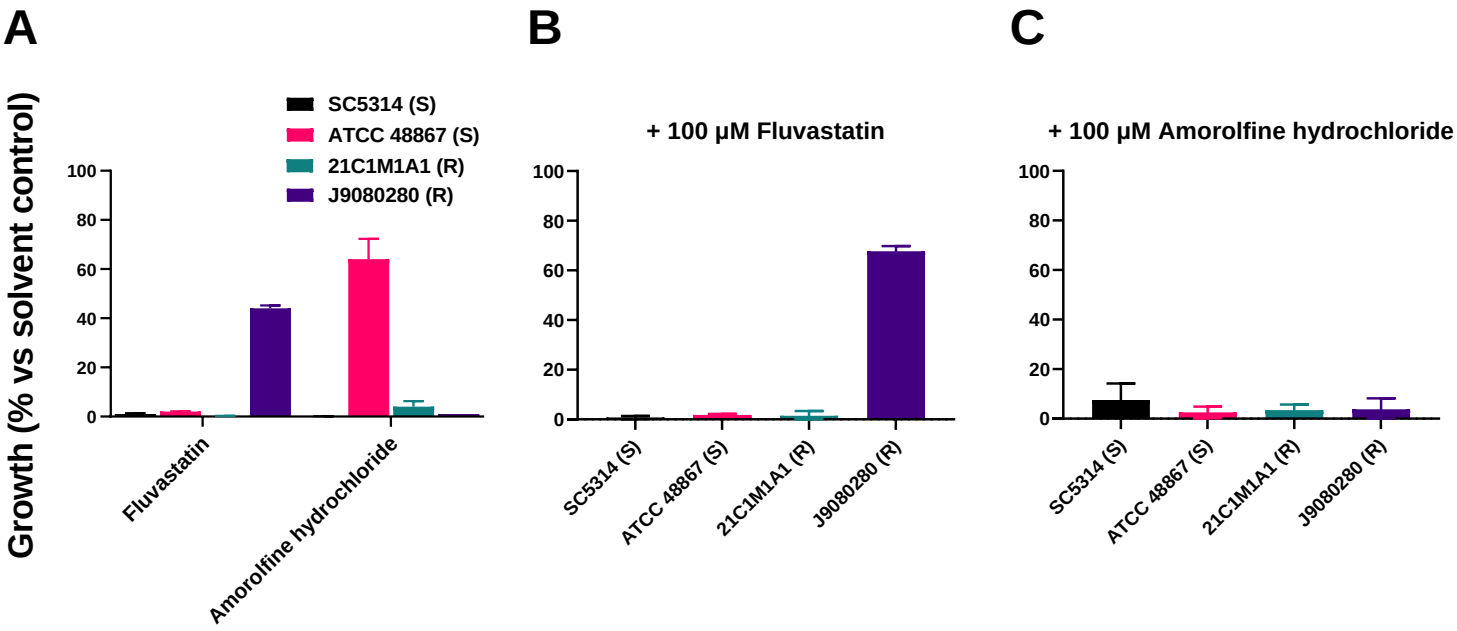

Figure 4.20. Validation of selected results from the Prestwick Chemical Library screening with *C. albicans*. Cells were treated overnight with fluvastatin or amorolfine hydrochloride at the indicated concentration. (A) Data derived from the screen (shown also in Figure 4.16). (B) Treatment with fluvastatin at the indicated concentration. Growth was measured using changes in OD_{600} across 24 hours at 37°C. The assay was conducted using a 96-well plate. Growth is compared to a solvent control and calculated as a percentage of growth. (C) Treatment with amorolfine hydrochloride at the indicated concentration, growth calculated as in (B). Each bar represents the mean of at least two independent experiments, +SEM. (R) = azole-resistant, (S) = azole sensitive.

4.4 Discussion

This chapter describes the characterisation of a novel drug-hypersensitivity phenotype in two azole-resistant clinical isolates of *C. albicans.* Drug-repurposing and the promise of collateral sensitivity are currently under-exploited in the area of drug resistant fungal control. The data presented here show how the drug resistance can render certain mutational backgrounds hypersensitive or, termed here, collaterally sensitive.
The hypersensitivity was not shared by additional clinical azole-resistant or -sensitive strains (additional 'WT's), showing that it was not a universal form of collateral sensitivity. Results suggested that the hypersensitivity was not the result of a slower growth rate, *ERG11* mutation or increased drug uptake. Additional mechanistic evaluation to elucidate the cause of hypersensitivity pointed to the involvement of potential glycosylation and/or cell wall integrity defects in the aminoglycoside hypersensitive isolates.

In addition, a high-throughput approach was implemented, where two azole-resistant strain/isolate containing the S405F mutation in *ERG11* and two azole-sensitive strain/isolate were used to widen the search for collateral sensitivity, focusing on FDA-approved compounds which might specifically inhibit azole-resistant strains. However, this screen did not reveal any hit compounds of this nature. Nevertheless, the possibility of CS cannot against azole-resistant *C. albicans* be completely excluded as the search was not exhaustive (i.e., only one chemical library was screened) and there were also some reproducibility issues with certain results from the screen. Knowledge of the mutational background of resistant strains can be important for deciding appropriate treatment strategies. The present identification of some link between cell wall integrity or glycosylation defects and hypersensitivity to drugs such as aminoglycosides could yet help inform novel clinical decision making in treatment options in the future.

4.4.1 Hypersensitivity of azole-resistant isolates to several approved agents

The hypersensitivity profiling of the three azole-resistant mutants initially focussed on the aminoglycoside class of approved drugs due to their involvement in several reported examples of collateral sensitivity (CS) (Lazar et al., 2013, Pal et al., 2015). The aim was to assess if the intrinsic resistance observed in *C. albicans* to paromomycin and hygromycin was retained in azole-resistant isolates. Moreover, additional information about possible hypersensitivity was hinted at through previous laboratory data, suggestive that azole-resistant isolates were hypersensitive to a synergistic combination of paromomycin and β-escin (Vallières et al., 2020). Hypersensitivity phenotypes were present consistently in two of the azole-resistant isolates (SCS119299X and J980280) towards several aminoglycosides, chloroquine, cyprodinil, chromate and azoxystrobin.

The data revealed that hypersensitivity was seen in drugs that required transport across the cell membrane and not present in cell wall synthesis or membrane acting drugs, suggesting that an increase in drug uptake or accumulation was important. One way of further looking into this could involve the use of efflux pump inhibitors, to see if this reduces the hypersensitivity. Aminoglycoside sensitivity in another human pathogen was also tested in this chapter using azole-resistant *A. fumigatus.* An increased use of the demethylase inhibitor (DMI) fungicides and similar inhibitors has incidentally increased the incidence of azole-resistance in the environment and thereby increases the chance to acquire a fungal infection with an azole-resistant isolate (Snelders et al., 2009). Interestingly, in the two azole-resistant isolates tested in this Chapter, a heightened sensitivity to aminoglycosides (specifically hygromycin) was also observed. A cross-species similarity in sensitivity profiles suggests that resistance to azoles shares some common incidental consequences for resistances to other drugs in potentially diverse fungi.

4.4.2 Mechanistic basis of hypersensitivity

Impacts of drug resistance on organismal fitness are well known, and can have implications for unrelated sensitivities (Melnyk et al., 2015). Therefore, it was considered that the azole-resistant aminoglycoside-hypersensitive (HS-R) isolates, which possess a reduced growth rate compared to the azole-sensitive laboratory strain, could be hypersensitive to several non-azole drugs because of resistance-associated fitness costs. Use of two approaches (reduced temperature or alternative inhibitor) enabled mimicry of the growth rate seen in the isolates of interest. However, this did not reproduce paromomycin hypersensitivity. Mimicry of slow growth using these different strategies is unlikely to reproduce the same growth defect in the HS-R isolates but provided insight into the overall fitness cost contribution to hypersensitivity. A fitness cost of slow growth alone is likely to be insufficient to explain the hypersensitivity, implicating another mechanism(s).

The *ERG11* gene in azole-resistant *C. albicans* is commonly mutated and numerous *ERG11* SNPs and overexpression mutations in ERG11 have been elucidated (Whaley et al., 2017). Sequencing of *ERG11* in the present isolates highlighted two previously validated non-synonymous SNPs, S405F and G448E (Flowers et al., 2015, Warrilow et al., 2019, Spettel et al., 2019). The S405F SNP was present in both HS-R isolates whereas G448E was only found in the other azole-resistant mutant that was not hypersensitive. This data suggested that the S405F mutation could be important for the HS-R phenotype. However, strains genetically modified to express the same SNP did not reproduce paromomycin hypersensitivity (and that was the case also for G488E), so the S405F mutation alone did not appear to explain the hypersensitivity observed. This result is consistent with previous literature, where despite being widely reported for its involvement in azole-resistance (Flowers et al., 2015), the S405F mutation has also previously been shown to be insufficient for azole-resistance in *C. albicans* (Oliveira-Carvalho and Del Negro, 2014) and suggests that additional factors could also contribute to the resistance/sensitivity phenotypes in the isolates tested in this study. It is noted

also that the SNPs were introduced in different genetic backgrounds to the isolates of interest in the present study, and it cannot be ruled out that genetic background has an influence. An ideal test would be to complement the SNPs in the isolates of interest, but given the limited time available, this was not attempted here.

Mechanistic exploration of CS often reports that uptake dynamics are one key mechanism involved, whereby there is increased uptake of the drugs(s) producing hypersensitivity (Roemhild et al., 2020). Using the fluorescent probe, rhodamine 6G (R6G) as a proxy substrate to measure uptake, the data revealed that the two HS-R isolates, if anything, exhibited decreased uptake suggesting that altered drug intake may not be the reason for hypersensitivity. This finding points to the potential involvement of an acquired increase in toxicity (Roemhild et al., 2020). For the non-sensitive azole-resistant isolate (J942148), assessment of R6G uptake revealed a considerable decrease in fluorescence, suggesting multiple mechanisms of resistance could be present; potentially in the form of increased drug efflux (i.e., overexpression of a drug efflux pump). R6G efflux has also been utilised as a tool for identification of *CDR1*-overexpressing azole-resistant *C. albicans*, where reduced R6G fluorescence indicates drug efflux mutations (Maesaki et al., 1999, Revie et al., 2022), which could aid the explanation for the lack of R6G fluorescence in J942148. Azole-resistance in *Candida albicans* is commonly reported to be the product of multiple mutations (Zhang et al., 2020) increasing the likelihood that J942148 possesses multiple mechanisms of azole-resistance.

Dean (1995) reported that *S. cerevisiae* cells had heightened in sensitivity towards aminoglycosides if they were defective in glycosylation (both early stage [endoplasmic reticulum] and late stage [Golgi] glycoprotein processing), an important cellular post-translational modification process. Related experimental testing in the present study identified two novel synergies in *S. cerevisiae* and/or *C. albicans*: between the aminoglycosides and tunicamycin, a known, potent inhibitor of N-linked glycosylation (Wu et al., 2018). Absence of this synergy in the HS-R isolates suggested that tunicamycin exposure may not

further impair glycosylation in these organisms, indicative of possible pre-existing glycosylation defects in these cells. This data suggested an involvement of glycosylation defects in the mechanism of aminoglycoside hypersensitivity of the two azole-resistant strains-of-interest. Additional experiments with calcofluor white and Congo red further supported the possibility of cell wall or glycosylation defects, with both HS-R isolates exhibiting hypersensitivity to these agents. The anticipated actions of tunicamycin and Congo red in our hands were corroborated by the fact that these agents acted synergistically when combined against the laboratory strain *C. albicans* SC5314, consistent with related targets of action. Previous research has shown that glycosylation defects can result in a decrease of *O*-mannosylated glycoproteins, and this is compensated by an increase in polysaccharides, such as chitin and glucans. These elevated glucan levels can result in enhanced sensitivities toward glucan-disturbing agents like Congo red (Prill et al., 2005). Nonetheless here, despite potential glycosylation defects, the hypersensitive isolates had significantly reduced β-(1-3)-glucan in the cell wall. It was proposed that a faciliatory relationship between cell wall integrity and glycosylation defects enables hypersensitivity in the mutants to an array of different agents. To test this hypothesis, Congo red was combined with tunicamycin in the wild-type laboratory strain (with no known mutations) and the results indicated a synergistic relationship. The hypersensitivity of the two azole-resistant mutants toward cell wall perturbing agents and aminoglycosides, with distinct different mechanisms of action point toward the involvement of an increase in permeability and therefore cellular uptake or an export defect specific to the drugs showing hypersensitivity.

Alternatively, the study by Dean (1995) discusses that aminoglycoside sensitivity because of glycosylation defects could be the consequence of the disruption to normal functioning glycoproteins (within the endomembrane system). It could be suggested that disruption to cell wall protein glycosylation, interferes with aminoglycoside detoxification once inside the cell, due to changes in functional activity or localization of these proteins which is highly

linked to glycosylation state, when mutated, leads to hypersensitivity. These findings exaggerate the complexity of drug resistance and how the mutational background can be informative in proposing treatment strategies e.g., combining a glycosylation-affecting agent with aminoglycosides.

4.4.3 Prestwick screening for collateral sensitivity identification

As aminoglycoside hypersensitivity proved not to be a common feature of all azole-resistant isolates, the study next cast the net wider in seeking evidence for collateral sensitivity in azole-resistant *C. albicans*. The present screen of an FDA-chemical approved chemical library for identifying compounds producing hypersensitivity only in azole-resistant isolate was, to our knowledge, the first attempt at such a CS screening approach against a fungal pathogen. Drug re-purposing screens against *Candida spp*. have identified several novel inhibitory compounds and combinatorial treatments which seek to bolster the current arsenal of treatments against the pathogens (Siles et al., 2013, Wall et al., 2018, Vallières et al., 2020). Despite a potential promising hit in the present study, follow-up validation revealed that it was a false-positive. Additional experiments revealed some further issues with reproducibility of certain screen results, and so it is equally possible there may have been a number of false negatives to which potential hit compounds could have been lost. Therefore, while the screening experiment was unsuccessful in identifying CS-displaying compounds specific to the azole-resistant mutants, it does not at all rule out future possibility of success. It should also be noted that the 100 µM concentration used for the library chemicals in the screen (following previous studies and manufacturers guidelines) could have been too low to distinguish any sensitivity differences between sensitive-and-resistant strains: this is supported by the lack of sensitivity observed for paromomycin detected by the screen. High-throughput screening is an invaluable resource. However, as a consequence of this approach, specific sensitivity differences, or hits, are likely to be missed or disproven in validation experiments (Bibette, 2012). *C. albicans* has an elevated intrinsic tolerance to many chemicals compared with *Saccharomyces cerevisiae* (Ksiezopolska and Gabaldon, 2018).

One example can be seen in the MIC to tunicamycin in Figure 4.11, and the use of higher chemical concentrations (even if too high for potential applications) than used here should be one approach to help identify CS interactions with this organism.

4.4.4 Conclusions and future work

Hypersensitivity of two clinical azole-resistant *C. albicans* isolates to several existing and approved drugs, suggested the possibility of CS in this study, although that proved inconsistent across other azole resistant isolates. Other studies have shown that CS is governed by a plethora of varied factors and that understanding the mechanisms involved are pivotal to permit clinical implementation (Nichol et al., 2019). Neither identified SNPs in the *ERG11* gene of the mutants nor drug uptake levels appeared sufficient to explain the CS of the two isolates of interest. Instead, results suggested an interaction of cell wall and/or glycosylation defects in the hypersensitivity phenotype. A chemical screen revealed no further indications of CS specific to azole-resistance. However, reproducibility and other issues were noted, and improvements embedded in future experiments could hold promise for finding novel CS interactions.

Future work may aim to look at specific glycosylation-deficient *Candida albicans* mutants to investigate further the involvement of glycosylation in the hypersensitivity phenotype alongside identifying the nature of any glycosylation defects in the azole-resistant hypersensitive isolates. Moreover, a synergistic relationship between cell wall integrity, glycosylation and aminoglycoside could be further explored in other pathogens of interest. This is particularly so considering that a protein-synthesis target of aminoglycoside drugs is so well documented, as opposed to any involvement with the cell wall. There is also still such promise for more rigorous screening approaches to find novel CS interactions in *C. albicans*, including through screening of additional chemical libraries. Moreover, *C. albicans* with a different mutational focus such as echinocandin resistance could also be used in a drug-repurposing or CS study in attempt to identify novel selective drugs. Identifying drugs that can be used

to selectively inhibit drug-resistant *Candida albicans* and finding novel solutions is imperative for bolstering the arsenal of treatment against this problematic clinical pathogen.

Chapter 5 – Exploring Mechanisms Governing Anti-attachment to (Meth)Acrylate Polymers in *Zymoseptoria tritici* and *Candida albicans*

5.1 Introduction

5.1.1 Polymer materials as alternatives to chemical actives

While antibiotics and other chemical actives are invaluable and routinely used in fungal control, the use of polymer materials can propose an alternative strategy for pathogen management. Polymers, first described in 1920 by German scientist, Hermann Staudinger, are formed by assemblies of simple structural units (monomers) resulting in the formation of a larger 3-dimensional structure. Natural polymers are evident throughout everyday life such as in human hair and cellulose, but can also be synthesised through man-made means (synthetic) (Staudinger, 1920, Maitz, 2015). Since they began to be practically used in the early twentieth century, use of synthetic polymers has grown so that they are now employed across many aspects of our lives and in industry, commercially from clothing and packaging to medical usage in biomaterials and combinatorial therapy (Hook et al., 2012, Peplow, 2016, O'Brien et al., 2019).

An extensive review by Maitz (2015) discussed the applications of biological, synthetic and hybrid polymers in clinical medicine. Examples include surgical/orthopaedic implants (e.g. bone cements) (Charnley, 1960, Kenny and Buggy, 2003), ophthalmology (e.g. contact lenses) (Lai et al., 1993, Nicolson and Vogt, 2001), dentistry (e.g. composites) (Bowen, 1962, Peutzfeldt, 1997) and *in vivo* applications (e.g. catheters) (Pickard et al., 2012). A further example of the application of polymers is seen in drug delivery systems, which can be classified into diffusion-controlled, solvent-activated (e.g. swelling) (Gao and Meury, 1996), chemically controlled (biodegradable) (Tamada and Langer, 1993) or externally triggered/responsive systems, i.e., 'smart polymers' (e.g. responsive to pH, temperature) (Lowman et al., 1999, Owens et al., 2007).

Another example of a pH-controlled delivery system used a copolymeric micelle loaded with itraconazole, which enhanced efficacy and improved treatment of *C. albicans* biofilms (Albayaty et al., 2020). In addition to drug delivery systems, polymers themselves can represent an alternative to antibiotics, harbouring bioactive properties that inhibit or kill pathogenic organisms, e.g. chitosan, which has been shown to inhibit phytopathogen growth (Hirano and Nagao, 1989). Antimicrobial polymers (AMP) can exhibit bioactivity in their inherent chemical structure or can provide a backbone to improve the potency of existing drugs (Chung et al., 2003). The design of AMPs is complex and benefits from the ability to integrate both structural and chemical manipulation to produce a diverse array of material types, certain forms capable of exhibiting antimicrobial activity against multidrug-resistant pathogens (Kamaruzzaman et al., 2019).

Moreover, as discussed earlier, combination therapies are of increasing importance in the control of multiple pathogens. Certain synthetic polymers, which alone do not display significant bioactivity, have been shown to act synergistically in combination with antifungal drugs in the control of the human pathogen *Candida albicans* and the common material spoilage fungus *Trichoderma virens* (O'Brien et al., 2019). O'Brien et al. (2019) employed renewable, bio-based bis-epoxy resin monomer from terpenes to generate epoxy-amine oligomers. These oligomers showed antifungal properties in combination with existing fungal inhibitors iodopropynyl-butylcarbamate (IPBC), proposed to effect the cell membrane permeability and fatty acid synthesis, and amphotericin B; reducing the MIC of IPBC up to 64-fold in *T. virens* and that of amphotericin B by 8-fold in *C. albicans* (O'Brien et al., 2019). A potential mechanism of synergy between the agents and oligomer was proposed to involve interaction with the fungal cell membrane, with polycations in the oligomer enabling leakage of cell contents.

5.1.2 Cell adhesion as a target for polymer applications

The adhesion of a microorganism to abiotic surfaces or biotic surfaces in/on host organisms is commonly followed by biofilm formation (often a polymicrobial biofilm), potentially seeding infections (Geesey et al., 1977, O'Toole et al., 2000). The problem of biofilms has been discussed with more detail in Chapter 1 (1.1.1). Regarding human pathogens, biofilm formation, usually made up of multiple microbial species, is commonly seen upon medical devices such as catheters and this presents a significant problem for successful patient therapy (Costerton et al., 2005). Adhesion to a plant surface is also a first critical step of infection by many phytopathogens. To address the problem of biofilm formation by microbial pathogens, the integration of knowledge from materials chemistry and microbiology could help provide solutions; allowing the evaluation of how the pathogen is able to attach and colonise the surface as well as the chemical surface properties that promote colonisation.

One study using bacterial pathogens of humans (*Pseudomonas aeruginosa, Staphylococcus aureus* and *E. coli*), used a high-throughput materials approach to identify specific polymers that the bacteria could not attach to (Hook et al., 2012). Hook et al. (2012) hypothesised that materials to prevent biofilm formation would be of greater efficacy than the development of agents to target a pre-formed biofilm. Their study used 'microarrays' of hundreds synthetic polymers to identify a number of materials that were resistant to bacterial attachment and, therefore, formation of the biofilm (Hook et al., 2012). Coating silicone with hit polymers achieved significant reduction (67-fold) in biofilm formation in *in vivo* testing in rats. The efficacy of these polymer-coated catheters are currently tested in European clinical trials.

5.1.3 Targeting adhesion in fungal pathogens

The adhesion of fungal pathogens can initiate infection in different settings including health care and agriculture. As discussed earlier, where biofilms are formed these additionally harbour intrinsic resistance that both complicates

and limit treatment options (Nobile and Johnson, 2015). Existing control strategies against adhering fungal pathogens include incorporation or application of antifungals or fungicides to the surface. An example of this is seen in the chemical pre-treatment of the catheter lumen with a high local antibiotic concentration; this is termed 'lock' therapy (Carratala, 2002, Cateau et al., 2011). Furthermore, in the control of fungal phytopathogens where adhesion to the leaf epidermis governs successful infection, chemical intervention is utilised (often sprayed) to prevent yield losses (Khan et al., 2021), with some formulations including adjuvant polymers to promote retention of the chemical active on the plant surface (Sevastos et al., 2020). In both of these environments the prolonged and excessive use of chemical intervention, where prevention of a relatively passive process (attachment) may suffice, contributes to the spread of resistance to a diminishing number of available drugs (Fisher et al., 2018, Almeida et al., 2019). Examples of targeting adhesion in fungal pathogens are illustrated in **Error! Reference source not found.**.

Targeting adhesion in fungal pathogens also offers the theoretical advantage of slowing resistance through the passive approach of preventing attachment, i.e., cells are not inhibited so presenting a weak selection pressure and it would also require a gain of (attachment) function, a significant evolutionary hurdle (Vallières et al., 2020). Following a similar approach to Hook et al. (2012), Vallières et al. (2020) employed the use of high-throughput acrylate/methacrylate-based polymer microarray screening to identify fungal anti-attachment materials. This study identified multiple materials that were resistant to attachment by both human and crop pathogens. One of the best performing polymer candidates against *C. albicans,* (R)-α-acryloyloxy-β,β-dimethyl-γ-butyrolactone (AODMBA), was also used in 3D inkjet printing to produce a voice prosthesis valve-flap exhibiting a 100% reduction in biofilm formation (*vs* commercial silicone) (Vallières et al., 2020). Furthermore, several anti-attachment polymers effective against fungal phytopathogens

Zymoseptoria tritici and *Botrytis cinerea* gave resistance to infection by the latter organism when sprayed to lettuce leaves (Vallières et al., 2020).

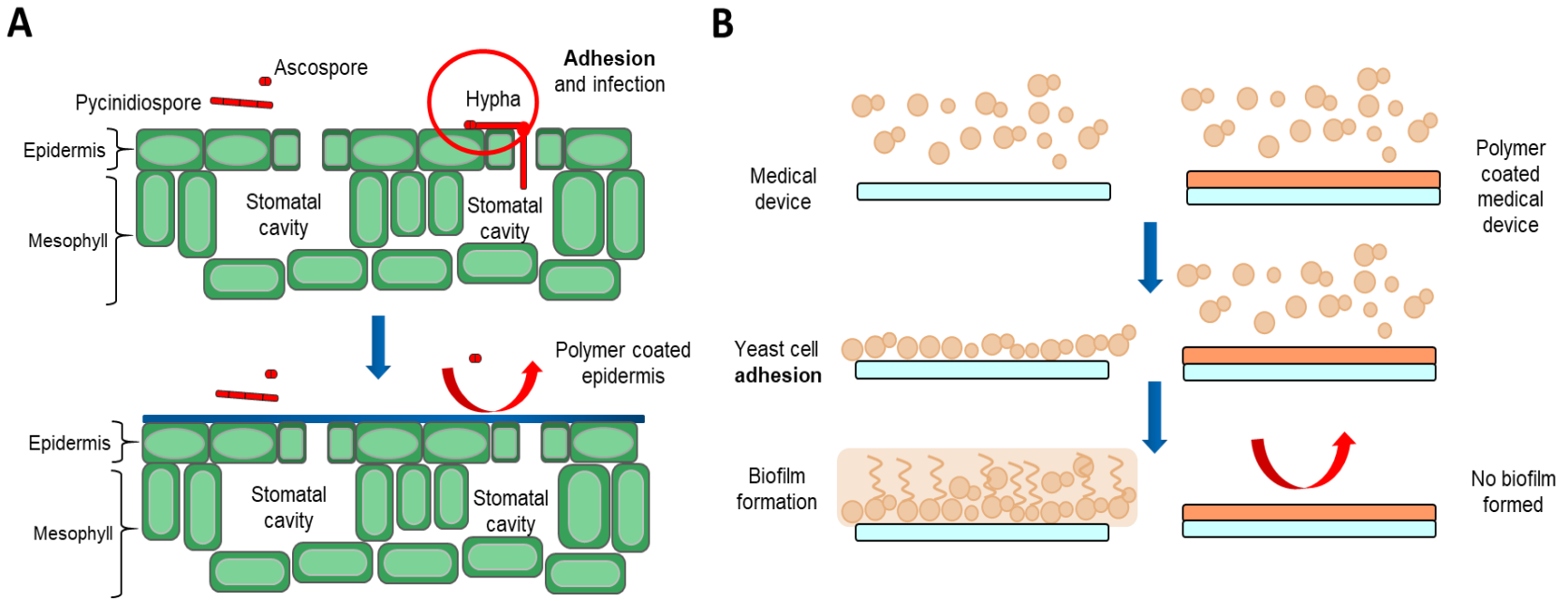

Figure 5.1. Illustration of two different surfaces where pathogen adhesion can be targeted using anti-attachment polymers. (A) *Zymoseptoria tritici* leaf infection, the red circle highlights the stomatal cavity being invaded by ascospore producing hypha. The addition of a polymer coat (blue) upon the leaf epidermis protects the plant from infection as ascospores/pycnidia are unable to attach. Note, this depiction is simplified as the polymer coating on leaves is unlikely to be continuous (Vallières et al., 2020). (A) Figure adapted from Steinberg et al. (2015). (B) *Candida albicans* biofilm formation upon medical device, yeast cells are prevented from attachment by coating of the medical device with an anti-attachment polymer and therefore the biofilm is not initiated.

Importantly, fungal anti-attachment materials that were investigated showed no toxicity against human and plant cells, supporting their potential to be implemented in clinical or agricultural settings (Vallières et al., 2020). Moreover, the biodegradation and accumulation of these synthetic polymers must also be evaluated before use.

Despite such advances in the discovery of materials capable of resisting fungal colonisation, biologically informed development of successful material is hindered by a limited mechanistic knowledge of how fungi interact with surfaces (Vallières et al., 2020). Previous studies that have focussed on understanding spore surface attachment have shown that attachment is influenced by several factors linked to the chemistry and physicochemistry of both the spore and material surface. Examples include surface hydrophobicity, surface wettability, fungal species and spore shape (Whitehead et al., 2011, Liauw et al., 2020). Moreover, an additional example of how the surface itself influences attachment is observed in the finding that surface charge modification upon an acrylic resin significantly decreased the attachment of *Candida albicans* (Park et al., 2008).

Therefore, this present study aims to elucidate properties of the fungus that are important for attachment, specifically against the human fungal pathogen *Candida albicans* (discussed in previous chapters) and in the fungal phytopathogen *Zymoseptoria tritici*. This ascomycete filamentous fungus causes 'Septoria leaf blotch' (STB), a devasting disease of wheat that is capable of causing up to 40% yield loss (Eyal and Wahl, 1973, Fones and Gurr, 2015). As a consequence of intensive breeding programmes favouring high yield production, susceptibility to STB became increased (Duba et al., 2018). As for most infectious crop diseases, management of STB is primarily controlled by chemical intervention, however the apoplastic hemi-biotrophic life cycle of *Z. tritici* complicates the decision on when to apply chemicals (Bosch et al., 2020). Evidence of infection is not present until 10 days post initial infection, when the symptomatic phase is established and chemical intervention is ineffective (Keon et al., 2007, Kettles and Kanyuka, 2016). The application of

chemicals must integrate prior knowledge of infection and diagnostics to prevent infection. The pathogens cell wall, unlike that of *C. albicans*, is relatively unexplored with the focus of studying the cell wall upon the β-(1,3)-glucan and chitin within the cell wall. Research has focussed on the involvement of these cell wall components as pathogen associated molecular pathogens (PAMP) in triggering wheat plant immune responses (Shetty et al., 2009, Zhou et al., 2020).

A consequence of mismanaged, late application of fungicides could contribute to the growing resistance of *Z. tritici* (Yamashita and Fraaije, 2018). The prevention of adhesion of *Z. tritici* spores (specifically pycnidiospores) to the leaf could present a passive, alternative approach to chemical intervention, which is facing increasing concerns both due to resistance and their toxicity to the surrounding environment (Commission, 2019).

5.1.4 Chapter Aims

This chapter sets out to gain a deeper understanding of mechanisms involved in fungal anti-attachment to candidate polymers and also explore how resistance could arise in the important fungal pathogens *C. albicans* and *Z. tritici*. One strategy will utilise accelerated evolution through multiple rounds of UV-mutagenesis and polymer selection. The tool of experimental evolution may enable identification of mutated genes that facilitate attachment and therefore development of our understanding on how resistance could occur. Moreover, another strategy aims to assess the importance of the cell wall components in attachment. This strategy will concentrate upon specific cell wall properties using selective fluorescent probes and single-cell analysis.

5.2 Materials and methods

5.2.1 Strains, culture and maintenance

Zymoseptoria tritici strain K4418 (kindly provided by Syngenta, UK) was routinely maintained and grown on Potato Dextrose Agar (PDA; Oxoid) or PD Broth (PDB; Sigma, UK) media. *Z. tritici* was grown for seven days on PDA from -80^{o}C glycerol stocks prior to harvesting of pycnidia for experimental use. *Candida albicans* strains CAF2-yCherry (kindly provided by R. Wheeler, University of Maine, USA) and SC5314 were also used, grown from -80^{o}C glycerol stocks at 37^{o}C for 48 h prior to use in experiments. Yeasts cells of *C. albicans* were maintained and grown in YPD (yeast extract, peptone, and dextrose) medium [2% peptone (Oxoid, Basingstoke, UK), 1% yeast extract (Oxoid), and 2% glucose]; where necessary, medium was solidified with 1.5% (w/v) agar (Sigma-Aldrich, UK).

5.2.2 Polymerisation using UV Curing

All monomers used were purchased from Sigma Aldrich (UK) and chemical structures can be found in Appendix D (D.1.). I was able to synthesise polymers using photo-initiation with ultra-violet (UV) curing of monomer as described in Vallières et al (2020). The synthesis of selected polymers involved the coating of 6.4 mm diameter wells of flat bottomed, polystyrene 96-well plates (Greiner Bio-One, Stonehouse, UK), to allow subsequent assessment of attachment by fungal cells. Polymerisation was initiated by addition of 2,2-dimethoxy-2-phenylacetophenone (DMPA, Sigma, UK) to a final concentration of 1% (w/v). Plates were prepared by adding 50 µl of the monomer solution (as provided by the manufacturer, with the addition of DMPA initiator) into each well. Plates were irradiated with UV (Blak-Ray XX-15L UV Bench Lamp, 230V ~50Hz, 15 Watt, 365nm) for 1 h within a Whitley DG250 Anaerobic Workstation (Don Whitley Scientific, UK)at O_2 < 2,000 ppm. The samples were dried at < 50 mTorr for 7 days within a vacuum oven (Fisher Scientific, UK). Wells were washed with 100% isopropanol (Sigma, UK), then sterile distilled water (SDW) and left in

SDW (100 µl per well) for 48 h at room temperature. The washing steps above were repeated after 48 h incubation followed by UV-sterilisation for 20 min prior to experimental use.

5.2.3 3D-printing of AODMBA-coupons

Coupons made using the (R)-α-acryloyloxy-β,β-dimethyl-γ-butyrolactone (AODMBA, Sigma, UK), abbreviated to AODMBA monomer were printed as described in Vallières et al. (2020) by Dr Yinfeng He (Centre for Additive Manufacturing, University of Nottingham). AODMBA associated ink formulations were prepared by dissolving 1% (w/v) 2,2-dimethoxy-2-phenylacetophenone (Sigma, UK) into 5 ml of the candidate monomer (as provided by the manufacturer). The mixture was stirred at 800 rev. min^{-1} at room temperature until initiator was fully dissolved. The ink was then purged with nitrogen gas for 15 min and filtered through a 5-µm nylon syringe filter. The final ink formulation was left at 4^{o}C overnight to degas. A Dimatix DMP-2830 material printer was used for printing, equipped with a 10-pl cartridge containing 16 nozzles, each with a square cross section with a side length of 21 µm. The jetting voltage and waveform were adjusted until stable droplet formation was achieved. A 365-nm UV light emitting diode (LED) unit (800 mW/cm^2) was used for in-line swath-by-swath ink curing after deposition. The whole printing process was carried out in a nitrogen environment, where the oxygen level was 0.2 ± 0.05%. The circular coupons were printed with the dimensions 5 mm diameter and 1.1 mm thickness. The coupons were dried at 37^{o}C inside a vacuum oven [at <50 mTorr]. The anti-attachment properties were assessed using the XTT assay (see Assessment of biofilm activity).

5.2.4 Thermal polymerisation and characterisation of mMAOES and AOHPMA

Polymerisation and characterisation was kindly carried out by Dr Valentina Cuzzucoli Crucitti (School of Chemistry, University of Nottingham).

Polymerisation via thiol-mediated free radical polymerisation

The protocol for the synthesis of polymerised mono-2-(Methacryloyloxy)ethyl succinate (mMAOES) and polymerised acryloyloxy-2-hydroxypropyl methacrylate (AOHPMA) by thiol-mediated free radical polymerisation was as follows. The appropriate quantities of the monomers and azobisisobutyronitrile (AIBN) (0.5 w/v with respect to the monomers) were introduced into the required volume of cyclohexanone with stirring. Dodecathiol (Sigma, UK) was added at a concentration of 1 or 65 mol% with respect to mMAOES (Sigma, UK) or AOHPMA (Sigma, UK), respectively. Finally, the reaction vessels were degassed in an ice bucket by purging with argon using a standard Schlenk line for at least 1 h. To commence the polymerisation reaction, the temperature was raised up to 75^{o}C using an oil bath. In order to leave the polymerisation of mMAOES to completion the reaction was allowed to continue for 18 h with continual stirring. In contrast, polyAOHPMA showed a gel state after 1 h of reaction, so the reaction was stopped after 50 min. Polymer purification was conducted by precipitation into an excess of heptane (polyAOHPMA) or chloroform (polymMAOES). The typical ratio of non-solvent to reaction medium was 5:1 v/v in order to enhance the precipitation process (and prevent polymer solubilisation). Finally, the precipitated materials were collected in a vial and left in a vacuum oven at 25^{o}C for at least 24h.

Polymer Characterisation by NMR and GPC

Nuclear Magnetic Resonance (NMR) spectra were recorded at 25^{o}C using Bruker AV400 and AV3400 spectrometers (400 MHz) using deuterated solvents. Chemical shifts were assigned in parts per million (ppm). Samples were dissolved in $CDCl_3$ (deuterated chloroform) and acetone-d6 to which chemical shifts are referenced. MestReNova 14.2.1 copyright 2021 (Mestrelab Research

S. L.) software was used for analysing the spectra. Analysis by Gel Permeation Chromatography (GPC) was performed using an Agilent 1260 Infinity instrument equipped with a double detector with the light scattering configuration. Two mixed C columns at 35^{o}C were employed, using tetrahydrofuran (THF) as the mobile phase with a flow rate of 1 ml min^{-1}. GPC samples were prepared in HPLC grade THF and filtered before injection. Analysis was carried out using Astra software. The number and weight average molecular weight (Mn and Mw) and polydispersity (Đ) for the polymers was calculated using narrow-distribution standards of poly(methyl methacrylate) for the calibration curve.

5.2.5 Coverslip spin coating of thermally cured polymers

To spin coat coverslips for use in microscopy, thermally polymerised AOHPMA and mMAOES were solubilised in 2% (w/v) toluene or isopropanol respectively using a hotplate stirrer, with mixing at 300 rev. min^{-1} and heating at 50^{o}C. A spin coater machine (MK7, Cordell, USA) was used, with a 13 mm diameter round coverslip (VWR Coverglass, UK) placed on top. Once added, a vacuum was applied to prevent the coverslip moving. Then, 25 µl of the solubilised polymer was added to the coverslip, covered and spin-coated at the 3000 rev. min^{-1} setting for 30 s. The coverslips were placed in 24-well polypropylene plates (Evergreen labware products, USA), dried for 7 days at 37^{o}C inside a vacuum oven [at <50 mTorr] and placed in dH_2O for two days before use in experiments. The anti-attachment properties of the coverslips were assessed using the XTT assay (see Assessment of biofilm activity), but here using 24-well plates and a volume of 1 ml, where 750 µl was then transferred to assess the XTT signal at 490 nm.

5.2.6 Assessment of biofilm activity

Biofilm metabolic activity during growth on polymer surfaces was measured by the XTT (tetrazolium salt, 2,3-bis[2-methyloxy-4-nitro-5-sulfophenyl]-2H-

tetrazolium-5-carboxanilide) reduction assay (Sigma, UK), using the method described by (Vallières et al., 2020), as described below for the two fungi studied here.

Zymoseptoria tritici was grown for 7 days on PDA and pycnidiospores were harvested using 80% tween. Hyphae were filtered out using a 40 µm nylon mesh cell strainer (Fisher Scientific, UK). Pycnidiospores were spun down for 5 min at 1900 *g* and resuspended in PDB. The spore suspension was counted using a haemocytometer and diluted to 2.5 x 10^6 spores ml^{-1} in PDB. Aliquots (100 µl) of this pycnidiospore suspension were transferred to wells of polymer-coated 96-well plates and incubated statically for 5 h at room temperature. Non-adherent pycnidiospores were removed by three gentle washes with PBS, then 100 µl of fresh medium was added to each well and plates were incubated at room temperature for up to a further 22 h. The wells were washed three times with PBS and the XTT reaction was initiated by adding XTT and menadione to PBS at final concentrations of 400 µg ml^{-1} and 25 µM respectively (final volume per well, 200 µl) (PBS was used instead of PDB as the XTT reaction does not work in PDB medium). After six hours, 100 µl of the reaction solution was transferred to fresh 96-well plates and the absorbance at 490 nm was measured using a BioTek EL800 microplate spectrophotometer. Comparison of the XTT (measure of metabolic activity) signal with the signal from non-coated control wells (polystyrene) enabled the calculation of percentage biofilm relative to that recorded in the control wells.

For *C. albicans,* single colonies from agar plates were used to inoculate YPD broth cultures in Erlenmeyer flasks and incubated overnight at 30°C with orbital shaking at 120 revolutions (rev.) min^{-1}. Cultures were washed twice in RPMI 1640 (+ L-glutamine and sodium bicarbonate, sterile filtered from Sigma, UK) and diluted to OD_{600} 0.015. Aliquots (100 µl) of the cell suspension were transferred to 96-well microtiter plates (Greiner Bio-One, Stonehouse, UK) coated with the polymers of interest and incubated statically for 2 h at 37°C. Non-adherent cells were removed by three washes with PBS and then 100 µl of fresh RPMI medium was added to each well, and plates were incubated at 37°C

for up to a further 22 h. The wells were washed three times with PBS, and the XTT reaction was initiated by adding XTT and menadione to RPMI to final concentrations of 210 µg ml^{-1} and 4.0 µM, respectively. After 2 hours, 100 µl of the reaction solutions were transferred to fresh 96-well plates and the procedure for spectrophotometric measurement was followed as described above. This experimental set-up acknowledges that media was not used for *Z. tritici* to avoid issues of autofluorescence and therefore direct comparisons to biofilm inhibition cannot be made with *C. albicans* where growth media was used during the experiment.

For assessment of biofilm on the polymer printed coupons or coated coverslips, the same procedures as above were used except that at each wash step the coupons/coverslips were transferred to fresh cell culture plates. This step was included to ensure attachment was only measured for cells attached to the materials of interest.

5.2.7 UV mutagenesis in *Candida albicans*

Starting generations used in this evolution experiment were picked from single colonies of *C. albicans* CAF2-ycherry grown on YPD agar plates and then grown in 50 ml Erlenmeyer flasks in YPD broth overnight at 30°C at 120 rev. min^{-1}. The three biological replicate cultures were diluted to OD_{600} 0.5 in 10 ml PBS and the suspension was placed in 5 cm petri dish with a sterile magnetic stirrer. The UV lamp (Sylvania G15T8 germicidal UV-C source, USA) switched on for sterilisation for 30 mins prior to use. An exposure height of 35 cm of the UV lamp source was used. A hot plate stirrer was added beneath the UV lamp source (Model, B212; J Bibby Science Products Limited, UK) a stirring power of five was applied at the start of UV exposure. To establish a UV-exposure time giving approximately 20% killing, at given time points 100 µl of cell suspension was transferred into 1.5 ml microcentrifuge tubes and immediately covered in foil. Tubes were kept at 4°C and in the dark for 1 h. To assess colony viability at zero time and in the different timed samples during UV-mutagenesis, samples

containing approximately 100 cells (estimated by counting with a haemocytometer) in 100 µl volumes were spread in triplicate onto 9 cm PDA petri dishes and grown at 30°C for 48 h before enumeration of colonies.

5.2.8 Accelerated evolution experiment in *Candida albicans*

The initial experiment established 30 sec of UV exposure was sufficient to achieve ~20% killing (see Figure 5.3) and therefore was used throughout this experiment. After 1 h at 4°C the cell suspensions were transferred to 15 ml centrifuge tubes and pelleted by 3.5 min centrifugation at 1900 *g*. Pellets were resuspended in 10 ml YPD and incubated in Erlenmeyer flasks overnight at 30°C, 120 rev min^{-1}. Frozen stocks (in 30% glycerol) from the overnight growth of UV-mutagenised cultures were kept for each round of UV-mutagenesis. 3D inkjet-printed AODMBA coupons were placed inside 96-well plates (Greiner, Bio-One, Stonehouse, UK) and 100 µl of the UV-mutagenised overnight culture adjusted to OD_{600} 0.25 was added. After 2 h incubation at 37°C, the coupons were washed three times with 100 µl of PBS to remove any non-attaching or loosely attaching yeast cells and the coupons were transferred into 10 ml of YPD in Erlenmeyer flasks and grown overnight. Samples were retained and frozen as stocks at -80°C after overnight growth. The experiment was continued by UV-mutagenesis of the overnight cultures as above and the process repeated. If the experiment was to be paused for any unforeseen reason, stocks from the most recent generation were used to resume the experiment. To monitor the AODMBA-attachment properties of cells after the rounds of UV-mutagenesis and culturing, 50 µl of frozen culture was grown overnight (as above, keeping an additional stock for future comparisons) and then diluted to use in the XTT assay (see Assessment of biofilm activity).

5.2.9 Fluorescent staining of *Zymoseptoria tritici* pycnidia and *Candida albicans* yeast cells

Z. tritici pycnidiospores were prepared as described earlier (see Assessment of biofilm activity). Pycnidiospores were centrifuged for 5 min at 1900 *g* and resuspended in PDB. Pycnidiospores were counted using a haemocytometer and the suspension diluted to 4 x 10^7 spores ml^{-1} in a 1.5 ml microcentrifuge tube. Pycnidiospores were pelleted at 7600 *g*, 10 min (18°C) and thoroughly resuspended in a mixture of PBS and fluorescent stain, described below (500 µl final volume). For *C. albicans*, strain SC5314, cultures were prepared as in Assessment of biofilm activity. Overnight cultures were washed in PBS, spun down for 3.5 min at 1900 *g* and diluted to OD_{600} 1.5 in RPMI 1640 medium. Cells were spun down again and thoroughly resuspended in a mixture of PBS and fluorescent stain (500 µl final volume).

For the fluorescent stains, FITC tagged Concanavalin A (Sigma, UK) was used at a final concentration of 80 µg ml^{-1} in buffer [containing dH_2O, 0.1 M sodium bicarbonate ($NaHCO_3$)]], from a 5 mg ml^{-1} stock solution [containing dH_2O, 0.1 M sodium bicarbonate ($NaHCO_3$)] . Trypan blue (Sigma, UK) was used at a final concentration of 20 µg ml^{-1} in PBS buffer, from a stock solution at 100 µg ml^{-1}. DAPI was used at a final concentration of 10 µg ml^{-1} in dH_2O, from a 1 mg ml^{-1} stock solution. Once the stain was added, the spore/cell samples were incubated at 21°C (*Z. tritici*) or 30°C (*C. albicans*) for 20 min. Stained samples were then washed twice in PBS and resuspended in PBS (*Z. tritici*) or RPMI 1640 (*C. albicans*). Samples (10 µl) of the stained samples were immediately mounted before observation by confocal microscopy (see below). These samples represented the whole cell population (i.e. both cells that may or may not attach to the glass/polymer coated coverslips). For samples representing the attaching cell subpopulations: in the case of *Z. tritici* pycnidiospores, stained suspensions were counted and diluted to 2.5 x 10^6 spores ml^{-1} and 1 ml added to a 24-well polystyrene plate (Greiner, Bio-One, Stonehouse, UK), with wells containing either a glass or AOHPMA polymer coated coverslip. After 5 h, the coverslips were washed three times with PBS and mounted onto microscope

slides. For *C. albicans,* the stained cell suspensions were diluted to OD_{600} 0.015 in RPMI 1640 medium and 1 ml added to wells as above but containing either a glass or mMAOES polymer coated coverslip. After 2 h incubation at 37°C the coverslips were washed three times with PBS and mounted onto microscope slides.

5.2.10 Observation of stained cells by confocal microscopy

For the confocal imaging of pycnidiospores or yeast cells attached to glass or polymer coated coverslips, a Zeiss LSM 880 confocal laser scanning microscope equipped with Airyscan Fast scanning (Zeiss, Germany) was used. Using Zen software, images were taken using X 40 magnification (with oil immersion) and 16 bit depth. Images were taken in a 2x2 tile scan, with three slices within a Z-stack. Three channels were used for imaging: GFP, Cy5 (far-red) and BFP filter. For each experiment, the laser power, contrast and gain were optimised for the whole population of cells (which was assumed to have the brightest fluorescence) and then the same settings were applied for all other conditions of interest. Excitation and emission wavelengths of the fluorochromes are listed in Table 5.1.

Stain	Excitation (nm)	Emission (nm)
FITC-Concanavalin A	495	519
Trypan blue	620	680
DAPI	359	457

Table 5.1. Excitation and emission wavelengths used for the confocal microscopy.

5.2.11 Statistical analysis

The statistical analyses in this chapter were performed as in Chapter Two, using Prism version 9.5.1.

5.3 Results

5.3.1 Pycnidiospore concentration is important for determining attachment

The process of attachment may involve a number of gene products and cell surface features and will be influenced also by the surface properties onto which the organism is attaching. As cell/spore concentration also may be a variable in experiments planned here, the impact of spore concentration was tested in a preliminary study using four different spore concentrations of *Z. tritici* (Figure 5.2A). It was evident that spore concentrations of 2.5 x 10^4 spores ml^{-1} and lower gave barely detectable attachment according to the XTT reduction assay. Unexpectedly, there was a decrease in detectable spore attachment when spore concentration was increased from 2.5 x 10^5 spores ml^{-1} to 2.5 x 10^6 spores ml^{-1}. This decrease in detectable attachment could be reflective of a quorum-sensing effect, where spore population density influences attachment. In response to this result, it was decided to use the spore concentration of 2.5 x 10^6 spores ml^{-1} in subsequent biofilm formation assessments, as this concentration has been used in published literature for the investigation of biofilm inhibition assays for other filamentous fungi including *Z. tritici* (Vallières et al., 2020). This data reveals the importance of consistency during preparation of pycnidiospore suspensions for comparing attachment ability in differing conditions (e.g. different polymer).

The preliminary experiments also emphasised how attachment of *Z. tritici* to different polymers AODMBA, (acryloyloxy-2-hydroxypropyl methacrylate (AOHPMA), isocyanatoethyl methacrylate (iCEMA) and polyethylene glycol diacrylate (PEGDA) is not uniform for all spores. That is, intermediate percentages of attachment suggested that some spores did attach, while others did not to each polymer (Figure 5.2B). An alternative possible explanation that the XTT activity was decreased for all spores was ruled out as the polymers are not active inhibitors (Vallières et al., 2020). This evidence for 'phenotypic heterogeneity' (Avery, 2006) was further explored as a potential tool for dissecting what cell features enable attachment or not onto the polymer.

The AOHPMA polymer was chosen for further investigation into heterogeneous attachment in *Z. tritici* and the AODMBA polymer was chosen for accelerated evolution experiments with *Candida albicans*.

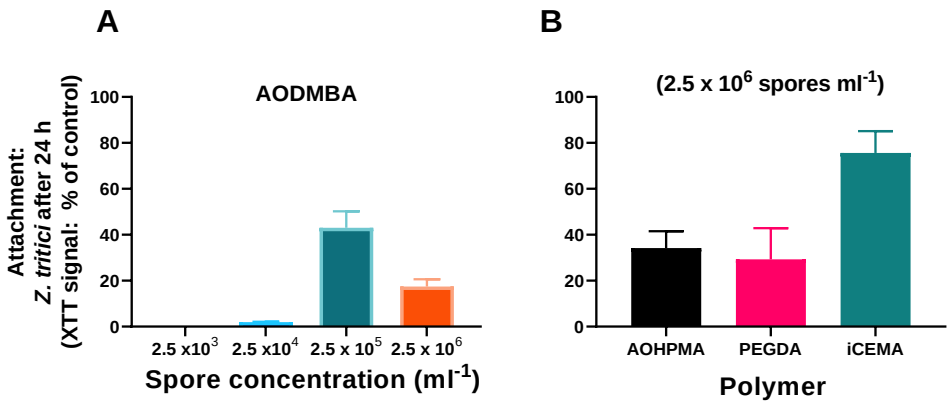

Figure 5.2. Influence of *Z. tritici* spore concentration on the level of attachment to polymer. (A) Attachment to AODMBA polymer at different spore concentrations. (B) Attachment to AOHPMA, PEGDA and iCEMA polymers. Attachment values were calculated using the XTT (metabolic activity signal) assay and OD_{490} readings, comparing this to a polystyrene control (normalised to 100%). Each bar represents the mean of three independent experiments. Error bars, + SD.

5.3.2 Optimisation of UV mutagenesis in *Candida albicans*

Due to the interruption of experiments experienced during the Coronavirus pandemic, it was decided that use of experimental evolution for gaining insight to genes determining polymer attachment mechanistic should be carried out with a fungal pathogen that possessed a faster growth rate than *Z. tritici*. This chosen pathogen was *Candida albicans*. UV-mutagenesis was optimised to provide a timepoint which gave ~80% survival, deemed a good threshold indicative of a reasonably high mutation rate. UV-mutagenesis was carried out in phosphate buffered saline (PBS) as YPD growth medium provided a protective effect against UV-light (shown in Appendix D, D.2). Recovery of viable cells declined by ~60% during the 60 sec exposure to UV (Figure 5.3).

Based on the results, 30 sec UV-exposure was chosen for further UV treatments as ~80% survival was observed.

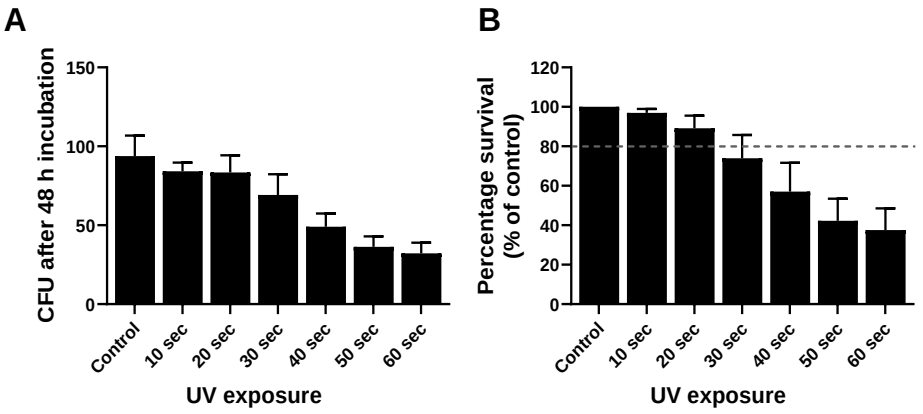

Figure 5.3. Optimisation of UV-mutagenesis in *C. albicans*. (A) Colony forming units (CFU) counted at 10-second increasing increments of UV exposure. *C. albicans* cells at OD_{600} 0.5 were exposed to UV-light in 10 ml of PBS, at an exposure height of 35 cm from the UV source with continuous mixing. Every 10 sec, aliquots of 100 µl were removed from the exposure, covered and kept at 4°C for one hour. Cells were diluted and spread onto YPD agar plates, enumerated after 48 h incubation at 37°C. (B) Percentage survival after UV mutagenesis plotted, calculated as a percentage of the control treatment without UV exposure, using data derived from (A). Bars represent the mean of three independent experiments, +SD.

5.3.3 AODMBA coupons maintain anti-attachment properties

After optimising the UV mutagenesis, the hit polymer chosen for the accelerated evolution experiment with *C. albicans*, AODMBA was used as a substrate to make inkjet 3D-printed forms for experiments. The polymer was chosen because of the the low-fungal attachment (< 25%) observed in *C. albicans* as well as the printability properties of the polymer, allowing a 'selection' to take place. The inkjet printability of the AODMBA polymer was first demonstrated by Vallières et al. (2020), where several factors including viscosity and surface tension were found to be suitable for AOMBA printing.

Therefore, AODMBA coupons were printed, and it was tested whether anti-attachment properties were retained. As can be seen in Figure 5.4, the coupons showed strong anti-attachment properties, supporting only ~10% of the attachment exhibited by *C. albicans* with the polystyrene control.

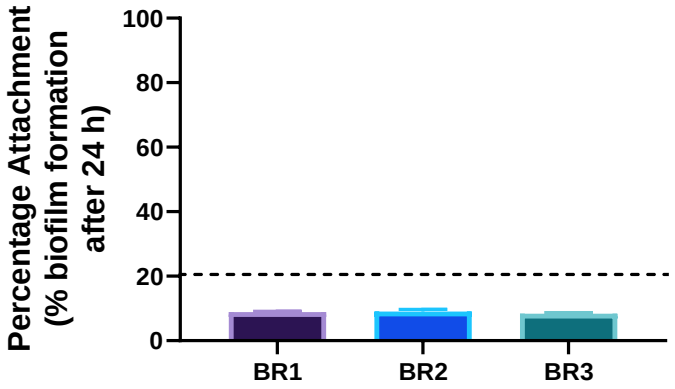

Figure 5.4. 3D-printed AODMBA coupons retain anti-attachment properties with *Candida albicans.* Attachment to 3D-printed coupons was assessed using the XTT-reduction assay with *C. albicans* strain CAF2-ycherry. Cells were incubated for 2h with AODMBA coupons before washing, transfer of coupons to fresh plates with fresh medium and further incubation up to 24 h, before XTT assay. Attachment was calculated as percentage compared to polystyrene controls for the respective biological repeats (BR). The dotted line points to 25% attachment, chosen as a threshold for quantifying a promising anti-attachment polymer. Bars represent the mean of three technical replicates, ±SD.

5.3.4 Accelerated 'evolution' strains do not show increased attachment

After confirming the suitability of the 3D-printed coupons for further work, an accelerated 'evolution' experiment was performed by subjecting *C. albicans* to seven rounds of UV-mutagenesis, outgrowth, selection of AODMBA-attaching cells and outgrowth again from the printed AODMBA coupons. A schematic for the evolution experiment is presented in Figure 5.5. Unfortunately, upon 3D-printing additional AODMBA coupons to continue with this experiment (after

conducting seven rounds of UV-mutagenesis and functional AODMBA coupon-selection), it was discovered upon testing the newly printed coupons that they had not retained their anti-attachment properties. This change coincided with a switch to a new printhead for printing. It was thought that the new printhead's printing properties negatively influenced the formulation and printed polymer performance. The data for the new printhead attachment can be found in Appendix D (D.3.).

In response to this technical problem, the attachment properties of the starting strains and the mutagenised generations with selection with AODMBA coupons (where anti-attachment properties were retained at ~10%, see Figure 5.4) were tested against 96-well plates coated with AODMBA (Figure 5.6A) and a promising AODMBA-co-TEGMA copolymer (Figure 5.6B) which has been shown to be effective against *Candida albicans* and various other fungal pathogens in preventing attachment (L. Crawford et al., in preparation). For AODMBA, testing with *C. albicans* yeast morphology, despite apparent slight increases in attachment across the three biological replicates after seven rounds of mutagenesis and selection, the attachment is not significantly increased compared to the starting strain. Furthermore, for AODMBA-co-TEGMA, the attachment did not significantly increase in the UV-mutagenesised strains selected with AODMBA. These results suggest the anti-attachment properties of the polymers show a robust, stable effect and, at least in the example of seven rounds of UV-mutagenesis and AODMBA selection, can withstand development of pathogen resistance to the anti-attachment effect.

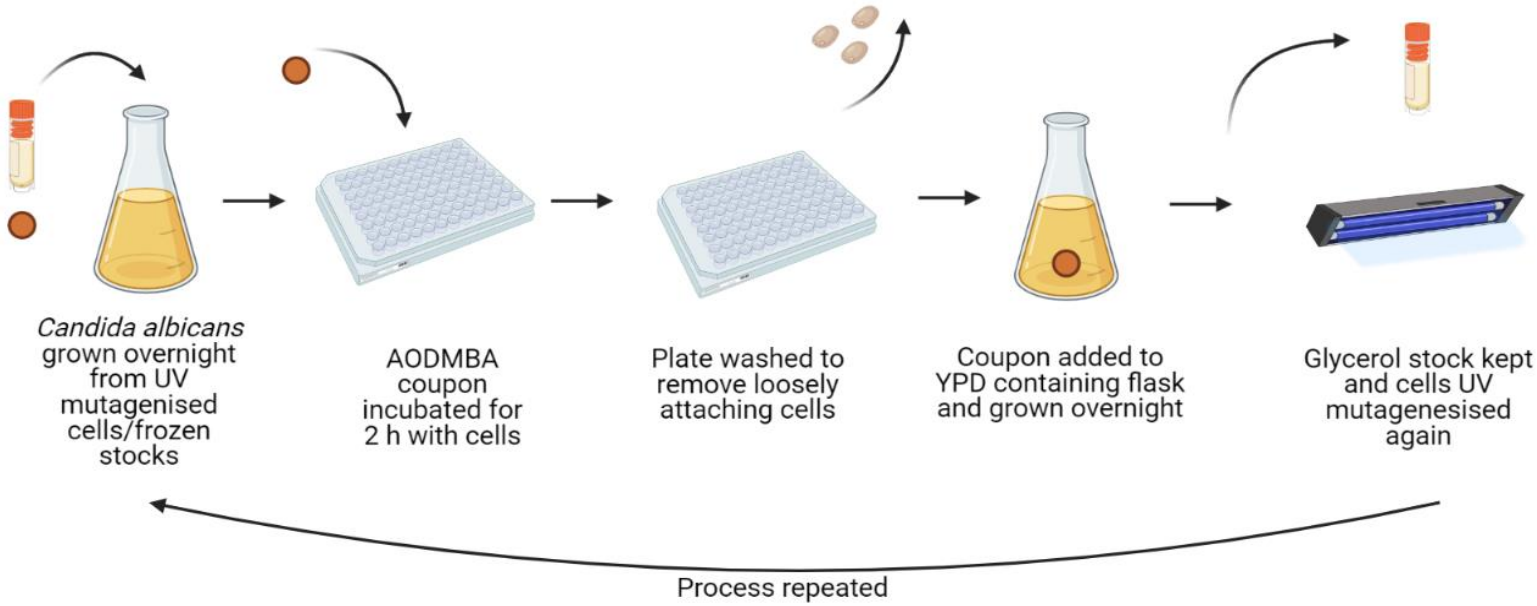

Figure 5.5. Schematic of the accelerated 'evolution' experiment using UV-mutagenesis in *C. albicans*. From left to right: The experiment begins with growing *C. albicans* (three biological replicates and two technical replicates) from colonies (first round) or from UV-mutagenised cells/stocks (subsequent rounds) in flasks containing YPD broth. Cultures are grown at 30°C overnight, diluted to an OD_{600} of 0.5 added to 96-well plates containing AODMBA-printed coupons, incubated at 37°C for 2 hours. Each well was washed three times with PBS to remove loosely attaching yeast cells. Coupons were added to flasks containing YPD and incubated overnight. Grown cultures samples were kept as glycerol stocks and diluted to OD_{600} 0.5 in phosphate buffered saline (PBS) for use in UV-mutagenesis. Mutagenised cells were washed and resuspended in YPD, grown overnight again and incubated with AODMBA coupons for the next round of selection. This process was repeated for multiple rounds. The figure was constructed using BioRender.

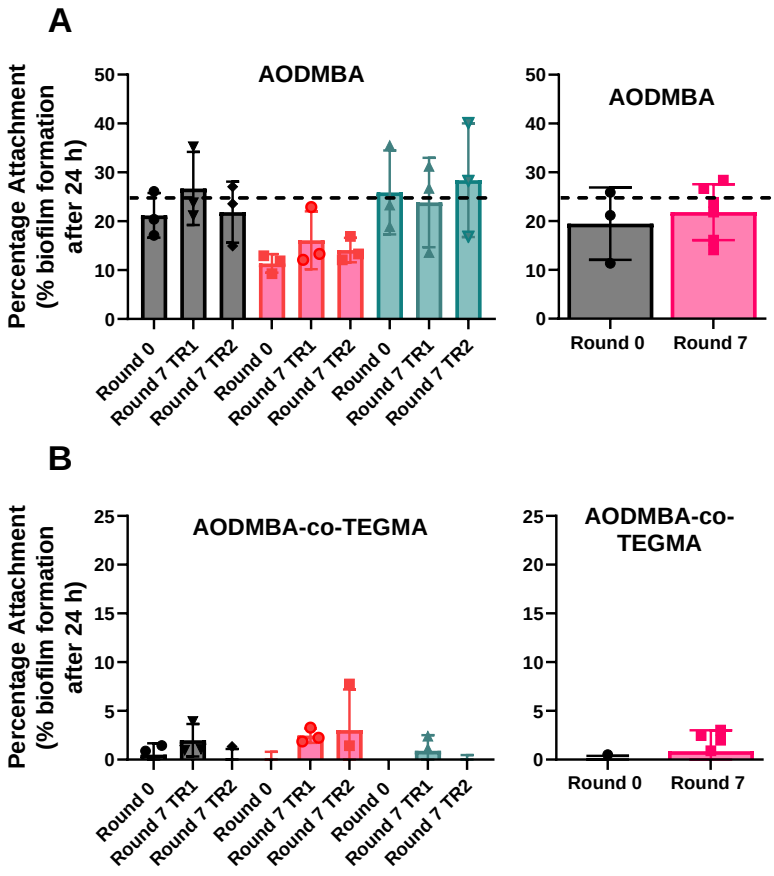

Figure 5.6. Anti-attachment properties tested against UV-mutagenised strains. Percentage attachment quantified using the XTT-metabolic activity assay after 24 h incubation with the indicated generations of *C. albicans* strain, CAF2-ycherry (experimental scheme shown in Figure 5.5). Attachment was calculated as a percentage of the polystyrene control (assumed to be 100%). (A) Attachment to AODMBA. (B) Attachment to AODMBA-co-TEGMA. Each point represents the mean of three independent experiments with each of the specified UV-mutagenised strains, error ±SD. Black bars represent biological replicate (BR) one, red bars represent BR two and green bars represent BR three. For the right hand panels, each bar is the average of the three biological replicates from the left hand panel, with the black bars representing Round 0 and red bars representing Round 7. TR = technical repeat for each biological replicate where UV mutagenesis and AODMBA selection was performed twice independently for an additional control. Data analysis using unpaired t-tests (comparing Round 0 and Round 7 for each biological replicate) revealed no significant differences. The dotted line points to 25% attachment, chosen for quantifying a promising anti-attachment polymer.

5.3.5 Spin coated mMAOES and AOHPMA polymer coverslips retain anti-attachment properties

In order to investigate the involvement of specific cell-wall properties in attachment and considering the cell-to-cell heterogeneity of the attachment phenotype described above, it was decided to compare the whole population of yeast cells/pycnidiospores to sub-populations that could attach to the polymer surfaces. Confocal laser scanning microscopy (CLSM) was used to assess selected cell surface properties according to staining with selective fluoroprobes. For achieving quantifiable images with CLSM a flat sample is desirable, to ensure that the image taken is of high resolution. Therefore, glass coverslips were spin-coated with thermally polymerised mono-2-(Methacryloyloxy)ethyl succinate (mMAOES), another promising polymer identified in the study by Vallieres *et al.* (2020) against *C. albicans*. This was chosen also as the protocol for mMAOES thermal polymerisation had already been optimised. for *C. albicans* or AOHPMA for *Z. tritici*. These polymers were chosen for microscopic analyses because thermal polymerisation protocols were optimised and possessed chemical suitability, such as not being brittle/prone to cracking. Spin coating enables polymer films to be made that are thin and uniformly distributed (Mouhamad et al., 2014, Muhammed Shameem et al., 2021).

Employment of the spin-coating method enabled the acquisition of images suitable for subsequent analysis. To assess the anti-attachment properties of polymer on the spin coated coverslips, XTT-reduction assays were performed with *C. albicans* on mMAOES and for *Z. tritici* on AOHPMA whilst also using glass coverslip as an additional material control. The attachment was calculated as a percentage compared to results for attachment to multi-well plates made from polystyrene. For *C. albicans* the mMAOES retained anti-attachment properties in the coverslip coatings, with mean attachment of ~8%, whereas for glass the mean attachment was ~64% compared to polystyrene (Figure 5.7A). For *Z. tritici*, AOHPMA coverslips also retained anti-attachment properties reflective of the data from previous AOHPMA experiments (Figure 5.2), with a

mean of ~30% attachment and with glass coverslips exhibiting ~76% attachment versus polystyrene (Figure 5.7B).

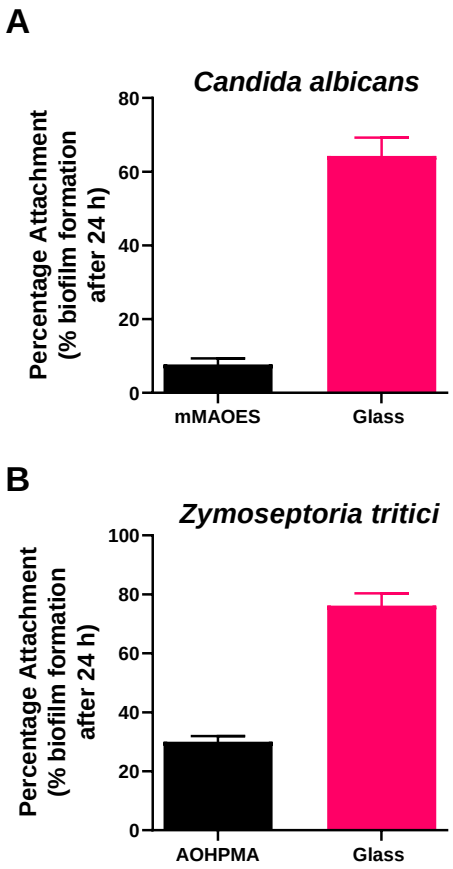

Figure 5.7. Anti-attachment properties retained in polymer-coated coverslips. (A) Biofilm formation was assessed using the XTT-reduction assay where *C. albicans* strain SC5314, at OD_{600} 0.015 was added to polystyrene, or glass/polymer coated coverslips. Loosely attaching cells were washed and plates were incubated for a further 24 h followed by XTT assay. (B) Similar experiment for *Z. tritici,* except supplied at 2.5 x 10^6 spores ml^{-1} with washing of loosely attaching cells after 5 h. Calculations were made comparing by XTT signal from cells/spores on uncoated or polymer coated glass coverslips versus multi-well plates made from polystyrene as the control. Each bar represents the mean of three independent experiments, error + SD.

5.3.6 Cell wall involvement in attaching cell populations

To investigate the outer cell wall properties, two probes were used initially. Concanavalin A tagged with Alexafluor 488 (FITC) was used as the lectin binds to α-(1-6)-mannan in the fungal cell wall (Tkacz et al., 1971, Fujikawa et al., 2009). Chitin was stained with trypan blue, being a stable, far-red dye with similar staining properties to calcofluor white which is widely used to stain chitin (Liesche et al., 2015). Calcofluor white (CFW) was not used in this experiment due to the need for cell quantification for subsequent image analysis which was carried out using the nuclear stain, DAPI (Tarnowski et al., 1991) , but is UV excitable like CFW meaning CFW could not be used.

Additional stains were also tested during optimisation experiments with aims to collect a more complete investigation into the involvement of cell wall components. One stain also tried was Eosin Y, to stain fungal chitosan (Fujikawa et al., 2009). The stain overlapped in fluorescence with concanavalin A, which would have prevented simultaneous staining (also excitable with FITC) and during optimisation experiments, issues with inconsistent spore/yeast cell staining were a recurrent problem, so for this experiment, Eosin Y was not pursued. Moreover, an additional stain, aniline blue which stains β-(1,3)-glucan (Lee et al., 2018) was used in initial experiments. However, the excitable fluorescence wavelength overlapped with DAPI, therefore prevented multiple staining and during optimisation the stain was not consistent despite following the same protocol, therefore aniline blue was not used in this experiment.

Initially several quality control tests were performed. First, to ensure that the polymer-coated coverslips did not interfere with any fluorescent signals, image analysis was performed on the 'whole' stained cell populations mounted onto coverslips; either uncoated glass or polymer coated. In the case of AOHPMA or mMAOES, spores or cells (respectively) on the polymer coated coverslips showed fluorescence from concanavalin A, DAPI or trypan blue staining that was comparable with spores or cells on glass (Figure 5.8). This indicates that

any differences identified between conditions in the attaching population would not be due to an artefact like polymer autofluorescence.

An additional control experiment was performed to validate the stability of the fluorescent stains during the attachment period of the experiment, to corroborate that any observed differences were genuine. In the experimental design, for *Z. tritici* there was an initial 5 hour incubation period to allow the pycnidiospores time to attach to the glass/polymer coverslips (see Methods 5.2.9). To assess if this attachment period affected the fluorescence of the stained population, the fluorescently stained spores were mounted to coverslips after 5 hours in solution (PBS). The data indicated that the attachment period has minimal impact on the fluorescence readings from spores for the three stains (Figure 5.9A). Similarly, for *C. albicans,* the 2 hour incubation period in solution (PBS) after fluorescent staining, used to allow cell attachment, showed minimal effect on fluorescence signals from cellular concanavalin A, DAPI or trypan blue (Figure 5.9B). These results indicated that the attachment period has minimal impact on the cell population fluorescence and therefore any differences in attached cell populations can be assumed not to be due to instability of fluorescent staining of cells.

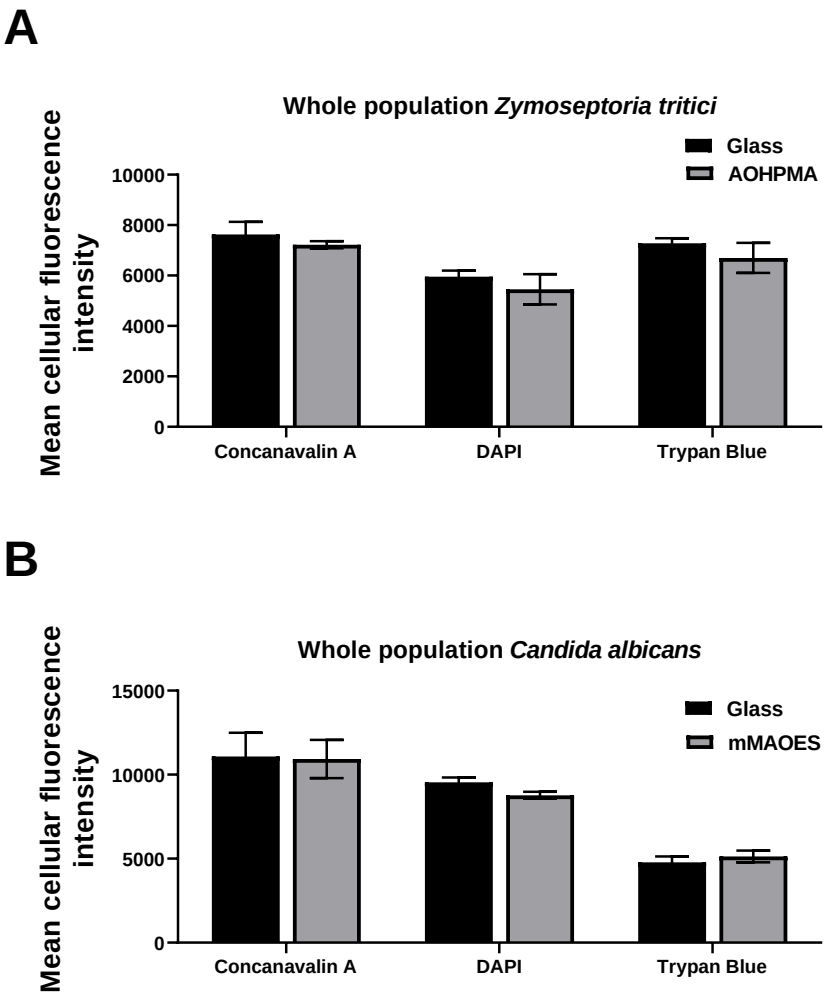

Figure 5.8. Cells on spin coated coverslips show comparable fluorescence to cells on glass coverslips. Whole population of *Z. tritici* spores mounted onto AOHPMA coated or uncoated glass coverslips (A) or mMAOES and *C. albicans*, strain SC5314 (B) stained with concanavalin A, DAPI or trypan blue, mounted onto uncoated glass or AOHPMA coated coverslips. Mean fluorescence intensity calculated (from single cell measurements) from a mean of three independent experiments. For each image ≥ 30 pycnidiospores/yeast cells were analysed. Image analysis performed in ImageJ. Error ±SD.

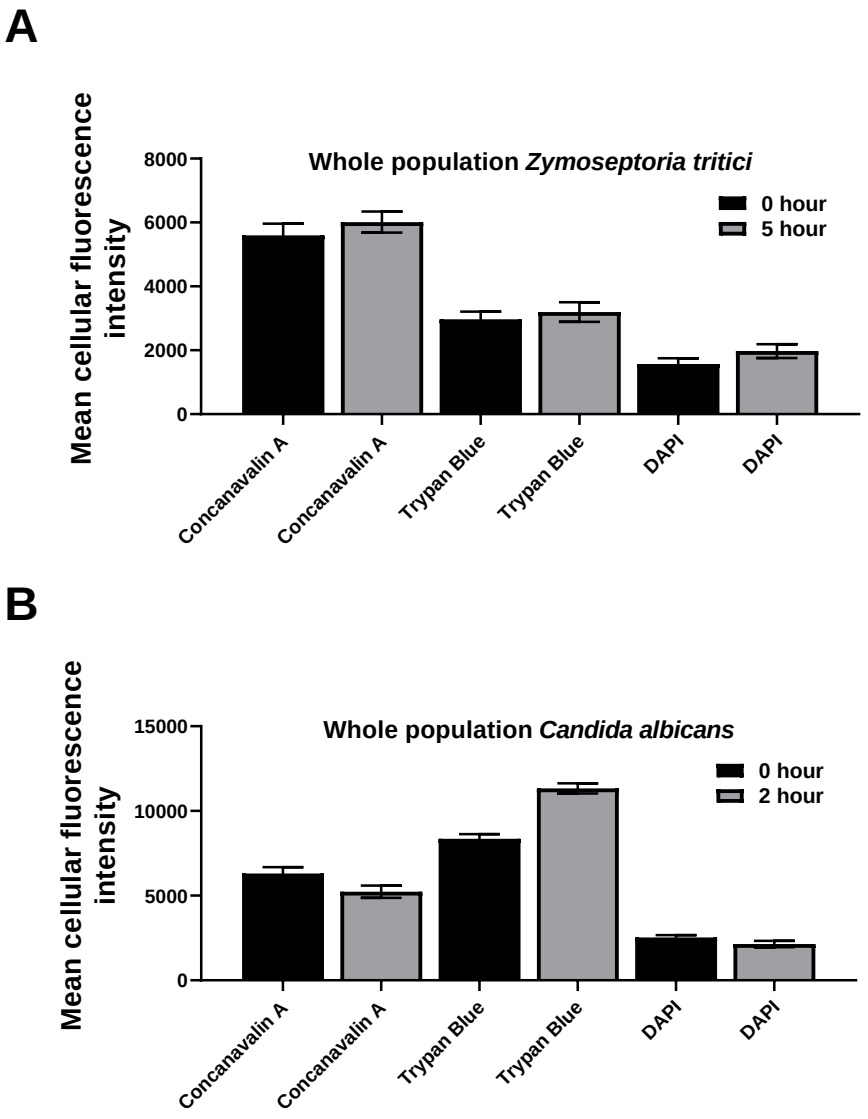

Figure 5.9. Attachment period has minimal influence on cellular fluorescence. Whole population of (A) *Z. tritici* mounted at 0 h or after a 5 h period in PBS solution or (B) *C. albicans*, strain SC5314, mounted at 0 h or after 2 h in PBS solution after fluorescent staining with stained with concanavalin A, DAPI or trypan blue. Mean fluorescence intensity calculated (from single cell measurements) from a mean of three independent experiments. For each image ≥ 30 yeast cells/pycnidiospores were analysed Image analysis performed in ImageJ. Error ±SD.

5.3.7 Attaching *Z. tritici* pycnidiospores show differences in cell wall properties compared with the whole spore-populations

Following on from the indication that AOHPMA-coated coverslips did not interfere with fluorescence signals from cells and that the attachment period also had minimal impact on fluorescence, the aim was to assess potential roles for certain outer and inner cell wall components in attachment, through staining of α-(1,6)-mannan and chitin respectively. As mentioned above, staining of other cell wall components were attempted and should be considered in future experiments in order to gain a more complete understanding of the involvement of the cell wall in attachment. From a simple visual assessment (Figure 5.10), there was a strikingly lower trypan blue fluorescence in the spore subpopulations that attached to glass or AOHPMA. For DAPI, the fluorescence also appears slightly lower in attaching cells. In the case of concanavalin A, all three cell populations appeared to exhibit similar fluorescence. To ensure that the brightness of the pycnidiospores was not skewed by not all attaching in the same focal plane, Z stacks were taken. For each image the different fluorescent channels used for the three stains are taken from the same field of view. Subsequent image analysis with ImageJ software then took the highest intensity value across the three stacks, allowing the maximum fluorescence intensity to be determined. This was performed for all conditions. For concanavalin A, the data suggested the possibility of a slightly lower fluorescence from cells of the whole population compared to attached pycnidiospores (Figure 5.11). However, this was not a significant effect ($p > 0.05$); there was a high variability in fluorescent intensities measured between experiments. For the nuclear stain, DAPI, used as a control for cell staining, the whole population shared a comparable fluorescence with pycnidiospores attached to glass and close to that of pycnidiospores attached to AOHPMA. Finally, for trypan blue, as suggested visually, there is a significantly lower signal compared with the whole population for pycnidiospores attached either to glass or to AOHPMA. The data indicates that whereas α-(1,6)-mannan content (concanavalin A staining) does not appear to

differ for attaching or entire (attaching + non-attaching) spore populations, according to trypan blue staining, the chitin content is lower for attaching spores. This suggests that high chitin is detrimental for attachment. It could be suggested that a lower chitin content could be reflective of a reduced cell wall flexibility in the spores that are capable of attaching to the glass or AOHPMA substrate. However, that did not differ whether attachment was to glass or to AOHPMA polymer.

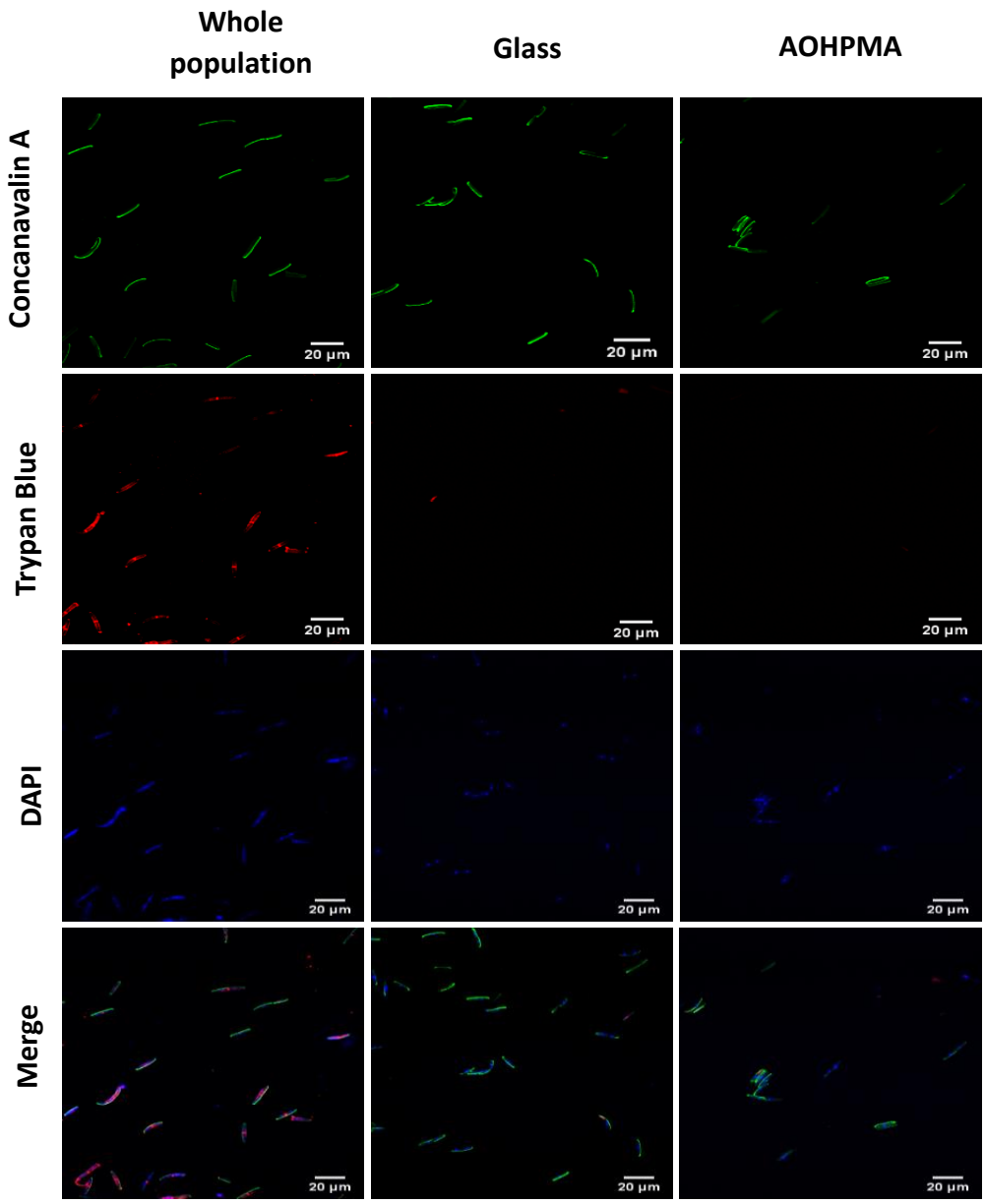

Figure 5.10. Confocal imaging of attaching and whole-culture populations of *Z. tritici* pycnidiospores. From top to bottom, the first panel represents pycnidiospore staining with concanavalin A (α-(1,6)-mannan), second panel channel with trypan blue (chitin) the third panel represents the nuclear stain DAPI, and the final panel is the merge of all three channels. From left to right, the first image of the panel represents the whole population before attachment, the middle image is the population attached to glass coverslips and the right image is the spore population attached to AOHPMA coated coverslips. Each image is taken using the Zen software and represents one slice from a Z stack of one image taken from three images taken across three independent experiments. For each image ≥ 30 cells were analysed. Scale bar = 20 µm.

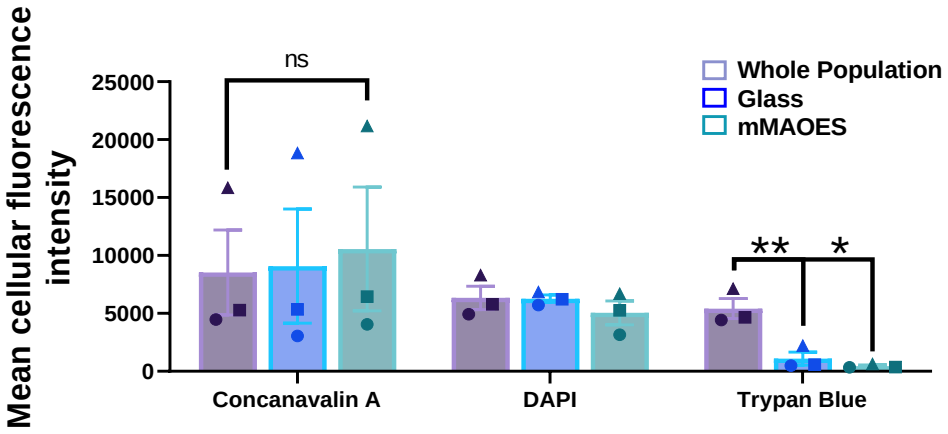

Figure 5.11. Mean fluorescence intensity of attaching and whole-culture populations of *Z. tritici* pycnidiospores. Fluorescence intensity was quantified in ImageJ, where single cell fluorescence was quantified across three Z stack slices and the maximum fluorescence value used for each cell. A mean value was taken for each experiment, and this was performed for three independent experiments for each stain and across the three conditions; with different replicate experiments distinguished by a different symbol and each bar representing a different condition; whole population (purple bar); attaching to glass (blue bar) or to AOHPMA (green bar). For each image ≥ 30 pycnidiospores were analysed. Error, ±SEM. Statistical comparison using paired t-tests; * $p < 0.05$, ** $p < 0.01$, ns = not significant.

5.3.8 Attaching *Candida albicans* yeast cells show differences in cell wall fluorescence compared with the whole cell-populations

Similar experiments as described for *Z. tritici* were also performed with *C. albicans,* with the mMAOES polymer. Preliminary quality control tests indicated that mMAOES, like AOHPMA, did not interfere with cell fluorescence readings (Figure 5.8B) and the signal was stable over the attachment period (Figure 5.9B) As for *Z. tritici*, confocal images were produced for the stained *C. albicans* cell (sub)populations (**Error! Reference source not found.**). For concanavalin A, cell fluorescence appeared comparable for all conditions. For the DAPI stain, the attaching cells appeared to a lower fluorescence than in the whole population. In the case of trypan blue, a stain for the inner cell wall (chitin) it was visibly evident that trypan staining was lower in attaching yeast

cell populations, both for glass and for mMAOES. Following quantification using ImageJ software (Figure 5.13, as described above for *Z. tritici*), for concanavalin A the mean cellular fluorescence intensity did not differ significantly for the attaching cells versus the whole cell population although a significant difference could have been masked by the variability between the mean fluorescence intensities in different experiments. For the DAPI cell-staining control, the mean fluorescence intensity appeared lower in both the attaching populations compared to the whole cell population, although again differences were not significant. Finally, in the case of trypan blue, there was a significant, > 10-fold lower mean cellular fluorescence intensity of the cell populations attached to glass or mMAOES. This data indicates that cells able to attach to either glass or mMAOES substrata are significantly reduced in their chitin content. This reduction in chitin levels in attaching spores could also reflect an enhanced flexibility, allowing the yeast cells to attach to the glass or AOHPMA substrate. A further experiment could be to look at exposed chitin levels using wheat germ agglutinin. As for *Z. tritici,* this effect was not specific for attachment to the polymer versus glass. The possibility also of a weaker, positive relationship between attachment and α-(1,6)-mannan content (concanavalin A fluorescence) cannot be completely discounted. The results were very similar for cells of *C. albicans* and spores of *Z. tritici*.

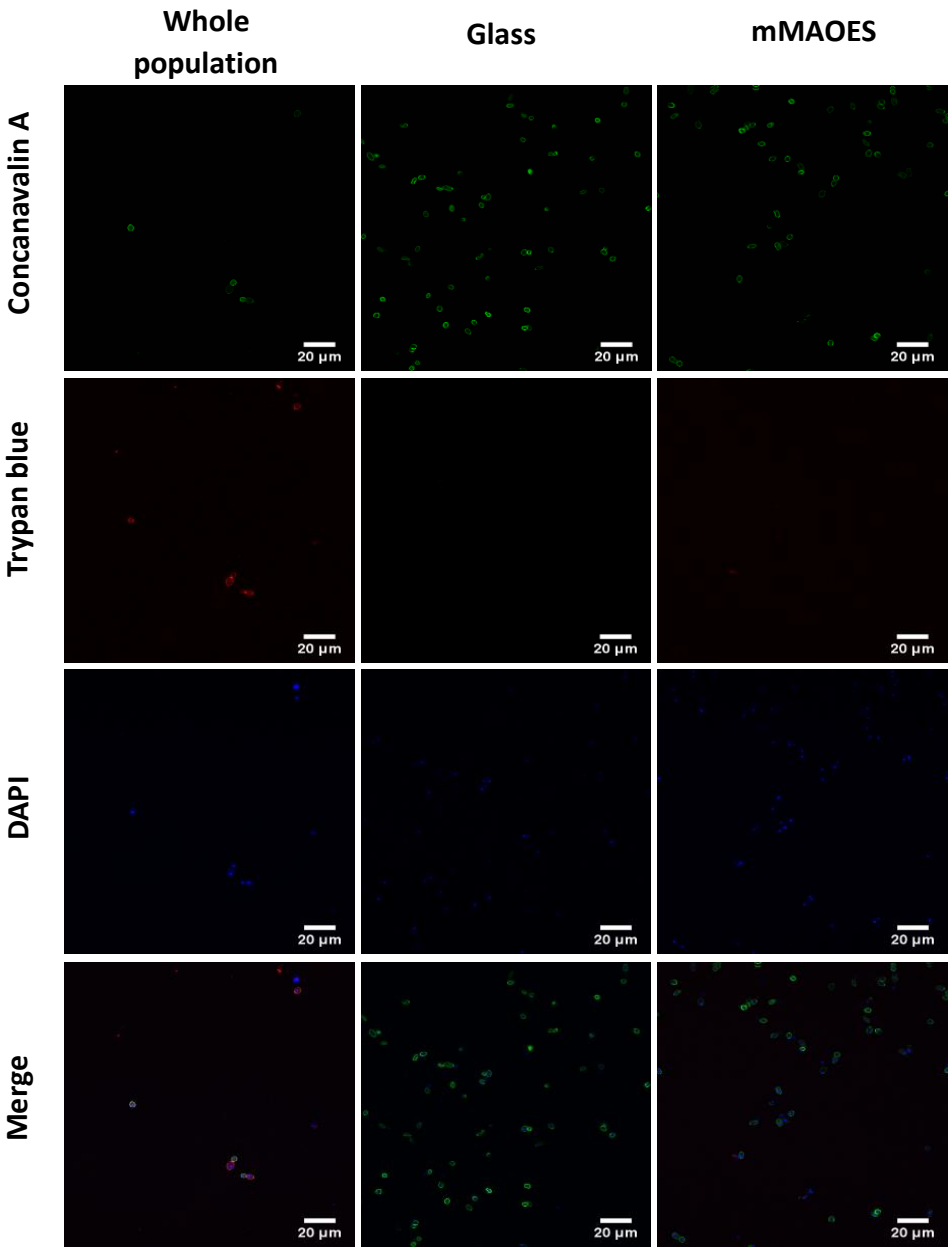

Figure 5.12. Confocal imaging of *C. albicans* yeast cells. From top to bottom, the first panel represents yeast cells, strain SC5314, stained with concanavalin A (α-(1,6)-mannan), second panel channel with trypan blue (chitin), the third panel represents the nuclear stain DAPI, and the final panel is the merge of all three channels. From left to right, the first image in the panel represents the whole population before attachment, the middle image is the population attached to glass coverslips and the right image is the cell population attached to mMAOES coated coverslips. Each image represents one slice from a Z stack of one image taken from three images taken across three independent experiments. For each image ≥ 30 yeast cells were analysed. Scale bar = 20 µm.

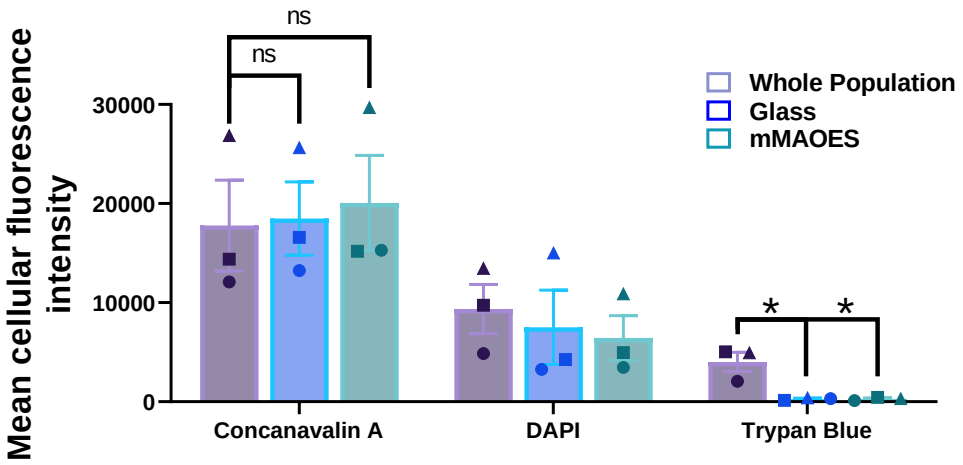

Figure 5.13. Mean cellular fluorescence intensity of *C. albicans* yeast cells, strain SC5314, across different conditions. Fluorescence intensity was quantified using ImageJ, where single cell fluorescence was quantified across three z stack slices and the maximum fluorescence value was used for each cell. A mean value was taken for each experiment, and this was performed for three independent experiments for each stain and across the three conditions; with different replicate experiments distinguished by a different symbol and each bar representing a different condition; whole population (purple bar); attaching to glass (blue bar) or to AOHPMA (green bar). For each image ≥ 30 yeast cells were analysed. Error, ±SEM. Statistical comparison using paired t-tests; * $p < 0.05$, ns = not significant.

5.4 Discussion

This chapter has focussed on developing our understanding of the mechanisms involved in the fungal anti-attachment properties of several polymers. One strategy utilised accelerated evolution and selection in the human fungal pathogen, *C. albicans,* focused on attachment to the hit polymer AODMBA. Across several rounds of UV mutagenesis and subsequent selection with AODMBA, despite unforeseen technical challenges interrupting the experiment, the yeast cell cultures had not gained improved attachment to the polymer or against additional AODMBA-co-TEGMA copolymer. An additional strategy was a preliminary study to assess cell wall features that may be important for fungal (anti-)attachment. Through confocal microscopy and image analysis, the cell/spore populations attaching to either glass or polymer showed significantly lower chitin content, according to trypan blue staining. These findings: (1) have indicated that anti-attachment phenotypes are relatively stable across rounds of mutagenesis and selection; (2) supported the idea that particular cell wall components are important for (anti)attachment. However, properties specific to polymer versus glass (anti)attachment were not identified in the current experimental setup with a focus on yeast cell adherence, these findings warrant further investigation in the future, particularly to extend the experimental focus to include the hyphal morphology of *C. albicans*.

5.4.1 *C. albicans* cells do not develop AODMBA resistance during accelerated evolution

Experimental evolution is a valuable strategy for elucidating genetic bases for phenotypes like resistance (to drugs etc.), often with a view to improving treatment or other means to help control resistance development (Santos-Lopez et al., 2022). Such experiments may incorporate mutagenesis steps, such as from ultra-violet light, to accelerate the emergence of potential resistance (Spencer and Spencer, 1996). One example by Mosbach et al. (2017) elucidated resistance of the fungal phytopathogen *Botrytis cinerea* to anilinopyrimidines

(AP) following UV-mutagenesis. The authors then used whole-genome sequencing and reverse genetics to characterise the AP resistance mechanism, which clustered around genes encoding proteins involved in mitochondrial function (Mosbach et al., 2017). This example illustrates one of many valuable types of output from accelerating resistance development, where the evolved resistance mechanism is informative of the drug mechanism of action. In our study, both continued UV-mutagenesis and selection were incorporated with aim to identify cells which had overcome polymer anti-attachment.

In this Chapter, mutagenesis plus selection experiments were performed with the phenotype of attachment to the hit anti-attachment polymer AODMBA. This polymer has shown potential for control of *C. albicans* colonisation, including drug-resistant strains whilst also possessing printability properties, which could be important for the production of medical devices e.g. catheters or voice prothesis flaps (Vallières et al., 2020). In the experiment conducted here, the inability of *C. albicans* to attach to AODMBA was retained. Therefore, at least for the seven rounds of UV-mutagenesis and the subsequent generations tested, there was no evidence for evolution to gain AODMBA-attachment function. This finding is positively important in indicating a relatively stable and robust nature of the anti-attachment phenotype against the yeast cell morphological form, providing further evidence supporting use of the polymer in medical applications. As shown through the Mosbach et al. (2017) study, genetic analysis of evolved mutants is informative for understanding how resistance can develop as well as mechanisms of action. Continuation of approaches like the evolution experiments with anti-attachment polymers are important for improving our understanding. However, while absence of attaching mutants does not help with that aim, it does provide experimental support for the hypothesis that development of attachment function, and therefore development of resistance presents a relatively large evolutionary hurdle for cells (Vallières et al., 2020).

5.4.2 Attaching populations exhibit cell wall differences

The fungal cell wall is important for pathogenesis and possesses a distinctiveness (e.g., humans do not possess a cell wall) which has rendered it a major focus of drug development (Arana et al., 2009). The importance of the fungal cell wall in attachment and subsequent pathogenesis has been unanimously accepted (Gow et al., 2017). Therefore, understanding the role of the cell wall in attachment to the polymers is a focus of interest for continued and lasting implementation. The fungal cell wall is complex with multiple components, including glucans, chitin and glycosylated cell wall proteins (Casadevall and Perfect, 1988, Garcia-Rubio et al., 2020). Using two stains (to stain the outer and inner cell wall) in this initial study of such cell wall components in (anti)attachment, roles for chitin or α-(1,6)-mannan were considered in attaching to the polymer materials, versus whole cell-populations. It is currently unknown if the polymers can 'bind' chitin. Fungal cell wall architecture is also well known exhibit species-specific differences (Free, 2013) and therefore two pathogens of interest were evaluated: the phytopathogen *Z. tritici* and human pathogen *C. albicans*.

In the pathogenesis of phytopathogens, the dispersal and attachment of the spore is of principal importance (Hamer et al., 1988, Osherov and May, 2001). Attachment to the plant host by spores can involve the production of adhesives, which are often classified into preformed (expressed prior to attachment, do not need time or metabolic activity for their production) (Schumacher et al., 2008) or secreted (where active metabolism is necessary for production once on the host) (Mercure et al., 1995). Spore adhesion is influenced by the attachment surface properties, hydrophobicity and temperature, which subsequently can influence germination and host colonisation (Jones and Epstein, 1990, Whitehead et al., 2011, Liauw et al., 2020, Vasselli and Shaw, 2022).

In addition to the abovementioned factors, the cell wall composition is likely to influence the spore attachment. In the present study, it was found *Z. tritici* pycnidiospores attached to either glass or AOHPMA coated coverslips had

significantly lower trypan blue staining than the starting cell populations, indicating lower chitin contents in these cells. There was also a hint of a possible relationship between α-(1,6)-mannan content and attachment, but there was considerable experiment-to experiment variation in the data. An increase in the mannan layer could suggest these spores have a thicker cell wall, which may be advantageous during attachment, and could also influence DAPI staining with less stain able to enter the fungal cell. A possibility that a larger outer mannan layer predisposes pycnidiospores to successful host colonisation would be consistent with a previous study that identified conidial mannan as important for conidial adhesion and cell wall organisation in *Aspergillus fumigatus* (Henry et al., 2016), both of which play important roles in successful attachment and infection. However these observations must be taken with caution as the composition and roles of components of the fungal cell wall differ between fungal species (Free, 2013).

Components of the fungal cell wall can also act as triggers of plant immune response, termed pathogen-associated molecular patterns (PAMPs) and PAMP-triggered immunity (PTI). It is known that for phytopathogens, particularly hemibiotroph's such as *Z. tritici*, remaining undetected is essential for successful infection and can be enabled by cell wall remodelling (Fujikawa et al., 2012). Chitin is a well-known PAMP, and enzymatic degradation of chitin (sub-nanomolar concentrations) can trigger PTI defence responses (Felix et al., 1993, Shinya et al., 2015). It could be hypothesised that attaching pycnidiospores are reduced in chitin to avoid triggering PTI and therefore promote successful host colonisation as a trade-off to the structural role chitin plays in the fungal cell wall. Wheat leaf surfaces are hydrophobic due to their waxy cuticle (Javelle et al., 2011) whilst spore surfaces of fungal pathogens are hydrophobic due to the presence of surface hydrophobins (Aimanianda et al., 2009). Spore hydrophobicity promotes successful dispersion and host colonisation (Cai et al., 2020). Chitin itself is also hydrophobic (Kang et al., 2018) and a decrease in chitin level is unlikely to be linked to an increase in the attachment of hydrophobic spores. Moreover, a change in the spore chitin level

is also not likely to change surface hydrophobicity due to its inner position and limited representation in the cell wall. Alternatively, low chitin in walls of some spores suggests increased composition of other cell surface component(s), with an increased flexibility allowing a larger surface area for attachment, which could drive a propensity of these spores to attach more. These proposed hypotheses warrant experimental scrutiny in future work.

Unlike many phytopathogens, the cell wall of *Candida albicans* is extremely well characterised for its composition, function and dynamics in these properties in response to changing environmental and stress conditions (Gow et al., 2017, Garcia-Rubio et al., 2020). The cell wall of *C. albicans* is the most well studied of any fungal pathogen (Gow and Hube, 2012). The outer cell wall mannan of *C. albicans* comprises 40% of dry cell wall weight and is referred to as a 'mask' for inner cell wall components, which elicit a strong immune response in the host, including β-(1,3)-glucan and chitin (Klis et al., 2001). Despite proposed immune shielding roles of the outer mannan layer, it has been found that this property is immune-cell specific: mannan acts as a shield in immune cells where Dectin-1 (recognising β-(1,3)-glucan) is the primary immune recognition receptor (Yadav et al., 2020). It was found that cells that had attached to mMAOES polymer of glass potentially exhibited an elevated α-(1,6)-mannan content, suggesting a possibility that attachment is favoured with a thicker outer cell mannan layer, which could also be suggested as a strategy to avoid host-cell recognition.

In the inner cell wall layer, chitin usually represents 1-3% (and can be up to 20%) of the *C. albicans* cell wall dry weight and is interconnected through β-(1,6)-glucan to the outer cell wall layer (Chattaway et al., 1968, Garcia-Rubio et al., 2020). Despite its comparatively small representation in the composition of the cell wall, chitin is essential for cell shape and viability (Bulawa et al., 1995, Mora-Montes et al., 2011). The cells attaching to glass and mMAOES substrata exhibited a significantly lower trypan blue (chitin) fluorescence. As suggested above for similar results for *Z. tritici* spores, low chitin in certain cells could be a strategy to limit host-recognition. Alternatively, low chitin in walls of some

yeast cells could also suggest, alike in *Z. tritici*, increased composition of other cell surface component(s), including an increase in flexibility, which increases the surface area for attachment, which could favour these yeast cells to attach more. Low chitin cells are likely to be less fit in other regards (Bulawa et al., 1995).

One aim of the chapter was to try to characterise cell wall features which may be important in enabling attachment to certain substrates (e.g. glass) but not the candidate anti-attachment polymers. The results supported the general approach used but did not themselves point a cell wall component that may distinguish attachment to these different surfaces: the reported effects were similar on glass or polymer. This is raised again in the future work suggestions below. A limitation of the present work was that it relied on fluorescent probes, a common concern about which is potential for cross-reaction, alongside other concerns with extrapolation to quantitative measures of specific cell constituents (Winterbourn, 2014). Nevertheless, the present results provide useful indicators which can inform future, more rigorous interrogation of such cell surface properties in polymer (anti)attachment phenotypes.

5.4.3 Conclusions and future work

Exploring the mechanisms involved in preventing attachment to different polymeric materials by medically and agriculturally important fungal pathogens could help inform their potential for and progression towards applications (Vallières et al., 2020). The attachment of such fungal cells to surfaces, as discussed in this chapter, is commonly a prerequisite for infection and can involve diverse strategies beyond those explored here; some of which include the production/secretion of adhesins and hydrophobins, surface charge effects as well as immune-masking (Yang et al., 2013, O'Driscoll et al., 2014, Desai and Mitchell, 2015, Kettles and Kanyuka, 2016, Gow et al., 2017).

Due to time constraints, the accelerated evolution experiment was undertaken in *C. albicans*, and was unexpectedly cut short due to printhead manufacturing

issues. It would be a priority to continue the accelerated evolution experiment using the AODMBA polymer, and should increase attachment arise with time, to evaluate the changes in these strains genetically. This would improve mechanistic understanding of anti-attachment and build knowledge towards potential for applications. It should also be valuable to carry out an evolution experiment in *Z. tritici*, to assess the robustness of the anti-attachment phenotype also in this phytopathogen. Little known about the process of spore attachment in *Z. tritici* (Steinberg, 2015). An experiment with *Z. tritici* had additionally been planned for a further hit polymer, DEGEEA, but could not be pursued due to the pandemic interruption and subsequent time constraints.

To establish proof of principle for the experimental approach with the cell wall probes, which capitalised on natural cell-to-cell variation in the attachment phenotype, only two cell wall components were investigated here. Potential roles for other components of the cell wall in polymer (anti)attachment would now be important to assess. Examples of additional cell wall components include specifically designed primary antibodies with fluorescent secondary antibodies, which have been used in the detection of α-(1-3)-glucan and β-(1-3)-glucan (Fujikawa et al., 2009). The results presented here indicate that cell wall variation between cells is important for the attachment phenotypes, in both the studied pathogens. Moreover, another approach could involve genome-wide evaluation (e.g. RNA-Seq) of yeast cells/pycnidiospores that had attached compared with the non-attaching cells, to cast the net wider in considering cell (wall) functions that may be mediating the differential phenotypes. Finally, the results highlighted here suggest cells low in chitin and with a higher mannan content in the case of *C. albicans*, are able to better attach to the polymer. In order to support these findings, relevant gene overexpression and knockout mutants could be tested. For example, chitin synthesis mutants of *C. albicans* are well described (Mora-Montes et al., 2011) and these could be tested against mMAOES to assess if they possess improved attachment properties compared to the background strain. For *Z. tritici,* genetic understanding of the pathogen is continually

improving, and chitin synthases have been identified but these have not yet been knocked out/overexpressed (Schuster et al., 2020).

Materials that passively prevent attachment of fungal pathogens offer a potentially promising strategy to prevent infection and biofilm formation, avoiding the use of chemical actives. Developing upon understanding of attachment in these pathogens is essential for mechanistic insights to (anti)attachment. This study has highlighted important findings regarding robustness of polymer anti-attachment phenotypes and potential importance of (low) cell wall chitin content for cell-cell variation in attachment, offering good bases for future development.

Chapter 6 – Summary and Concluding Remarks

6.1 Summary of results

In Chapter 2 and 3 of this thesis, the studies focussed on the exploration and the use of natural products (NP) in combination against fungal pathogens. Through the use of a pairwise high-throughput screening approach (Chapter 2), many potential synergistic NP combinations were identified. Importantly several combinations exhibited broad-spectrum activity, suggesting NP synergies could be used across multiple fungi. Moreover, the complexity of NP interactions was explored within Chapter 3, where a NP with uncoupling (of oxidative phosphorylation) activity was synergistic with a number of other NPs and commonly used antifungals. It would be important to assess potential host toxicity and durability (to resistance development) of these synergistic interactions, both to develop our understanding of synergy and to encourage their practical application. These findings suggest that synergy amongst NPs is a common occurrence, and this could be further exploited in a larger screening programme for identification of additional potent combinations for fungal pathogen control.

In Chapter 4, collateral sensitivity (CS) in azole-resistant *C. albicans* was explored using a drug-repurposing strategy. CS is relatively unexplored in fungal pathogens and this study aimed to assess if CS was present in azole-resistant *C. albicans*. Two mutants exhibited a strong hypersensitivity to an array of different non-antifungals, further exploration of the sensitivity revealed the potential involvement of cell wall integrity and glycosylation defects. Moreover, screening of an FDA-approved library did not identify any CS-displaying compounds in the mutants. Taken together, these findings suggest that CS is not very common in azole-resistant *C. albicans*. Future research could focus on pursuing the presence of CS in different drug-resistance backgrounds using high-throughput repurposing libraries.

In Chapter 5, the robustness and potential mechanisms relevant to the passive anti- fungal-attachment properties of certain methacrylate polymers were assessed. An evolution-based experiment within *C. albicans*, revealed that this organism did not readily overcome the anti-attachment properties of the hit polymer AODMBA. This experiment, whilst highlighting the polymer is able to resist attachment, focussed on the yeast morphological form of *C. albicans*. To establish a more complete understanding of the durability of the polymer, future work should also incorporate the hyphal morphological form. Both *C. albicans* and *Z. tritici* showed significantly lower chitin content in glass- or polymer- attached cells, which could reflect an immune evasion strategy or more simply that the physical properties of low-chitin walls enable better attachment to the flat surfaces. These findings begin to elucidate the complexity in how fungi are able to attach to polymeric surfaces and future work could use additional fluorescent probes for additional cell wall features and/or relevant genetically manipulated strains to deepen our understanding of how attachment is prevented in these materials.

6.2 Key themes and discussion

In this thesis, alternative approaches to control fungal pathogens are explored using different methodologies. In Chapters 2 and 4, high-throughput screening was used to search for novel compound-combinations or chemical-genetic interactions (i.e. drug sensitivity in genetically azole-resistant strains), with either NP or FDA-approved chemical libraries. The focus upon NPs and FDA-approved compounds was chosen to address growing consumer concerns and legislative restrictions. Identification of activities of interest that can also be safely used, potentially without the need to follow the slow and expensive drug-development pipeline offer exciting prospects for microbial pathogen control (Boyd et al., 2021).

Moreover, all experimental chapters include a goal to develop mechanistic understanding of the inhibitory activity of the chosen control method.

In Chapters 2 and 3 the use of relevant deletion mutants linked to the NP mechanism of action, among other approaches, helped to indicate important roles for mitochondrial depolarisation and uncoupling of oxidative phosphorylation in synergistic NP combinations. Using the model organism *S. cerevisiae* facilitated experimental testing of specific biological functions such as ergosterol biosynthesis and ROS defence (Hanson, 2018). For Chapters 2, 3 and 4, insights to observed sensitivity profiles (synergies or hypersensitivity) were gained through the use of agents where mechanistic understanding was already established.

In addition, for Chapters 4 and 5 the cell wall was one focus of experimental attention. As discussed in Chapter 1, the fungal cell wall is an attractive target for drug development as it is absent from humans. Moreover, fungal cell wall composition is dynamic and well-studied in the context of pathogenesis, stress response and resistance development (Gow and Lenardon, 2022). In Chapter 4, fluorescence probing of the immunogenic β-(1,3)-glucan component of the cell wall helped as part of the investigation to the apparent collateral sensitivity phenotype. Data suggested that the mutants of interest had decreased β-(1,3)-glucan cell wall content, indicating cell wall differences between the mutants that exhibited drug hypersensitivity and the non-sensitive strains. Moreover, in Chapter 5, fluorescence probing was further exploited to look at specific cell wall components; in that case establishing certain relationships with attachment phenotypes.

6.3 Thesis conclusions and future work

The experimental work performed in this thesis has laid a groundwork for further research upon the three methods of fungal pathogen control explored. For the work focussing on natural product combinations, it is important to assess the toxicity of the synergistic combinations against human and plant cells. Moreover, *in vivo* potency of the synergies pursued would be a key priority in forwarding their practical applications for fungal control. In addition,

further assessment of the potential use of uncoupling agents such as the NP sclareol would be prioritised, with both assessment within targeted combinations of interest and/or through a pairwise screening approach.

In the area of drug-repurposing to discover collaterally sensitive interactions, here against azole-resistant *C. albicans*, as discussed at the end of Chapter 4, it would be important to assess additional drug-resistance profiles in *C. albicans*, such as in echinocandin-resistant strains. Expanding research outside of azole-resistance could continue to assess if the phenomenon of collateral sensitivity is something that can be exploited for fungal pathogen control.

Finally, in the characterisation of fungal anti-attachment phenotypes, the question of durability against evolution of attachment development still requires further (longer-term) experimentation, encouraged by promising findings presented in Chapter 5. It would also be a priority to further elucidate the cell wall properties that determine fungal attachment/non-attachment specifically to candidate polymers of interest, as these may offer a 'passive' alternative to undesirable chemical-actives in several fungal control applications.

Appendices

Professional Internship for PhD Students; Reflective Statement

Note to examiners:

This statement is included as an appendix to the thesis in order that the thesis accurately captures the PhD training experienced by the candidate as a BBSRC Doctoral Training Partnership student. The Professional Internship for PhD Students is a compulsory 3-month placement which must be undertaken by DTP students. It is usually centred on a specific project and must not be related to the PhD project. This reflective statement is designed to capture the skills development which has taken place during the student's placement and the impact on their career plans it has had.

For my PIP I was able to secure a placement during the COVID-19 pandemic (August 2020) within the Medizinische Hochschule Hannover, a partner institute of the German Centre for Infection Research (DZIF) working under the supervision of Professor Thomas Schulz and Dr. Jasmin Zischke. The Schulz group work on developing therapeutics and biological understanding of several human viruses. My project involved working on the human oncogenic virus, Kaposi Sarcoma Herpesvirus (KSHV). KSHV is a devastating oncogenic virus where several advances have been made in the implementation of combination antiretroviral therapies, however further therapeutic developments are still need for the development of new treatments. More specifically, my project was designed to investigate the involvement of proteins that are potentially complexed and/or phosphorylated by the thymidine/tyrosine kinase (TK) ORF21. This project focussed on the potential interacting proteins ORF6, ORF59 and ORF67.

Recent laboratory data identified TK as essential for the pro-drug activation of several antivirals and importantly is also inhibited by clinically approved tyrosine kinases (Beauclair et al. 2020). TK presents an exciting, novel therapeutic target against KSHV. This finding lead to the need to further investigate the proteins that are interacting with and potentially also phosphorylation targets of TK to improve our understanding of this process and which could offer additional therapeutic potential against lytic KSHV. The outcomes of the placement project were successful in molecular cloning of

three expression plasmids containing the ORFs of interest, and due to time constraints only ORF6 was transfected and tested in bead-based immunoprecipitation 'pull-down' experiments. Initial data suggested that ORF6 is not physically interacting or phosphorylated by ORF21. These findings pose additional questions into how ORF6 interacts with ORF21 or into the validity of the mass-spectrometry data.

Within my PIP I learnt a plethora of skills both inside and outside of the laboratory environment. In the area of laboratory techniques, I was able to work closely with one of the post-doctoral researchers and they were able to share many techniques with me during the placement. Some examples of techniques I was exposed to on my PIP which I have not done so within my PhD project include molecular cloning and bacterial transformation, human cell culture, transfection (specifically lipofection), immunoblotting and immunoprecipitation experiments. Moreover, whilst not directly linked to my project, I also learnt how to seed cells in 3D culture. Unfortunately due to the pandemic, I was asked to return to the UK before the end of the three months, meaning I was unable to learn all the techniques proposed however the experience was invaluable in helping with my experimental design and independence as it was a steep learning curve in a different field of research.

Aside from laboratory techniques I also undertook personal development, gaining confidence to speak with other researchers in a different country with different rhythms of what is normal. This experience pushed me outside of my comfort zone (e.g. with a different language) and encouraged me to think about my future career plans. I was determined to complete my placement in a country outside of the UK, although this proved difficult with the COVID-19 pandemic (for example, my initial placement in Seattle was cancelled and having to cut my placement two weeks short to return to the UK) I thoroughly enjoyed my experience. Finally, this experience solidified my view that I would like to remain in a laboratory-setting after my PhD as there are still so many things I have not yet been exposed to or able to take part in to promote the forwarding of our scientific understanding.

Appendix A

A.1. Raw data from the Puretitre library screen. The data can be accessed using the following private link: **https://figshare.com/s/e44bcb1aaa6050a9c59d**

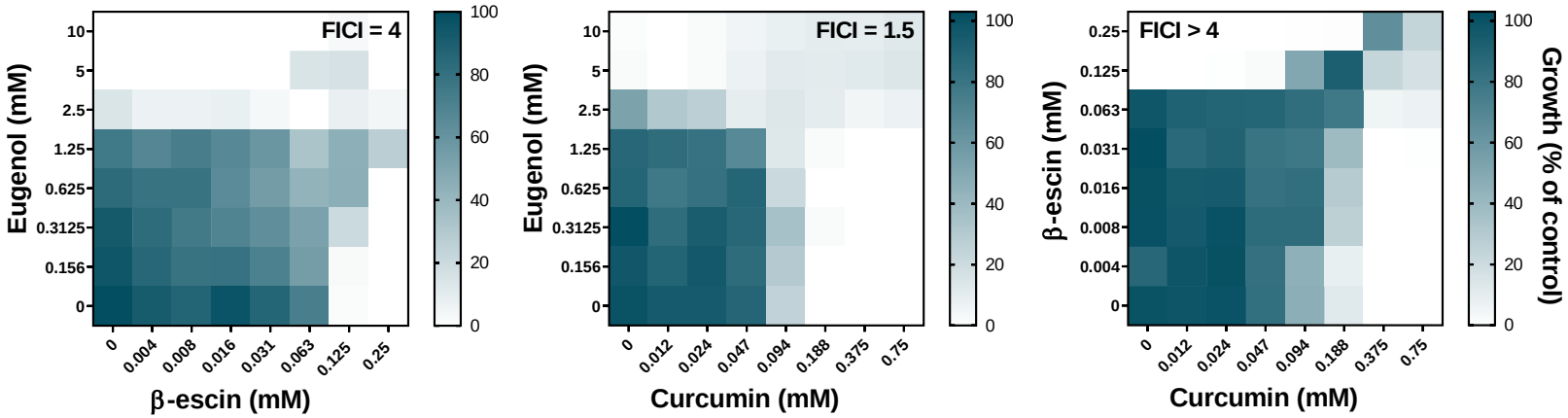

A.2. Checkerboard assays of combinatorial growth-effects of eugenol, β-escin and curcumin in *S. cerevisiae* strain BY4743. Assays were performed according to EUCAST procedure in YPD broth with S. cerevisiae BY4743 at the indicated concentrations of eugenol, ß-escin and curcumin. Growth values (scale to the right) represent means from three independent experiments, calculated as percentages of growth (OD_{600}) with the NPs relative to the minus-NP control. FICI, fractional inhibitory concentration index, calculated from data after 24 h growth at 30°C; growth values < 5% were assigned as no-growth (Hsieh et al., 1993). Corresponding data for *S. cerevisiae* W303 are shown in Figure 2.1.

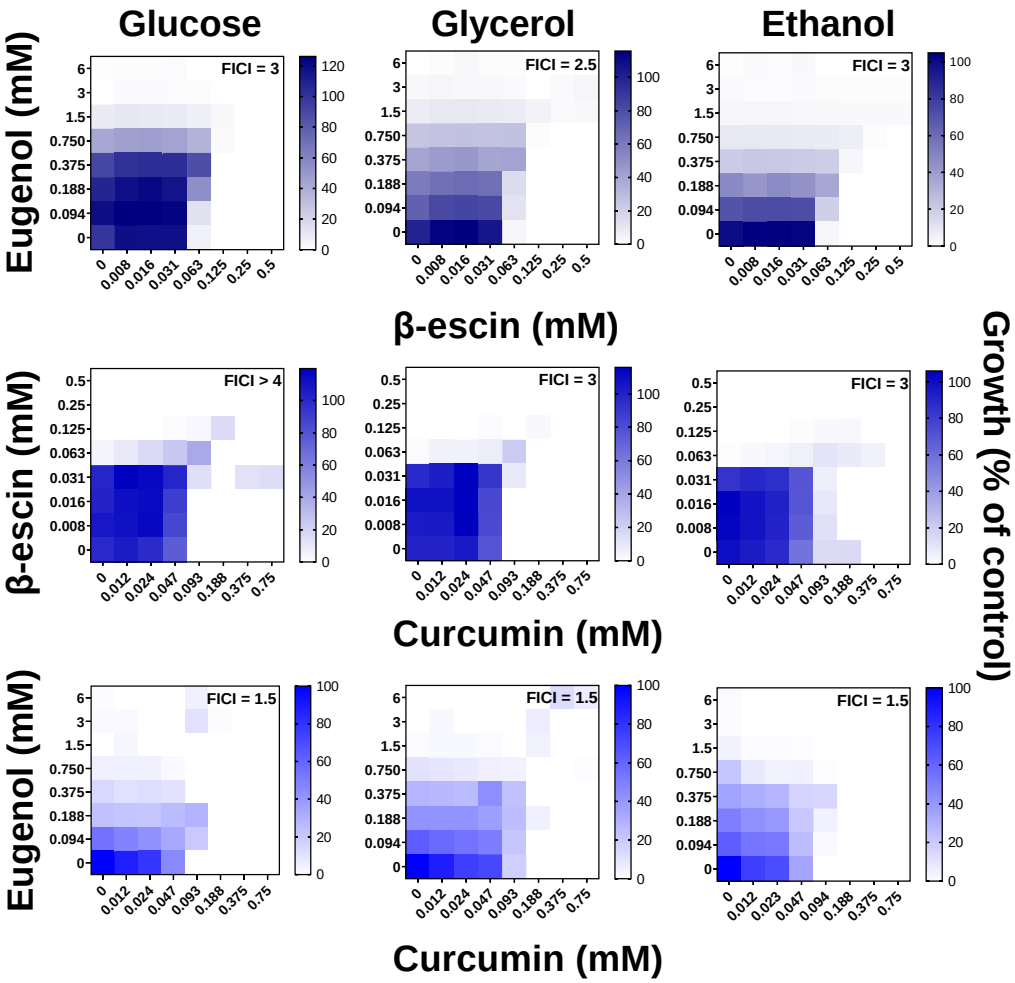

A.3. Checkerboard assays of combinatorial growth-effects performed according to EUCAST procedure in YP broth (+2% either glucose, glycerol or ethanol) with *S. cerevisiae* W303 at the indicated concentrations of eugenol, ß-escin and curcumin. The growth values represent the mean of three independent experiments calculated as percentages of growth (OD_{600}) with the natural products relative to the minus-NP control. FICI, fractional inhibitory concentration index, calculated from the data after 24 h growth at 30°C and where growth < 5% of the control was assigned as no-growth.

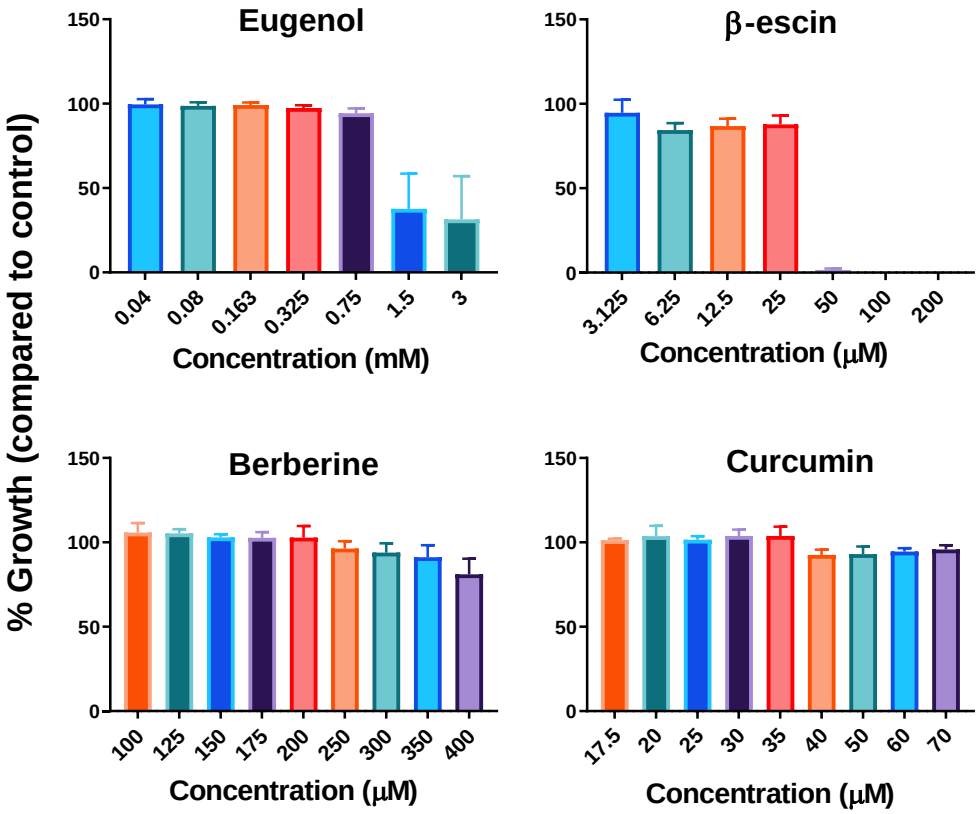

A.4. Characterisation of sub inhibitory concentrations (SIC) of selected NPs in *S. cerevisiae* W303. Growth was assessed (OD_{600}) after 24 h incubation in YPD broth with the indicated concentrations of eugenol, curcumin, β-escin or berberine. Percentage growth was calculated by comparison with OD_{600} obtained for solvent-only, no-drug controls. Mean values + SEM from three independent experiments are plotted.

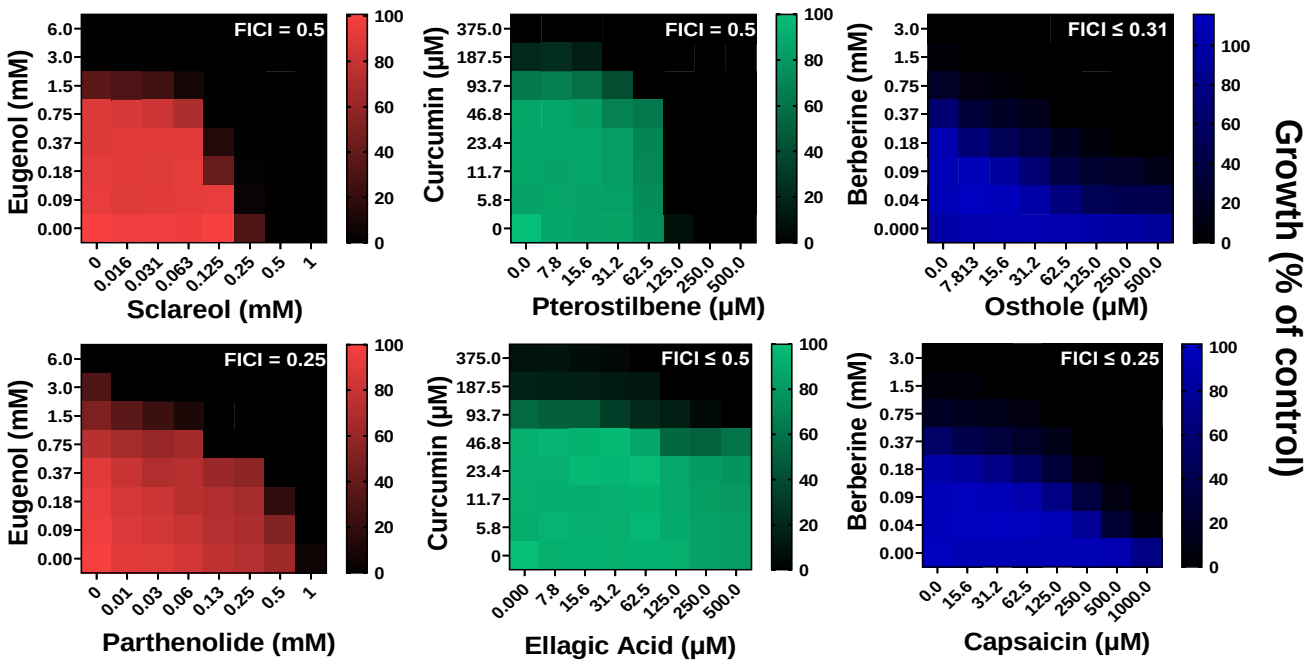

A.5. Checkerboard corroboration in *S. cerevisiae* W303 of additional synergies arising from the prior screen. Checkerboard assays of combinatorial growth-effects performed according to EUCAST procedure in YPD broth with *S. cerevisiae* W303 at the specified concentrations of the indicated natural products. The growth values represent the mean of three independent experiments calculated as percentages of growth (OD_{600}) with the natural products relative to the minus-NP control, after 24 h growth at 30°C. FICI, fractional inhibitory concentration index, where growth < 5% of the control was assigned as no-growth.

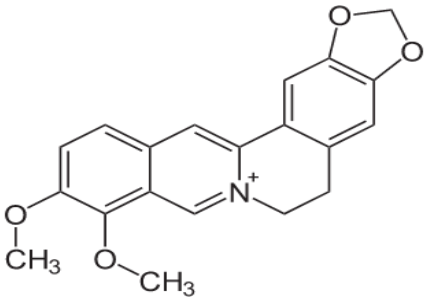

Berberine hydrochloride

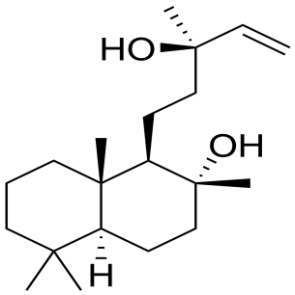

Sclareol

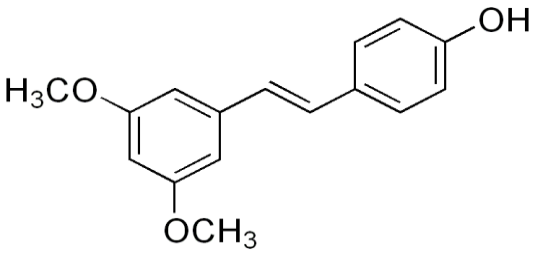

Pterostilbene

A.6. Chemical structures of library compounds giving the strongest effect strengths from each screen and validated in Figure 2.4B.

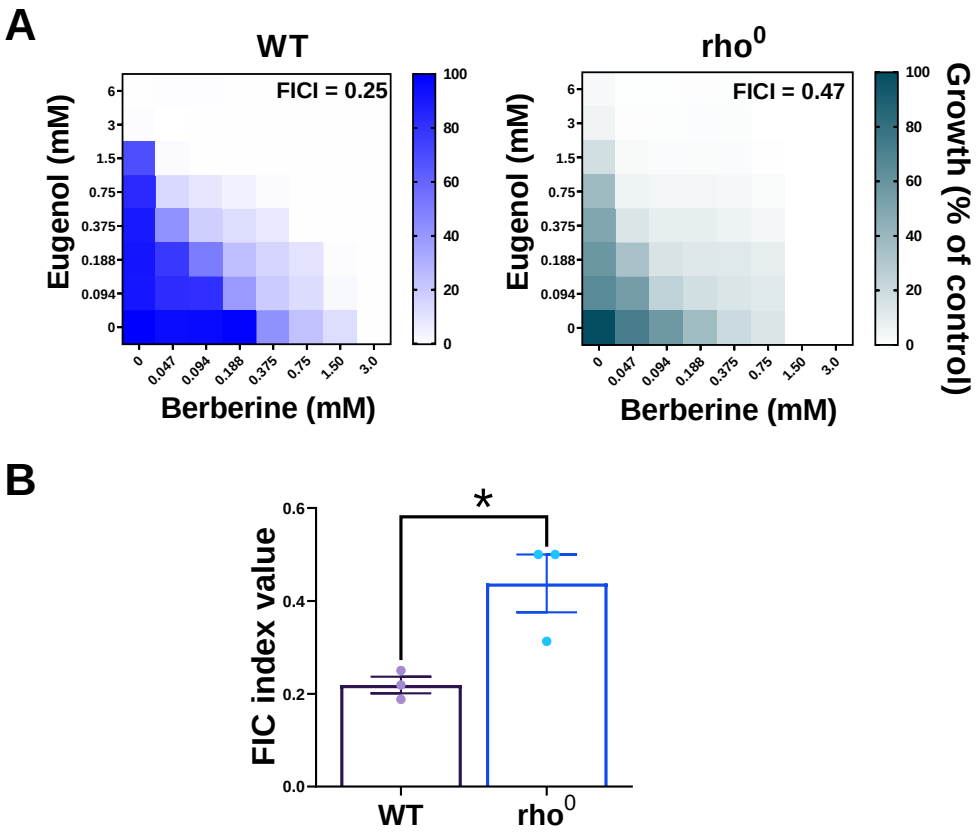

A.7. Checkerboard assessment of EUG + BER synergy in wild type and rho^0 *S. cerevisiae*. (A) Checkerboard assays of combinatorial growth-effects performed according to EUCAST procedure in YPD broth with *S. cerevisiae* W303 (WT) and a derived rho^0 mutant at the indicated concentrations of eugenol and berberine. The growth values represent the mean of three independent experiments calculated as percentages of growth (OD_{600}) with the natural products relative to the minus-NP control, after 24 h growth at 30°C. FICI, fractional inhibitory concentration index, calculated from the data and where growth < 5% of the control was assigned as no-growth.(Hsieh et al., 1993) (B) Fractional inhibitory concentration indices determined from three independent checkerboard experiments, with bar-height showing mean ±SEM. *, $p < 0.05$, according to unpaired t-test.

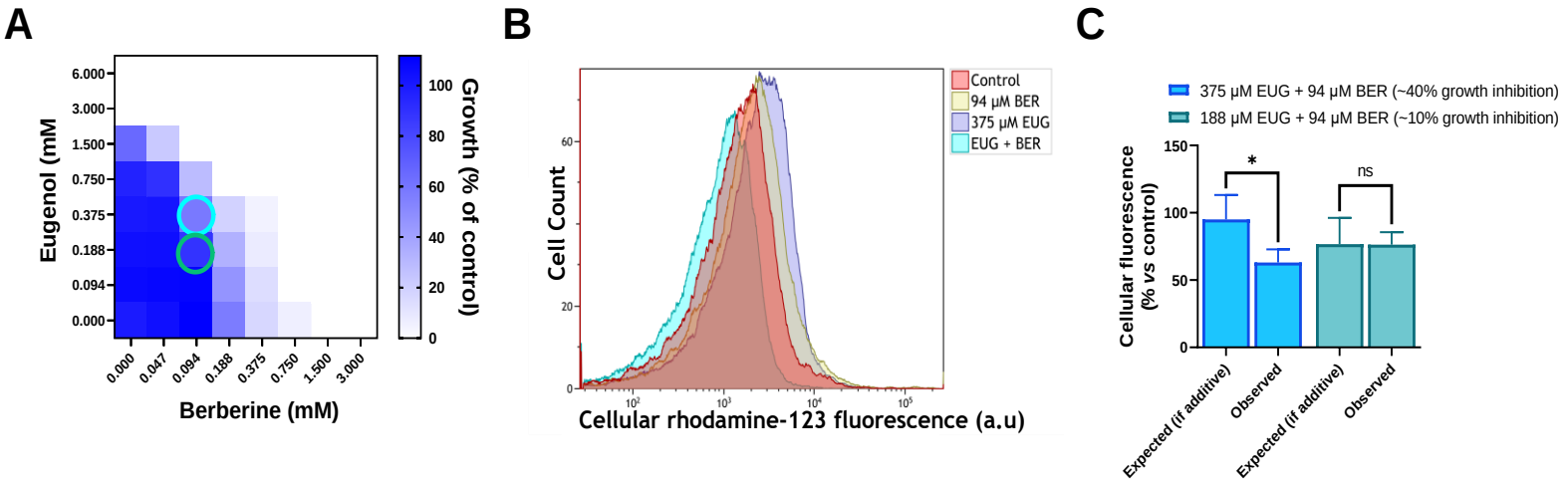

A.8. Mitochondrial membrane depolarization persists in eugenol- and berberine-treated *C. albicans* cells (A) Checkerboard assays of combinatorial growth-effects were performed as described in Figures 1 and 4; combination concentrations are circled where subsequently tested for mitochondrial membrane depolarization (B,C). (B) Flow cytometric histograms for cells incubated for 24 h without (control) or with the indicated concentrations of EUG and BER and stained with rhodamine 123; a.u., arbitrary units. (C) Observed effects of combinations were obtained experimentally from median fluorescence of rhodamine 123-stained cells exposed to the EUG + BER combination (derived from corresponding flow cytometric data as in B), normalized to the no drug control (100%). Expected effects were calculated by multiplication of the two % median-fluorescence determinations obtained for the corresponding individual-compound effects. Values represent means +SEM from three independent experiments: *, p <0.05 according to paired, one-tailed t-test. EUG, Eugenol; BER, Berberine.

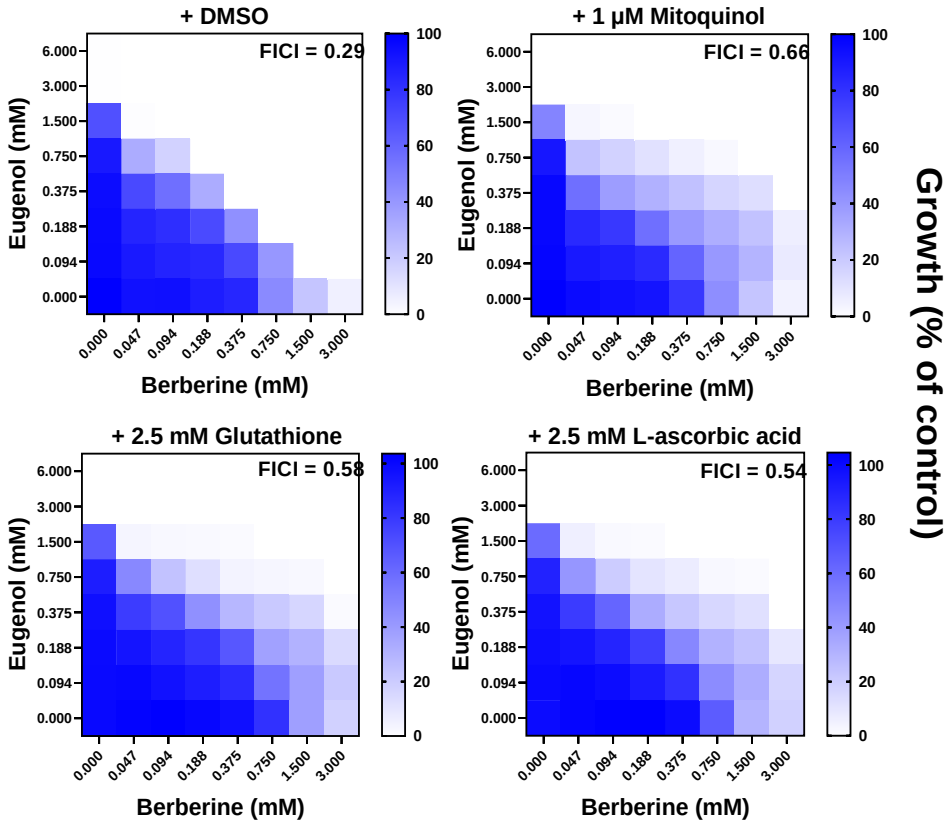

A.9. Checkerboard assessment of EUG + BER synergy with or without the addition of different antioxidants. Checkerboard assays of combinatorial growth-effects performed according to EUCAST procedure in YPD broth with *S. cerevisiae* W303 at the indicated concentrations of eugenol and berberine with the inclusion of the indicated antioxidant concentrations. The growth values represent the mean of three independent experiments calculated as percentages of growth (OD_{600}) with the natural products relative to the minus-NP control, after 24 h growth at 30°C. FICI, fractional inhibitory concentration index values were calculated from the data and where growth < 5% of the control was assigned as no-growth.

Appendix B

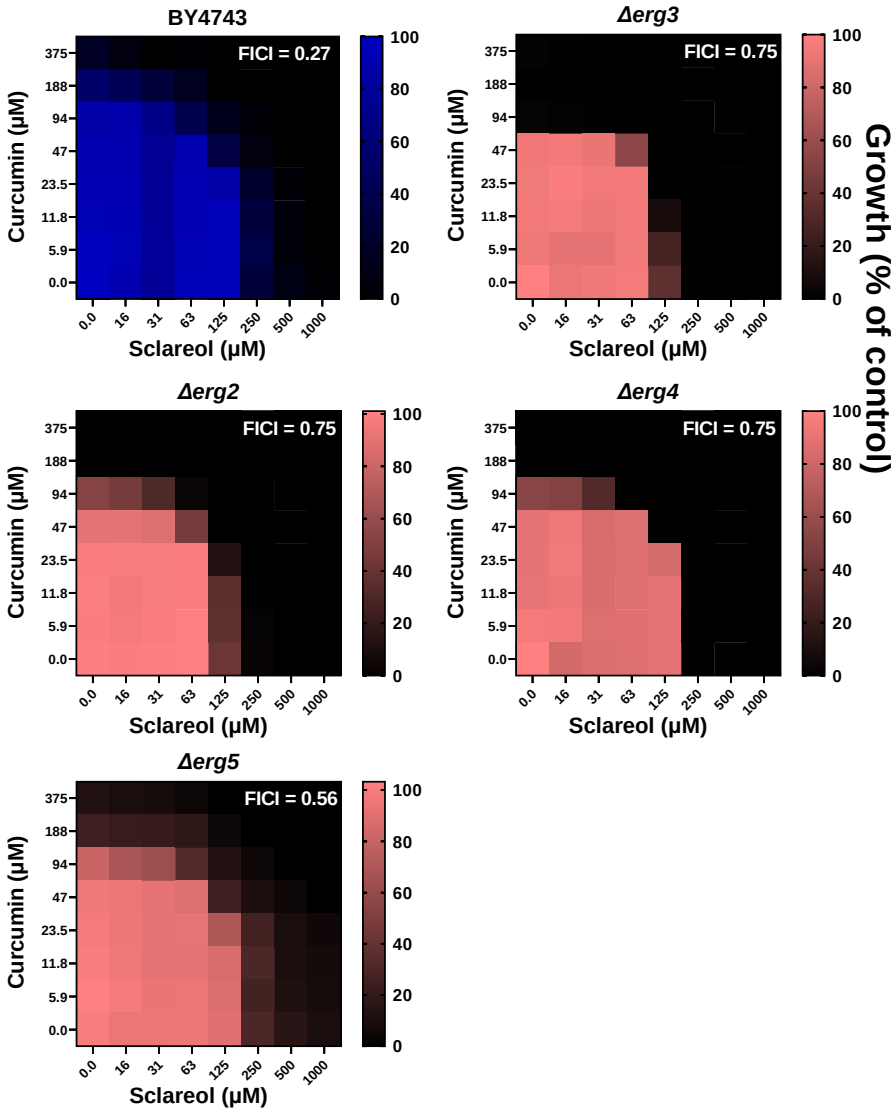

Appendix B.1. Synergy between curcumin and sclareol removed in mutants of the ergosterol synthesis pathway. Checkerboard assays of combinatorial growth-effects performed according to EUCAST procedure in YPD broth (+2% glucose) in *S. cerevisiae,* strain BY4743 (background strain) and in the indicated homozygous deletion mutants at the indicated concentrations of sclareol and curcumin. The growth values represent the mean of three independent experiments calculated as percentages of growth (OD_{600}) with the natural products relative to the minus-NP control, after 24 h growth at 30°C. FICI, fractional inhibitory concentration index values, calculated from the data and where growth < 5% of the control was assigned as no-growth (Hsieh et al., 1993).

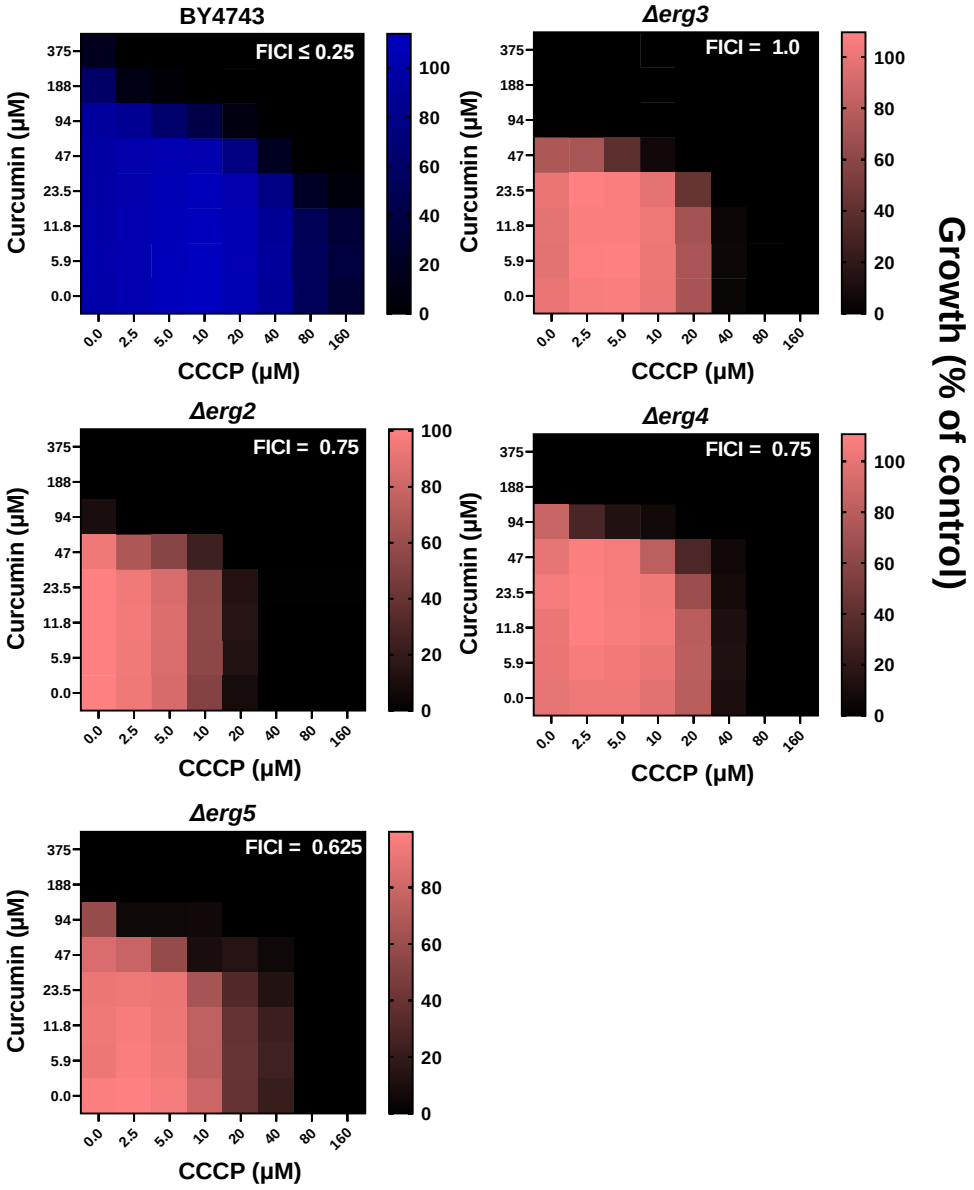

Appendix B.2. Synergy between curcumin and CCCP removed in mutants of the ergosterol biosynthesis pathway. Checkerboard assays of combinatorial growth-effects performed according to EUCAST procedure in YPD broth (+2% glucose) in *S. cerevisiae,* strain BY4743 (background strain) and in the shown homozygous deletion mutants at the indicated concentrations of CCCP and curcumin. The growth values represent the mean of three independent experiments calculated as percentages of growth (OD_{600}) with the natural products relative to the minus-NP control, after 24 h growth at 30°C. FICI, fractional inhibitory concentration index values, calculated from the data and where growth < 5% of the control was assigned as no-growth (Hsieh et al., 1993).

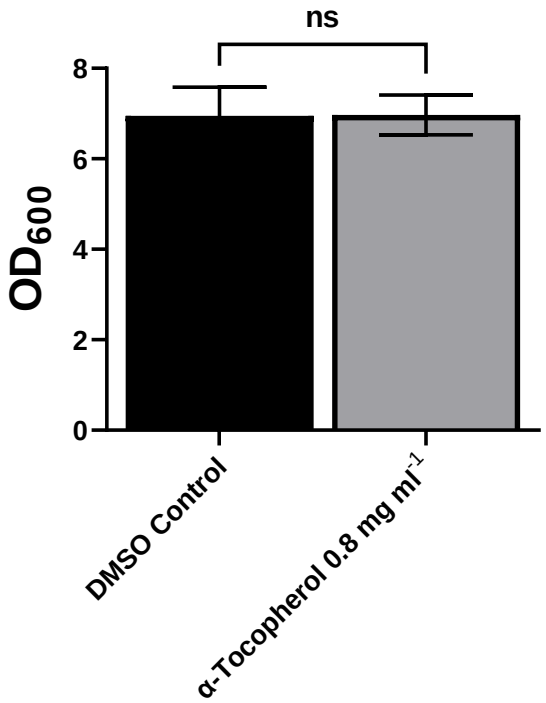

Appendix B.3. Growth comparison between DMSO solvent and α-tocopherol show no significant difference. Checkerboard analysis between eugenol and sclareol as shown in Figure 3.7 using OD_{600} as a measure of growth. The bar height represents the growth using OD_{600} of *S. cerevisiae* strain W303 exposed only to solvent from eugenol and sclareol, with the addition of DMSO solvent (at the same concentration of α-tocopherol) or exposed to exposed only to solvent from eugenol and sclareol and α-tocopherol at 0.8 mg ml^{-1}. Each bar represents the mean of three independent experiments, error plotted ±SD.

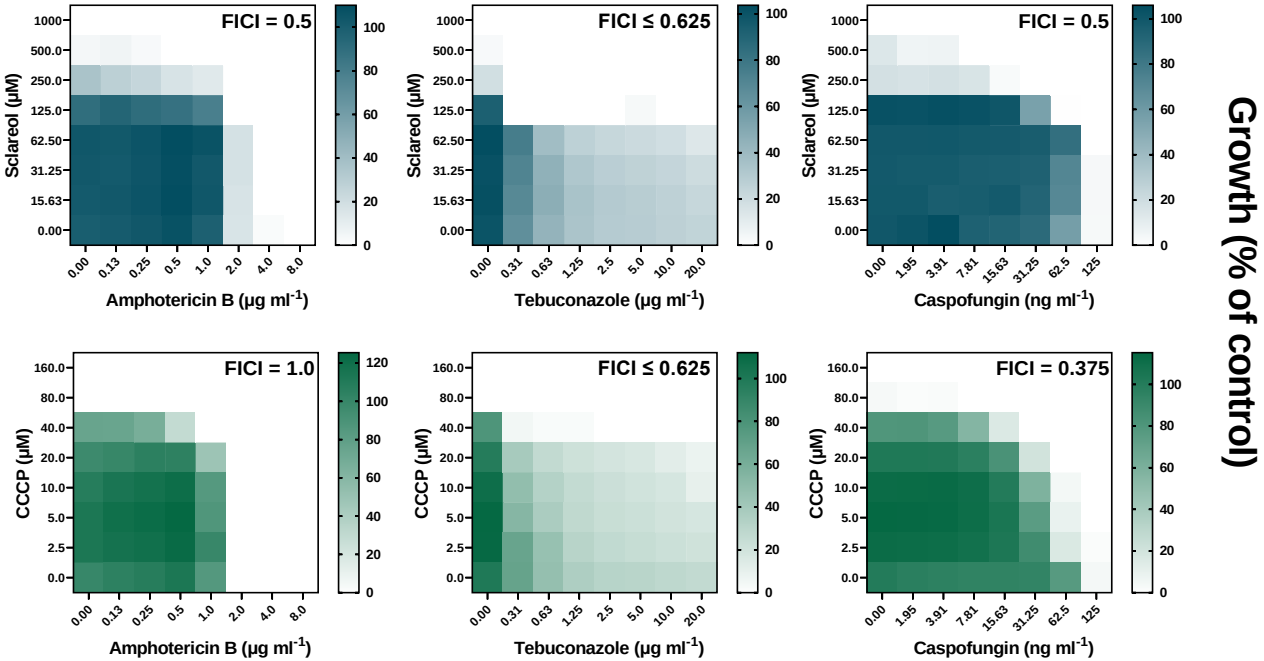

Appendix B.4 Interaction of uncoupling agents with commonly used antifungals. Checkerboard assays of combinatorial growth-effects performed according to EUCAST procedure in YPD broth (+2% glucose) in *S. cerevisiae,* strain W303 at the indicated concentrations of sclareol, CCCP, amphotericin B, tebuconazole and caspofungin. The growth values represent the mean of three independent experiments calculated as percentages of growth (OD_{600}) with the natural products relative to the minus-NP control, after 24 h growth at 30°C. FICI, fractional inhibitory concentration index values, calculated from the data and where growth < 5% of the control was assigned as no-growth (Hsieh et al., 1993).

Appendix C

Ingredient	Quantity (per Litre)
p-Aminobenzoic Acid	400 mg
Thiamine HCl	50 mg
d-Biotin	2 mg
Nicotinic Acid	100 mg
Pyridoxine Hydrochloride	250 mg
Choline Chloride	1.4 g
Riboflavin	100 mg

C.1. Aspergillus Vitamin Solution ingredients.

Ingredient	Quantity (per Litre)
Potassium Chloride (KCl)	26 g
Magnesium Sulphate ($MgSO_4.7H_2O$)	26 g
Potassium diHydrogen Phosphate (KH_2PO_4)	76 g
Aspergillus Trace Elements Solution	10 ml

C.2. Aspergillus salt solution ingredients.

Ingredient	Quantity (per Litre)
Sodium Tetraborate Decahydrate ($Na_2B_4O_7.10H_2O$)	40 mg
Copper Sulphate Pentahydrate ($CuSO_4.5H_2O$)	800 mg
Ferric Orthophosphate Monohydrate ($FePO_4.H_2O$)	800 mg
Manganese Sulphate Tetrahydrate($MnSO_4.4H_2O$)	800 mg
Sodium Molybdate Dihydrate ($NaMoO_4.2H_2O$)	800 mg
Zinc Sulphate ($ZnSO_4$)	8 g

C.3. Aspergillus trace elements solution ingredients.

C.4. DNA Sequencing Data for *ERG11*. Red highlighted codons indicate non-synonymous SNPS causing amino acid changes in the protein. Blue highlighting indicate the start and end of gene ORF.

SC5314 – Laboratory wild-type strain.

ATGGCTATTGTTGAAACTGTCATTGATGGCATTAATTATTTTTTGTCCCTTAG
TGTTACACAACAGATCAGTATATTATTAGGGGTTCCATTTGTTTACAACTTAG
TATGGCAATATTTATATTCATTAAGAAAAGATAGAGCTCCATTAGTGTTTTAT
TGGATTCCTTGGTTTGGTTCTGCAGCTTCATATGGTCAACAACCTTATGAATT
TTTCGAATCATGTCGTCAAAAGTATGGTGATGTATTTTCATTTATGTTATTAG
GGAAAATTATGACGGTTTATTTAGGTCCAAAAGGTCATGAATTTGTTTTCAAT
GCTAAATTATCTGATGTTTCTGCTGAAGATGCTTATAAGCATTTAACTACTCC
AGTTTTCGGTACAGGGGTTATTTATGATTGTCCAAATTCCAGATTAATGGAAC
AAAAAAAATTTGCTAAATTTGCTTTGACTACTGATTCATTTAAAAGATATGTT
CCTAAGATTAGAGAAGAAATTTTGAATTATTTTGTTACTGATGAAAGTTTCAA
ATTGAAAGAAAAAACTCATGGGGTTGCCAATGTTATGAAAACTCAACCAGAAA
TTACTATTTTCACTGCTTCAAGATCTTTATTTGGTGATGAAATGAGAAGAATT
TTTGACCGTTCATTTGCTCAACTATATTCTGATTTAGATAAAGGTTTTACCCC
TATTAATTTTGTTTTCCCTAATTTACCTTTACCTCATTATTGGAGACGTGATG
CTGCTCAAAAGAAAATCTCTGCTACTTATATGAAAGAAATTAAACTGAGAAGA
GAACGTGGTGATATTGATCCAAATCGTGATTTAATTGATTCCTTATTGATTCA
TTCAACTTATAAAGATGGTGTGAAAATGACTGATCAAGAAATTGCTAATCTTT
TAATTGGTATTCTTATGGGTGGTCAACATACTTCTGCTTCTACTTCTGCTTGG
TTCTTGTTACATTTAGGTGAAAAACCTCATTTACAAGATGTTATTTATCAAGA
AGTTGTTGAATTATTGAAAGAAAAAGGTGGTGATTTGAATGATTTGACTTATG
AAGATTTACAAAAATTACCATCAGTCAATAACACTATTAAGGAAACTCTCAGA
ATGCATATGCCATTACATTCTATTTTTAGAAAAGTTACTAACCCATTAAGAAT
CCCTGAAACCAATTATATTGTTCCAAAAGGTCATTATGTTTTAGTTTCTCCAG
GTTATGCTCATACTAGTGAAAGATATTTTGATAACCCTGAAGATTTTGATCCA
ACTAGATGGGATACTGCTGCTGCCAAAGCTAATTCTGTTTCATTTAACTCTTC
TGATGAAGTTGATTATGGGTTTGGGAAAGTTTCTAAAGGGGTTTCTTCACCTT
ATTTACCATTTGGTGGTGGTAGACATAGATGTATTGGGGAACAATTTGCTTAT
GTTCAATTGGGAACCATTTTAACTACTTTTGTTTATAACTTAAGATGGACTAT
TGATGGTTATAAAGTGCCTGACCCTGATTATAGTTCAATGGTGGTTTTACCTA
CTGAACCAGCAGAAATCATTTGGGAAAAAAGAGAAACTTGTATGTTTTAA

J942148 – Azole resistant clinical isolate, not hypersensitive.

ATGGCTATTGTTGAAACTGTCATTGATGGCATTAATTATTTTTTGTCCCTTAG
TGTTACACAACAGATCAGTATATTATTAGGGGTTCCATTTGTTTACAACTTAG
TATGGCAATATTTATATTCATTAAGAAAAGATAGAGCTCCATTAGTGTTTTAT
TGGATTCCTTGGTTTGGTTCTGCAGCTTCATATGGTCAACAACCTTATGAATT
TTTTGAATCATGTCGTCAAAAGTATGGTGATGTATTTTCATTTATGTTATTAG
GGAAAATTATGACGGTTTATTTAGGTCCAAAAGGTCATGAATTTGTTTTCAAT
GCTAAATTATCTGATGTTTCTGCTGAAGATGCTTATAAACATTTAACTACTCC
AGTTTTCGGTAAAGGGGTTATTTATGATTGTCCAAATTCTAGATTAATGGAAC
AAAAAAAATTTGCTAAATTTGCTTTGACTACTGATTCATTTAAAAGATATGTT
CCTAAGATTAGAGAAGAAATTTTGAATTATTTTGTTACTGATGAAAGTTTCAA
ATTGAAAGAAAAAACTCATGGGGTTGCCAATGTTATGAAAACTCAACCAGAAA

TTACTATTTTCACTGCTTCAAGATCTTTATTTGGTGATGAAATGAGAAGAATT
TTTGACCGTTCATTTGCTCAATTATATTCTGATTTAGATAAAGGTTTTACCCC
TATTAATTTTGTTTTCCCTAATTTACCTTTACCTCATTATTGGAGACGTGATG
CTGCTCAAAAGAAAATCTCTGCTACTTATATGAAAGAAATTAAACTGAGAAGA
GACCGTGGTGATATTGATCCAAATCGTGATTTAATTGATTCCTTATTGATTCA
TTCAACTTATAAAGATGGTGTGAAAATGACTGATCAAGAAATTGCTAATCTTT
TAATTGGTATTCTTATGGGT**G**GTCAACATACTTCTGCTTCTACTTCTGCTTGG
TTCTTGTTACATTTAGGTGAAAAACCTCATTTACAAGATGTTATTTATCAAGA
AGTTGTTGAATTGTTGAAAGAAAAAGGTGGTGATTTGAATGATTTGACTTATG
AAGATTTACAAAAATTACCATCAGTCAATAACACTATTAAGGAAACTCTTAGA
ATGCATATGCCATTACATTCTATTTTTAGAAAAGTTACTAACCCATTAAGAAT
CCCTGAAACCAATTATATTGTTCCAAAAGGTCATTATGTTTTAGTTTCTCCAG
GTTATGCTCATACTAGTGAAAGATATTTTGATAACCCTGAAGATTTTGATCCA
ACTAGATGGGATACTGCTGCTGCCAAAGCTAATTCTGTTTCATTTAACTCTTC
TGATGAAGTTGATTATGAGTTTGGGAAAGTTTCTAAAGGGGTTTCTTCACCTT
ATTTACCATTTGGTGGTGGTAGACATAGATGTATTGGGGAACAATTTGCTTAT
GTTCAATTGGGAACCATTTTAACTACTTTTGTTTATAACTTAAGATGGACTAT
TGATGGTTATAAAGTGCCTGACCCTGATTATAGTTCAATGGTGGTTTTACCTA
CTGAACCAGCAGAAATCATTTGGGAAAAAAGAGAAACTTGTATGTTTTAA

J980280 – Azole-resistant clinical isolate and hypersensitive.

ATGGCTATTGTTGAAACTGTCATTGATGGCATTAATTATTTTTTGTCCCTTAG
TGTTACACAACAGATCAGTATATTATTAGGGGTTCCATTTGTTTACAACTTAG
TATGGCAATATTTATATTCATTAAGAAAAGATAGAGCTCCATTAGTGTTTTAT
TGGATTCCTTGGTTTGGTTCTGCAGCTTCATATGGTCAACAACCTTATGAATT
TTTTGAATCATGTCGTCAAAAGTATGGTGATGTATTTTCATTTATGTTATTAG
GGAAAATTATGACGGTTTATTTAGGTCCAAAAGGTCATGAATTTGTTTTCAAT
GCTAAATTATCTGATGTTTCTGCTGAAGATGCTTATAAACATTTAACTACTCC
AGTTTTCGGTAAAGGGGTTATTTATGATTGTCCAAATTCTAGATTAATGGAAC
AAAAAAAATTTGCTAAATTTGCTTTGACTACTGATTCATTTAAAAGATATGTT
CCTAAGATTAGAGAAGAAATTTTGAATTATTTTGTTACTGATGAAAGTTTCAA
ATTGAAAGAAAAAACTCATGGGGTTGCCAATGTTATGAAAACTCAACCAGAAA
TTACTATTTTCACTGCTTCAAGATCTTTATTTGGTGATGAAATGAGAAGAATT
TTTGACCGTTCATTTGCTCAATTATATTCTGATTTAGATAAAGGTTTTACCCC
TATTAATTTTGTTTTCCCTAATTTACCTTTACCTCATTATTGGAGACGTGATG
CTGCTCAAAAGAAAATCTCTGCTACTTATATGAAAGAAATTAAACTGAGAAGA
GACCGTGGTGATATTGATCCAAATCGTGATTTAATTGATTCCTTATTGATTCA
TTCAACTTATAAAGATGGTGTGAAAATGACTGATCAAGAAATTGCTAATCTTT
TAATTGGTATTCTTATGGGT**G**GTCAACATACTTCTGCTTCTACTTCTGCTTGG
TTCTTGTTACATTTAGGTGAAAAACCTCATTTACAAGATGTTATTTATCAAGA
AGTTGTTGAATTGTTGAAAGAAAAAGGTGGTGATTTGAATGATTTGACTTATG
AAGATTTACAAAAATTACCATCAGTCAATAACACTATTAAGGAAACTCTTAGA
ATGCATATGCCATTACATTCTATTTTTAGAAAAGTTACTAACCCATTAAGAAT
CCCTGAAACCAATTATATTGTTCCAAAAGGTCATTATGTTTTAGTTTTTCCAG
GTTATGCTCATACTAGTGAAAGATATTTTGATAACCCTGAAGATTTTGATCCA
ACTAGATGGGATACTGCTGCTGCCAAAGCTAATTCTGTTTCATTTAACTCTTC
TGATGAAGTTGATTATGGGTTTGGGAAAGTTTCTAAAGGGGTTTCTTCACCTT
ATTTACCATTTGGTGGTGGTAGACATAGATGTATTGGGGAACAATTTGCTTAT
GTTCAATTGGGAACCATTTTAACTACTTTTGTTTATAACTTAAGATGGACTAT

TGATGGTTATAAAGTGCCTGACCCTGATTATAGTTCAATGGTGGTTTTACCTA
CTGAACCAGCAGAAATCATTTGGGAAAAAAGAGAAACTTGTATGTTTTAA

SCS119299X – Azole-resistant clinical isolate and hypersensitive.

ATGGCTATTGTTGAAACTGTCATTGATGGCATTAATTATTTTTTGTCCCTTAG
TGTTACACAACAGATCAGTATATTATTAGGGGTTCCATTTGTTTACAACTTAG
TATGGCAATATTTATATTCATTAAGAAAAGATAGAGCTCCATTAGTGTTTTAT
TGGATTCCTTGGTTTGGTTCTGCAGCTTCATATGGTCAACAACCTTATGAATT
TTTTGAATCATGTCGTCAAAAGTATGGTGATGTATTTTCATTTATGTTATTAG
GGAAAATTATGACGGTTTATTTAGGTCCAAAAGGTCATGAATTTGTTTTCAAT
GCTAAATTATCTGATGTTTCTGCTGAAGATGCTTATAAACATTTAACTACTCC
AGTTTTCGGTAAAGGGGTTATTTATGATTGTCCAAATTCTAGATTAATGGAAC
AAAAAAAATTTGCTAAATTTGCTTTGACTACTGATTCATTTAAAAGATATGTT
CCTAAGATTAGAGAAGAAATTTTGAATTATTTTGTTACTGATGAAAGTTTCAA
ATTGAAAGAAAAAACTCATGGGGTTGCCAATGTTATGAAAACTCAACCAGAAA
TTACTATTTTCACTGCTTCAAGATCTTTATTTGGTGATGAAATGAGAAGAATT
TTTGACCGTTCATTTGCTCAATTATATTCTGATTTAGATAAAGGTTTTACCCC
TATTAATTTTGTTTTCCCTAATTTACCTTTACCTCATTATTGGAGACGTGATG
CTGCTCAAAAGAAAATCTCTGCTACTTATATGAAAGAAATTAAACTGAGAAGA
GACCGTGGTGATATTGATCCAAATCGTGATTTAATTGATTCCTTATTGATTCA
TTCAACTTATAAAGATGGTGTGAAAATGACTGATCAAGAAATTGCTAATCTTT
TAATTGGTATTCTTATGGGTGGTCAACATACTTCTGCTTCTACTTCTGCTTGG
TTCTTGTTACATTTAGGTGAAAAACCTCATTTACAAGATGTTATTTATCAAGA
AGTTGTTGAATTGTTGAAAGAAAAAGGTGGTGATTTGAATGATTTGACTTATG
AAGATTTACAAAAATTACCATCAGTCAATAACACTATTAAGGAAACTCTTAGA
ATGCATATGCCATTACATTCTATTTTTAGAAAAGTTACTAACCCATTAAGAAT
CCCTGAAACCAATTATATTGTTCCAAAAGGTCATTATGTTTTAGTTTTTCCAG
GTTATGCTCATACTAGTGAAAGATATTTTGATAACCCTGAAGATTTTGATCCA
ACTAGATGGGATACTGCTGCTGCCAAAGCTAATTCTGTTTCATTTAACTCTTC
TGATGAAGTTGATTATGGGTTTGGGAAAGTTTCTAAAGGGGTTTCTTCACCTT
ATTTACCATTTGGTGGTGGTAGACATAGATGTATTGGGGAACAATTTGCTTAT
GTTCAATTGGGAACCATTTTAACTACTTTTGTTTATAACTTAAGATGGACTAT
TGATGGTTATAAAGTGCCTGACCCTGATTATAGTTCAATGGTGGTTTTACCTA
CTGAACCAGCAGAAATCATTTGGGAAAAAAGAGAAACTTGTATGTTTTAA

21C1M1A1 – S405F genetically modified into SC5314. Azole-resistant but not hypersensitive.

ATGGCTATTGTTGAAACTGTCATTGATGGCATTAATTATTTTTTGTCCCTTAG
TGTTACACAACAGATCAGTATATTATTAGGGGTTCCATTTGTTTACAACTTAG
TATGGCAATATTTATATTCATTAAGAAAAGATAGAGCTCCATTAGTGTTTTAT
TGGATTCCTTGGTTTGGTTCTGCAGCTTCATATGGTCAACAACCTTATGAATT
TTTTGAATCATGTCGTCAAAAGTATGGTGATGTATTTTCATTTATGTTATTAG
GGAAAATTATGACGGTTTATTTAGGTCCAAAAGGTCATGAATTTGTTTTCAAT
GCTAAATTATCTGATGTTTCTGCTGAAGATGCTTATAAACATTTAACTACTCC
AGTTTTCGGTAAAGGGGTTATTTATGATTGTCCAAATTCTAGATTAATGGAAC
AAAAAAAATTTGCTAAATTTGCTTTGACTACTGATTCATTTAAAAGATATGTT
CCTAAGATTAGAGAAGAAATTTTGAATTATTTTGTTACTGATGAAAGTTTCAA
ATTGAAAGAAAAAACTCATGGGGTTGCCAATGTTATGAAAACTCAACCAGAAA

TTACTATTTTCACTGCTTCAAGATCTTTATTTGGTGATGAAATGAGAAGAATT
TTTGACCGTTCATTTGCTCAATTATATTCTGATTTAGATAAAGGTTTTACCCC
TATTAATTTTGTTTTCCCTAATTTACCTTTACCTCATTATTGGAGACGTGATG
CTGCTCAAAAGAAAATCTCTGCTACTTATATGAAAGAAATTAAACTGAGAAGA
GACCGTGGTGATATTGATCCAAATCGTGATTTAATTGATTCCTTATTGATTCA
TTCAACTTATAAAGATGGTGTGAAAATGACTGATCAAGAAATTGCTAATCTTT
TAATTGGTATTCTTATGGGT**G**GTCAACATACTTCTGCTTCTACTTCTGCTTGG
TTCTTGTTACATTTAGGTGAAAAACCTCATTTACAAGATGTTATTTATCAAGA
AGTTGTTGAATTGTTGAAAGAAAAAGGTGGTGATTTGAATGATTTGACTTATG
AAGATTTACAAAAATTACCATCAGTCAATAACACTATTAAGGAAACTCT**T**AGA
ATGCATATGCCATTACATTCTATTTTTAGAAAAGTTACTAACCCATTAAGAAT
CCCTGAAACCAATTATATTGTTCCAAAAGGTCATTATGTTTTAGTT**TT**CCAG
GTTATGCTCATACTAGTGAAAGATATTTTGATAACCCTGAAGATTTTGATCCA
ACTAGATGGGATACTGCTGCTGCTAAAGCCAATTCTGTTTCATTTAACTCTTC
TGATGAAGTTGATTATGGGTTTGGGAAAGTTTCTAAAGGGGTTTCTTCACCTT
ATTTACCATTTGGTGGTGGTAGACATAGATGTATTGGGGAACAATTTGCTTAT
GTTCAATTAGGAACCATTTTAACTACTTTTGTTTATAACTTAAGATGGACTAT
TGATGGTTATAAAGTGCCTGACCCTGATTATAGTTCAATGGTGGTTTTACCTA
CTGAACCAGCAGAAATCATTTGGGAAAAAAGAGAAACTTGTATGTTTTAA

20NA11A57A – G488E genetically modified into SC5314. Azole-resistant but not hypersensitive. Azole-resistant.

ATGGCTATTGTTGAAACTGTCATTGATGGCATTAATTATTTTTTGTCCCTTAG
TGTTACACAACAGATCAGTATATTATTAGGGGTTCCATTTGTTTACAACTTAG
TATGGCAATATTTATATTCATTAAGAAAAGATAGAGCTCCATTAGTGTTTTAT
TGGATTCCTTGGTTTGGTTCTGCAGCTTCATATGGTCAACAACCTTATGAATT
TTTCGAATCATGTCGTCAAAAGTATGGTGATGTATTTTCATTTATGTTATTAG
GGAAAATTATGACGGTTTATTTAGGTCCAAAAGGTCATGAATTTGTTTTCAAT
GCTAAATTATCTGATGTTTCTGCTGAAGATGCTTATAAGCATTTAACTACTCC
AGTTTTCGGTACAGGGGTTATTTATGATTGTCCAAATTCCAGATTAATGGAAC
AAAAAAAATTTGCTAAATTTGCTTTGACTACTGATTCATTTAAAAGATATGTT
CCTAAGATTAGAGAAGAAATTTTGAATTATTTTGTTACTGATGAAAGTTTCAA
ATTGAAAGAAAAAACTCATGGGGTTGCCAATGTTATGAAAACTCAACCAGAAA
TTACTATTTTCACTGCTTCAAGATCTTTATTTGGTGATGAAATGAGAAGAATT
TTTGACCGTTCATTTGCTCAACTATATTCTGATTTAGATAAAGGTTTTACCCC
TATTAATTTTGTTTTCCCTAATTTACCTTTACCTCATTATTGGAGACGTGATG
CTGCTCAAAAGAAAATCTCTGCTACTTATATGAAAGAAATTAAACTGAGAAGA
GAACGTGGTGATATTGATCCAAATCGTGATTTAATTGATTCCTTATTGATTCA
TTCAACTTATAAAGATGGTGTGAAAATGACTGATCAAGAAATTGCTAATCTTT
TAATTGGTATTCTTATGGGTGGTCAACATACTTCTGCTTCTACTTCTGCTTGG
TTCTTGTTACATTTAGGTGAAAAACCTCATTTACAAGATGTTATTTATCAAGA
AGTTGTTGAATTATTGAAAGAAAAAGGTGGTGATTTGAATGATTTGACTTATG
AAGATTTACAAAAATTACCATCAGTCAATAACACTATTAAGGAAACTCTTAGA
ATGCATATGCCATTACATTCTATTTTTAGAAAAGTTACTAACCCATTAAGAAT
CCCTGAAACCAATTATATTGTTCCAAAAGGTCATTATGTTTTAGTTTCTCCAG
GTTATGCTCATACTAGTGAAAGATATTTTGATAACCCTGAAGATTTTGATCCA
ACTAGATGGGATACTGCTGCTGCCAAAGCTAATTCTGTTTCATTTAACTCTTC
TGATGAAGTTGATTATG**AA**GTTTGGGAAAGTTTCTAAAGGGGTTTCTTCACCTT

ATTTACCATTTGGTGGTGGTAGACATAGATGTATTGGGGAACAATTTGCTTAT
GTTCAATTGGGAACCATTTTAACTACTTTTGTTTATAACTTAAGATGGACTAT
TGATGGTTATAAAGTGCCTGACCCTGATTATAGTTCAATGGTGGTTTTACCTA
CTGAACCAGCAGAAATCATTTGGGAAAAAAGAGAAACTTGTATGTTTTAA

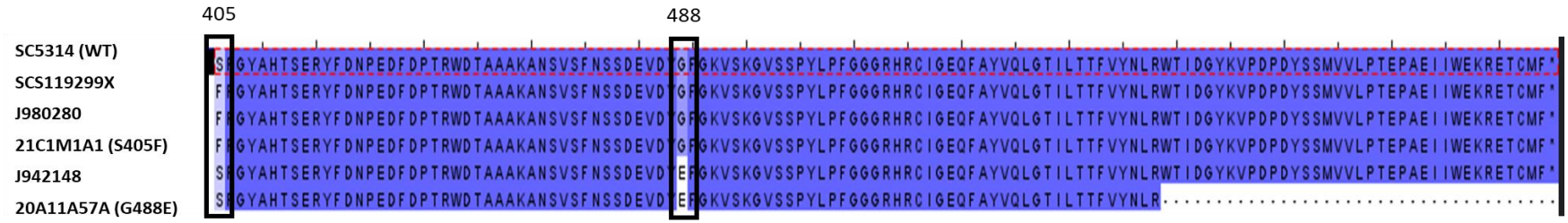

C.5. Protein alignment of *ERG11* for azole-resistant mutants including genetically engineered (GE) mutants and clinical isolates, comparing to SC5314 (WT) control. The alignment shows the protein sequence from amino acid position 405 to the end of the protein. Indicated at the top of the alignment, shown with black boxes are the two SNPS of interest, serine to phenylalanine at position 405, shared by SCS119299X, J980280 and 21C1M1A1 (GE mutant) and glycine to glutamic acid at position 488 shared by J942148 and 20A11A57A (GE mutant).

Strain	MIC Tebuconazole
SC5314 'WT'	≤[a] 4 µg ml^{-1}
21C1M1A1 (S405F)	32 µg ml^{-1}
20NA11A57A (G488E)	32 µg ml^{-1}

C.6. Minimum inhibitory concentration (MIC) values for *Candida albicans.* MIC towards tebuconazole for the genetically engineered strains and the laboratory 'WT' were determined using the CLSI method after 24 h incubation at 37°C. [a] = where the MIC could be below the stated concentration but was the lowest concentration used in the experiment.

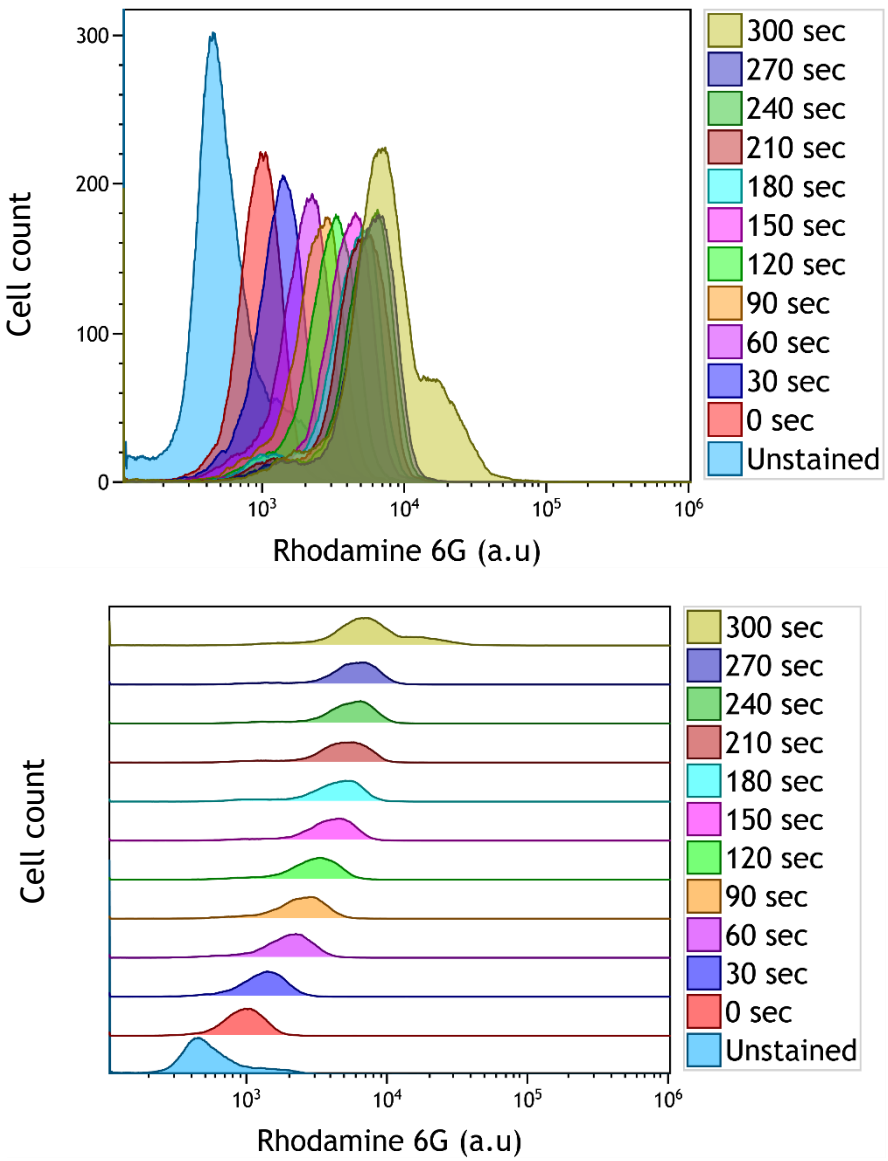

C.7. Rhodamine 6G optimisation. Both plots show flow cytometric peaks from one biological repeat assessing cellular fluorescence using the rhodamine-6G probe, top plot is with peaks overlapping, bottom plot is an overlay of the data. The plots show a changing incubation time from initial addition of R6G, from 0 min to five min at 30 second intervals, at a cell concentration of OD_{600} 2.0 in YP (+ 2% glucose) medium. The samples were then washed three times in PBS and kept on ice. Fluorescence was quantified by analysing 20,000 cells using a Beckman Coulter FC500, FITC filter. Analysis was performed in Kaluza software.

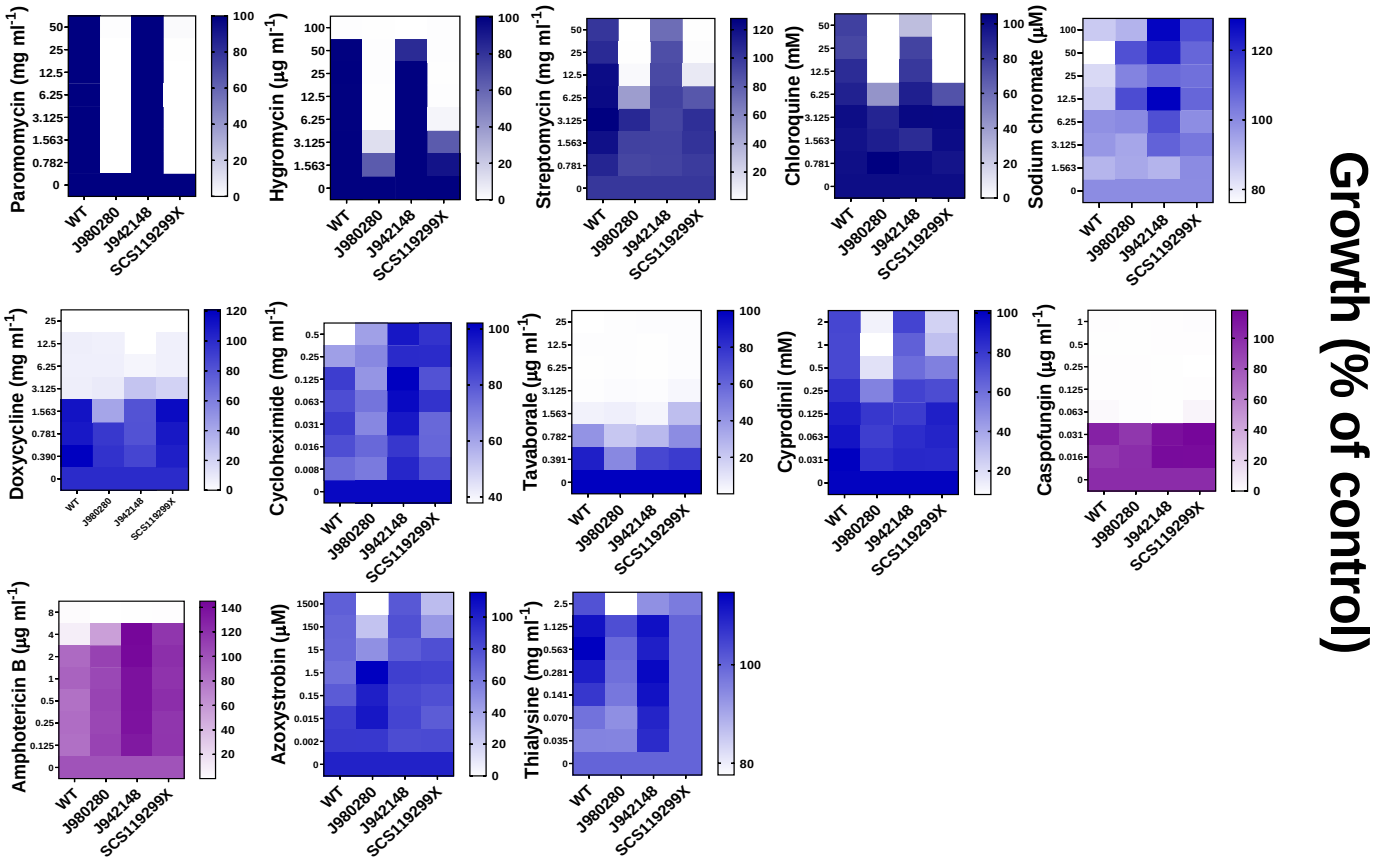

C.8. Hypersensitivity profile of *Candida albicans* azole-resistant mutants compared with SC5314 (WT). Navy/blue heatmaps represent drugs with mechanisms of action inside the cell, purple graphs represent drugs with mode of actions in cell wall/membrane targets. Each heat map represents the mean of three independent experiments.

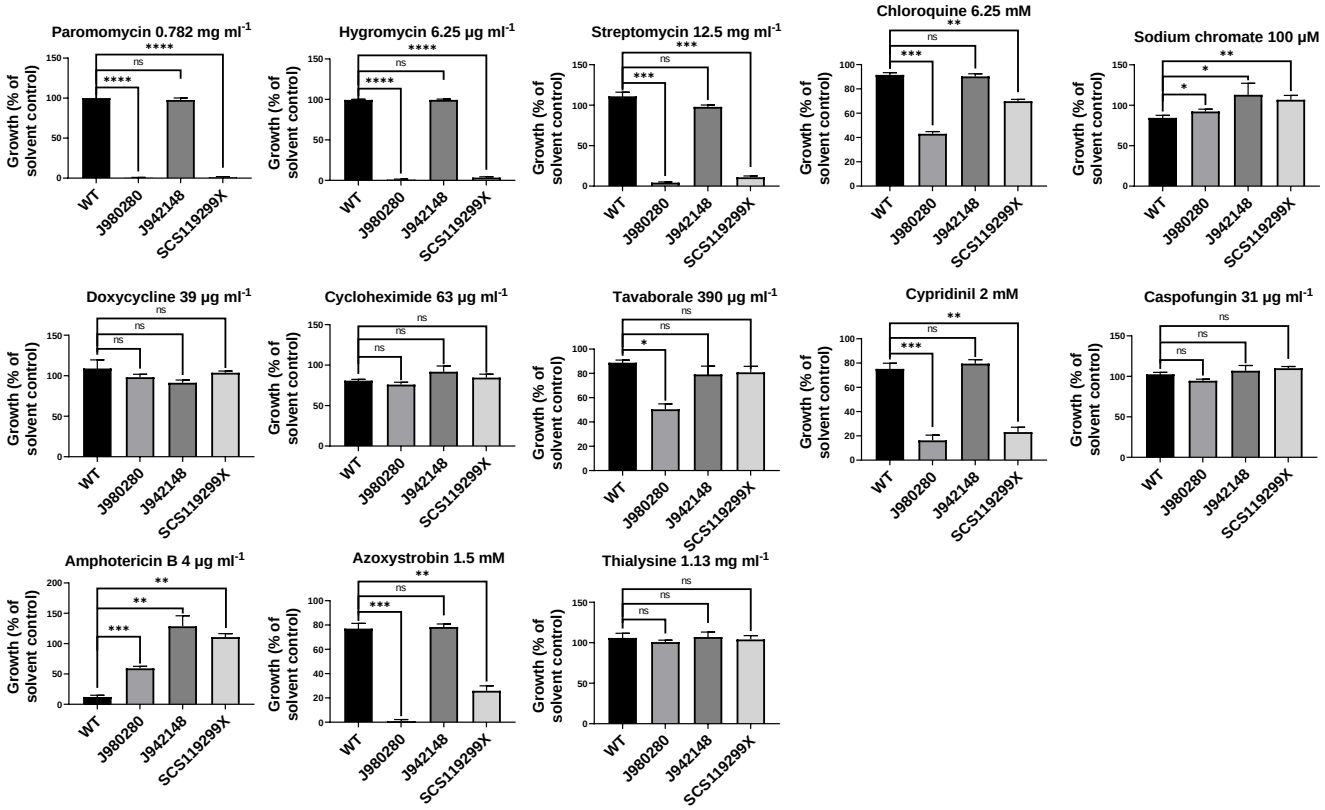

C.9. Sensitivities of *C. albicans* 'WT' SC5314 and azole-resistant isolates to different compounds. A specific concentration from **C.8**. chosen to compare between the 'WT' strain and azole-resistant isolates. Each bar represents the mean of three independent experiments, error + SD. Statistical comparison used unpaired t-tests, ns, not significant, * $p < 0.05$, ** $p < 0.01$, *** $p < 0.001$ and **** $p < 0.0001$.

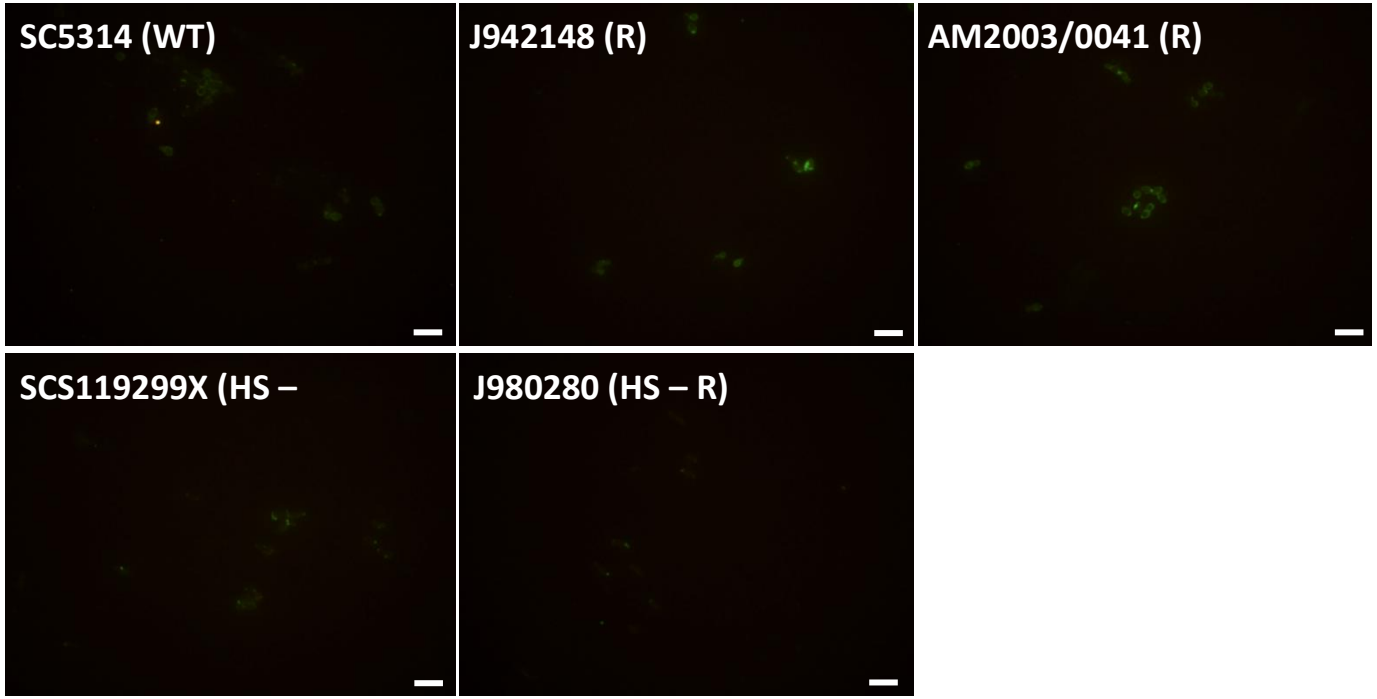

C.10. *Candida albicans* cells stained for β-(1,3)-glucan using Fc-Dectin-1 antibody (FITC). The cells were grown to mid-exponential phase in YEPD (+2% glucose), washed, fixed in 4% PFA and stained for Fc-Dectin-1 (FITC). The strain/isolate is indicated in the top left of the image. WT, wild type, R, azole-resistant, HS – R, hypersensitive and azole-resistant. Scale bar represents 20 µM.

C.11. Raw data from the Prestwick library screening with *Candida albicans* can be found using this private link:
https://figshare.com/s/ade89ab284523eef0c57

Appendix D

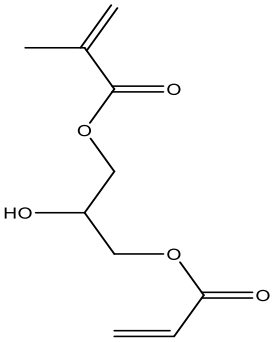

Acryloyloxy-2-hydroxypropyl methacrylate

AOHPMA

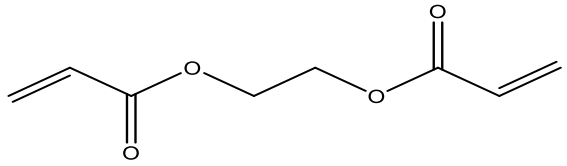

Polyethylene glycol diacrylate

PEGDA

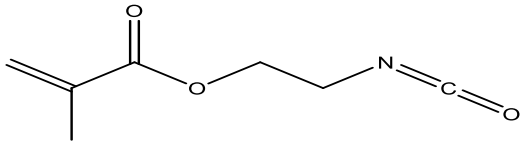

Isocyanatoethyl methacrylate

iCEMA

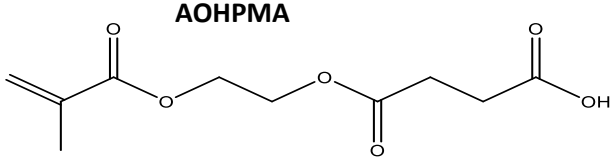

mono-2-(Methacryloyloxy)ethyl succinate

mMAOES

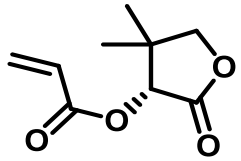

(R)-α-Acryloyloxy-β,β-dimethyl-γ-butyrolactone

AODMBA

D.1. Polymer structures used in this study. The chemical structure, full chemical name and abbreviation are listed for each of polymer.

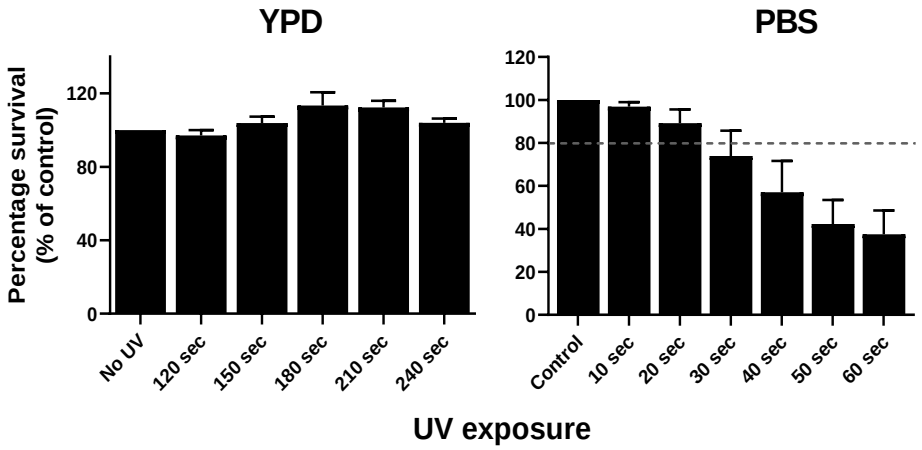

D.2. YPD media provides protective effect under UV-exposure in *C. albicans*. *C. albicans* cells at OD_{600} 0.5 were exposed to UV-light in 10 ml of YPD or PBS, at an exposure height of 35 cm from the UV lamp source with continuous mixing. At increasing increments, aliquots of 100 µl were removed from the exposure, covered and kept at 4 ^{o}C for one hour. Cells were diluted and spread onto YPD agar plates, enumerated after 48 h incubation at 37^{o}C and calculated as a percentage of the untreated control. Each bar represents the mean of three independent experiments. Error + SD.

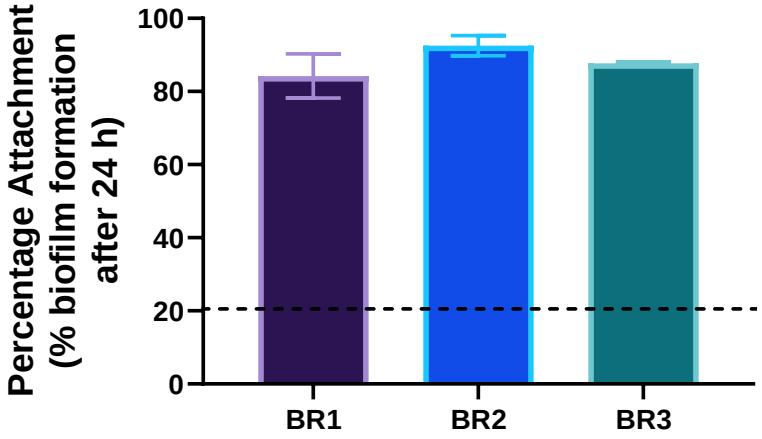

D.3. Anti-attachment properties of AODMBA-printed coupons printed with new printhead. Attachment to 3D-printed coupons was assessed using the XTT-reduction assay, attachment was calculated as percentage compared to polystyrene controls for respective biological repeats (BR). Bars represent the mean of three technical replicates, ±SD.

References

Achilles, J., Muller, S., Bley, T. & Babel, W. 2004. Affinity of single *S. cerevisiae* cells to 2-NBDglucose under changing substrate concentrations. *Cytometry A,* 61**,** 88-98.

Adams, P. B. & Ayers, W. A. 1979. Ecology of *Sclerotinia* species. *Phytopathology,* 69**,** 899-904.

Agostini, M. L., Andres, E. L., Sims, A. C., Graham, R. L., Sheahan, T. P., Lu, X., Smith, E. C., Case, J. B., Feng, J. Y., Jordan, R., Ray, A. S., Cihlar, T., Siegel, D., Mackman, R. L., Clarke, M. O., Baric, R. S. & Denison, M. R. 2018. Coronavirus susceptibility to the antiviral remdesivir (GS-5734) is mediated by the viral polymerase and the proofreading exoribonuclease. *mBio,* 9**,** e00221-18.

Ahmad, A., Khan, A., Khan, L. A. & Manzoor, N. 2010a. In vitro synergy of eugenol and methyleugenol with fluconazole against clinical *Candida* isolates. *J. Med. Microbiol.,* 59**,** 1178-1184.

Ahmad, A., Khan, A., Yousuf, S., Khan, L. A. & Manzoor, N. 2010b. Proton translocating ATPase mediated fungicidal activity of eugenol and thymol. *Fitoterapia,* 81**,** 1157-1162.

Aimanianda, V., Bayry, J., Bozza, S., Kniemeyer, O., Perruccio, K., Elluru, S. R., Clavaud, C., Paris, S., Brakhage, A. A., Kaveri, S. V., Romani, L. & Latge, J. P. 2009. Surface hydrophobin prevents immune recognition of airborne fungal spores. *Nature,* 460**,** 1117-1121.

Albayaty, Y. N., Thomas, N., Ramirez-Garcia, P. D., Davis, T. P., Quinn, J. F., Whittaker, M. R. & Prestidge, C. A. 2020. pH-Responsive copolymer micelles to enhance itraconazole efficacy against *Candida albicans* biofilms. *J. Mater. Chem. B.,* 8**,** 1672-1681.

Aldholmi, M., Marchand, P., Ourliac-Garnier, I., Le Pape, P. & Ganesan, A. 2019. A decade of antifungal leads from natural products: 2010-2019. *Pharmaceuticals,* 12**,** 182.

Almeida, F., Rodrigues, M. L. & Coelho, C. 2019. The still underestimated problem of fungal diseases worldwide. *Front. Microbiol.,* 10**,** 214-218.

Alves, J. C. O., Ferreira, G. F., Santos, J. R., Silva, L. C. N., Rodrigues, J. F. S., Neto, W. R. N., Farah, E. I., Santos, A. R. C., Mendes, B. S., Sousa, L., Monteiro, A. S., Dos Santos, V. L., Santos, D. A., Perez, A. C., Romero, T. R. L., Denadai, A. M. L. & Guzzo, L. S. 2017. Eugenol induces phenotypic alterations and increases the oxidative burst in *Cryptococcus*. *Front. Microbiol.,* 8**,** 2419-2430.

Andreoli, T. E. & Monahan, M. 1968. The interaction of polyene antibiotics with thin lipid membranes. *J. Gen. Physiol.,* 52**,** 300-325.

Andriole, V. T. 2000. Current and future antifungal therapy: new targets for antifungal therapy. *Int. J. Antimicrob. Agents,* 16**,** 317-321.

Anonymous 2017. Stop neglecting fungi. *Nat. Microbiol.,* 2**,** 17120.

Antinori, S., Milazzo, L., Sollima, S., Galli, M. & Corbellino, M. 2016. Candidemia and invasive candidiasis in adults: A narrative review. *Eur. J. Intern. Med.,* 34**,** 21-28.

Apjok, G., Boross, G., Nyerges, A., Fekete, G., Lazar, V., Papp, B., Pal, C. & Csorgo, B. 2019. Limited evolutionary conservation of the phenotypic effects of antibiotic resistance mutations. *Mol. Biol. Evol.,* 36**,** 1601-1611.

Appleby, R. D., Porteous, W. K., Hughes, G., James, A. M., Shannon, D., Wei, Y. H. & Murphy, M. P. 1999. Quantitation and origin of the mitochondrial membrane potential in human cells lacking mitochondrial DNA. *Eur. J. Biochem.,* 262**,** 108-116.

Arana, D. M., Prieto, D., Roman, E., Nombela, C., Alonso-Monge, R. & Pla, J. 2009. The role of the cell wall in fungal pathogenesis. *Microb. Biotechnol.,* 2**,** 308-320.

Arendrup, M. C., Cuenca-Estrella, M., Lass-Florl, C., Hope, W. & Eucast, A. 2012. EUCAST technical note on the EUCAST definitive document EDef 7.2: method for the determination of broth dilution minimum inhibitory concentrations of antifungal agents for yeasts EDef 7.2 (EUCAST-AFST). *Clin. Microbiol. Infect.,* 18**,** E246-247.

Arendrup, M. C. & Patterson, T. F. 2017. Multidrug-Resistant *Candida*: Epidemiology, Molecular Mechanisms, and Treatment. *J. Infect. Dis.,* 216**,** S445-S451.

Atanasov, A. G., Zotchev, S. B., Dirsch, V. M. & Supuran, C. T. 2021. Natural products in drug discovery: advances and opportunities. *Nat. Rev. Drug. Discov.,* 20**,** 200-216.

Attiq, A., Jalil, J., Husain, K. & Ahmad, W. 2018. Raging the war against inflammation with natural products. *Front. Pharmacol.,* 9**,** 976-1002.

Augostine, C. R. & Avery, S. V. 2022. Discovery of natural products with antifungal potential through combinatorial synergy. *Front. Microbiol.,* 13**,** 866840.

Avenot, H. F. & Michailides, T. J. 2010. Progress in understanding molecular mechanisms and evolution of resistance to succinate dehydrogenase inhibiting (SDHI) fungicides in phytopathogenic fungi. *Crop Prot.,* 29**,** 643-651.

Avery, S. V. 2006. Microbial cell individuality and the underlying sources of heterogeneity. *Nat. Rev. Microbiol.,* 4**,** 577-587.

Avery, S. V., Singleton, I., Magan, N. & Goldman, G. H. 2019. The fungal threat to global food security. *Fungal Biol.,* 123**,** 555-557.

Baell, J. & Walters, M. A. 2014. Chemistry: Chemical con artists foil drug discovery. *Nature,* 513**,** 481-483.

Baell, J. B. 2016. Feeling nature's PAINS: Natural products, natural product drugs, and pan assay interference compounds (PAINS). *J. Nat. Prod.,* 79**,** 616-628.

Balashov, S. V., Park, S. & Perlin, D. S. 2006. Assessing resistance to the echinocandin antifungal drug caspofungin in *Candida albicans* by profiling mutations in *FKS1*. *Antimicrob. Agents Chemother.,* 50**,** 2058-2063.

Bankina, B., Bimšteine, G., Arhipova, I., Kaņeps, J. & Stanka, T. 2018. Importance of agronomic practice on the control of wheat leaf diseases. *Agriculture,* 8**,** 56-64.

Barbosa, C., Romhild, R., Rosenstiel, P. & Schulenburg, H. 2019. Evolutionary stability of collateral sensitivity to antibiotics in the model pathogen *Pseudomonas aeruginosa*. *Elife,* 8**,** e51481.

Barbosa, C., Trebosc, V., Kemmer, C., Rosenstiel, P., Beardmore, R., Schulenburg, H. & Jansen, G. 2017. Alternative evolutionary paths to bacterial antibiotic resistance cause distinct collateral effects. *Mol. Biol. Evol.,* 34**,** 2229-2244.

Bartlett, D. W., Clough, J. M., Godwin, J. R., Hall, A. A., Hamer, M. & Parr-Dobrzanski, B. 2002. The strobilurin fungicides. *Pest Manag. Sci.,* 58**,** 649-662.

Basra, P., Alsaadi, A., Bernal-Astrain, G., O'Sullivan, M. L., Hazlett, B., Clarke, L. M., Schoenrock, A., Pitre, S. & Wong, A. 2018. Fitness tradeoffs of antibiotic resistance in extraintestinal pathogenic *Escherichia coli*. *Genome Biol. Evol.,* 10**,** 667-679.

Bates, D. W., Su, L., Yu, D. T., Chertow, G. M., Seger, D. L., Gomes, D. R., Dasbach, E. J. & Platt, R. 2001. Mortality and costs of acute renal failure associated with amphotericin B therapy. *Clin. Infect. Dis.,* 32**,** 686-693.

Becker, W. F., Von Jagow, G., Anke, T. & Steglich, W. 1981. Oudemansin, strobilurin A, strobilurin B and myxothiazol: new inhibitors of the bc 1 segment of the respiratory chain with an E-β-methoxyacrylate system as common structural element. *FEBS Letters,* 132**,** 329-333.

Beigel, J. H., Tomashek, K. M., Dodd, L. E., Mehta, A. K., Zingman, B. S., Kalil, A. C., Hohmann, E., Chu, H. Y., Luetkemeyer, A., Kline, S., Lopez de Castilla, D., Finberg, R. W., Dierberg, K., Tapson, V., Hsieh, L., Patterson, T. F., Paredes, R., Sweeney, D. A., Short, W. R., Touloumi, G., Lye, D. C., Ohmagari, N., Oh, M. D., Ruiz-Palacios, G. M., Benfield, T., Fatkenheuer, G., Kortepeter, M. G., Atmar, R. L., Creech, C. B., Lundgren, J., Babiker, A. G., Pett, S., Neaton, J. D., Burgess, T. H., Bonnett, T., Green, M., Makowski, M., Osinusi, A., Nayak, S., Lane, H. C. & Members, A.-S. G. 2020. Remdesivir for the treatment of Covid-19 - Final report. *N. Engl. J. Med.,* 383**,** 1813-1826.

Ben-Ami, R. 2018. Treatment of invasive candidiasis: A narrative review. *J. Fungi,* 4.

Ben-Ami, R., Garcia-Effron, G., Lewis, R. E., Gamarra, S., Leventakos, K., Perlin, D. S. & Kontoyiannis, D. P. 2011. Fitness and virulence costs of *Candida albicans FKS1* hot spot mutations associated with echinocandin resistance. *J. Infect. Dis.,* 204**,** 626-635.

Bibette, J. 2012. Gaining confidence in high-throughput screening. *PNAS USA,* 109**,** 649-650.

Bisson, J., McAlpine, J. B., Friesen, J. B., Chen, S. N., Graham, J. & Pauli, G. F. 2016. Can invalid bioactives undermine natural product-based drug discovery? *J. Med. Chem.,* 59**,** 1671-1690.

Bongomin, F., Gago, S., Oladele, R. O. & Denning, D. W. 2017. Global and multi-national prevalence of fungal diseases-estimate precision. *J. Fungi* 3**,** 57.

Bosch, F., Blake, J., Gosling, P., Helps, J. C. & Paveley, N. 2020. Identifying when it is financially beneficial to increase or decrease fungicide dose as resistance develops: An evaluation from long-term field experiments. *Plant Pathol.,* 69**,** 631-641.

Bourdichon, F., Casaregola, S., Farrokh, C., Frisvad, J. C., Gerds, M. L., Hammes, W. P., Harnett, J., Huys, G., Laulund, S., Ouwehand, A., Powell, I. B., Prajapati, J. B., Seto, Y., Ter Schure, E., Van Boven, A., Vankerckhoven, V., Zgoda, A., Tuijtelaars, S. & Hansen, E. B. 2012. Food fermentations: microorganisms with technological beneficial use. *Int. J. Food Microbiol.,* 154**,** 87-97.

Bowen, R. L. 1962. *Dental filling material comprising vinyl-silanetreated fused silica and a binder consisting of the reaction product of bis phenol and glycidyi methacrylate*. USA patent application.

Boyd, N. K., Teng, C. & Frei, C. R. 2021. Brief overview of approaches and challenges in new antibiotic development: A focus on drug repurposing. *Front. Cell. Infect. Microbiol.,* 11**,** 684515.

Braga, P. C., Sasso, M. D., Culici, M. & Alfieri, M. 2007. Eugenol and thymol, alone or in combination, induce morphological alterations in the envelope of *Candida albicans*. *Fitoterapia,* 78**,** 396-400.

Brown, A. J. P., Gow, N. A. R., Warris, A. & Brown, G. D. 2019. Memory in fungal pathogens promotes immune evasion, colonisation, and infection. *Trends Microbiol.,* 27**,** 219-230.

Brown, G. D., Denning, D. W., Gow, N. A., Levitz, S. M., Netea, M. G. & White, T. C. 2012. Hidden killers: human fungal infections. *Sci. Transl. Med.,* 4**,** 165rv13.

Brown, G. D. & Gordon, S. 2001. Immune recognition: A new receptor for [beta]-glucans. *Nature,* 413**,** 36-37.

Brown, J. K., Chartrain, L., Lasserre-Zuber, P. & Saintenac, C. 2015. Genetics of resistance to *Zymoseptoria tritici* and applications to wheat breeding. *Fungal Genet. Biol.,* 79**,** 33-41.

Buied, A., Moore, C. B., Denning, D. W. & Bowyer, P. 2013. High-level expression of *cyp51B* in azole-resistant clinical *Aspergillus fumigatus* isolates. *J. Antimicrob. Chemother.,* 68**,** 512-514.

Bulawa, C. E., Miller, D. W., Henry, L. K. & Becker, J. M. 1995. Attenuated virulence of chitin-deficient mutants of *Candida albicans*. *PNAS USA,* 92**,** 10570-10574.
Cai, F., Gao, R., Zhao, Z., Ding, M., Jiang, S., Yagtu, C., Zhu, H., Zhang, J., Ebner, T., Mayrhofer-Reinhartshuber, M., Kainz, P., Chenthamara, K., Akcapinar, G. B., Shen, Q. & Druzhinina, I. S. 2020. Evolutionary compromises in fungal fitness: hydrophobins can hinder the adverse dispersal of conidiospores and challenge their survival. *ISME J.,* 14**,** 2610-2624.
Cai, Q., He, B., Kogel, K. H. & Jin, H. 2018. Cross-kingdom RNA trafficking and environmental RNAi-nature's blueprint for modern crop protection strategies. *Curr. Opin. Microbiol.,* 46**,** 58-64.
Campêlo, M. C. S., Medeiros, J. M. S. & Silva, J. B. A. 2019. Natural products in food preservation. *Int. Food Res. J.,* 26**,** 41-46.
Carratala, J. 2002. The antibiotic-lock technique for therapy of 'highly needed' infected catheters. *Clin. Microbiol. Infect.,* 8**,** 282-289.
Casadevall, A. & Perfect, J. 1988. *Cryptococcus neoformans,* Washington DC, ASM.
Cateau, E., Berjeaud, J. M. & Imbert, C. 2011. Possible role of azole and echinocandin lock solutions in the control of *Candida* biofilms associated with silicone. *Int. J. Antimicrob. Agents,* 37**,** 380-384.
Ceri, H., Olson, M. E., Stremick, C., Read, R. R., Morck, D. & Buret, A. 1999. The Calgary Biofilm Device: new technology for rapid determination of antibiotic susceptibilities of bacterial biofilms. *J .Clin. Microbiol.,* 37**,** 1771-1776.
Charnley, J. 1960. Anchorage of the femoral head prosthesis to the shaft of the femur. *J. Bone Jt. Surg. ,* 42**,** 28-30.
Chattaway, F. W., Holmes, M. R. & Barlow, A. J. 1968. Cell wall composition of the mycelial and blastospore forms of *Candida albicans*. *J. Gen. Microbiol.,* 51**,** 367-376.
Cheeseman, K. H. 1993. Lipid peroxidation and cancer. *In:* B., H. & ARUOMA, O. I. (eds.) *DNA and free radicals.* London, UK: Ellis Horwood. 109-144.
Chen, L., Heng, J., Qin, S. & Bian, K. 2018. A comprehensive understanding of the biocontrol potential of *Bacillus velezensis* LM2303 against Fusarium head blight. *PLoS One,* 13**,** e0198560.
Cheng, F., Kovacs, I. A. & Barabasi, A. L. 2019. Network-based prediction of drug combinations. *Nat. Commun.,* 10**,** 1197.
Cheung, N., Tian, L., Liu, X. & Li, X. 2020. The destructive fungal pathogen *Botrytis cinerea*-insights from genes studied with mutant analysis. *Pathogens,* 9**,** 923.
Chin, N. X., Weitzman, I. & Della-Latta, P. 1997. In vitro activity of fluvastatin, a cholesterol-lowering agent, and synergy with flucanazole and itraconazole against *Candida* species and *Cryptococcus neoformans*. *Antimicrob. Agents Chemother.,* 41**,** 850-852.
Chowdhary, A., Sharma, C., Hagen, F. & Meis, J. F. 2014. Exploring azole antifungal drug resistance in *Aspergillus fumigatus* with special reference to resistance mechanisms. *Future Microbiol.,* 9**,** 697-711.
Chung, D., Papadakis, S. E. & Yam, K. L. 2003. Evaluation of a polymer coating containing triclosan as the antimicrobial layer for packaging materials. *Int. J. Food Sci. Technol.,* 38**,** 165-169.
Clancy, C. J. & Nguyen, M. H. 2013. Finding the "missing 50%" of invasive candidiasis: how nonculture diagnostics will improve understanding of disease spectrum and transform patient care. *Clin. Infect. Dis.,* 56**,** 1284-1292.
Cokol, M., Li, C. & Chandrasekaran, S. 2018. Chemogenomic model identifies synergistic drug combinations robust to the pathogen microenvironment. *PLoS Comput. Biol.,* 14**,** e1006677.

Commission, E. 2019. Concerning the non-renewal of the approval of the active substance chlorothalonil.

Cools, H. J., Bayon, C., Atkins, S., Lucas, J. A. & Fraaije, B. A. 2012. Overexpression of the sterol 14alpha-demethylase gene (*MgCYP51*) in *Mycosphaerella graminicola* isolates confers a novel azole fungicide sensitivity phenotype. *Pest Manag. Sci.,* 68**,** 1034-1040.

Coste, A. T., Karababa, M., Ischer, F., Bille, J. & Sanglard, D. 2004. *TAC1*, transcriptional activator of *CDR* genes, is a new transcription factor involved in the regulation of *Candida albicans* ABC transporters *CDR1* and *CDR2*. *Eukaryot. Cell,* 3**,** 1639-1652.

Costerton, J. W., Montanaro, L. & Arciola, C. R. 2005. Biofilm in implant infections: its production and regulation. *Int. J. Artif. Organs,* 28**,** 1062-1068.

Cottagnoud, P., Cottagnoud, M. & Tauber, M. G. 2003. Vancomycin acts synergistically with gentamicin against penicillin-resistant pneumococci by increasing the intracellular penetration of gentamicin. *Antimicrob. Agents Chemother.,* 47**,** 144-7.

Cottier, F., Sherrington, S., Cockerill, S., Del Olmo Toledo, V., Kissane, S., Tournu, H., Orsini, L., Palmer, G. E., Perez, J. C. & Hall, R. A. 2019. Remasking of *Candida albicans* beta-glucan in response to environmental pH is regulated by quorum sensing. *mBio,* 10**,** mBio.02347-19.

Cowen, L. E., Sanglard, D., Howard, S. J., Rogers, P. D. & Perlin, D. S. 2014. Mechanisms of antifungal drug resistance. *Cold Spring Harb. Perspect. Med.,* 5**,** a019752.

Crystal, A. S., Shaw, A. T., Sequist, L. V., Friboulet, L., Niederst, M. J., Lockerman, E. L., Frias, R. L., Gainor, J. F., Amzallag, A., Greninger, P., Lee, D., Kalsy, A., Gomez-Caraballo, M., Elamine, L., Howe, E., Hur, W., Lifshits, E., Robinson, H. E., Katayama, R., Faber, A. C., Awad, M. M., Ramaswamy, S., Mino-Kenudson, M., Iafrate, A. J., Benes, C. H. & Engelman, J. A. 2014. Patient-derived models of acquired resistance can identify effective drug combinations for cancer. *Science,* 346**,** 1480-1486.

Csermely, P., Korcsmaros, T., Kiss, H. J., London, G. & Nussinov, R. 2013. Structure and dynamics of molecular networks: a novel paradigm of drug discovery: a comprehensive review. *Pharmacol. Ther.,* 138**,** 333-408.

da Silva, A. R., de Andrade Neto, J. B., da Silva, C. R., Campos Rde, S., Costa Silva, R. A., Freitas, D. D., do Nascimento, F. B., de Andrade, L. N., Sampaio, L. S., Grangeiro, T. B., Magalhaes, H. I., Cavalcanti, B. C., de Moraes, M. O. & Nobre Junior, H. V. 2016a. Berberine antifungal activity in fluconazole-resistant pathogenic yeasts: Action mechanism evaluated by flow cytometry and biofilm growth inhibition in *Candida* spp. *Antimicrob. Agents. Chemother.,* 60**,** 3551-3557.

da Silva, L. P., Pereira Coutinho, A., Heleno, R. H., Tenreiro, P. Q. & Ramos, J. A. 2016b. Dispersal of fungi spores by non-specialized flower-visiting birds. *J. Avian Biol.,* 47**,** 438-442.

Darvishi, E., Omidi, M., Bushehri, A. A., Golshani, A. & Smith, M. L. 2013. The antifungal eugenol perturbs dual aromatic and branched-chain amino acid permeases in the cytoplasmic membrane of yeast. *PLoS One,* 8**,** e76028.

Das, B., Mandal, D., Dash, S. K., Chattopadhyay, S., Tripathy, S., Dolai, D. P., Dey, S. K. & Roy, S. 2016. Eugenol provokes ROS-mediated membrane damage-associated antibacterial activity against clinically isolated multidrug-resistant *Staphylococcus aureus* strains. *Infect. Dis.,* 9**,** 11-19.

Davies, C. R., Wohlgemuth, F., Young, T., Violet, J., Dickinson, M., Sanders, J., Vallières, C. & Avery, S. V. 2021. Evolving challenges and strategies for fungal control in the food supply chain. *Fungal Biol. Rev.,* 36**,** 15-26.

Davis-Hanna, A., Piispanen, A. E., Stateva, L. I. & Hogan, D. A. 2008. Farnesol and dodecanol effects on the *Candida albicans* Ras1-cAMP signalling pathway and the regulation of morphogenesis. *Mol. Microbiol.,* 67**,** 47-62.

de Oliveira, H. C., Monteiro, M. C., Rossi, S. A., Peman, J., Ruiz-Gaitan, A., Mendes-Giannini, M. J. S., Mellado, E. & Zaragoza, O. 2019. Identification of off-patent compounds that present antifungal activity against the emerging fungal pathogen *Candida auris*. *Front. Cell. Infect. Microbiol.,* 9**,** 83-93.

Dean, N. 1995. Yeast glycosylation mutants are sensitive to aminoglycosides. *PNAS USA,* 92**,** 1287-1291.

Dean, R., Van Kan, J. A., Pretorius, Z. A., Hammond-Kosack, K. E., Di Pietro, A., Spanu, P. D., Rudd, J. J., Dickman, M., Kahmann, R., Ellis, J. & Foster, G. D. 2012. The Top 10 fungal pathogens in molecular plant pathology. *Mol. Plant Pathol.,* 13**,** 414-30.

Debonne, E., Van Bockstaele, F., Samapundo, S., Eeckhout, M. & Devlieghere, F. 2018. The use of essential oils as natural antifungal preservatives in bread products. *J. Essent. Oil Res.,* 30**,** 309-318.

Degala, H. L., Scott, J. R., Rico Espinoza, F. I., Mahapatra, A. K. & Kannan, G. 2019. Synergistic effect of ozonated and electrolyzed water on the inactivation kinetics of *Escherichia coli* on goat meat. *J. Food Saf.,* 40**,** e12740.

Del Pilar Martinez-Diz, M., Diaz-Losada, E., Andres-Sodupe, M., Bujanda, R., Maldonado-Gonzalez, M. M., Ojeda, S., Yacoub, A., Rey, P. & Gramaje, D. 2021. Field evaluation of biocontrol agents against black-foot and Petri diseases of grapevine. *Pest Manag. Sci.,* 77**,** 697-708.

Demine, S., Renard, P. & Arnould, T. 2019. Mitochondrial uncoupling: A key controller of biological processes in physiology and diseases. *Cells,* 8**,** 795.

Denning, D. W. 2002. Echinocandins: a new class of antifungal. *J. Antimicrob. Chemother.,* 49**,** 889-891.

Denning, D. W. & Bromley, M. J. 2015. Infectious disease. How to bolster the antifungal pipeline. *Science,* 347**,** 1414-1416.

Desai, J. V. & Mitchell, A. P. 2015. *Candida albicans* biofilm development and its genetic control. *Microbiol. Spectr.,* 3**,** MB-0005-2014.

Dhamgaye, S., Devaux, F., Vandeputte, P., Khandelwal, N. K., Sanglard, D., Mukhopadhyay, G. & Prasad, R. 2014. Molecular mechanisms of action of herbal antifungal alkaloid berberine, in *Candida albicans*. *PLoS One,* 9**,** e104554.

Donlan, R. M. 2002. Biofilms: microbial life on surfaces. *Emerg. Infect. Dis.,* 8**,** 881-890.

Drewello, R. & Weissmann, R. 1997. Microbially influenced corrosion of glass. *Appl. Microbiol. Biotechnol.,* 47**,** 337-346.

Duba, A., Goriewa-Duba, K. & Wachowska, U. 2018. A review of the interactions between wheat and wheat pathogens: *Zymoseptoria tritic*i, *Fusarium* spp. and *Parastagonospora nodorum*. *Int. J. Mol. Sci.,* 19**,** 1138.

El-Azizi, M. 2007. Enhancement of the *in vitro* activity of amphotericin B against the biofilms of non-albicans *Candida* spp. by rifampicin and doxycycline. *J. Med. Microbiol.,* 56**,** 645-649.

El-Sharkawy, H. H. A., Rashad, Y. M. & Ibrahim, S. A. 2018. Biocontrol of stem rust disease of wheat using arbuscular mycorrhizal fungi and *Trichoderma* spp. *Physiol. Mol. Plant. Path.,* 103**,** 84-91.

El Ghaouth, A., Wilson, C. L. & Wisniewski, M. 2003. Control of postharvest decay of apple fruit with *Candida saitoana* and induction of defense responses. *Phytopathology,* 93**,** 344-348.

Eyal, Z. & Wahl, I. A. 1973. Physiologic specialisation of *Septoria tritici*. *Phytopathology,* 63**,** 1087-1091.

FAO 2011. Global food losses and food waste - Extent, causes and prevention. *In:* NATIONS, F. A. A. O. O. T. U. (ed.). Rome.

FAO/WHO 1982. Evaluation of certain food additives and contaminants : twenty-sixth report of the Joint FAO/WHO Expert Committee on Food Additives. *Meeting held in Rome [from 19 to 28 April 1982]. World Health Organization*.

Farha, M. A. & Brown, E. D. 2019. Drug repurposing for antimicrobial discovery. *Nat. Microbiol.,* 4**,** 565-577.

Fazly, A., Jain, C., Dehner, A. C., Issi, L., Lilly, E. A., Ali, A., Cao, H., Fidel, P. L., Jr., Rao, R. P. & Kaufman, P. D. 2013. Chemical screening identifies filastatin, a small molecule inhibitor of *Candida albicans* adhesion, morphogenesis, and pathogenesis. *PNAS USA,* 110**,** 13594-13599.

Felix, G., Regenass, M. & Boller, T. 1993. Specific perception of subnanomolar concentrations of chitin fragments by tomato cells: induction of extracellular alkalinization, changes in protein phosphorylation, and establishment of a refractory state. *Plant J.,* 4**,** 307-316.

Feng, Y., Huang, Y., Zhan, H., Bhatt, P. & Chen, S. 2020. An overview of strobilurin fungicide degradation: current status and future perspective. *Front. Microbiol.,* 11**,** 389-400.

Filtenborg, O., Frisvad, J. C. & Thrane, U. 1996. Moulds in food spoilage. *Int. J. Food Microbiol.,* 33**,** 85-102.

Finkel, J. S., Xu, W., Huang, D., Hill, E. M., Desai, J. V., Woolford, C. A., Nett, J. E., Taff, H., Norice, C. T., Andes, D. R., Lanni, F. & Mitchell, A. P. 2012. Portrait of *Candida albicans* adherence regulators. *PLoS Pathog.,* 8**,** e1002525.

Fisher, M. C., Hawkins, N. J., Sanglard, D. & Gurr, S. J. 2018. Worldwide emergence of resistance to antifungal drugs challenges human health and food security. *Science,* 360**,** 739-742.

Fisher, N., Meunier, B. & Biagini, G. A. 2020. The cytochrome bc(1) complex as an antipathogenic target. *FEBS Lett.,* 594**,** 2935-2952.

Flowers, S. A., Colon, B., Whaley, S. G., Schuler, M. A. & Rogers, P. D. 2015. Contribution of clinically derived mutations in *ERG11* to azole resistance in *Candida albicans*. *Antimicrob. Agents Chemother.,* 59**,** 450-460.

Fones, H. & Gurr, S. 2015. The impact of *Septoria tritic*i blotch disease on wheat: An EU perspective. *Fungal Genet. Biol.,* 79**,** 3-7.

Fones, H. N., Bebber, D. P., Chaloner, T. M., Kay, W. T., Steinberg, G. & Gurr, S. J. 2020. Threats to global food security from emerging fungal and oomycete crop pathogens. *Nature Food,* 1**,** 332-342.

Formanek, P. E. & Dilling, D. F. 2019. Advances in the diagnosis and management of invasive fungal disease. *Chest,* 156**,** 834-842.

Fraaije, B. A., Bayon, C., Atkins, S., Cools, H. J., Lucas, J. A. & Fraaije, M. W. 2012. Risk assessment studies on succinate dehydrogenase inhibitors, the new weapons in the battle to control Septoria leaf blotch in wheat. *Mol. Plant Pathol.,* 13**,** 263-275.

Fraaije, B. A., Cools, H. J., Fountaine, J., Lovell, D. J., Motteram, J., West, J. S. & Lucas, J. A. 2005. Role of ascospores in further spread of QoI-resistant cytochrome *b* alleles (G143A) in field populations of *Mycosphaerella graminicola*. *Phytopathology,* 95**,** 933-941.

Frade, J. P. & Arthington-Skaggs, B. A. 2010. Effect of serum and surface characteristics on *Candida albicans* biofilm formation. *Mycoses,* 54**,** e154-162.

Francisco, C. S., Ma, X., Zwyssig, M. M., McDonald, B. A. & Palma-Guerrero, J. 2019. Morphological changes in response to environmental stresses in the fungal plant pathogen *Zymoseptoria tritici*. *Sci. Rep.,* 9**,** 9642.

Free, S. J. 2013. Fungal cell wall organization and biosynthesis. *Adv. Genet.,* 81**,** 33-82.

Frija, L. M., Frade, R. F. & Afonso, C. A. 2011. Isolation, chemical, and biotransformation routes of labdane-type diterpenes. *Chem. Rev.,* 111**,** 4418-4452.

Fujikawa, T., Kuga, Y., Yano, S., Yoshimi, A., Tachiki, T., Abe, K. & Nishimura, M. 2009. Dynamics of cell wall components of *Magnaporthe grisea* during infectious structure development. *Mol. Microbiol.,* 73**,** 553-570.

Fujikawa, T., Sakaguchi, A., Nishizawa, Y., Kouzai, Y., Minami, E., Yano, S., Koga, H., Meshi, T. & Nishimura, M. 2012. Surface alpha-1,3-glucan facilitates fungal stealth infection by interfering with innate immunity in plants. *PLoS Pathog.,* 8**,** e1002882.

Gallis, H. A., Drew, R. H. & Pickard, W. W. 1990. Amphotericin B: 30 years of clinical experience. *Rev. Infect. Dis.,* 12**,** 308-329.

Gao, J., Wang, H., Li, Z., Wong, A. H., Wang, Y. Z., Guo, Y., Lin, X., Zeng, G., Liu, H., Wang, Y. & Wang, J. 2018. *Candida albicans* gains azole resistance by altering sphingolipid composition. *Nat. Commun.,* 9**,** 4495.

Gao, P. & Meury, R. H. 1996. Swelling of hydroxypropyl methylcellulose matrix tablets. 1. Characterization of swelling using a novel optical imaging method. *J. Pharm. Sci.,* 85**,** 725-731.

Garcia-Rubio, R., de Oliveira, H. C., Rivera, J. & Trevijano-Contador, N. 2020. The fungal cell wall: *Candida*, *Cryptococcus*, and *Aspergillus* species. *Front. Microbiol.,* 10**,** 2993.

Garcia-Solache, M. A. & Casadevall, A. 2010. Global warming will bring new fungal diseases for mammals. *mBio,* 1**,** e00061-10.

Geesey, G. G., Richardson, W. T., Yeomans, H. G., Irvin, R. T. & Costerton, J. W. 1977. Microscopic examination of natural sessile bacterial populations from an alpine stream. *Can. J. Microbiol.,* 23**,** 1733-1736.

George, C., Kuriakose, S., George, S. & Mathew, T. 2011. Antifungal activity of silver nanoparticle-encapsulated β-cyclodextrin against human opportunistic pathogens. *Supramol. Chem.,* 23**,** 593-597.

Georgopapadakou, N. H. & Walsh, T. J. 1996. Antifungal agents: chemotherapeutic targets and immunologic strategies. *Antimicrob. Agents Chemother.,* 40**,** 279-291.

Georgopoulos, S. G., Alexandri, E. & Chrysayi, M. 1972. Genetic evidence for the action of oxathiin and thiazole derivatives on the succinic dehydrogenase system of *Ustilago maydis* mitochondria. *J. Bacteriol.,* 110**,** 809-817.

Ghannoum, M. A. & Rice, L. B. 1999. Antifungal agents: Mode of action, mechanisms of resistance, and correlation of these mechanisms with bacterial resistance. *Clin. Microbiol. Rev.,* 12**,** 501-518.

Gil, M. I., López-Gálvez, F., Andújar, S., Moreno, M. & Allende, A. 2019. Disinfection by-products generated by sodium hypochlorite and electrochemical disinfection in different process wash water and fresh-cut products and their reduction by activated carbon. *Food Control,* 100**,** 46-52.

Gill, A. O. & Holley, R. A. 2006. Inhibition of membrane bound ATPases of *Escherichia coli* and Listeria monocytogenes by plant oil aromatics. *Int. J. Food Microbiol.,* 111**,** 170-174.

Glicksberg, B. S., L., L., Cheng, W. Y., Shameer, K., J., H., Castellanos, R., Ma, M., Shi, L., Shah, H., Dudley, J. T. & Chen, R. 2015. An integrative pipeline for multi-modal discovery of disease relationships. *Pac. Symp. Biocomput.,* 20**,** 407-418.

Goddard, M. R., Anfang, N., Tang, R., Gardner, R. C. & Jun, C. 2010. A distinct population of *Saccharomyces cerevisiae* in New Zealand: evidence for local dispersal by insects and human-aided global dispersal in oak barrels. *Environ. Microbiol.,* 12**,** 63-73.

Gomez-Gaviria, M., Vargas-Macias, A. P., Garcia-Carnero, L. C., Martinez-Duncker, I. & Mora-Montes, H. M. 2021. Role of protein glycosylation in interactions of medically relevant fungi with the host. *J. Fungi,* 7**,** 875-905.

Górski, A., Bollyky, P. L., Przybylski, M., Borysowski, J., Miedzybrodzki, R., Jonczyk-Matysiak, E. & Weber-Dabrowska, B. 2018. Perspectives of phage therapy in non-bacterial infections. *Front. Microbiol.,* 9**,** 1-6.

Gostinčar, C., Zajc, J., Lenassi, M., Plemenitaš, A., de Hoog, S., Al-Hatmi, A. M. S. & Gunde-Cimerman, N. 2018. Fungi between extremotolerance and opportunistic pathogenicity on humans. *Fungal Divers.,* 93**,** 195-213.

Gow, N. A. & Hube, B. 2012. Importance of the *Candida albicans* cell wall during commensalism and infection. *Curr. Opin. Microbiol.,* 15**,** 406-412.

Gow, N. A. R., Latge, J. P. & Munro, C. A. 2017. The fungal cell wall: structure, biosynthesis, and function. *Microbiol. Spectr.,* 5**,** FUNK-0035-2016.

Gow, N. A. R. & Lenardon, M. D. 2022. Architecture of the dynamic fungal cell wall. *Nat. Rev. Microbiol.***,** 1-12.

Gray, K. C., Palacios, D. S., Dailey, I., Endo, M. M., Uno, B. E., Wilcock, B. C. & Burke, M. D. 2012. Amphotericin primarily kills yeast by simply binding ergosterol. *PNAS USA,* 109**,** 2234-2239.

Gsaller, F., Hortschansky, P., Furukawa, T., Carr, P. D., Rash, B. & Capilla, J. 2016. Sterol biosynthesis and azole tolerance is governed by the opposing actions of SrbA and the CCAAT binding complex. *PLOS Pathogens,* 12**,** e1005775.

Hakulinen, J. K., Hering, J., Branden, G., Chen, H., Snijder, A., Ek, M. & Johansson, P. 2017. MraY-antibiotic complex reveals details of tunicamycin mode of action. *Nat. Chem. Biol.,* 13**,** 265-267.

Hall, R. A. 2015. Dressed to impress: impact of environmental adaptation on the *Candida albicans* cell wall. *Mol. Microbiol.,* 97**,** 7-17.

Hall, R. A. & Gow, N. A. R. 2013. Mannosylation in *Candida albicans*: role in cell wall function and immune recognition. *Mol. Microbiol.,* 90**,** 1147-1161.

Hall, R. A., Turner, K. J., Chaloupka, J., Cottier, F., De Sordi, L., Sanglard, D., Levin, L. R., Buck, J. & Muhlschlegel, F. A. 2011. The quorum-sensing molecules farnesol/homoserine lactone and dodecanol operate via distinct modes of action in *Candida albicans*. *Eukaryot. Cell,* 10**,** 1034-1042.

Hamer, J. E., Howard, R. J., Chumley, F. G. & Valent, B. 1988. A mechanism for surface attachment in spores of a plant pathogenic. *Science,* 239**,** 288-290.

Hanson, P. K. 2018. *Saccharomyces cerevisiae*: A unicellular model genetic organism of enduring importance. *Curr. Protoc. Essent. Lab. Tech.,* 16**,** e21.

Haro-Reyes, T., Diaz-Peralta, L., Galvan-Hernandez, A., Rodriguez-Lopez, A., Rodriguez-Fragoso, L. & Ortega-Blake, I. 2022. Polyene antibiotics physical chemistry and their effect on lipid membranes; impacting biological processes and medical applications. *Membranes,* 12**,** 681.

Hawksworth, D. L. & Lucking, R. 2017. Fungal diversity revisited: 2.2 to 3.8 million species. *Microbiol. Spectr.,* 5**,** FUNK-00522016.

He, L., Cui, K., Song, Y., Li, T., Liu, N., Mu, W. & Liu, F. 2020. Activity of the novel succinate dehydrogenase inhibitor fungicide pydiflumetofen against SDHI-

sensitive and SDHI-resistant isolates of *Botrytis cinerea* and efficacy against gray mold. *Plant Dis.,* 104**,** 2168-2173.
He, M., Du, M., Fan, M. & Bian, Z. 2007. In vitro activity of eugenol against *Candida albicans* biofilms. *Mycopathologia,* 163**,** 137-143.
Healey, K. R. & Perlin, D. S. 2018. Fungal resistance to echinocandins and the MDR phenomenon in *Candida glabrata*. *J. Fungi,* 4**,** 105-119.
Heaney, S. P., Hall, A. A., Davies, S. A. & Olaya, G. 2000. Resistance to fungicides in the QoI-STAR cross-resistance group: current perspectives. *The BCPC Conference.* Brighton, UK: British Crop Protection Council Farnham, UK.
Heick, T. M., Justesen, A. F. & Jørgensen, L. N. 2017. Anti-resistance strategies for fungicides against wheat pathogen *Zymoseptoria tritici* with focus on DMI fungicides. *Crop Prot.,* 99**,** 108-117.
Heilmann, C. J., Schneider, S., Barker, K. S., Rogers, P. D. & Morschhauser, J. 2010. An A643T mutation in the transcription factor Upc2p causes constitutive *ERG11* upregulation and increased fluconazole resistance in *Candida albicans*. *Antimicrob. Agents Chemother.,* 54**,** 353-359.
Henry, C., Fontaine, T., Heddergott, C., Robinet, P., Aimanianda, V., Beau, R., Beauvais, A., Mouyna, I., Prevost, M. C., Fekkar, A., Zhao, Y., Perlin, D. & Latge, J. P. 2016. Biosynthesis of cell wall mannan in the conidium and the mycelium of *Aspergillus fumigatus*. *Cell Microbiol.,* 18**,** 1881-1891.
Hiemenz, J. W. & Walsh, T. J. 1996. Lipid formulations of amphotericin B: recent progress and future directions. *Clin. Infect. Dis.,* 22 133-144.
Hirano, S. & Nagao, N. 1989. Effects of chitosan, pectic acid lysozyme, and chitinase on the growth of several phytopathogens. *Agric. Biol. Chem.,* 53**,** 3065-3066.
Höfs, S., Mogavero, S. & Hube, B. 2016. Interaction of *Candida albicans* with host cells: virulence factors, host defense, escape strategies, and the microbiota. *J. Microbiol.,* 54**,** 149-169.
Holland, S. L., Ghosh, E. & Avery, S. V. 2010. Chromate-induced sulfur starvation and mRNA mistranslation in yeast are linked in a common mechanism of Cr toxicity. *Toxicol. In Vitro,* 24**,** 1764-1767.
Hon, T., Lee, H. C., Hu, Z., Iyer, V. R. & Zhang, L. 2005. The heme activator protein Hap1 represses transcription by a heme-independent mechanism in *Saccharomyces cerevisiae*. *Genetics,* 169**,** 1343-1352.
Hook, A. L., Chang, C. Y., Yang, J., Luckett, J., Cockayne, A., Atkinson, S., Mei, Y., Bayston, R., Irvine, D. J., Langer, R., Anderson, D. G., Williams, P., Davies, M. C. & Alexander, M. R. 2012. Combinatorial discovery of polymers resistant to bacterial attachment. *Nat. Biotechnol.,* 30**,** 868-875.
Hsieh, M. H., Yu, C. M., Yu, V. L. & Chow, J. W. 1993. Synergy assessed by checkerboard a critical analysis. *Diagn. Microbiol. Infect. Dis.,* 16**,** 343-349.
Hsieh, Y. H., Deng, J. S., Pan, H. P., Liao, J. C., Huang, S. S. & Huang, G. J. 2017. Sclareol ameliorate lipopolysaccharide-induced acute lung injury through inhibition of MAPK and induction of HO-1 signaling. *Int. Immunopharmacol.,* 44**,** 16-25.
Hua, L., Yong, C., Zhanquan, Z., Boqiang, L., Guozheng, Q. & Shiping, T. 2018. Pathogenic mechanisms and control strategies of *Botrytis cinerea* causing post-harvest decay in fruits and vegetables. *Food Qual. Saf.,* 2**,** 111-119.
Hussain, T., Shukla, G. S. & Chandra, S. V. 1987. Effects of cadmium on superoxide dismutase and lipid peroxidation in liver and kidney of growing rats: *in vivo* and i*n vitro* studies. *Pharmacol. Toxicol.,* 60**,** 355-358.
Imamovic, L. & Sommer, M. O. A. 2013. Use of collateral sensitivity networks to design drug cycling protocols that avoid resistance development. *Sci. Transl. Med.,* 5**,** 204ra132.

Iobbi, V., Brun, P., Bernabe, G., Dougue Kentsop, R. A., Donadio, G., Ruffoni, B., Fossa, P., Bisio, A. & De Tommasi, N. 2021. Labdane diterpenoids from *Salvia tingitana* Etl. synergize with clindamycin against methicillin-resistant *Staphylococcus aureus*. *Molecules,* 26**,** 6681.

Isham, N. & Ghannoum, M. A. 2010. Antifungal activity of miconazole against recent *Candida* strains. *Mycoses,* 53**,** 434-437.

Jaber, Q. Z., Bibi, M., Ksiezopolska, E., Gabaldon, T., Berman, J. & Fridman, M. 2020. Elevated vacuolar uptake of fluorescently labeled antifungal drug caspofungin predicts echinocandin resistance in pathogenic yeast. *ACS Cent. Sci.,* 6**,** 1698-1712.

Jacobsen, I. D. & Hube, B. 2017. *Candida albicans* morphology: still in focus. *Expert Rev. Anti. Infect. Ther.,* 15**,** 327-330.

Jacobsen, I. D., Luttich, A., Kurzai, O., Hube, B. & Brock, M. 2014. *In vivo* imaging of disseminated murine *Candida albicans* infection reveals unexpected host sites of fungal persistence during antifungal therapy. *J. Antimicrob. Chemother.,* 69**,** 2785-2796.

Jamal, M., Ahmad, W., Andleeb, S., Jalil, F., Imran, M., Nawaz, M. A., Hussain, T., Ali, M., Rafiq, M. & Kamil, M. A. 2018. Bacterial biofilm and associated infections. *J. Chin. Med. Assoc.,* 81**,** 7-11.

Javelle, M., Vernoud, V., Rogowsky, P. M. & Ingram, G. C. 2011. Epidermis: the formation and functions of a fundamental plant tissue. *New Phytol.,* 189**,** 17-39.

Jenks, J. D. & Hoenigl, M. 2018. Treatment of Aspergillosis. *J. Fungi* 4.

Jensen, R. H., Astvad, K. M., Silva, L. V., Sanglard, D., Jorgensen, R., Nielsen, K. F., Mathiasen, E. G., Doroudian, G., Perlin, D. S. & Arendrup, M. C. 2015. Stepwise emergence of azole, echinocandin and amphotericin B multidrug resistance in vivo in *Candida albicans* orchestrated by multiple genetic alterations. *J. Antimicrob. Chemother.,* 70**,** 2551-2555.

Jia, J., Zhu, F., Ma, X., Cao, Z., Cao, Z. W., Li, Y., Li, Y. X. & Chen, Y. Z. 2009. Mechanisms of drug combinations: interaction and network perspectives. *Nat. Rev. Drug Discov.,* 8**,** 111-128.

Jiao, Y., Wilkinson, J. t., Christine Pietsch, E., Buss, J. L., Wang, W., Planalp, R., Torti, F. M. & Torti, S. V. 2006. Iron chelation in the biological activity of curcumin. *Free Radic. Biol. Med.,* 40**,** 1152-1160.

Jimenez-Ortigosa, C., Moore, C., Denning, D. W. & Perlin, D. S. 2017. Emergence of echinocandin resistance due to a point mutation in the *fks1* gene of *Aspergillus fumigatus* in a patient with chronic pulmonary aspergillosis. *Antimicrob. Agents Chemother.,* 61**,** e01277-17.

Jones, D. & Watson, D. 1969. Parasitism and lysis by soil fungi of *Sclerotinia sclerotiorum* (Lib.) de Bary, a phytopathogenic fungus. *Nature,* 224**,** 287-288.

Jones, M. J. & Epstein, L. 1990. Adhesion of macroconidia to the plant surface and virulence of *Nectria haematococca*. *Appl. Environ. Microbiol.,* 56**,** 3772-3778.

Jørgensen, L. N., Matzen, N., Heick, T. M., Havis, N., Holdgate, S., Clark, B., Blake, J., Glazek, M., Korbas, M., Danielewicz, J., Maumene, C., Rodemann, B., Weigand, S., Kildea, S., Bataille, C., Brauna-Morževska, E., Gulbis, K., Ban, R., Berg, G., Semaskiene, R. & Stammler, G. 2020. Decreasing azole sensitivity of *Z. tritici* in Europe contributes to reduced and varying field efficacy. *J. Plant. Dis. Prot.,* 128**,** 287-301.

Jørgensen, L. N., Nielsen, G. C., Ørum, J. E., Jensen, J. E. & Pinnschmidt, H. O. 2008. Integrating disease control in winter wheat – optimizing fungicide input. *Outlooks Pest Manag.,* 19**,** 206-213.

Jurczuk, M., Brzoska, M. M., Moniuszko-Jakoniuk, J., Galazyn-Sidorczuk, M. & Kulikowska-Karpinska, E. 2004. Antioxidant enzymes activity and lipid peroxidation in liver and kidney of rats exposed to cadmium and ethanol. *Food. Chem. Toxicol.,* 42**,** 429-438.

Kaczmarek, M., Avery, S. V. & Singleton, I. 2019. Microbes associated with fresh produce: sources, types and methods to reduce spoilage and contamination. *Adv. Appl. Microbiol.,* 107**,** 29-82.

Kamaruzzaman, N. F., Tan, L. P., Hamdan, R. H., Choong, S. S., Wong, W. K., Gibson, A. J., Chivu, A. & Pina, M. F. 2019. Antimicrobial Polymers: The Potential Replacement of Existing Antibiotics? *Int. J. Mol. Sci.,* 20**,** 2747-2778.

Kanagaraj, J., Panda, R. C. & Kumar, M. V. 2020. Trends and advancements in sustainable leather processing: Future directions and challenges—A review. *J. Environ. Chem. Eng.,* 8**,** 1-13.

Kang, X., Kirui, A., Muszynski, A., Widanage, M. C. D., Chen, A., Azadi, P., Wang, P., Mentink-Vigier, F. & Wang, T. 2018. Molecular architecture of fungal cell walls revealed by solid-state NMR. *Nat. Commun.,* 9**,** 2747.

Kankanala, P., Czymmek, K. & Valent, B. 2007. Roles for rice membrane dynamics and plasmodesmata during biotrophic invasion by the blast fungus. *Plant Cell,* 19**,** 706-724.

Kasianowicz, J., Benz, R. & McLaughlin, S. 1984. The kinetic mechanism by which CCCP (carbonyl cyanide m-chlorophenylhydrazone) transports protons across membranes. *J. Membr. Biol.,* 82**,** 179-190.

Kenny, S. M. & Buggy, M. 2003. Bone cements and fillers: a review. *J. Mater. Sci. Mater. Med.,* 14**,** 923-938.

Kenwood, B. M., Weaver, J. L., Bajwa, A., Poon, I. K., Byrne, F. L., Murrow, B. A., Calderone, J. A., Huang, L., Divakaruni, A. S., Tomsig, J. L., Okabe, K., Lo, R. H., Cameron Coleman, G., Columbus, L., Yan, Z., Saucerman, J. J., Smith, J. S., Holmes, J. W., Lynch, K. R., Ravichandran, K. S., Uchiyama, S., Santos, W. L., Rogers, G. W., Okusa, M. D., Bayliss, D. A. & Hoehn, K. L. 2014. Identification of a novel mitochondrial uncoupler that does not depolarize the plasma membrane. *Mol. Metab.,* 3**,** 114-123.

Keon, J., Antoniw, J., Carzaniga, R., Deller, S., Ward, J. L., Baker, J. M., Beale, M. H., Hammond-Kosack, K. & Rudd, J. J. 2007. Transcriptional adaptation of *Mycosphaerella graminicola* to programmed cell death (PCD) of its susceptible wheat host. *Mol. Plant Microbe Interact.,* 20**,** 178-193.

Kettles, G. J. & Kanyuka, K. 2016. Dissecting the molecular interactions between wheat and the fungal pathogen *Zymoseptoria tritici*. *Front. Plant. Sci.,* 7**,** 508-515.

Khan, A., Ahmad, A., Akhtar, F., Yousuf, S., Xess, I., Khan, L. A. & Manzoor, N. 2011. Induction of oxidative stress as a possible mechanism of the antifungal action of three phenylpropanoids. *FEMS Yeast Res.,* 11**,** 114-122.

Khan, M., Khan, A. U., Hasan, M., Yadav, K. K., Pinto, M. M. C., Malik, N., Yadav, V. K., Khan, A. H., Islam, S. & Sharma, G. K. 2021. Agro-nanotechnology as an emerging field: A novel sustainable approach for improving plant growth by reducing biotic stress. *Appl. Sci.,* 11**,** 2282.

Khang, C. H., Berruyer, R., Giraldo, M. C., Kankanala, P., Park, S. Y., Czymmek, K., Kang, S. & Valent, B. 2010. Translocation of *Magnaporthe oryzae* effectors into rice cells and their subsequent cell-to-cell movement. *Plant Cell,* 22**,** 1388-1403.

Kim, J. Y. 2016. Human fungal pathogens: Why should we learn? *J. Microbiol.,* 54**,** 145-148.

Kim, R., Khachikian, D. & Reboli, A. C. 2007. A comparative evaluation of properties and clinical efficacy of the echinocandins. *Expert Opin. Pharmacother.,* 8**,** 1479-1492.

Kirikyali, N., P., D., J., L., Hawkins. N & Fraaije, B. A. 2017. Azole and SDHI sensitivity status of *Zymoseptoria tritici* field populations sampled in France, Germany and the UK during 2015 *In:* DEISING, H. B., FRAAIJE, B. A., MEHL, A., OERKE, E. C., SIEROTZKI, H. & STAMMLER, G. (eds.) *Modern fungicides and antifungal compounds.* VIII. Deutsche Phytomedizinische Gesellschaft, Braunschweig. 153-158.

Klis, F. M., de Groot, P. & Hellingwerf, K. 2001. Molecular organization of the cell wall of *Candida albicans*. *Med. Mycol.,* 39 1-8.

Koch, A., Biedenkopf, D., Furch, A., Weber, L., Rossbach, O., Abdellatef, E., Linicus, L., Johannsmeier, J., Jelonek, L., Goesmann, A., Cardoza, V., McMillan, J., Mentzel, T. & Kogel, K. H. 2016. An RNAi-based control of *Fusarium graminearum* infections through spraying of long dsRNAs involves a plant passage and is controlled by the fungal silencing machinery. *PLoS Pathog.,* 12**,** e1005901.

Koseki, S. & Isobe, S. 2007. Microbial control of fresh produce using electrolyzed water. *Jpn. Agric. Res. Q.,* 41**,** 273-282.

Kotler-Brajtburg, J., Price, H. D., Medoff, G., Schlessinger, D. & Kobayashi, G. S. 1974. Molecular basis for the selective toxicity of amphotericin B for yeast and filipin for animal cells. *Antimicrob. Agents Chemother.,* 5**,** 377-382.

Kou, L., Bhutia, Y. D., Yao, Q., He, Z., Sun, J. & Ganapathy, V. 2018. Transporter-guided delivery of nanoparticles to improve drug permeation across cellular barriers and drug exposure to selective cell types. *Front. Pharmacol.,* 9**,** 1-27.

Kozel, T. R. & Wickes, B. 2014. Fungal diagnostics. *Cold Spring. Harb. Perspect. Med.,* 4**,** a019299.

Krisch, J., Tserennadmid, R. & Vágvölgyi, C. 2011. Essential oils against yeast and moulds causing food spoilage. *In:* MÉNDEZ-VILAS, A. (ed.) *Science against microbial pathogens: communicating current research and technological advances* Formatex Research Center.

Kristanc, L., Bozic, B., Jokhadar, S. Z., Dolenc, M. S. & Gomiscek, G. 2019. The pore-forming action of polyenes: From model membranes to living organisms. *Biochim. Biophys. Acta Biomembr.,* 1861**,** 418-430.

Ksiezopolska, E. & Gabaldon, T. 2018. Evolutionary emergence of drug resistance in *Candida* opportunistic pathogens. *Genes,* 9**,** 461-486.

Lai, Y., Wilson, A. & Zantos, S. 1993. Contact lens. *Kirk-Othmer Encyclopedia of Chemical Technology.* New York: Wiley. 191-218.

Lamoth, F. & Calandra, T. 2017. Early diagnosis of invasive mould infections and disease. *J. Antimicrob. Chemother.,* 72**,** 19-28.

Lara, H. H., Ixtepan-Turrent, L., Jose Yacaman, M. & Lopez-Ribot, J. 2020. Inhibition of *Candida auris* biofilm formation on medical and environmental surfaces by silver nanoparticles. *ACS Appl. Mater. Interfaces.,* 12**,** 21183-21191.

Lazar, V., Pal Singh, G., Spohn, R., Nagy, I., Horvath, B., Hrtyan, M., Busa-Fekete, R., Bogos, B., Mehi, O., Csorgo, B., Posfai, G., Fekete, G., Szappanos, B., Kegl, B., Papp, B. & Pal, C. 2013. Bacterial evolution of antibiotic hypersensitivity. *Mol. Syst. Biol.,* 9**,** 700.

Lee, K. K., Kubo, K., Abdelaziz, J. A., Cunningham, I., de Silva Dantas, A., Chen, X., Okada, H., Ohya, Y. & Gow, N. A. R. 2018. Yeast species-specific, differential inhibition of beta-1,3-glucan synthesis by poacic acid and caspofungin. *Cell Surf.,* 3**,** 12-25.

Lefebvre, S., Cook, L. A. & Griffiths, M. A. 2019. Consumer perceptions of genetically modified foods: a mixed-method approach. *J. Consum. Mark.,* 36**,** 113-123.

Lehar, J., Krueger, A. S., Avery, W., Heilbut, A. M., Johansen, L. M., Price, E. R., Rickles, R. J., Short, G. F., 3rd, Staunton, J. E., Jin, X., Lee, M. S., Zimmermann, G. R. & Borisy, A. A. 2009. Synergistic drug combinations tend to improve therapeutically relevant selectivity. *Nat. Biotechnol.,* 27**,** 659-666.

Leon-Buitimea, A., Garza-Cervantes, J. A., Gallegos-Alvarado, D. Y., Osorio-Concepcion, M. & Morones-Ramirez, J. R. 2021. Nanomaterial-based antifungal therapies to combat fungal diseases aspergillosis, coccidioidomycosis, mucormycosis, and candidiasis. *Pathogens,* 10**,** 1303-1325.

Leroux, P., Bach, J., Debieu, D., Fillinger, S., Fritz, R. & Walker, A. S. 2008. Modes of action of sterol biosynthesis inhibitors and resistance phenomena in fungi. *In:* DEHNE, H. W., DEISING, H. B., GISI, U., KUCK, K. H., RUSSELL, P. E. & LYR, H. (eds.) *Modern Fungicides and Antifungal Compounds* V.Braunschweig, Germany: Deutsche Phytomedizinische Gesellschaft. 85-92.

Leslie, J. F. & Summerell, B. A. 2006. *The Fusarium laboratory manual,* Iowa, Blackwell Publishing.

Levitz, S. M., Harrison, T. S., Tabuni, A. & Liu, X. 1997. Chloroquine induces human mononuclear phagocytes to inhibit and kill *Cryptococcus neoformans* by a mechanism independent of iron deprivation. *J. Clin. Invest.,* 100**,** 1640-1646.

Leyva Salas, M., Mounier, J., Valence, F., Coton, M., Thierry, A. & Coton, E. 2017. Antifungal microbial agents for food biopreservation—A review. *Microorganisms,* 5**,** 37-72.

Li, D. D., Zhao, L. X., Mylonakis, E., Hu, G. H., Zou, Y., Huang, T. K., Yan, L., Wang, Y. & Jiang, Y. Y. 2014. In vitro and in vivo activities of pterostilbene against *Candida albicans* biofilms. *Antimicrob. Agents Chemother.,* 58**,** 2344-2355.

Li, F., Svarovsky, M. J., Karlsson, A. J., Wagner, J. P., Marchillo, K., Oshel, P., Andes, D. & Palecek, S. P. 2007. Eap1p, an adhesin that mediates *Candida albicans biofilm* formation *in vitro* and *in vivo*. *Eukaryot. Cell,* 6**,** 931-939.

Li, P., Seneviratne, C. J., Alpi, E., Vizcaino, J. A. & Jin, L. 2015. Delicate metabolic control and coordinated stress response critically determine antifungal tolerance of *Candida albicans* biofilm persisters. *Antimicrob. Agents. Chemother.,* 59**,** 6101-6112.

Li, W., Deng, Y., Ning, Y., He, Z. & Wang, G. L. 2020. Exploiting broad-spectrum disease resistance in crops: from molecular dissection to breeding. *Annu. Rev. Plant Biol.***,** 575-603.

Liauw, C. M., Slate, A. J., Butler, J. A., Wilson-Nieuwenhuis, J. S. T., Deisenroth, T., Preuss, A., Verran, J. & Whitehead, K. A. 2020. The effect of surface hydrophobicity on the attachment of fungal conidia to substrates of polyvinyl acetate and polyvinyl alcohol. *J. Polym. Environ.,* 28**,** 1450-1464.

Liesche, J., Marek, M. & Gunther-Pomorski, T. 2015. Cell wall staining with Trypan blue enables quantitative analysis of morphological changes in yeast cells. *Front. Microbiol.,* 6**,** 107-115.

Liu, Q., Niu, H., Zhang, W., Mu, H., Sun, C. & Duan, J. 2015. Synergy among thymol, eugenol, berberine, cinnamaldehyde and streptomycin against planktonic and biofilm-associated food-borne pathogens. *Lett. Appl. Microbiol.,* 60**,** 421-430.

Lo, H. J., Köhler, J. R., DiDomenico, B., Loebenberg, D., Cacciapuoti, A. & Fink, G. R. 1997. Nonfilamentous *C. albicans* mutants are avirulent. *Cell,* 90**,** 939-949.

Lohse, M. B., Gulati, M., Johnson, A. D. & Nobile, C. J. 2018. Development and regulation of single- and multi-species *Candida albicans* biofilms. *Nat. Rev. Microbiol.,* 16**,** 19-31.

Lowman, A. M., Morishita, M., Kajita, M., Nagai, T. & Peppas, N. A. 1999. Oral delivery of insulin using pH-responsive complexation gels. *J. Pharm. Sci.,* 88**,** 933-937.

Lu, Y., Su, C. & Liu, H. 2014. *Candida albicans* hyphal initiation and elongation. *Trends Microbiol.,* 22**,** 707-714.

Lu, Y., Su, C., Solis, N. V., Filler, S. G. & Liu, H. 2013. Synergistic regulation of hyphal elongation by hypoxia, CO(2), and nutrient conditions controls the virulence of Candida albicans. *Cell Host Microbe.,* 14**,** 499-509.

Lv, J., Liu, G., Ju, Y., Sun, Y. & Guo, W. 2022. Prediction of synergistic antibiotic combinations by graph learning. *Front. Pharmacol.,* 13**,** 849006.

Maertens, J. A. 2004. History of the development of azole derivatives. *Clin. Microbiol. Infect.,* 10 1-10.

Maesaki, S., Marichal, P., Vanden Bossche, H., Sanglard, D. & Kohno, S. 1999. Rhodamine 6G efflux for the detection of CDR1-overexpressing azole-resistant *Candida albicans* strains. *J. Antimicrob. Chemother.,* 44**,** 27-31.

Maitz, M. F. 2015. Applications of synthetic polymers in clinical medicine. *Biosurface Biotribology,* 1**,** 161-176.

Majewska, M. L., Rola, K. & Zubek, S. 2017. The growth and phosphorus acquisition of invasive plants *Rudbeckia laciniata* and *Solidago gigantea* are enhanced by arbuscular mycorrhizal fungi. *Mycorrhiza,* 27**,** 83-94.

Marchese, A., Barbieri, R., Coppo, E., Orhan, I. E., Daglia, M., Nabavi, S. F., Izadi, M., Abdollahi, M., Nabavi, S. M. & Ajami, M. 2017. Antimicrobial activity of eugenol and essential oils containing eugenol: A mechanistic viewpoint. *Crit. Rev. Microbiol.,* 43**,** 668-689.

Marcus, A. I., Zhou, J., O'Brate, A., Hamel, E., Wong, J., Nivens, M., El-Naggar, A., Yao, T. P., Khuri, F. R. & Giannakakou, P. 2005. The synergistic combination of the farnesyl transferase inhibitor lonafarnib and paclitaxel enhances tubulin acetylation and requires a functional tubulin deacetylase. *Cancer Res.,* 65**,** 3883-3893.

Marian, M. & Shimizu, M. 2019. Improving performance of microbial biocontrol agents against plant diseases. *J. Gen. Plant Pathol.,* 85**,** 329-336.

Marichal, P., Gorrens, J. & Vanden Bossche, H. 1985. The action of itraconazole and ketoconazole on growth and sterol synthesis in *Aspergillus fumigatus* and *Aspergillus niger*. *Sabouraudia,* 23**,** 13-21.

Marichal, P., Koymans, L., Willemsens, S., Bellens, D., Verhasselt, P., Luyten, W., Borgers, M., Ramaekers, F. C. S., Odds, F. C. & Vanden Bossche, H. 1999. Contribution of mutations in the cytochrome P450 14alpha-demethylase (Erg11p, Cyp51p) to azole resistance in *Candida albicans*. *Microbiology,* 145**,** 2701-2713.

Marini, G., Nuske, E., Leng, W., Alberti, S. & Pigino, G. 2020. Reorganization of budding yeast cytoplasm upon energy depletion. *Mol. Biol. Cell,* 31**,** 1232-1245.

Mayer, F. L., Wilson, D. & Hube, B. 2013. *Candida albicans* pathogenicity mechanisms. *Virulence,* 4**,** 119-128.

Maymon, M., Sela, N., Shpatz, U., Galpaz, N. & Freeman, S. 2020. The origin and current situation of *Fusarium oxysporum* f. sp. *cubense* tropical race 4 in Israel and the Middle East. *Sci. Rep.,* 10**,** 1590-1601.

McCartney, H. A. 1994. Dispersal of spores and pollen from crops. *Grana,* 33**,** 76-80.

McDougall, P. 2001. Crop protection and agricultural biotechnology consultants. *Report 249.*

Melnyk, A. H., Wong, A. & Kassen, R. 2015. The fitness costs of antibiotic resistance mutations. *Evol. Appl.,* 8**,** 273-283.

Mendgen, K. & Deising, H. 1993. Infection structures of fungal plant pathogens - a cytological and physiological evaluation. *New Phytol.,* 124**,** 193-213.

Mendoza, L., SepÚLveda, C., Melo, R. & Cotoras, M. 2015. Characterization of the antifungal activity against *Botrytis cinerea* of sclareol and 13-epi-sclareol, two labdane-type diterpenoids. *J. Chil. Chem. Soc.,* 60**,** 3024-3028.

Mercure, E. W., Kunoh, H. & Nicholson, R. L. 1995. Visualization of materials released from adhered, ungerminated conidia of *Colletotrichum graminicola*. *Physiol. Mol. Plant. Path.,* 46**,** 121-135.

Min, K., Neiman, A. M. & Konopka, J. B. 2020. Fungal Pathogens: Shape-Shifting Invaders. *Trends Microbiol.***,** 1-12.

Moghadamtousi, S. Z., Kadir, H. A., Hassandarvish, P., Tajik, H., Abubakar, S. & Zandi, K. 2014. A review on antibacterial, antiviral, and antifungal activity of curcumin. *Biomed. Res. Int.,* 2014**,** 1-12.

Mora-Montes, H. M., Netea, M. G., Ferwerda, G., Lenardon, M. D., Brown, G. D., Mistry, A. R., Kullberg, B. J., O'Callaghan, C. A., Sheth, C. C., Odds, F. C., Brown, A. J., Munro, C. A. & Gow, N. A. 2011. Recognition and blocking of innate immunity cells by *Candida albicans* chitin. *Infect. Immun.,* 79**,** 1961-1970.

Morones-Ramirez, J. R., Winkler, J. A., Spina, C. S. & Collins, J. J. 2013. Silver enhances antibiotic activity against gram-negative bacteria. *Sci. Transl. Med.,* 5**,** 190ra81.

Morton, M. J. & Main, M. J. 2013. Use of escin as a perforating agent on the IonWorks quattro automated electrophysiology platform. *J. Biomol. Screen.,* 18**,** 128-134.

Mosbach, A., Edel, D., Farmer, A. D., Widdison, S., Barchietto, T., Dietrich, R. A., Corran, A. & Scalliet, G. 2017. Anilinopyrimidine resistance in *Botrytis cinerea* is linked to mitochondrial function. *Front. Microbiol.,* 8**,** 2361.

Moscou, M. J. & van Esse, H. P. 2017. The quest for durable resistance. *Science,* 358**,** 1541-1542.

Mouhamad, Y., Mokarian-Tabari, P., Clarke, N., Jones, R. A. L. & Geoghegan, M. 2014. Dynamics of polymer film formation during spin coating. *J. Appl. Physics,* 116.

Moyes, D. L., Wilson, D., Richardson, J. P., Mogavero, S., Tang, S. X., Wernecke, J., Hofs, S., Gratacap, R. L., Robbins, J., Runglall, M., Murciano, C., Blagojevic, M., Thavaraj, S., Forster, T. M., Hebecker, B., Kasper, L., Vizcay, G., Iancu, S. I., Kichik, N., Hader, A., Kurzai, O., Luo, T., Kruger, T., Kniemeyer, O., Cota, E., Bader, O., Wheeler, R. T., Gutsmann, T., Hube, B. & Naglik, J. R. 2016. Candidalysin is a fungal peptide toxin critical for mucosal infection. *Nature,* 532**,** 64-68.

Muhammed Shameem, M., Sasikanth, S. M., Annamalai, R. & Ganapathi Raman, R. 2021. A brief review on polymer nanocomposites and its applications. *Mater. Today,* 45**,** 2536-2539.

Munck, C., Gumpert, H. K., Wallin, A. I., Wang, H. H. & Sommer, M. O. 2014. Prediction of resistance development against drug combinations by collateral responses to component drugs. *Sci. Transl. Med.,* 6**,** 262ra156.

Murad, A. M., Leng, P., Straffon, M., Wishart, J., Macaskill, S., MacCallum, D., Schnell, N., Talibi, D., Marechal, D., Tekaia, F., d'Enfert, C., Gaillardin, C., Odds, F. C. & Brown, A. J. 2001. NRG1 represses yeast-hypha morphogenesis and hypha-specific gene expression in *Candida albicans*. *EMBO J.,* 20**,** 4742-4752.

Nations, U. 2019. World Population Prospects Data Booklet. *In:* DIVISION, D. O. E. A. S. A. P. (ed.). New York, USA.
Neag, M. A., Mocan, A., Echeverria, J., Pop, R. M., Bocsan, C. I., Crisan, G. & Buzoianu, A. D. 2018. Berberine: Botanical occurrence, traditional uses, extraction methods, and relevance in cardiovascular, metabolic, hepatic, and renal disorders. *Front. Pharmacol.,* 9**,** 557-586.
Nett, J. E., Sanchez, H., Cain, M. T. & Andes, D. R. 2010. Genetic basis of *Candida* biofilm resistance due to drug-sequestering matrix glucan. *J. Infect. Dis.,* 202**,** 171-175.
Newman, D. J. & Cragg, G. M. 2016. Natural products as sources of new drugs from 1981 to 2014. *J. Nat. Prod.,* 79**,** 629-661.
Newman, D. J. & Cragg, G. M. 2020. Natural products as sources of new drugs over the nearly four decades from 01/1981 to 09/2019. *J. Nat. Prod.,* 83**,** 770-803.
Nichol, D., Rutter, J., Bryant, C., Hujer, A. M., Lek, S., Adams, M. D., Jeavons, P., Anderson, A. R. A., Bonomo, R. A. & Scott, J. G. 2019. Antibiotic collateral sensitivity is contingent on the repeatability of evolution. *Nat. Commun.,* 10**,** 334.
Nicolson, P. C. & Vogt, J. 2001. Soft contact lens polymers: an evolution. *Biomaterials,* 22**,** 3273-3283.
Ning, Y., Liu, W. & Wang, G. L. 2017. Balancing immunity and yield in crop plants. *Trends. Plant. Sci.,* 22**,** 1069-1079.
Nishimoto, A. T., Sharma, C. & Rogers, P. D. 2019. Molecular and genetic basis of azole antifungal resistance in the opportunistic pathogenic fungus *Candida albicans*. *J. Antimicrob. Chemother.,* 75**,** 257-270.
Niu, G. & Li, W. 2019. Next-generation drug discovery to combat antimicrobial resistance. *Trends Biochem. Sci.,* 44**,** 961-972.
Nobile, C. J., Andes, D. R., Nett, J. E., Smith, F. J., Yue, F., Phan, Q. T., Edwards, J. E., Filler, S. G. & Mitchell, A. P. 2006. Critical role of Bcr1-dependent adhesins in *C. albicans* biofilm formation *in vitro* and *in vivo*. *PLoS Pathog.,* 2**,** e63.
Nobile, C. J. & Johnson, A. D. 2015. *Candida albicans* biofilms and human disease. *Annu. Rev. Microbiol.,* 69**,** 71-92.
Nosanchuk, J. D. 2013. Review of human pathogenic fungi: Molecular biology and pathogenic mechanisms. *Front. Microbiol.,* 6**,** 86.
Nosengo, N. 2016. Can you teach old drugs new tricks? *Nature* 534**,** 314–316.
O'Driscoll, A., Kildea, S., Doohan, F., Spink, J. & Mullins, E. 2014. The wheat-*Septoria* conflict: a new front opening up? *Trends. Plant. Sci.,* 19**,** 602-610.
O'Toole, G., Kaplan, H. B. & Kolter, R. 2000. Biofilm formation as microbial development. *Annu. Rev. Microbiol.,* 54**,** 49-79.
O'Brien, D. M., Vallieres, C., Alexander, C., Howdle, S. M., Stockman, R. A. & Avery, S. V. 2019. Epoxy–amine oligomers from terpenes with applications in synergistic antifungal treatments. *J. Mater. Chem. B.***,** 5222-5229.
O'Neill, J. 2016. Tackling drug-resistant infections globally: Final report and recommendation. *The review on antimicrobial resistance.* London: Wellcome Trust.
Ocampo, P. S., Lazar, V., Papp, B., Arnoldini, M., Abel zur Wiesch, P., Busa-Fekete, R., Fekete, G., Pal, C., Ackermann, M. & Bonhoeffer, S. 2014. Antagonism between bacteriostatic and bactericidal antibiotics is prevalent. *Antimicrob. Agents Chemother.,* 58**,** 4573-4582.
Odds, F. C. 2003. Synergy, antagonism, and what the chequerboard puts between them. *J. Antimicrob. Chemother.,* 52**,** 1.
Ogar, A., Tylko, G. & Turnau, K. 2015. Antifungal properties of silver nanoparticles against indoor mould growth. *Sci. Total Environ.,* 521**,** 305-314.

Olivares, J., Alvarez-Ortega, C., Linares, J. F., Rojo, F., Kohler, T. & Martinez, J. L. 2012. Overproduction of the multidrug efflux pump MexEF-OprN does not impair *Pseudomonas aeruginosa* fitness in competition tests, but produces specific changes in bacterial regulatory networks. *Environ. Microbiol.,* 14**,** 1968-1981.

Oliveira-Carvalho, V. & Del Negro, G. M. 2014. Is the S405F mutation in *Candida albicans ERG11* gene sufficient to confer resistance to fluconazole? *J. Mycol. Med.,* 24**,** 241-242.

Oliveira, P. M., Zannini, E. & Arendt, E. K. 2014. Cereal fungal infection, mycotoxins, and lactic acid bacteria mediated bioprotection: from crop farming to cereal products. *Food Microbiol.,* 37**,** 78-95.

Omrane, S., Sghyer, H., Audeon, C., Lanen, C., Duplaix, C., Walker, A. S. & Fillinger, S. 2015. Fungicide efflux and the MgMFS1 transporter contribute to the multidrug resistance phenotype in *Zymoseptoria tritici* field isolates. *Environ. Microbiol.,* 17**,** 2805-2823.

Orlita, A. 2004. Microbial biodeterioration of leather and its control: a review. *Int. Biodeterior. Biodegradation,* 53**,** 157-163.

Ors, M. E., Randoux, B., Selim, S., Siah, A., Couleaud, G., Maumené, C., Sahmer, K., Halama, P. & Reignault, P. 2018. Cultivar-dependent partial resistance and associated defence mechanisms in wheat against *Zymoseptoria tritici*. *Plant Pathol.,* 67**,** 561-572.

Osherov, N. & May, G. S. 2001. The molecular mechanisms of conidial germination. *FEMS Microbiol. Lett.,* 199**,** 153-160.

Ou, S. H. 1980. Pathogen variability and host resistance in rice blast disease. *Annu. Rev. Phytopathol.,* 18**,** 167-187.

Owens, D. E., Eby, J. K., Jian, Y. & Peppas, N. A. 2007. Temperature-responsive polymer–gold nanocomposites as intelligent therapeutic systems. *J. Biomed. Mater. Res. A,* 83A**,** 692-695.

Pal, C., Papp, B. & Lazar, V. 2015. Collateral sensitivity of antibiotic-resistant microbes. *Trends Microbiol.,* 23**,** 401-407.

Pal, K. K. & Gardener, B. M. 2006. Biological control of plant pathogens. *Plant Health Instr.,* 2**,** 1117-1142.

Palmer, C. L. & Skinner, W. 2002. *Mycosphaerella graminicola*: latent infection, crop devastation and genomics. *Mol. Plant Pathol.,* 3**,** 63-70.

Paolini, G. V., Shapland, R. H., van Hoorn, W. P., Mason, J. S. & Hopkins, A. L. 2006. Global mapping of pharmacological space. *Nat. Biotechnol.,* 24**,** 805-815.

Pappas, P. G., Kauffman, C. A., Andes, D. R., Clancy, C. J., Marr, K. A., Ostrosky-Zeichner, L., Reboli, A. C., Schuster, M. G., Vazquez, J. A., Walsh, T. J., Zaoutis, T. E. & Sobel, J. D. 2016. Clinical practice guideline for the management of candidiasis: 2016 Update by the infectious diseases society of America. *Clin. Infect. Dis.,* 62**,** e1-50.

Park, S. E., Blissett, R., Susarla, S. M. & Weber, H. P. 2008. *Candida albicans* adherence to surface-modified denture resin surfaces. *J. Prosthodont.,* 17**,** 365-369.

Parnell, J. J., Berka, R., Young, H. A., Sturino, J. M., Kang, Y., Barnhart, D. M. & DiLeo, M. V. 2016. From the lab to the farm: An industrial perspective of plant beneficial microorganisms. *Front. Plant Sci.,* 7**,** 1110.

Parsek, M. R. & Greenberg, E. P. 2005. Sociomicrobiology: the connections between quorum sensing and biofilms. *Trends Microbiol.,* 13**,** 27-33.

Parsons, A. B., Lopez, A., Givoni, I. E., Williams, D. E., Gray, C. A., Porter, J., Chua, G., Sopko, R., Brost, R. L., Ho, C. H., Wang, J., Ketela, T., Brenner, C., Brill, J. A., Fernandez, G. E., Lorenz, T. C., Payne, G. S., Ishihara, S., Ohya, Y., Andrews, B., Hughes, T. R., Frey, B. J., Graham, T. R., Andersen, R. J. & Boone, C. 2006.

Exploring the mode-of-action of bioactive compounds by chemical-genetic profiling in yeast. *Cell,* 126**,** 611-625.

Penner, J. C., Ferreira, J. A. G., Secor, P. R., Sweere, J. M., Birukova, M. K., Joubert, L. M., Haagensen, J. A. J., Garcia, O., Malkovskiy, A. V., Kaber, G., Nazik, H., Manasherob, R., Spormann, A. M., Clemons, K. V., Stevens, D. A. & Bollyky, P. L. 2016. Pf4 bacteriophage produced by *Pseudomonas aeruginosa* inhibits *Aspergillus fumigatus* metabolism via iron sequestration. *Microbiology,* 162**,** 1583-1594.

Peplow, M. 2016. Fantastic plastics. *Nature,* 536**,** 266-268.

Perfect, J. R. 2017. The antifungal pipeline: a reality check. *Nat. Rev. Drug Discov.,* 16**,** 603-616.

Peutzfeldt, A. 1997. Resin composites in dentistry: the monomer systems. *Eur. J. Oral Sci.,* 105**,** 97-116.

Piarroux, R. P., Romain, T., Martin, A., Vainqueur, D., Vitte, J., Lachaud, L., Gangneux, J. P., Gabriel, F., Fillaux, J. & Ranque, S. 2019. Multicenter evaluation of a novel immunochromatographic test for anti-aspergillus IgG detection. *Front. Cell Infect. Microbiol.,* 9**,** 12.

Pickard, R., Lam, T., MacLennan, G., Starr, K., Kilonzo, M., McPherson, G., Gillies, K., McDonald, A., Walton, K., Buckley, B., Glazener, C., Boachie, C., Burr, J., Norrie, J., Vale, L., Grant, A. & N'Dow, J. 2012. Antimicrobial catheters for reduction of symptomatic urinary tract infection in adults requiring short-term catheterisation in hospital: a multicentre randomised controlled trial. *The Lancet,* 380**,** 1927-1935.

Prasad, S., Gupta, S. C., Tyagi, A. K. & Aggarwal, B. B. 2014. Curcumin, a component of golden spice: from bedside to bench and back. *Biotechnol. Adv.,* 32**,** 1053-1064.

Prill, S. K., Klinkert, B., Timpel, C., Gale, C. A., Schroppel, K. & Ernst, J. F. 2005. PMT family of *Candida albicans*: five protein mannosyltransferase isoforms affect growth, morphogenesis and antifungal resistance. *Mol. Microbiol.,* 55**,** 546-560.

Pritchard, J. R., Bruno, P. M., Gilbert, L. A., Capron, K. L., Lauffenburger, D. A. & Hemann, M. T. 2013. Defining principles of combination drug mechanisms of action. *PNAS USA,* 110**,** E170-179.

Pushpakom, S., Iorio, F., Eyers, P. A., Escott, K. J., Hopper, S., Wells, A., Doig, A., Guilliams, T., Latimer, J., McNamee, C., Norris, A., Sanseau, P., Cavalla, D. & Pirmohamed, M. 2019. Drug repurposing: progress, challenges and recommendations. *Nat. Rev. Drug. Discov.,* 18**,** 41-58.

Qian, L., Qi, S., Wang, Z., Magnuson, J. T., Volz, D. C., Schlenk, D., Jiang, J. & Wang, C. 2021. Environmentally relevant concentrations of boscalid exposure affects the neurobehavioral response of zebrafish by disrupting visual and nervous systems. *J. Hazard. Mater.,* 404**,** 124083.

Qu, S., Yang, K., Chen, L., Liu, M., Geng, Q., He, X., Li, Y., Liu, Y. & Tian, J. 2019. Cinnamaldehyde, a promising natural preservative against *Aspergillus flavus*. *Front. Microbiol.,* 10**,** 2895.

Quan, H., Cao, Y. Y., Xu, Z., Zhao, J. X., Gao, P. H., Qin, X. F. & Jiang, Y. Y. 2006. Potent in vitro synergism of fluconazole and berberine chloride against clinical isolates of *Candida albicans* resistant to fluconazole. *Antimicrob. Agents Chemother.,* 50**,** 1096-1099.

Ramage, G., Bachmann, S., Patterson, T. F., Wickes, B. L. & Lopez-Ribot, J. L. 2002a. Investigation of multidrug efflux pumps in relation to fluconazole resistance in *Candida albicans* biofilms. *J. Antimicrob. Chemother.,* 49**,** 973-980.

Ramage, G., Saville, S. P., Wickes, B. L. & López-Ribot, J. L. 2002b. Inhibition of *Candida albicans* biofilm formation by farnesol, a quorum-sensing molecule. *Appl. Environ. Microbiol.,* 68**,** 5459-5463.

Rashad, Y., M. & Moussa, T. A. A. 2020. Biocontrol agents for fungal plant diseases management. *In:* N., E.-W., M., S. & M., A.-H. (eds.) *Cottage industry of biocontrol agents and their applications.* Springer, Cham. 337-363.

Reboli, A. C., Rotstein, C., Pappas, P. G., Chapman, S. W., Kett, D. H., Kumar, D., Betts, R., Wible, M., Goldstein, B. P., Schranz, J., Krause, D. S. & Walsh, T. J. 2007. Anidulafungin versus fluconazole for invasive candidiasis. *N. Engl. J. Med.,* 356**,** 2472-2482.

Revie, N. M., Iyer, K. R., Maxson, M. E., Zhang, J., Yan, S., Fernandes, C. M., Meyer, K. J., Chen, X., Skulska, I., Fogal, M., Sanchez, H., Hossain, S., Li, S., Yashiroda, Y., Hirano, H., Yoshida, M., Osada, H., Boone, C., Shapiro, R. S., Andes, D. R., Wright, G. D., Nodwell, J. R., Del Poeta, M., Burke, M. D., Whitesell, L., Robbins, N. & Cowen, L. E. 2022. Targeting fungal membrane homeostasis with imidazopyrazoindoles impairs azole resistance and biofilm formation. *Nat. Commun.,* 13**,** 3634.

Reygaert, W. C. 2018. An overview of the antimicrobial resistance mechanisms of bacteria. *AIMS Microbiol.,* 4**,** 482-501.

Ribes, S., Fuentes, A., Talens, P. & Barat, J. M. 2018. Prevention of fungal spoilage in food products using natural compounds: A review. *Crit. Rev. Food Sci. Nutr.,* 58**,** 2002-2016.

Rock, F. L., Mao, W., Yaremchuk, A., Tukalo, M., Crepin, T., Zhou, H., Zhang, Y. K., Hernandez, V., Akama, T., Baker, S. J., Plattner, J. J., Shapiro, L., Martinis, S. A., Benkovic, S. J., Cusack, S. & Alley, M. R. 2007. An antifungal agent inhibits an aminoacyl-tRNA synthetase by trapping tRNA in the editing site. *Science,* 316**,** 1759-1761.

Rodaki, A., Bohovych, I. M., Enjalbert, B., Young, T., Odds, F. C., Gow, N. A. & Brown, A. J. 2009. Glucose promotes stress resistance in the fungal pathogen *Candida albicans*. *Mol. Biol. Cell,* 20**,** 4845-4855.

Rodrigues, A., Gutierrez-Patricio, S., Miller, A. Z., Saiz-Jimenez, C., Wiley, R., Nunes, D., Vilarigues, M. & Macedo, M. F. 2014. Fungal biodeterioration of stained-glass windows. *Int. Biodeterior. Biodegradation,* 90**,** 152-160.

Rodrigues, T., Reker, D., Schneider, P. & Schneider, G. 2016. Counting on natural products for drug design. *Nat. Chem.,* 8**,** 531-541.

Rodriguez, D. L., Quail, M. M., Hernday, A. D. & Nobile, C. J. 2020. Transcriptional circuits regulating developmental processes in *Candida albicans*. *Front. Cell Infect. Microbiol.,* 10**,** 605711.

Roemer, T. & Krysan, D. J. 2014. Antifungal drug development: challenges, unmet clinical needs, and new approaches. *Cold Spring Harb. Perspect. Med.,* 1**,** a019703.

Roemhild, R., Linkevicius, M. & Andersson, D. I. 2020. Molecular mechanisms of collateral sensitivity to the antibiotic nitrofurantoin. *PLoS Biol.,* 18**,** e3000612.

Rojas Tayo, E. C., Jørgensen, H. J. L., Jensen, B. & Collinge, D. B. 2018. Fusarium diseases: biology and management perspectives. *Integrated disease management of wheat and barley.* Burleigh Dodds Science Publishing Limited. 23-45.

Ruby, A. J., Kuttan, G., Dinesh Babu, K., Rajasekharan, K. N. & Kuttan, R. 1995. Anti-tumour and antioxidant activity of natural curcuminoids. *Cancer Lett.,* 94**,** 79-83.

Rybak, J. M., Cuomo, C. A. & P., D. R. 2022. The molecular and genetic basis of antifungal resistance in the emerging fungal pathogen *Candida auris*. *Curr. Opin. Microbiol.,* 70.

Ryder, L. S., Cruz-Mireles, N., Molinari, C., Eisermann, I., Eseola, A. B. & Talbot, N. J. 2022. The appressorium at a glance. *J. Cell Sci.,* 135**,** jcs259857.

Sanglard, D. 2016. Emerging threats in antifungal-resistant fungal pathogens. *Front. Med.,* 15**,** 11.

Sanglard, D., Kuchler, K., Ischer, F., Pagani, J. L., Monod, M. & Bille, J. 1995. Mechanisms of resistance to azole antifungal agents in *Candida albicans* isolates from AIDS patients involve specific multidrug transporters. *Antimicrob. Agents Chemother.,* 39**,** 2378-2386.

Sanglard, D. & Odds, F. C. 2002. Resistance of *Candida* species to antifungal agents: molecular mechanisms and clinical consequences. *Lancet Infect. Dis.,* 2**,** 73-85.

Santos-Lopez, A., Fritz, M. J., Lombardo, J. B., Burr, A. H. P., Heinrich, V. A., Marshall, C. W. & Cooper, V. S. 2022. Evolved resistance to a novel cationic peptide antibiotic requires high mutation supply. *Evol. Med. Public Health,* 10**,** 266-276.

Satish, S., Jimenez-Ortigosa, C., Zhao, Y., Lee, M. H., Dolgov, E., Kruger, T., Park, S., Denning, D. W., Kniemeyer, O., Brakhage, A. A. & Perlin, D. S. 2019. Stress-induced changes in the lipid microenvironment of beta-(1,3)-d-glucan synthase cause clinically important echinocandin resistance in *Aspergillus fumigatus*. *mBio,* 10**,** e00779-19.

Satish, S. & Perlin, D. S. 2019. Echinocandin resistance in *Aspergillus fumigatus* has broad implications for membrane lipid perturbations that influence drug-target interactions. *Microbiol. Insights,* 12**,** 1-4.

Saville, S. P., Lazzell, A. L., Bryant, A. P., Fretzen, A., Monreal, A., Solberg, E. O., Monteagudo, C., Lopez-Ribot, J. L. & Milne, G. T. 2006. Inhibition of filamentation can be used to treat disseminated candidiasis. *Antimicrob. Agents Chemother.,* 50**,** 3312-3216.

Scherlach, K., Graupner, K. & Hertweck, C. 2013. Molecular bacteria-fungi interactions: effects on environment, food, and medicine. *Annu. Rev. Microbiol.,* 67**,** 375-397.

Schmeling, B. V. & Kulka, M. 1966. Systemic fungicidal activity of 1,4-oxathiin derivatives. *Science,* 152**,** 659-660.

Schneider-Poetsch, T., Ju, J., Eyler, D. E., Dang, Y., Bhat, S., Merrick, W. C., Green, R., Shen, B. & Liu, J. O. 2010. Inhibition of eukaryotic translation elongation by cycloheximide and lactimidomycin. *Nat. Chem. Biol.,* 6**,** 209-217.

Schumacher, C. F., Steiner, U., Dehne, H. W. & Oerke, E. C. 2008. Localized adhesion of nongerminated *Venturia inaequalis* conidia to leaves and artificial surfaces. *Phytopathology,* 98**,** 760-768.

Schuster, M., Guiu-Aragones, C. & Steinberg, G. 2020. Class V chitin synthase and beta(1,3)-glucan synthase co-travel in the same vesicle in *Zymoseptoria tritici*. *Fungal Genet. Biol.,* 135**,** 103286.

Schwenninger, S. M. & Meile, L. 2004. A mixed culture of *Propionibacterium jensenii* and *Lactobacillus paracasei* subsp. *paracasei* inhibits food spoilage yeasts. *Syst. Appl. Microbiol.,* 27**,** 229-237.

Selbmann, L. 2019. Extreme-fungi and the benefits of a stressing life. *Life,* 9**,** 31.

Serasinghe, M. N., Gelles, J. D., Li, K., Zhao, L., Abbate, F., Syku, M., Mohammed, J. N., Badal, B., Rangel, C. A., Hoehn, K. L., Celebi, J. T. & Chipuk, J. E. 2018. Dual suppression of inner and outer mitochondrial membrane functions augments apoptotic responses to oncogenic MAPK inhibition. *Cell Death Dis.,* 9**,** 29-42.

Sevastos, A. A., Thomson, N. R., Lindsay, C., Padia, F. & Khutoryanskiy, V. V. 2020. Rainfastness of agrochemical formulations based on N-vinyl pyrrolidone polymers and their interpolymer complexes with poly(acrylic acid). *Eur. Polym. J.,* 134**,** 109852.

Shafi, J., Tian, H. & Ji, M. 2017. *Bacillus* species as versatile weapons for plant pathogens: a review. *Biotechnol. Biotechnol. Equip.,* 31**,** 446-459.

Sharma, M., Dhamgaye, S., Singh, A. & Prasad, R. 2012. Lipidome analysis reveals antifungal polyphenol curcumin affects membrane lipid homeostasis. *Front. Biosci. (Elite Ed),* 4**,** 1195-1209.

Sharma, M., Manoharlal, R., Puri, N. & Prasad, R. 2010. Antifungal curcumin induces reactive oxygen species and triggers an early apoptosis but prevents hyphae development by targeting the global repressor TUP1 in *Candida albicans*. *Biosci. Rep.,* 30**,** 391-404.

Sharma, M., Manoharlal, R., Shukla, S., Puri, N., Prasad, T., Ambudkar, S. V. & Prasad, R. 2009. Curcumin modulates efflux mediated by yeast ABC multidrug transporters and is synergistic with antifungals. *Antimicrob. Agents Chemother.,* 53**,** 3256-3265.

Shetty, N. P., Jensen, J. D., Knudsen, A., Finnie, C., Geshi, N., Blennow, A., Collinge, D. B. & Jorgensen, H. J. 2009. Effects of beta-1,3-glucan from *Septoria tritici* on structural defence responses in wheat. *J. Exp. Bot.,* 60**,** 4287-4300.

Shi, H.-Z., Chang, W.-Q., Zhang, M. & Lou, H.-X. 2019. Two natural molecules preferentially inhibit azole-resistant *Candida albicans* with MDR1 hyperactivation. *Chin. J. Nat. Med.,* 17**,** 209-217.

Shichiri, M., Yoshida, Y., Ishida, N., Hagihara, Y., Iwahashi, H., Tamai, H. & Niki, E. 2011. alpha-Tocopherol suppresses lipid peroxidation and behavioral and cognitive impairments in the Ts65Dn mouse model of Down syndrome. *Free Radic. Biol. Med.,* 50**,** 1801-1811.

Shinya, T., Nakagawa, T., Kaku, H. & Shibuya, N. 2015. Chitin-mediated plant-fungal interactions: catching, hiding and handshaking. *Curr. Opin. Plant Biol.,* 26**,** 64-71.

Shrestha, R., Johnson, E. & Byrne, F. L. 2021. Exploring the therapeutic potential of mitochondrial uncouplers in cancer. *Mol. Metab.,* 51**,** 101222.

Siles, S. A., Srinivasan, A., Pierce, C. G., Lopez-Ribot, J. L. & Ramasubramanian, A. K. 2013. High-throughput screening of a collection of known pharmacologically active small compounds for identification of *Candida albicans* biofilm inhibitors. *Antimicrob. Agents Chemother.,* 57**,** 3681-3687.

Six, D. L. & Wingfield, M. J. 2011. The role of phytopathogenicity in bark beetle-fungus symbioses: a challenge to the classic paradigm. *Annu. Rev. Entomol.,* 56**,** 255-272.

Slater, E. C. 1973. The mechanism of action of the respiratory inhibitor, antimycin. *Biochim. Biophys. Acta Bioenerg.,* 301**,** 129-154.

Slaven, J. W., Anderson, M. J., Sanglard, D., Dixon, G. K., Bille, J., Roberts, I. S. & Denning, D. W. 2002. Increased expression of a novel *Aspergillus fumigatus* ABC transporter gene, atrF, in the presence of itraconazole in an itraconazole resistant clinical isolate. *Fungal Genet. Biol.,* 36**,** 199-206.

Snelders, E., Huis In 't Veld, R. A., Rijs, A. J., Kema, G. H., Melchers, W. J. & Verweij, P. E. 2009. Possible environmental origin of resistance of *Aspergillus fumigatus* to medical triazoles. *Appl. Environ. Microbiol.,* 75**,** 4053-4057.

Song, D., Hao, J. & Fan, D. 2020. Biological properties and clinical applications of berberine. *Front. Med.,* 14**,** 564-582.

Sparks, T. C., Wessels, F. J., Lorsbach, B. A., Nugent, B. M. & Watson, G. B. 2019. The new age of insecticide discovery-the crop protection industry and the impact of natural products. *Pestic. Biochem. Physiol.,* 161**,** 12-22.

Spencer, J. F. T. & Spencer, D. M. 1996. Mutagenesis in yeast. *In:* EVANS, I. H. (ed.) *Yeast Protocols, methods in cell and molecular biology* Totowa, New Jersey: Human Press Inc. 17-39.

Spettel, K., Barousch, W., Makristathis, A., Zeller, I., Nehr, M., Selitsch, B., Lackner, M., Rath, P. M., Steinmann, J. & Willinger, B. 2019. Analysis of antifungal resistance genes in *Candida albicans* and *Candida glabrata* using next generation sequencing. *PLoS One,* 14**,** e0210397.

Spitzer, M., Robbins, N. & Wright, G. D. 2017. Combinatorial strategies for combating invasive fungal infections. *Virulence,* 8**,** 169-185.

Staudinger, H. 1920. Über Polymerisation. *Ber. Dtsch. Chem. Ges.,* 53**,** 1073-1085.

Steinbach, W. J., Mitchell, T. G., Schell, W. A., Espinel-Ingroff, A., Coico, R. F., Walsh, T. J. & Perfect, J. R. 2003. Status of medical mycology education. *Med. Mycol.,* 41**,** 457-467.

Steinberg, G. 2015. Cell biology of *Zymoseptoria tritici*: Pathogen cell organization and wheat infection. *Fungal Genet. Biol.,* 79**,** 17-23.

Sterflinger, K. 2010. Fungi: Their role in deterioration of cultural heritage. *Fungal Biol. Rev.,* 24**,** 47-55.

Stewart, P. S. 1996. Theoretical aspects of antibiotic diffusion into microbial biofilms. *Antimicrob. Agents Chemother.,* 40**,** 2517–2522.

Strähle, U., Scholz, S., Geisler, R., Greiner, P., Hollert, H., Rastegar, S., Schumacher, A., Selderslaghs, I., Weiss, C., Witters, H. & Braunbeck, T. 2012. Zebrafish embryos as an alternative to animal experiments - a commentary on the definition of the onset of protected life stages in animal welfare regulations. *Reprod. Toxicol.,* 33**,** 128-132.

Strzelczyk, A. B., Kuroczkin, J. & Krumbein, W. E. 1987. Studies on the microbial degradation of ancient leather bookbindings: Part I. *Int. Biodeterior.,* 23**,** 3-27.

Sucher, A. J., Chahine, E. B. & Balcer, H. E. 2009. Echinocandins: the newest class of antifungals. *Ann. Pharmacother.,* 43**,** 1647-1657.

Talevi, A. & Bellera, C. L. 2020. Challenges and opportunities with drug repurposing: finding strategies to find alternative uses of therapeutics. *Expert Opin. Drug Discov.,* 15**,** 397-401.

Tamada, J. A. & Langer, R. 1993. Erosion kinetics of hydrolytically degradable polymers. *PNAS USA,* 90**,** 552-526.

Tarnowski, B. I., Spinale, F. G. & Nicholson, J. H. 1991. DAPI as a useful stain for nuclear quantitation. *Biotech. Histochem.,* 66**,** 296-302.

Thomson, P., Mayayo, E., Lopez-Fernandez, L., Guarro, J. & Capilla, J. 2017. Combined antifungal therapy against systemic murine infections by rare *Cryptococcus* species. *Mycoses,* 60**,** 112-117.

Tillman, R. W., Siegel, M. R. & Long, J. W. 1973. Mechanism of action and fate of the fungicide chlorothalonil (2,4,5,6-tetrachloroisophthalonitrile) in biological systems. *Pestic. Biochem. Physiol.,* 3**,** 160-167.

Tkacz, J. S., Cybulska, E. B. & Lampen, J. O. 1971. Specific staining of wall mannan in yeast cells with fluorescein-conjugated concanavalin A. *J. Bacteriol.,* 105**,** 1-5.

Tobin, M. B., Peery, R. B. & Skatrud, P. L. 1997. Genes encoding multiple drug resistance-like proteins in *Aspergillus fumigatus* and *Aspergillus flavus*. *Gene,* 200**,** 11-23.

Torriani, S. F., Melichar, J. P., Mills, C., Pain, N., Sierotzki, H. & Courbot, M. 2015. *Zymoseptoria tritici*: A major threat to wheat production, integrated approaches to control. *Fungal Genet. Biol.,* 79**,** 8-12.

Tudela, J. A., López-Gálvez, F., Allende, A., Hernández, N., Andújar, S., Marín, A., Garrido, Y. & Gil, M. I. 2019. Operational limits of sodium hypochlorite for different fresh produce wash water based on microbial inactivation and disinfection by-products (DBPs). *Food Control,* 104**,** 300-307.

Tuite, M. F. & McLaughlin, C. S. 1984. The effects of paromomycin on the fidelity of translation in a yeast cell-free system. *Biochim. Biophys. Acta.,* 783**,** 166-170.

Tyers, M. & Wright, G. D. 2019. Drug combinations: a strategy to extend the life of antibiotics in the 21st century. *Nat. Rev. Microbiol.,* 17**,** 141-155.

Ulanowska, M. & Olas, B. 2021. Biological properties and prospects for the application of eugenol-a review. *Int. J. Mol. Sci.,* 22**,** 1-12.

Umetsu, N. & Shirai, Y. 2020. Development of novel pesticides in the 21st century. *J. Pestic. Sci.,* 45**,** 54-74.

Uppuluri, P., Chaturvedi, A. K., Srinivasan, A., Banerjee, M., Ramasubramaniam, A. K., Kohler, J. R., Kadosh, D. & Lopez-Ribot, J. L. 2010. Dispersion as an important step in the *Candida albicans* biofilm developmental cycle. *PLoS Pathog.,* 6**,** e1000828.

Vallières, C., Hook, A. L., He, Y., Crucitti, V. C., Figueredo, G., Davies, C. R., Burroughs, L., Winkler, D. A., Wildman, R. D., Irvine, D. J., Alexander, M. R. & Avery, S. V. 2020. Discovery of (meth)acrylate polymers that resist colonization by fungi associated with pathogenesis and biodeterioration. *Sci. Adv.,* 6**,** eaba6574.

Vallières, C., Raulo, R., Dickinson, M. & Avery, S. V. 2018. Novel combinations of agents targeting translation that synergistically inhibit fungal pathogens. *Front. Microbiol.,* 9**,** 2355.

Vallières, C., Singh, N., Alexander, C. & Avery, S. V. 2020. Repurposing nonantifungal approved drugs for synergistic targeting of fungal pathogens. *ACS Infect. Dis.,* 6**,** 2950-2958.

van Baarlen, P., Woltering, E. J., Staats, M. & van Kan, J. A. 2007. Histochemical and genetic analysis of host and non-host interactions of Arabidopsis with three *Botrytis* species: an important role for cell death control. *Mol. Plant. Pathol.,* 8**,** 41-54.

van Esse, H. P., Reuber, T. L. & van der Does, D. 2020. Genetic modification to improve disease resistance in crops. *New Phytol.,* 225**,** 70-86.

van Lenteren, J. C., Bolckmans, K., Köhl, J., Ravensberg, W. J. & Urbaneja, A. 2017. Biological control using invertebrates and microorganisms: plenty of new opportunities. *BioControl,* 63**,** 39-59.

Vasselli, J. G. & Shaw, B. D. 2022. Fungal spore attachment to substrata. *Fungal Biol. Rev.,* 41**,** 2-9.

Vermes, A., van Der Sijs, H. & Guchelaar, H. J. 2000. Flucytosine: correlation between toxicity and pharmacokinetic parameters. *Chemotherapy,* 46**,** 86-94.

Verweij, P. E., Chowdhary, A., Melchers, W. J. & Meis, J. F. 2016. Azole resistance in *Aspergillus fumigatus*: Can we retain the clinical use of mold-active antifungal azoles? *Clin. Infect. Dis.,* 62**,** 362-368.

Vincent, B. M., Lancaster, A. K., Scherz-Shouval, R., Whitesell, L. & Lindquist, S. 2013. Fitness trade-offs restrict the evolution of resistance to amphotericin B. *PLoS Biol.,* 11**,** e1001692.

Vowinckel, J., Hartl, J., Marx, H., Kerick, M., Runggatscher, K., Keller, M. A., Mulleder, M., Day, J., Weber, M., Rinnerthaler, M., Yu, J. S. L., Aulakh, S. K., Lehmann, A., Mattanovich, D., Timmermann, B., Zhang, N., Dunn, C. D., MacRae, J. I.,

Breitenbach, M. & Ralser, M. 2021. The metabolic growth limitations of petite cells lacking the mitochondrial genome. *Nat. Metab.,* 3**,** 1521-1535.
Wall, G., Chaturvedi, A. K., Wormley, F. L., Jr., Wiederhold, N. P., Patterson, H. P., Patterson, T. F. & Lopez-Ribot, J. L. 2018. Screening a repurposing library for inhibitors of multidrug-resistant *Candida auris* identifies ebselen as a repositionable candidate for antifungal drug development. *Antimicrob. Agents Chemother.,* 62**,** e01084-18.
Waltenberger, B., Mocan, A., Smejkal, K., Heiss, E. H. & Atanasov, A. G. 2016. Natural products to counteract the epidemic of cardiovascular and metabolic disorders. *Molecules,* 21**,** 807.
Walter, H., Glattli, A., Grote, T. & Stammler, G. 2011. New fungicides and new modes of action. *In:* DEHNE, H. W., DEISING, H. B., GISI, U., KUCK, K. H. & LYR, H. (eds.) *Modern fungicides and antifungal compounds* VI. Braunschweig, Germany.: DPG. 47-54.
Wang, H., Kong, F., Sorrell, T. C., Wang, B., McNicholas, P., Pantarat, N., Ellis, D., Xiao, M., Widmer, F. & Chen, S. C. 2009. Rapid detection of *ERG11* gene mutations in clinical *Candida albicans* isolates with reduced susceptibility to fluconazole by rolling circle amplification and DNA sequencing. *BMC Microbiol.,* 9**,** 167.
Wang, L., He, H. S., Yu, H. L., Zeng, Y., Han, H., He, N., Liu, Z. G., Wang, Z. Y., Xu, S. J. & Xiong, M. 2015. Sclareol, a plant diterpene, exhibits potent antiproliferative effects via the induction of apoptosis and mitochondrial membrane potential loss in osteosarcoma cancer cells. *Mol. Med. Rep.,* 11**,** 4273-4278.
Warrilow, A. G., Nishimoto, A. T., Parker, J. E., Price, C. L., Flowers, S. A., Kelly, D. E., Rogers, P. D. & Kelly, S. L. 2019. The evolution of azole resistance in *Candida albicans* sterol 14alpha-demethylase (CYP51) through incremental amino acid substitutions. *Antimicrob. Agents Chemother.,* 63**,** e02586-18.
Watts, H. J., Veacute Ry, A. A., Perera, T. H. S., Davies, J. M. & Gow, N. A. R. 1998. Thigmotropism and stretch-activated channels in the pathogenic fungus *Candida albicans*. *Microbiology,* 144 (Pt 3)**,** 689-695.
Wei, Y., Mao, S. & Tu, K. 2014. Effect of preharvest spraying *Cryptococcus laurentii* on postharvest decay and quality of strawberry. *Biol. Control,* 73**,** 68-74.
Whaley, S. G., Berkow, E. L., Rybak, J. M., Nishimoto, A. T., Barker, K. S. & Rogers, P. D. 2017. Azole antifungal resistance in *Candida albicans* and emerging non-albicans *Candida* species. *Front. Microbiol.,* 7**,** 2173.
Whitehead, K. A., Deisenroth, T., Preuss, A., Liauw, C. M. & Verran, J. 2011. The effect of surface properties on the strength of attachment of fungal spores using AFM perpendicular force measurements. *Colloids Surf. B.,* 82**,** 483-489.
WHO 2022. WHO fungal priority pathogens list to guide research, development and public health action. Geneva: World Health Organization.
Wieczorek, T. M., Berg, G., Semaškienė, R., Mehl, A., Sierotzki, H., Stammler, G., Justesen, A. F. & Jørgensen, L. N. 2015. Impact of DMI and SDHI fungicides on disease control and *CYP51* mutations in populations of *Zymoseptoria tritici* from Northern Europe. *Eur. J. Plant Pathol.,* 143**,** 861-871.
Williams, A. J., Murrell, M., Brammah, S., Minchenko, J. & Christodoulou, J. 1999. A novel system for assigning the mode of inheritance in mitochondrial disorders using cybrids and rhodamine 6G. *Hum. Mol. Genet.,* 8**,** 1691-1697.
Williams, R. B. & Lorenz, M. C. 2020. Multiple alternative carbon pathways combine to promote *Candida albicans* stress resistance, immune interactions, and virulence. *mBio,* 11**,** e03070-19.
Williamson, B., Tudzynski, B., Tudzynski, P. & van Kan, J. A. 2007. *Botrytis cinerea*: the cause of grey mould disease. *Mol. Plant Pathol.,* 8**,** 561-580.

Winterbourn, C. C. 2014. The challenges of using fluorescent probes to detect and quantify specific reactive oxygen species in living cells. *Biochim. Biophys. Acta.,* 1840**,** 730-738.

Wohlgemuth, F., Gomes, R. L., Singleton, I., Rawson, F. J. & Avery, S. V. 2020. Top-down characterization of an antimicrobial sanitizer, leading from quenchers of efficacy to mode of action. *Front. Microbiol.,* 11**,** 575157.

Wright, G. D. 2019. Unlocking the potential of natural products in drug discovery. *Microb. Biotechnol.,* 12**,** 55-57.

Wu, J., Chen, S., Liu, H., Zhang, Z., Ni, Z., Chen, J., Yang, Z., Nie, Y. & Fan, D. 2018. Tunicamycin specifically aggravates ER stress and overcomes chemoresistance in multidrug-resistant gastric cancer cells by inhibiting N-glycosylation. *J. Exp. Clin. Cancer. Res.,* 37**,** 272.

Wuyts, J., Van Dijck, P. & Holtappels, M. 2018. Fungal persister cells: The basis for recalcitrant infections? *PLoS Pathog.,* 14**,** e1007301.

Xiang, M. J., Liu, J. Y., Ni, P. H., Wang, S., Shi, C., Wei, B., Ni, Y. X. & Ge, H. L. 2013. Erg11 mutations associated with azole resistance in clinical isolates of *Candida albicans*. *FEMS Yeast Res.,* 13**,** 386-393.

Xu, Y., Chen, L. & Li, C. 2008. Susceptibility of clinical isolates of *Candida* species to fluconazole and detection of *Candida albicans ERG11* mutations. *J. Antimicrob. Chemother.,* 61**,** 798-804.

Xu, Y., Wang, Y., Yan, L., Liang, R. M., Dai, B. D., Tang, R. J., Gao, P. H. & Jiang, Y. Y. 2009. Proteomic analysis reveals a synergistic mechanism of fluconazole and berberine against fluconazole-resistant *Candida albicans*: endogenous ROS augmentation. *J. Proteome. Res.,* 8**,** 5296-5304.

Yadav, B., Mora-Montes, H. M., Wagener, J., Cunningham, I., West, L., Haynes, K., Brown, A. J. P. & Gow, N. A. R. 2020. Differences in fungal immune recognition by monocytes and macrophages: N-mannan can be a shield or activator of immune recognition. *Cell Surf.,* 6**,** 100042.

Yamashita, M. & Fraaije, B. 2018. Non-target site SDHI resistance is present as standing genetic variation in field populations of *Zymoseptoria tritici*. *Pest Manag. Sci.,* 74**,** 672-681.

Yang, F., Li, W. & Jorgensen, H. J. 2013. Transcriptional reprogramming of wheat and the hemibiotrophic pathogen *Septoria tritici* during two phases of the compatible interaction. *PLoS One,* 8**,** e81606.

Yang, F., Zhang, L., Wakabayashi, H., Myers, J., Jiang, Y., Cao, Y., Jimenez-Ortigosa, C., Perlin, D. S. & Rustchenko, E. 2017. Tolerance to caspofungin in *Candida albicans* is associated with at least three distinctive mechanisms that govern expression of *FKS* genes and cell wall remodeling. *Antimicrob. Agents Chemother.,* 61**,** e00071-17.

Yang, M., Jaaks, P., Dry, J., Garnett, M., Menden, M. P. & Saez-Rodriguez, J. 2020. Stratification and prediction of drug synergy based on target functional similarity. *NPJ Syst. Biol. Appl.,* 6**,** 16.

Yanicostas, C. & Soussi-Yanicostas, N. 2021. SDHI fungicide toxicity and associated adverse outcome pathways: What can zebrafish tell us? *Int. J. Mol. Sci.,* 22**,** 12362.

Yeh, P., Tschumi, A. I. & Kishony, R. 2006. Functional classification of drugs by properties of their pairwise interactions. *Nat. Genet.,* 38**,** 489-494.

Yousfi, H., Ranque, S., Cassagne, C., Rolain, J. M. & Bittar, F. 2020. Identification of repositionable drugs with novel antimycotic activity by screening the Prestwick Chemical Library against emerging invasive moulds. *J. Glob. Antimicrob. Resist.,* 21**,** 314-317.

Zadoks, J. C. 1985. Cereal rusts, dogs and stars in antiquity. *Cereal. Rusts Bull.,* 13**,** 1-10.

Zarnowski, R., Westler, W. M., Lacmbouh, G. A., Marita, J. M., Bothe, J. R., Bernhardt, J., Lounes-Hadj Sahraoui, A., Fontaine, J., Sanchez, H., Hatfield, R. D., Ntambi, J. M., Nett, J. E., Mitchell, A. P. & Andes, D. R. 2014. Novel entries in a fungal biofilm matrix encyclopedia. *MBio,* 5**,** e01333-14.

Zeng, X.-H., Zeng, X.-J. & Li, Y.-Y. 2003. Efficacy and safety of berberine for congestive heart failure secondary to ischemic or idiopathic dilated cardiomyopathy. *Am. J. Cardiol.,* 92**,** 173-176.

Zhang, M. R., Zhao, F., Wang, S., Lv, S., Mou, Y., Yao, C. L., Zhou, Y. & Li, F. Q. 2020. Molecular mechanism of azoles resistant *Candida albicans* in a patient with chronic mucocutaneous candidiasis. *BMC Infect. Dis.,* 20**,** 126.

Zhao, W. H., Hu, Z. Q., Okubo, S., Hara, Y. & Shimamura, T. 2001. Mechanism of synergy between epigallocatechin gallate and beta-lactams against methicillin-resistant *Staphylococcus aureus*. *Antimicrob. Agents Chemother.,* 45**,** 1737-1742.

Zheng, G. Q., Kenney, P. M. & Lam, L. K. 1992. Sesquiterpenes from clove (*Eugenia caryophyllata*) as potential anticarcinogenic agents. *J. Nat. Prod.,* 55**,** 999-1003.

Zheng, W., Sun, W. & Simeonov, A. 2018. Drug repurposing screens and synergistic drug-combinations for infectious diseases. *Br. J. Pharmacol.,* 175**,** 181-191.

Zhou, B., Benbow, H. R., Brennan, C. J., Arunachalam, C., Karki, S. J., Mullins, E., Feechan, A., Burke, J. I. & Doohan, F. M. 2020. Wheat encodes small, secreted proteins that contribute to resistance to *Septoria tritici* blotch. *Front. Genet.,* 11**,** 469.